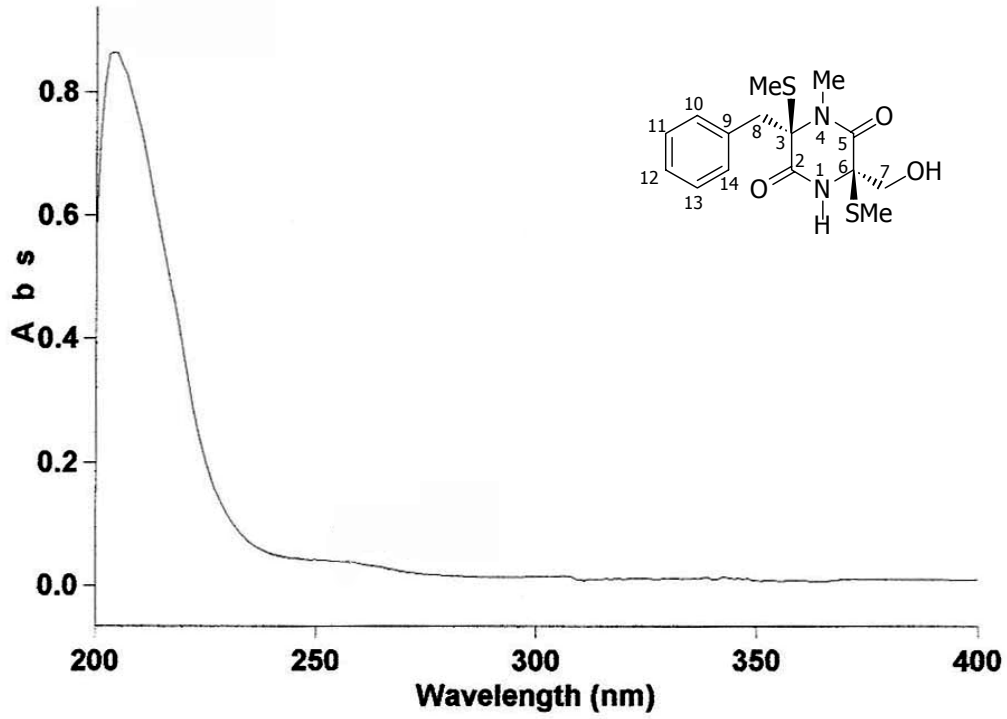

Figure 31. UV spectrum of compound **51**

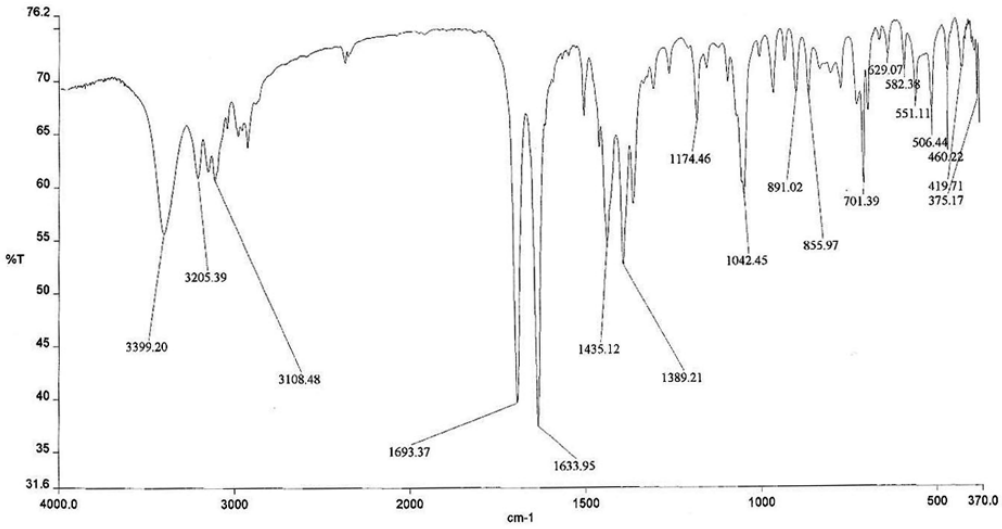

Figure 32. IR spectrum of compound **51**

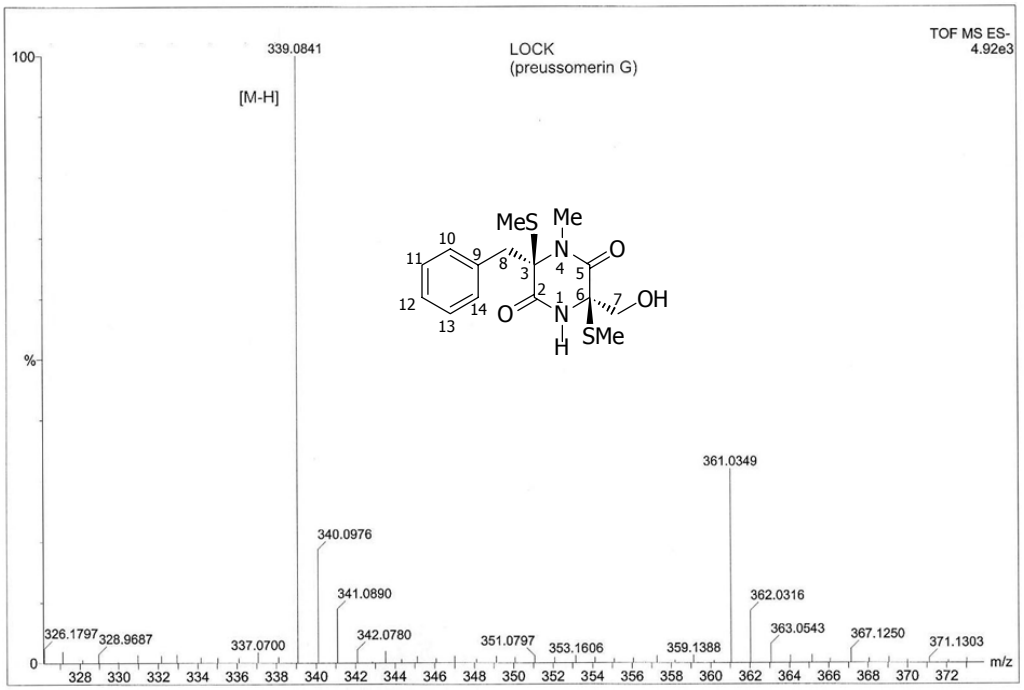

Figure 33. HRMS spectrum of compound **51**

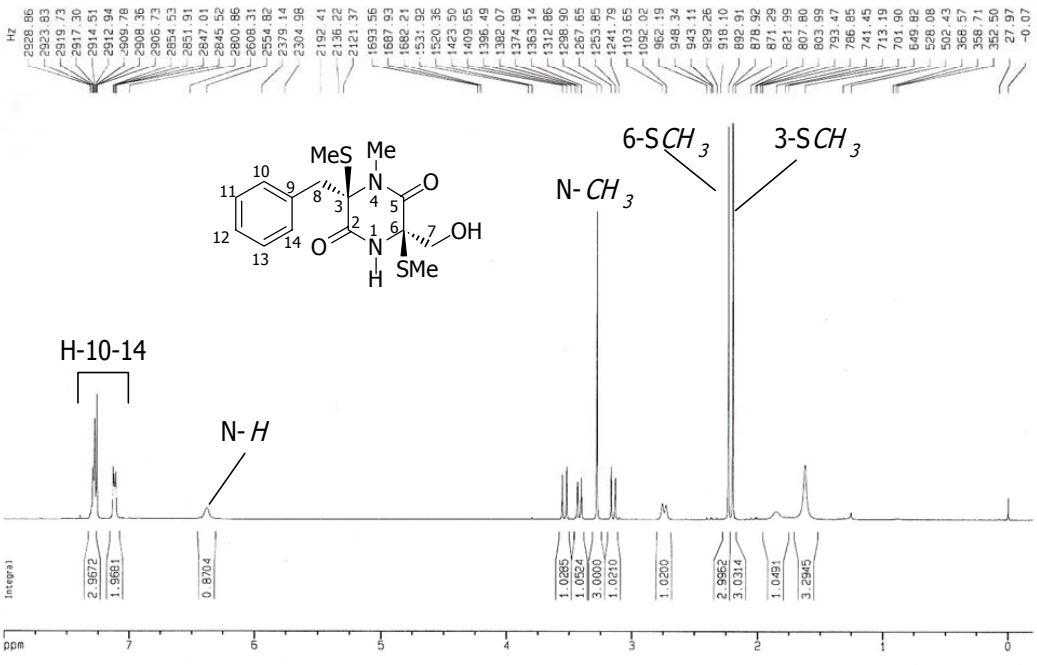

Figure 34. ^{1}H NMR ($CDCl_3$) spectrum of compound **51**

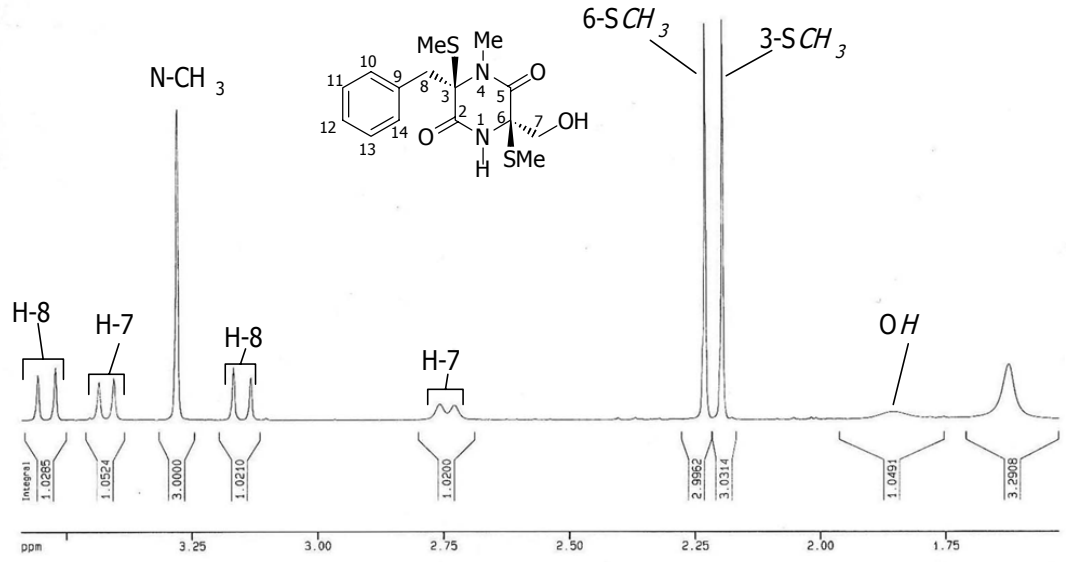

Figure 35. Expansion of ^{1}H NMR ($CDCl_3$) spectrum of compound **51**

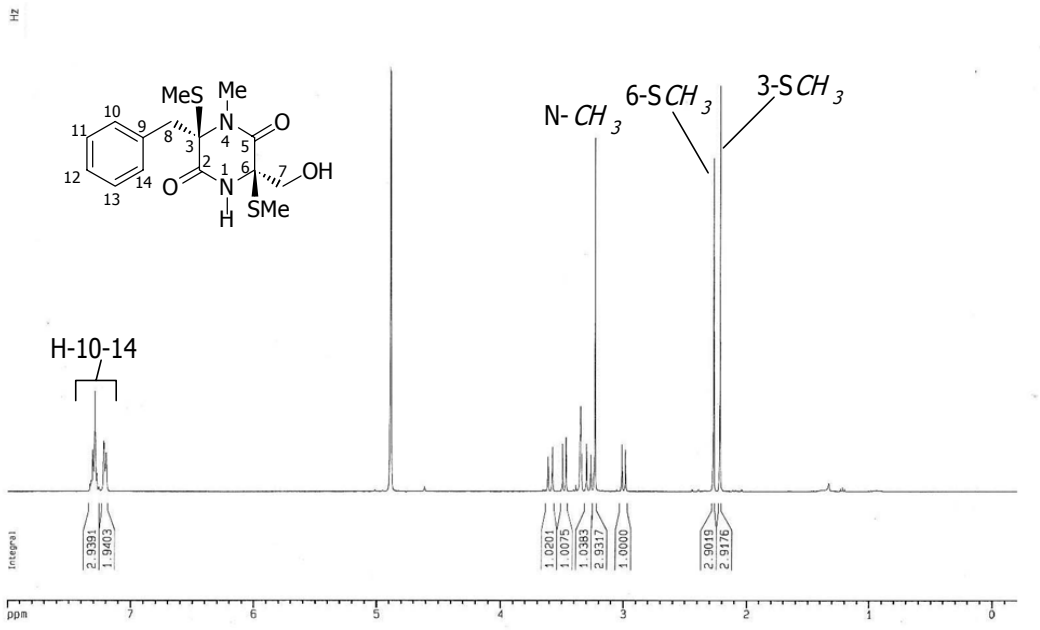

Figure 36. ^{1}H NMR (MeOH-d_4) spectrum of compound **51**

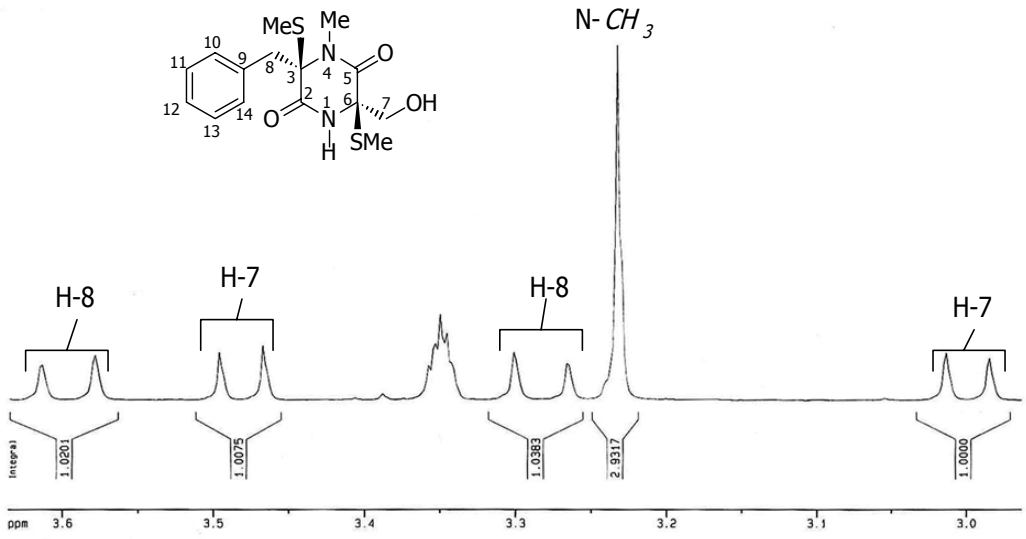

Figure 37. Expansion of ^{1}H NMR (MeOH-d_4) spectrum of compound **51**

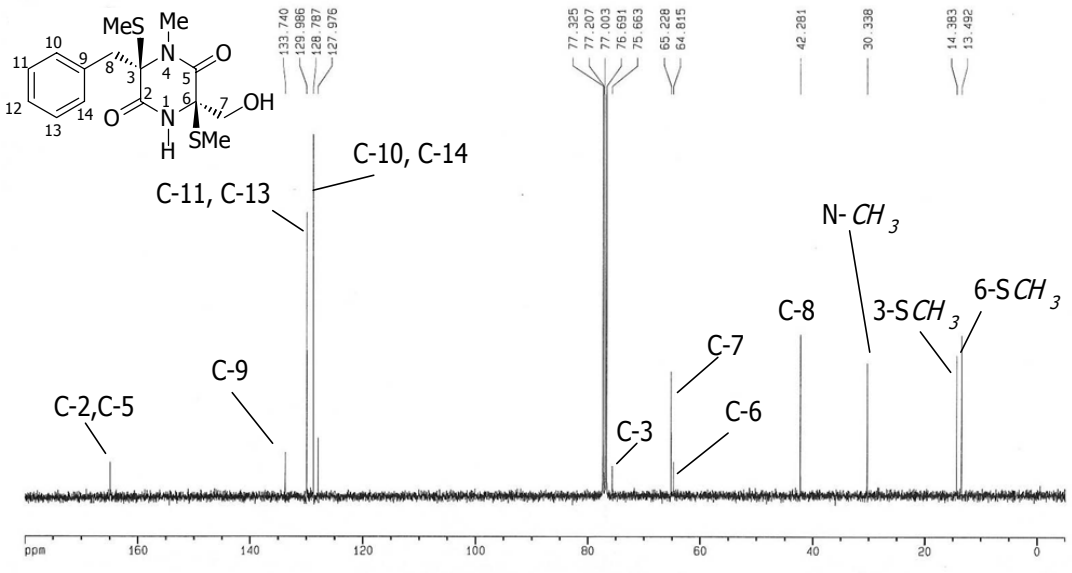

Figure 38. ^{13}C NMR ($CDCl_3$) spectrum of compound **51**

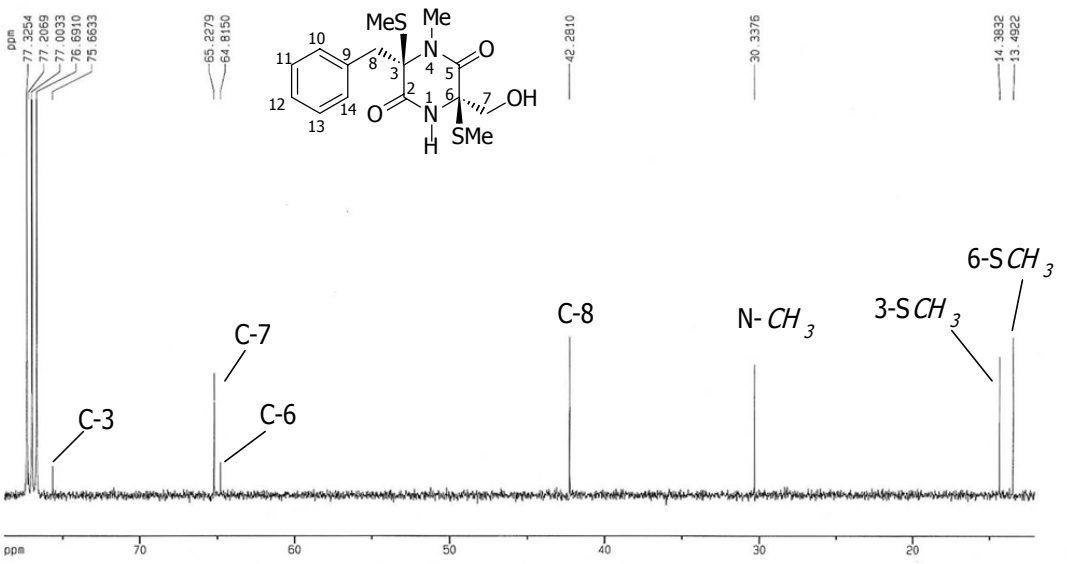

Figure 39. Expansion A of ^{13}C NMR ($CDCl_3$) spectrum of compound **51**

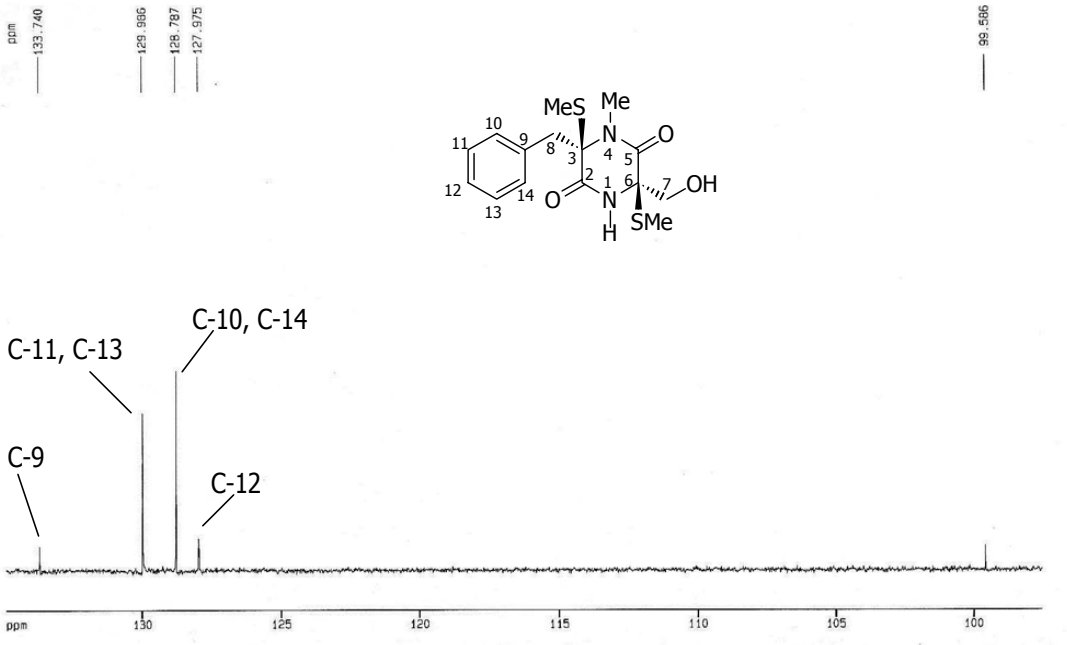

Figure 40. Expansion B of ^{13}C NMR ($CDCl_3$) spectrum of compound **51**

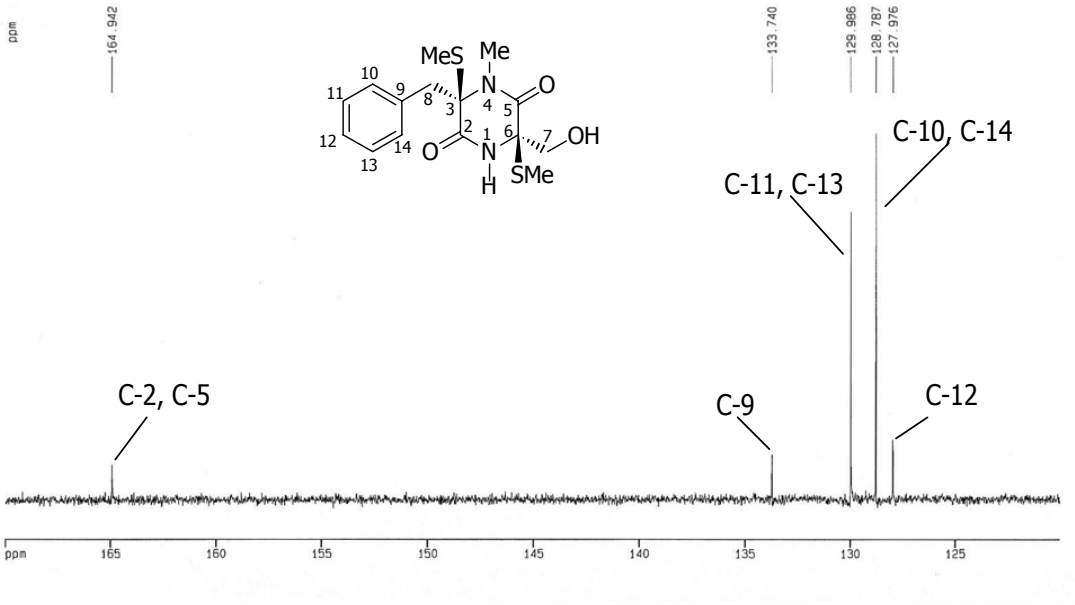

Figure 41. Expansion C of ^{13}C NMR ($CDCl_3$) spectrum of compound **51**

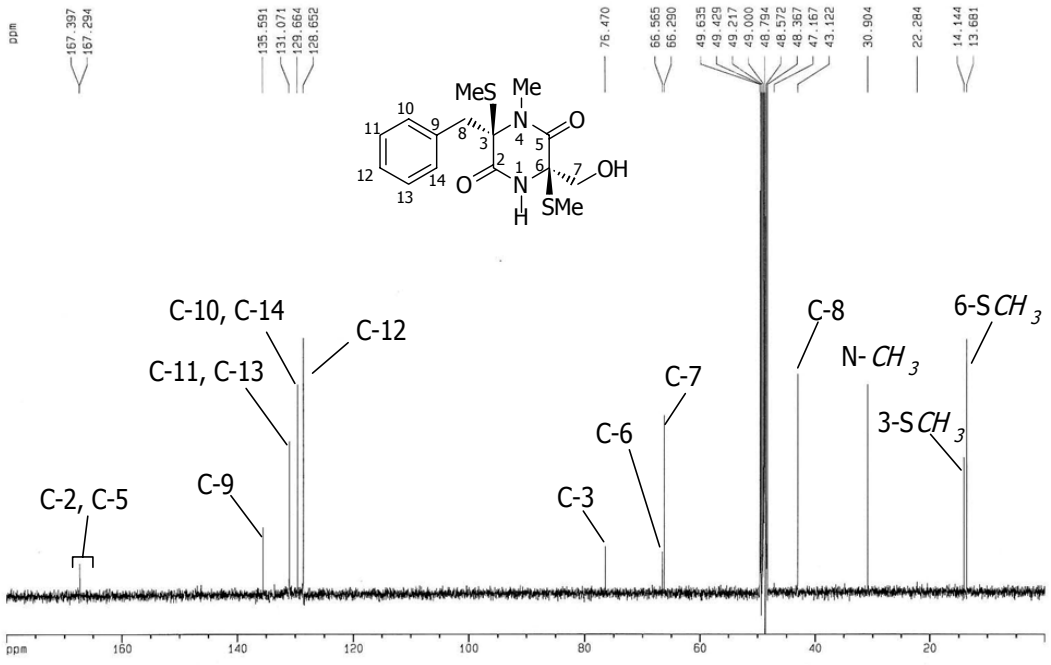

Figure 42. ^{13}C NMR (MeOH- d_4) spectrum of compound **51**

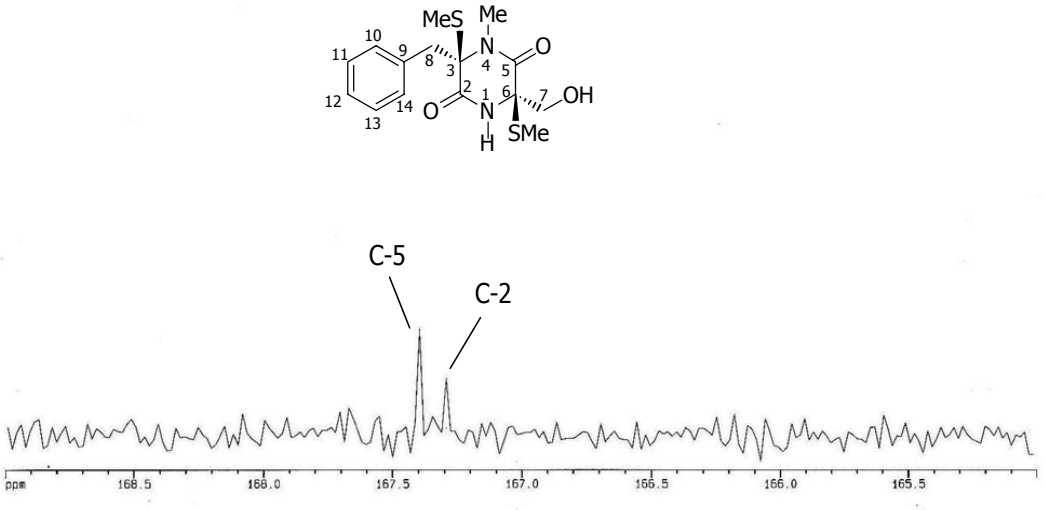

Figure 43. Expansion of ^{13}C NMR (MeOH- d_4) spectrum of compound **51**

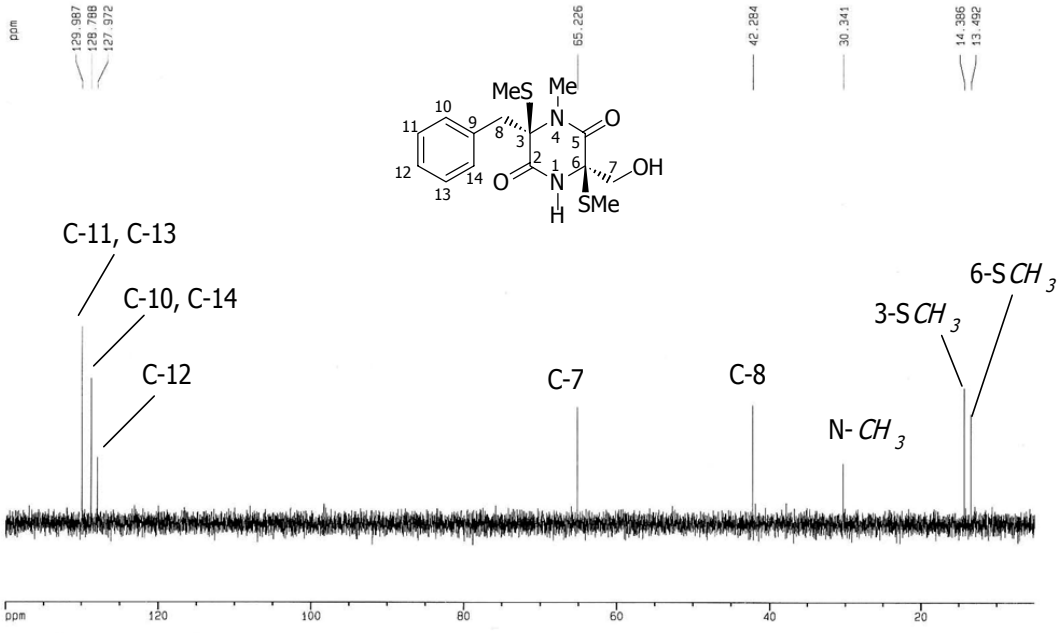

Figure 44. DEPT 45 ($CDCl_3$) spectrum of compound **51**

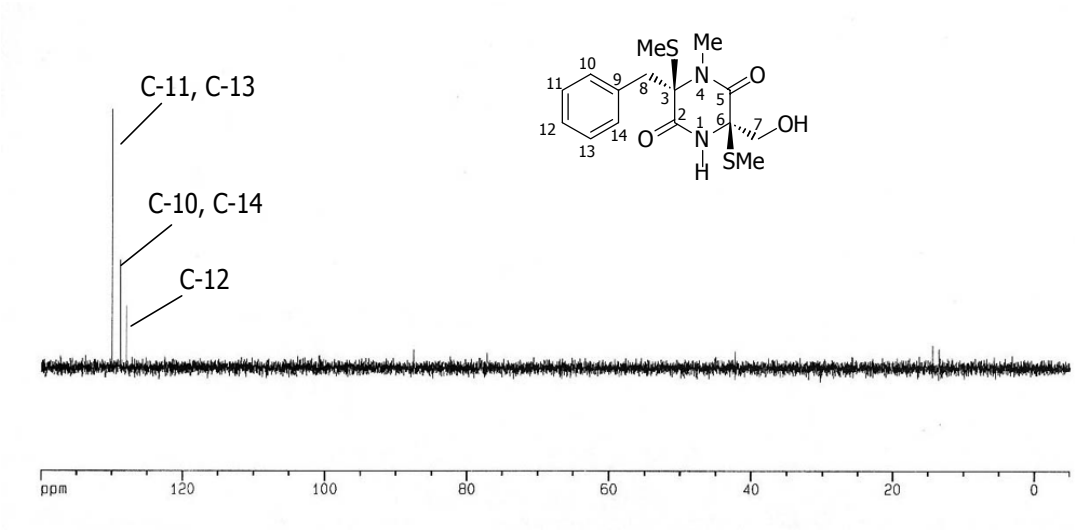

Figure 45. DEPT 90 ($CDCl_3$) spectrum of compound **51**

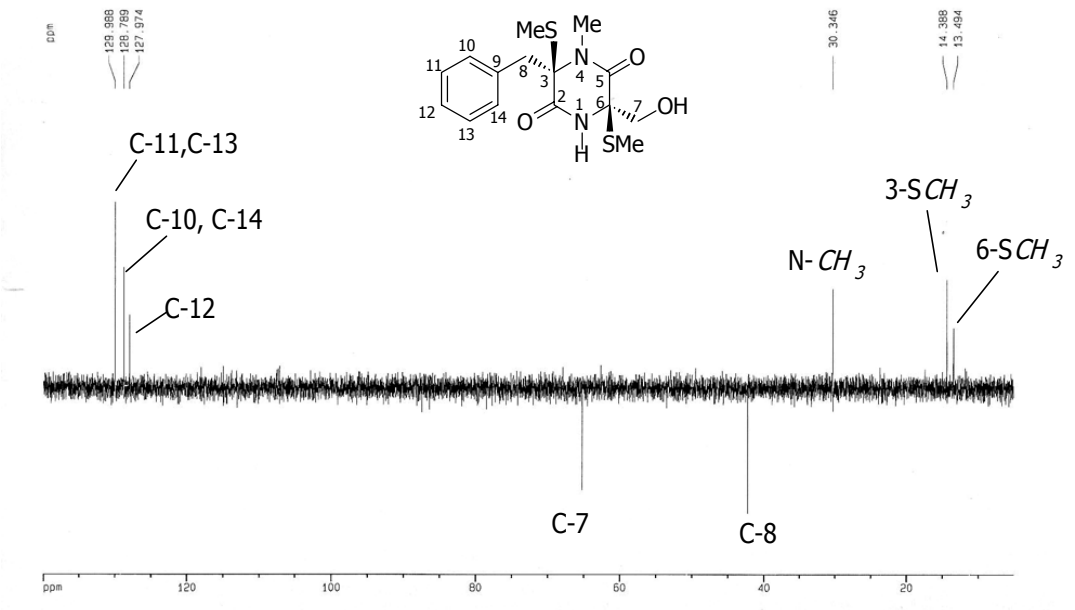

Figure 46. DEPT 135 ($CDCl_3$) spectrum of compound **51**

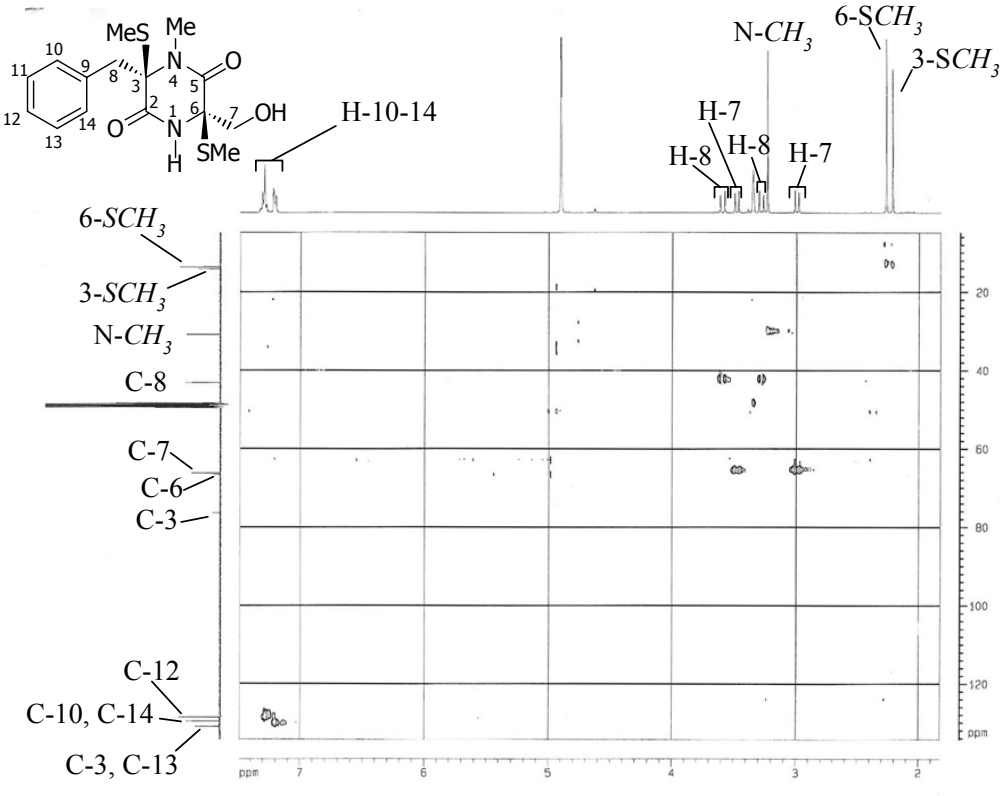

Figure 47. HMQC (MeOH- d_4) spectrum of compound **51**

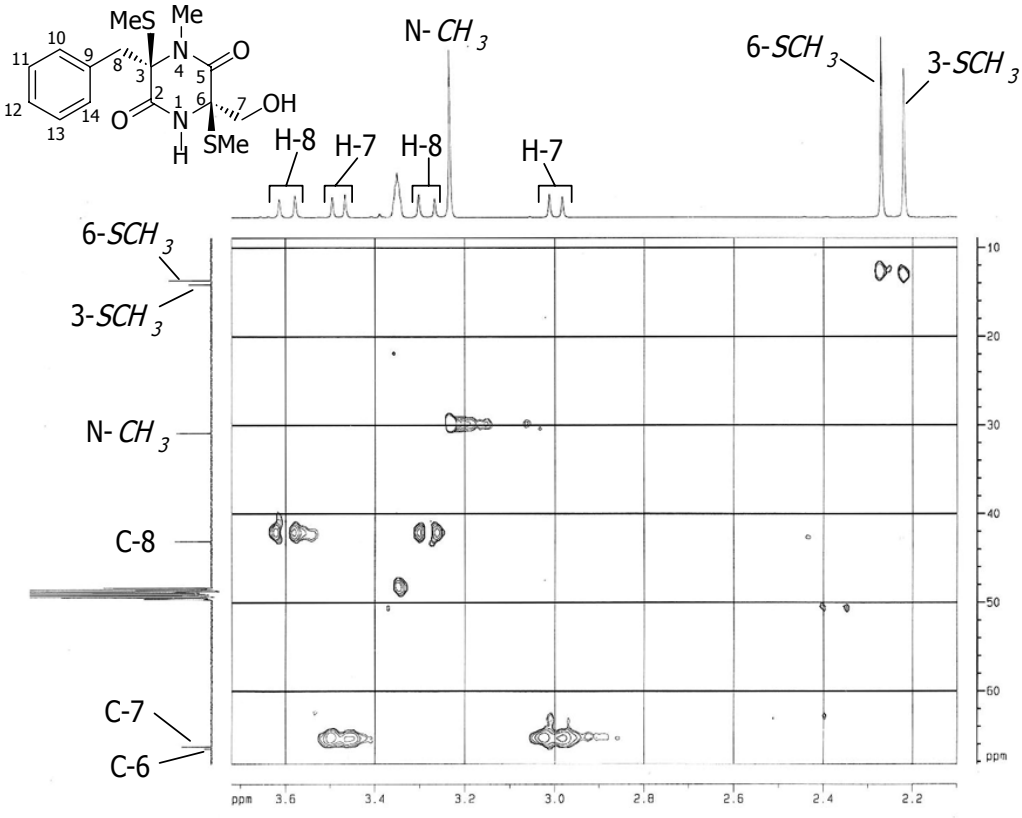

Figure 48. Expansion A of HMQC (MeOH- d_4) spectrum of compound **51**

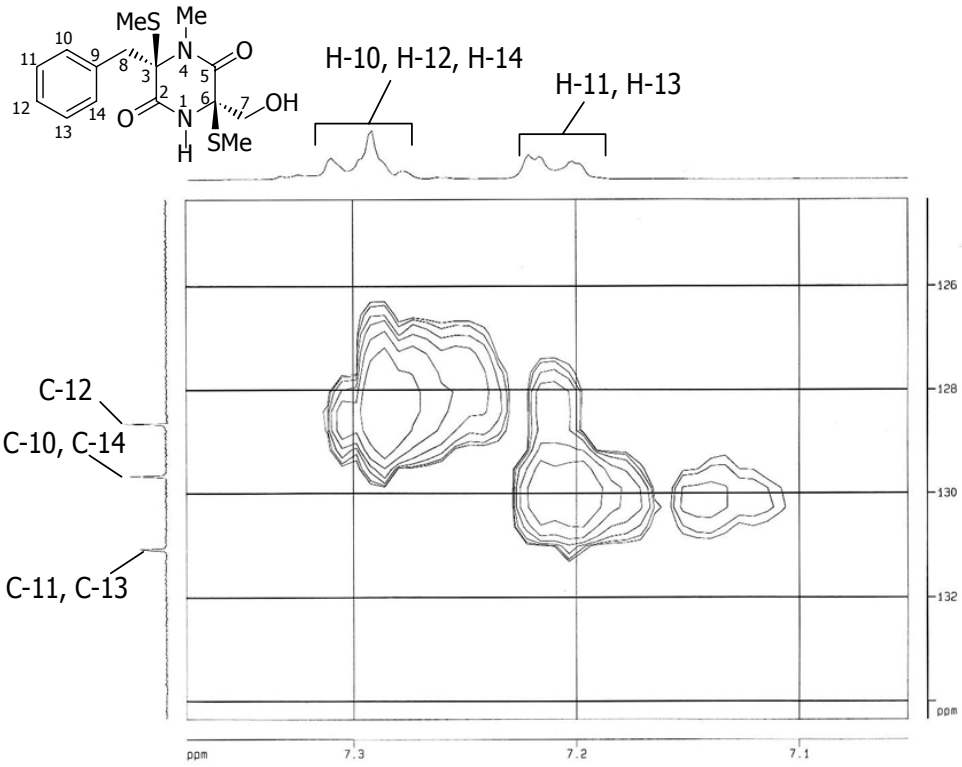

Figure 49. Expansion B of HMQC (MeOH- d_4) spectrum of compound **51**

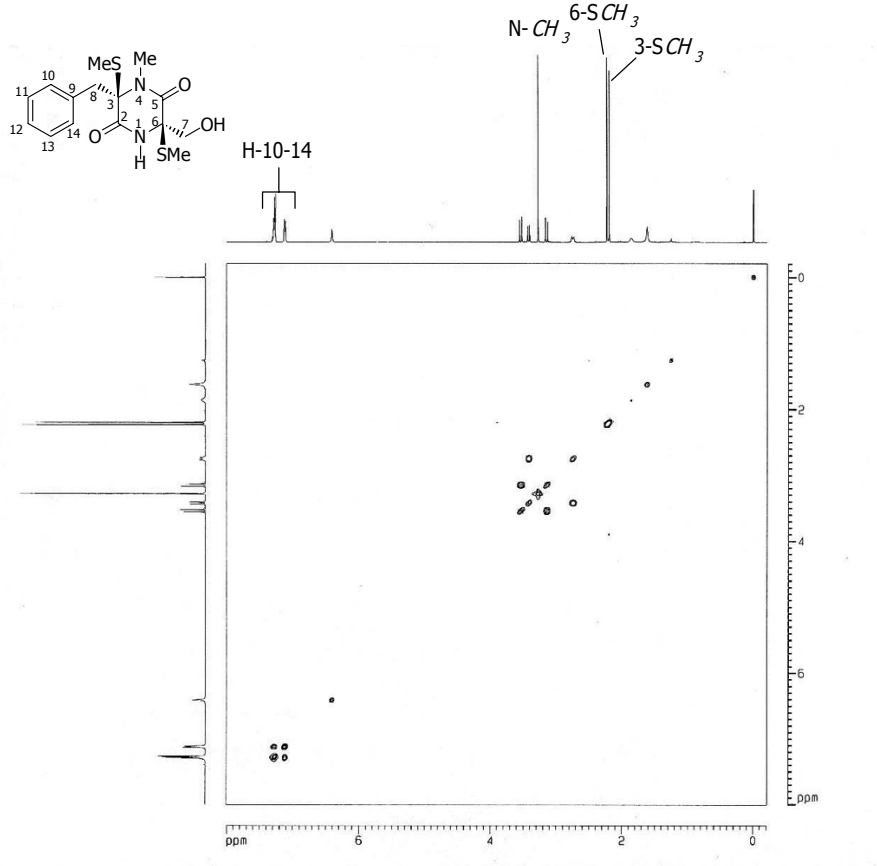

Figure 50. COSY ($CDCl_3$) spectrum of compound **51**

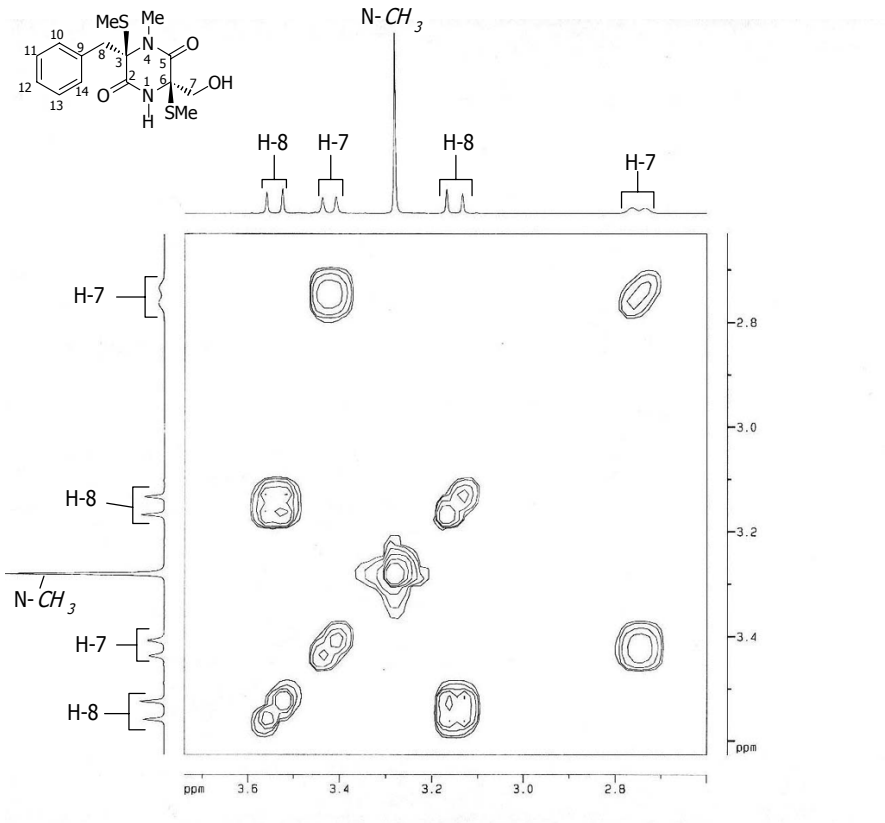

Figure 51. Expansion A of COSY ($CDCl_3$) spectrum of compound **51**

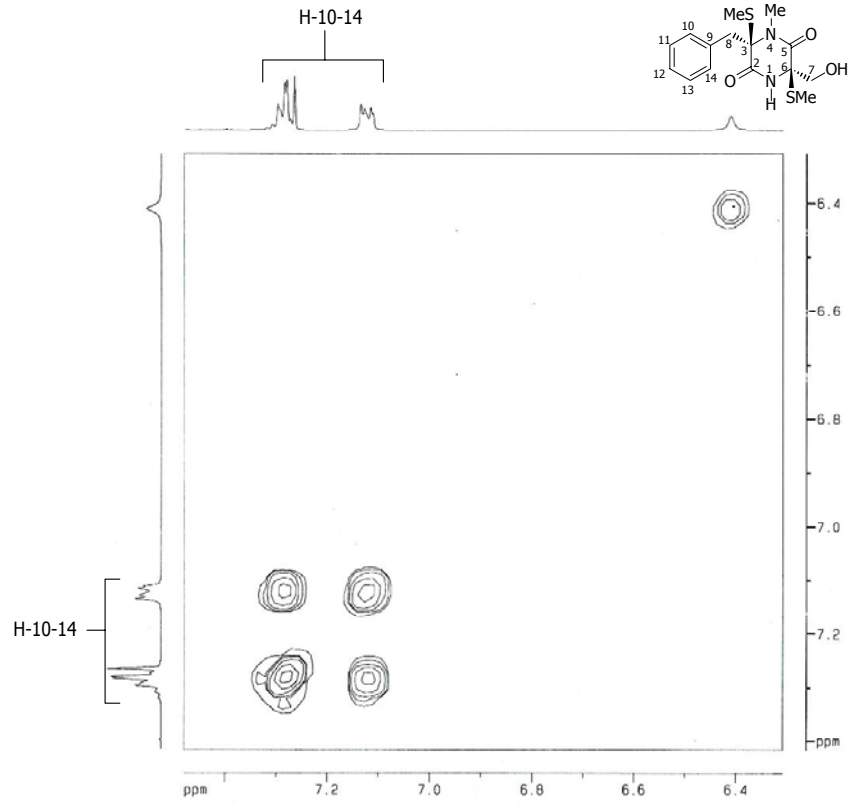

Figure 52. Expansion B of COSY ($CDCl_3$) spectrum of compound **51**

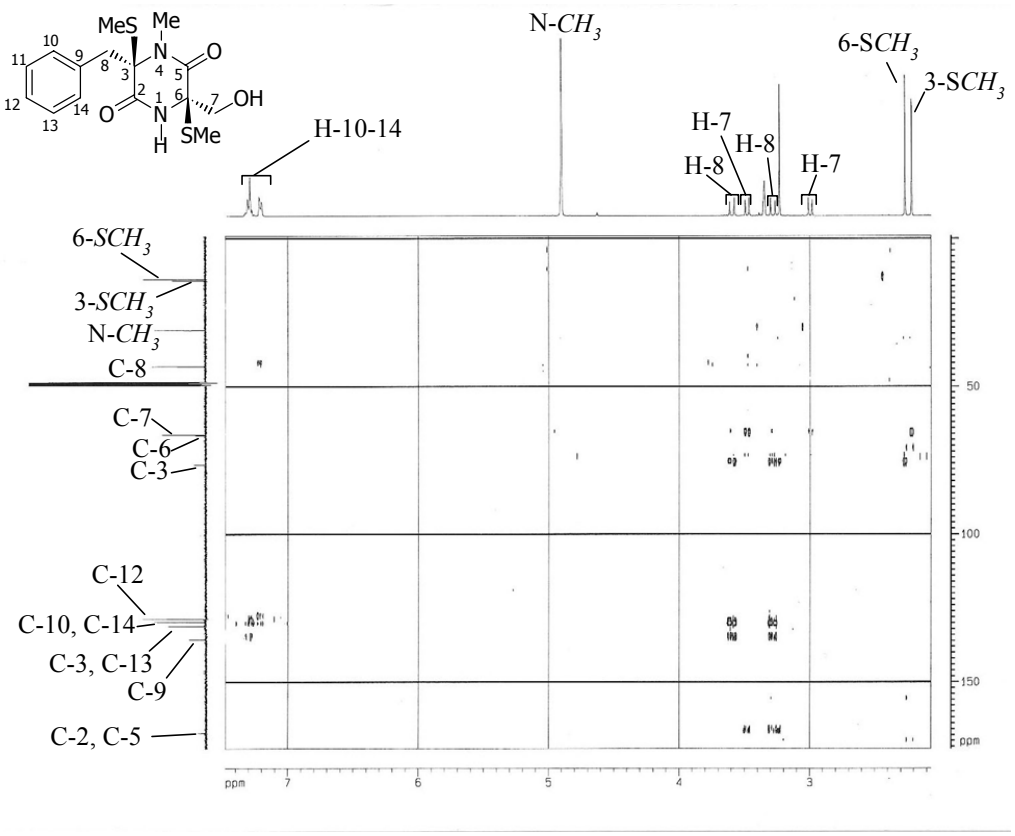

Figure 53. HMBC (MeOH- d_4, d6=110 msec) spectrum of compound **51**

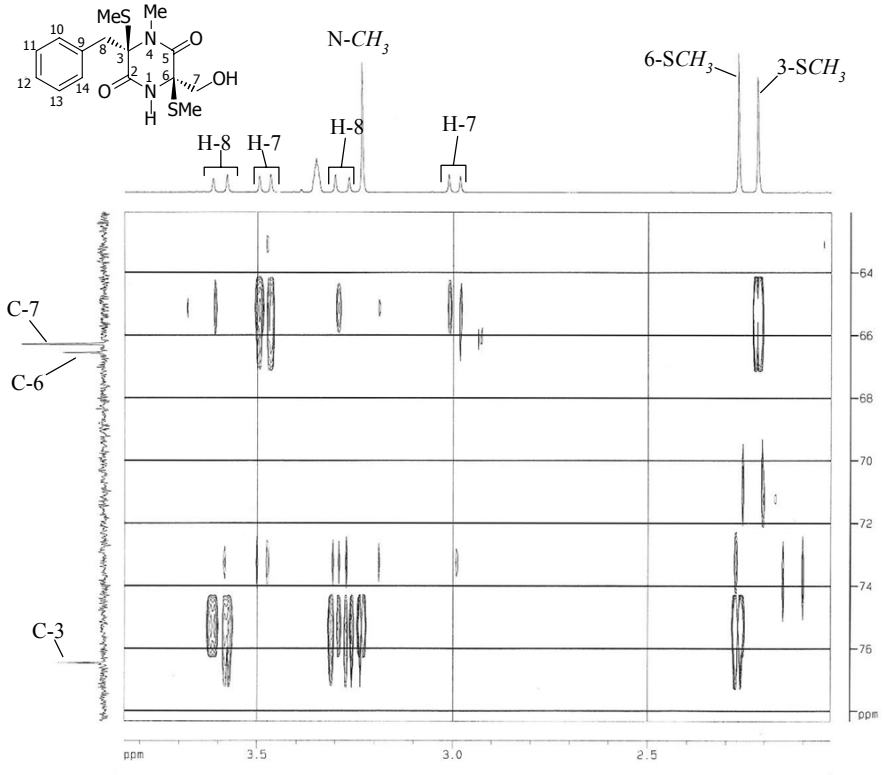

Figure 54. Expansion A of HMBC (MeOH- d_4, d6=110 msec) spectrum of compound **51**

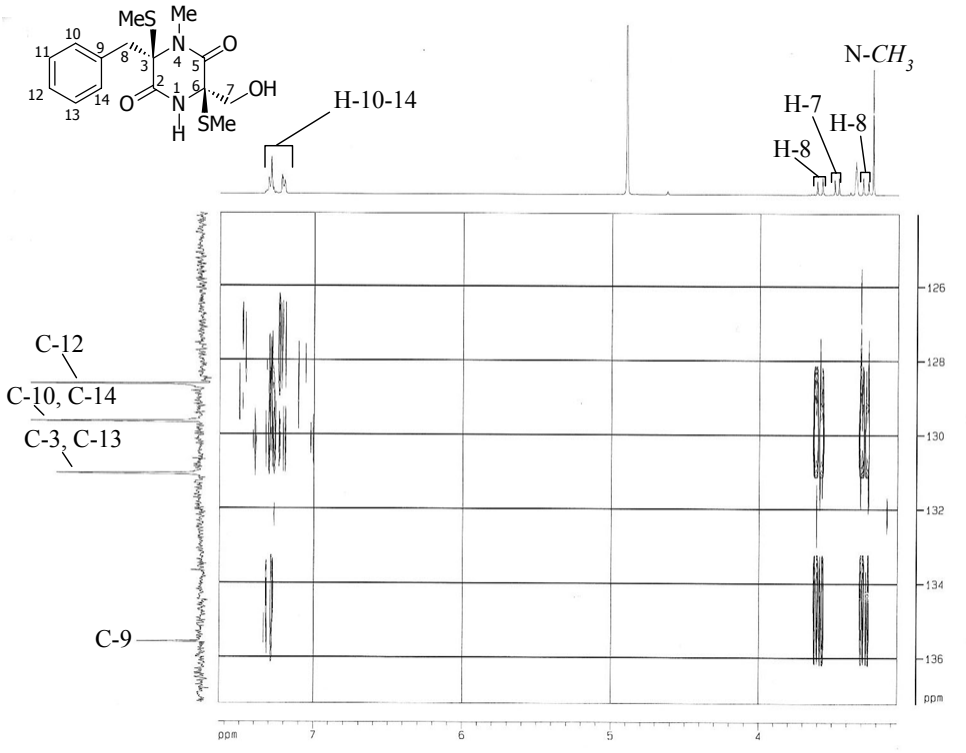

Figure 55. Expansion B of HMBC (MeOH- d_4, d6=110 msec) spectrum of compound **51**

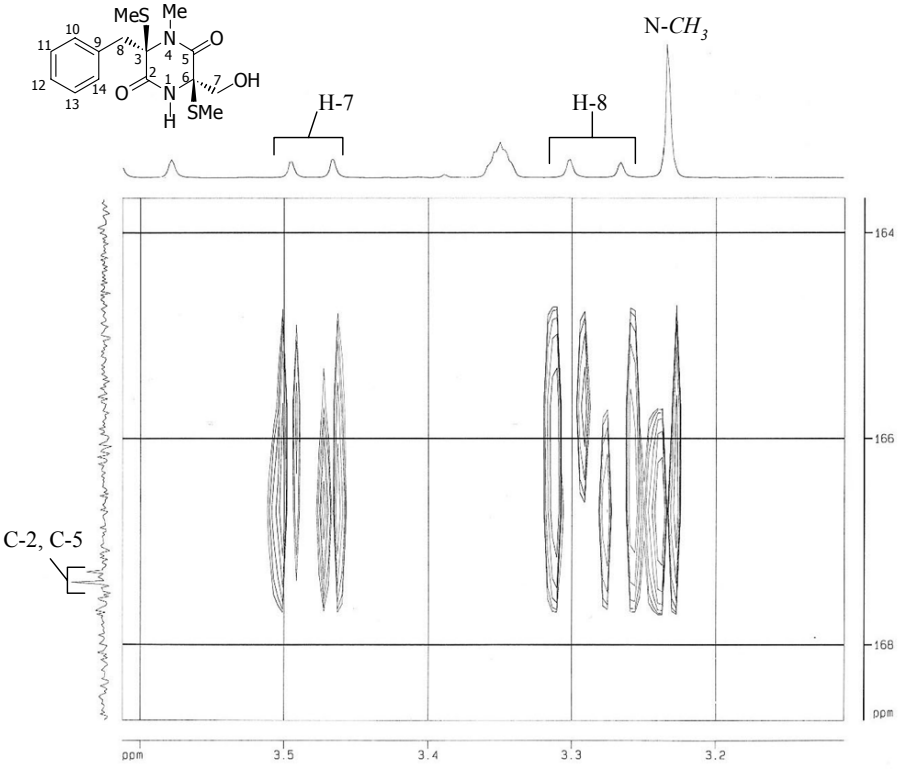

Figure 56. Expansion C of HMBC (MeOH- d_4, d6=110 msec) spectrum of compound **51**

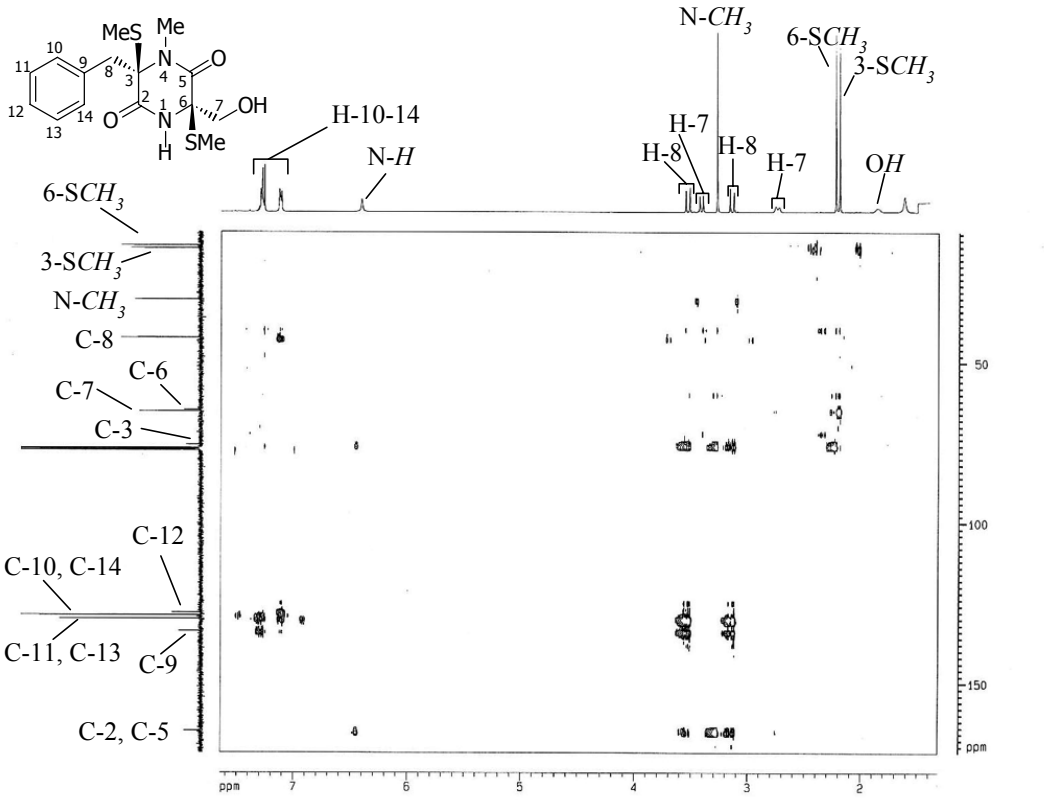

Figure 57. HMBC ($CDCl_3$) spectrum of compound **51**

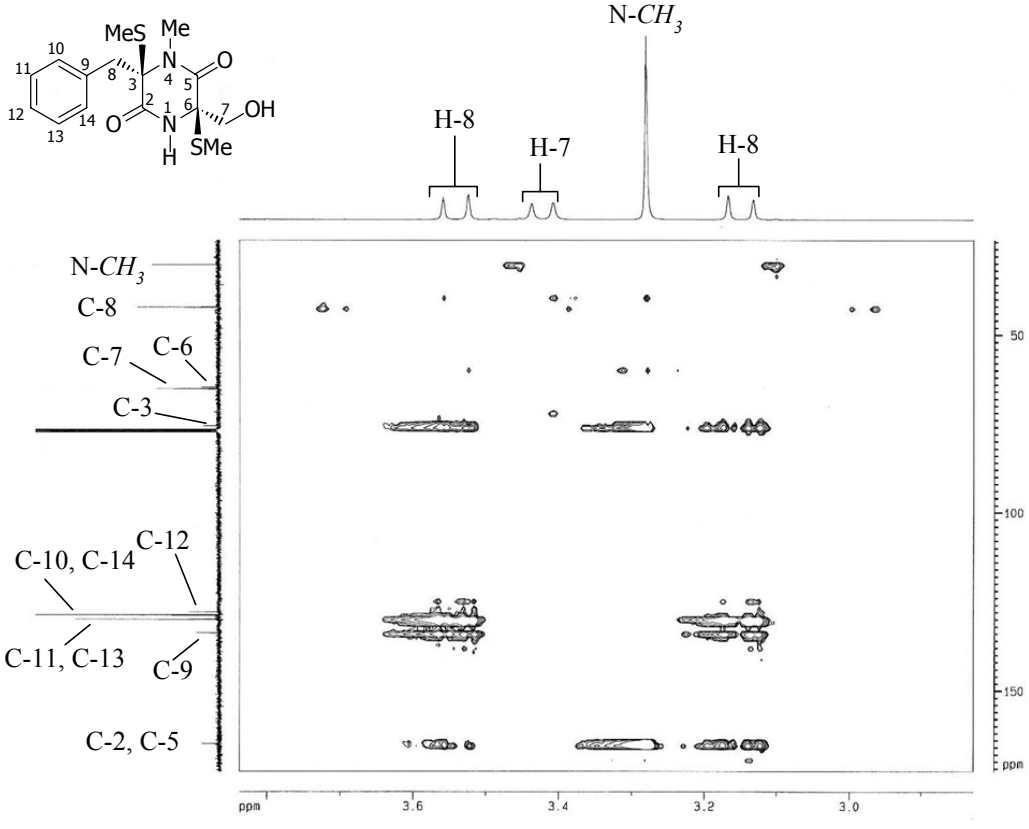

Figure 58. Expansion A of HMBC ($CDCl_3$) spectrum of compound **51**

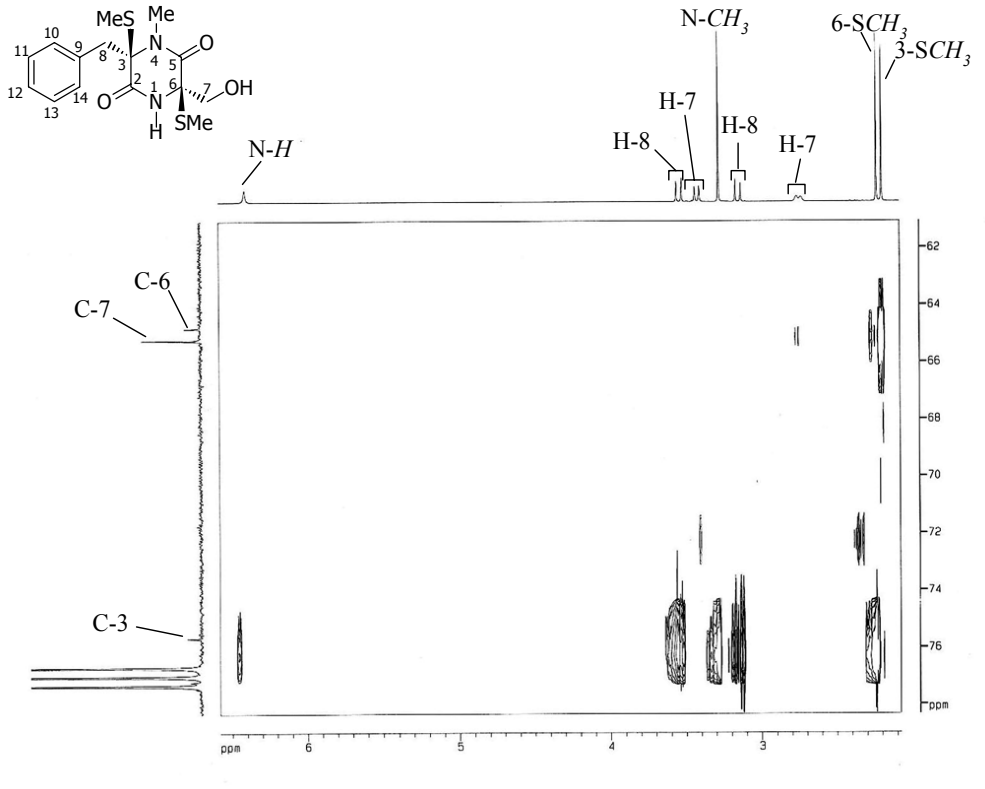

Figure 59. Expansion B of HMBC ($CDCl_3$) spectrum of compound **51**

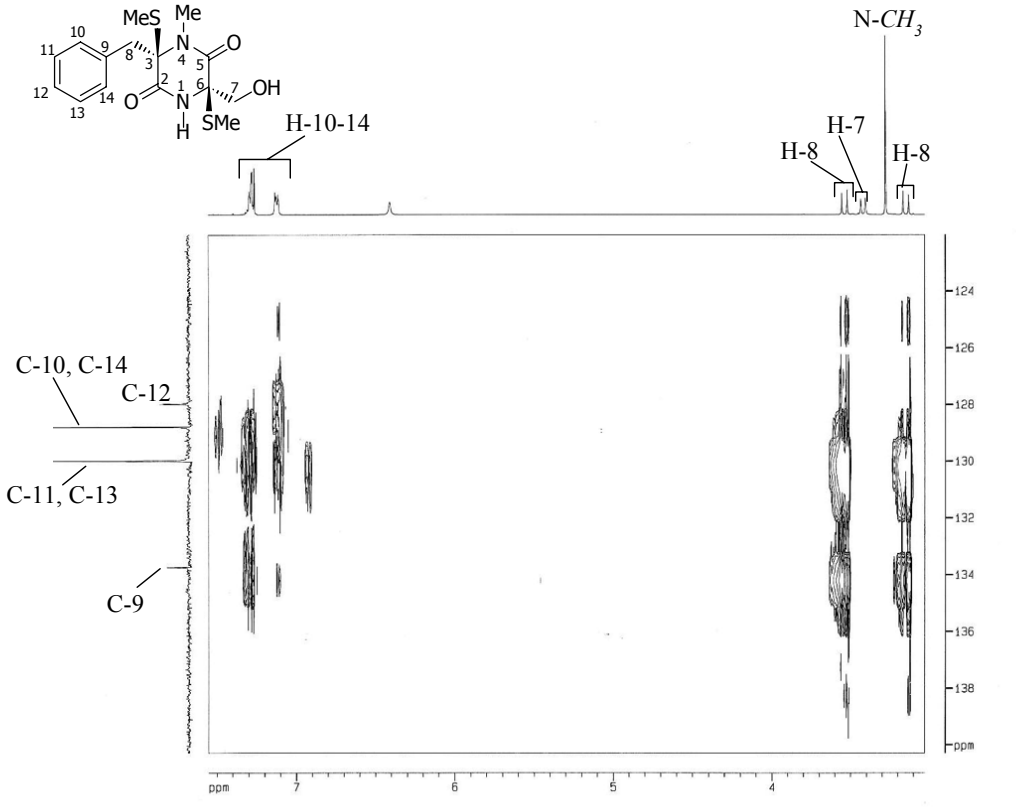

Figure 60. Expansion C of HMBC ($CDCl_3$) spectrum of compound **51**

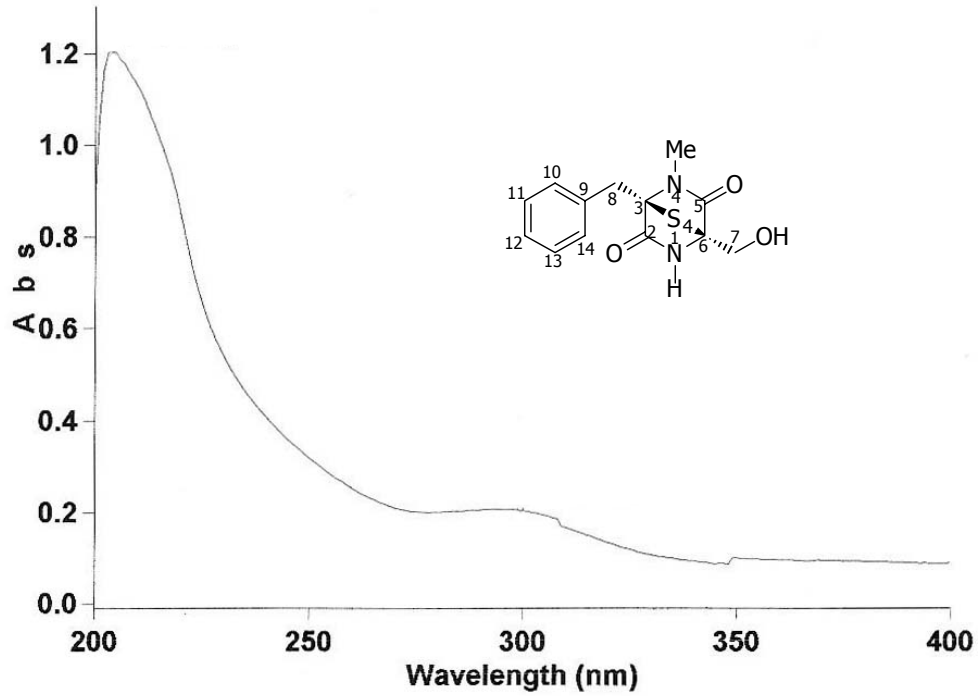

Figure 61. UV spectrum of compound **52**

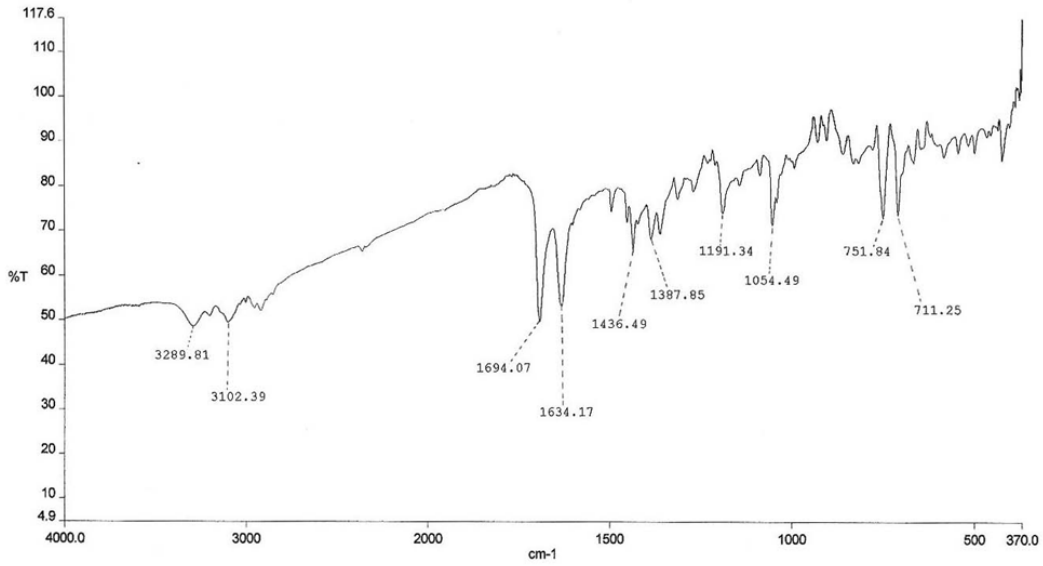

Figure 62. IR spectrum of compound **52**

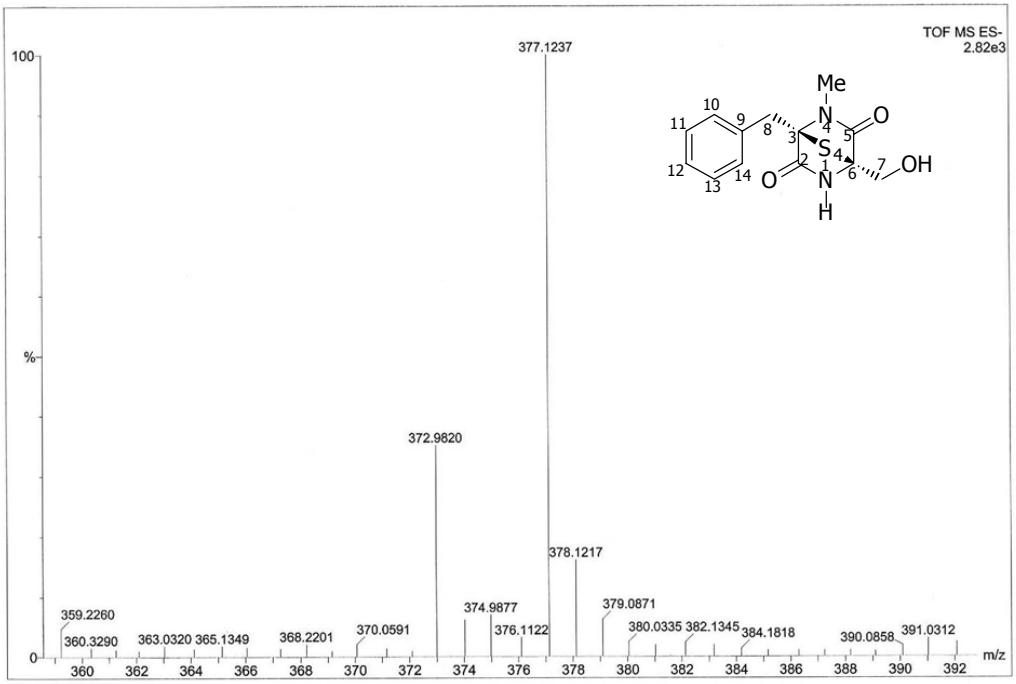

Figure 63. HRMS spectrum of compound **52**

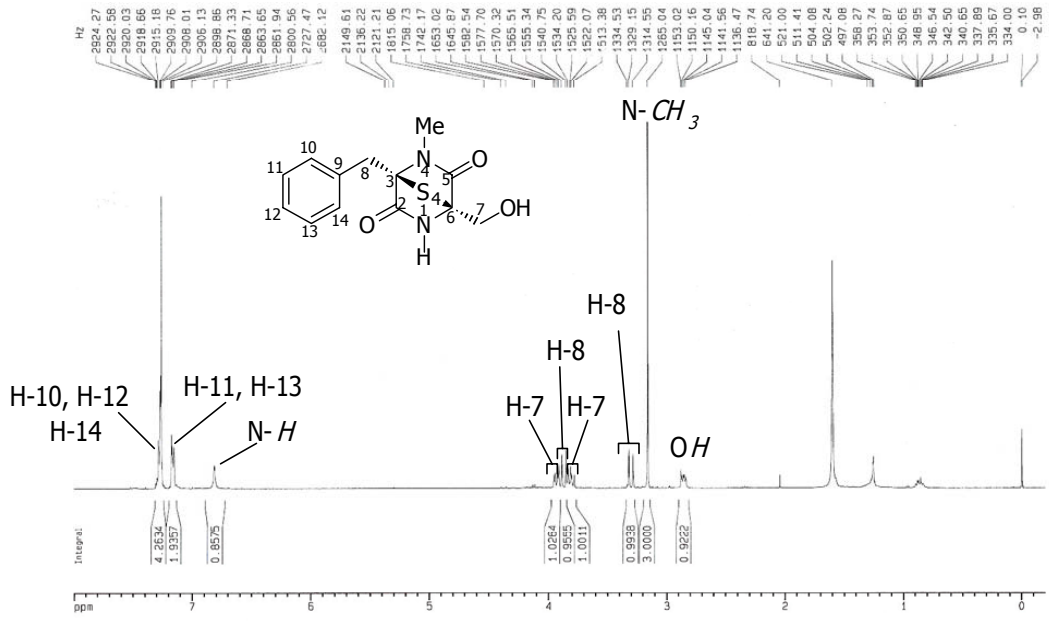

Figure 64. ^{1}H NMR ($CDCl_3$) spectrum of compound **52**

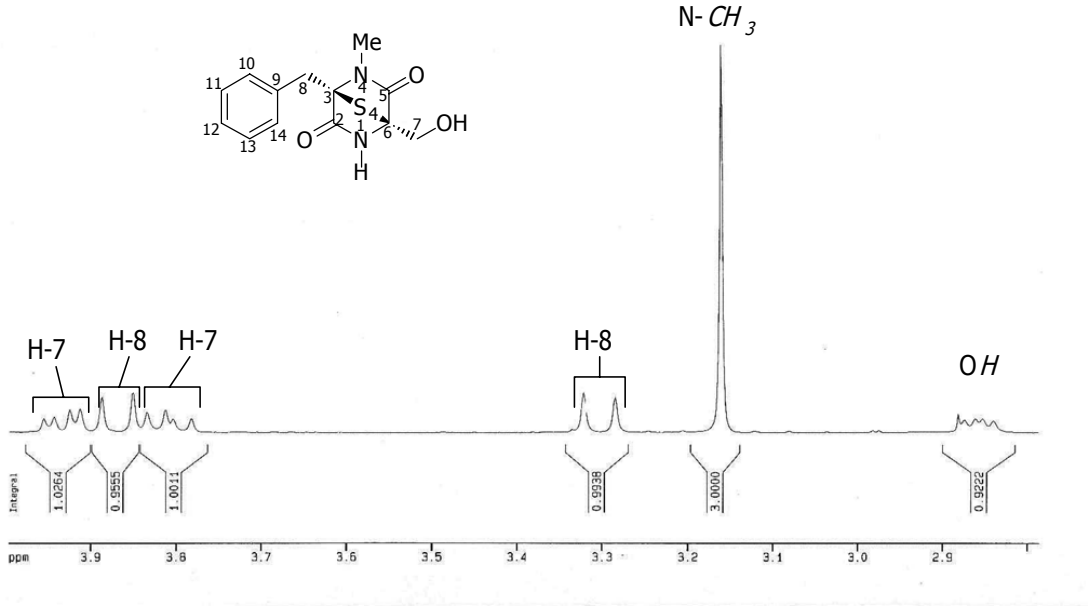

Figure 65. Expansion of ^{1}H NMR ($CDCl_3$) spectrum of compound **52**

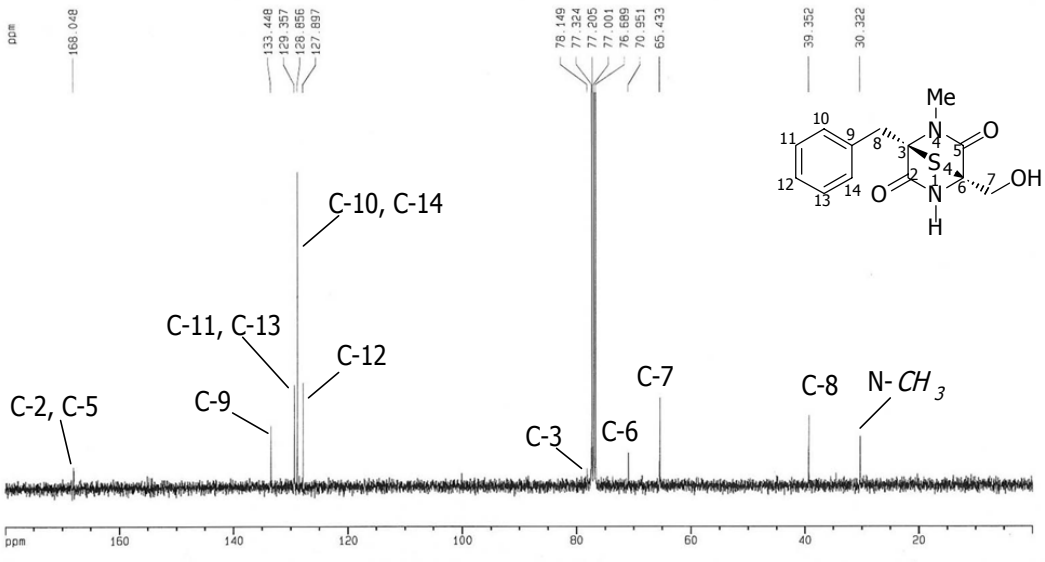

Figure 66. ^{13}C NMR spectrum of compound **52**

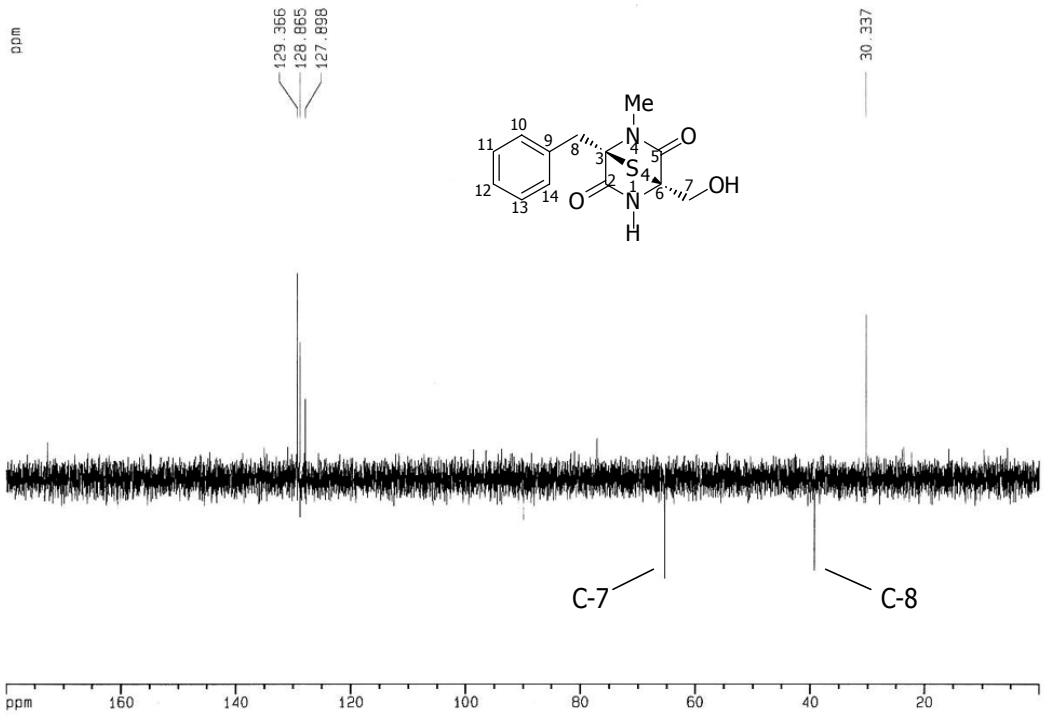

Figure 67. DEPT 135 spectrum of compound **52**

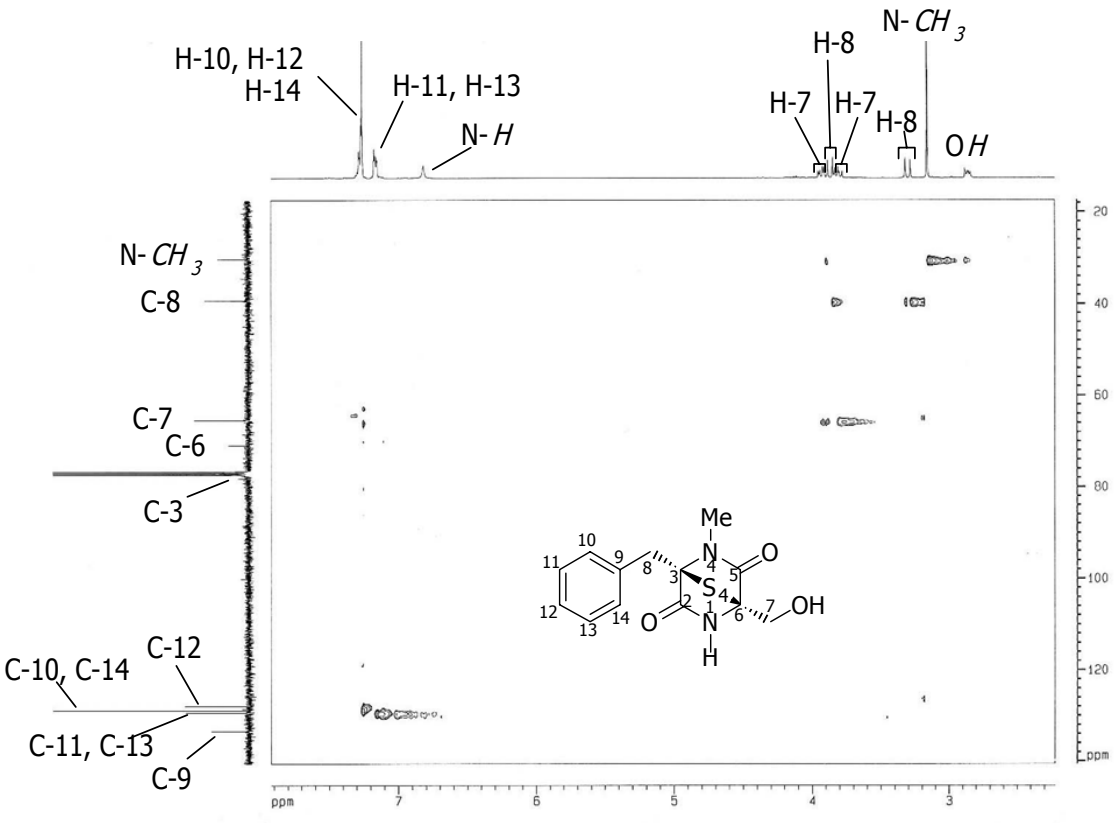

Figure 68. HMQC spectrum of compound **52**

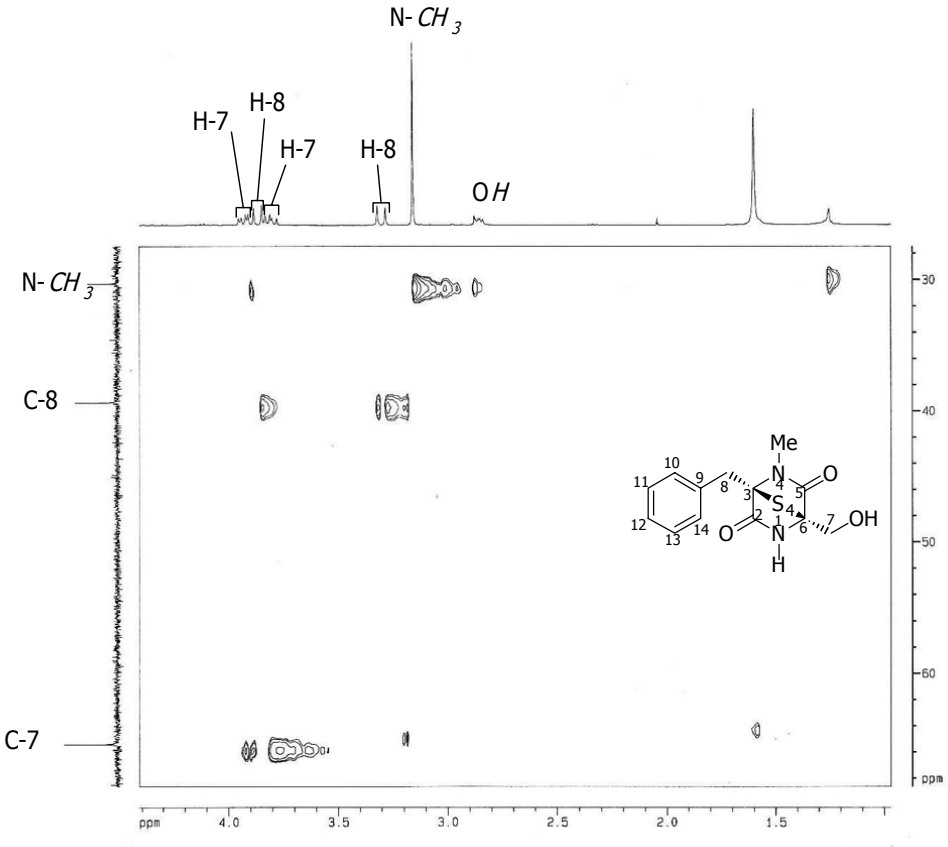

Figure 69. Expansion A of HMQC spectrum of compound **52**

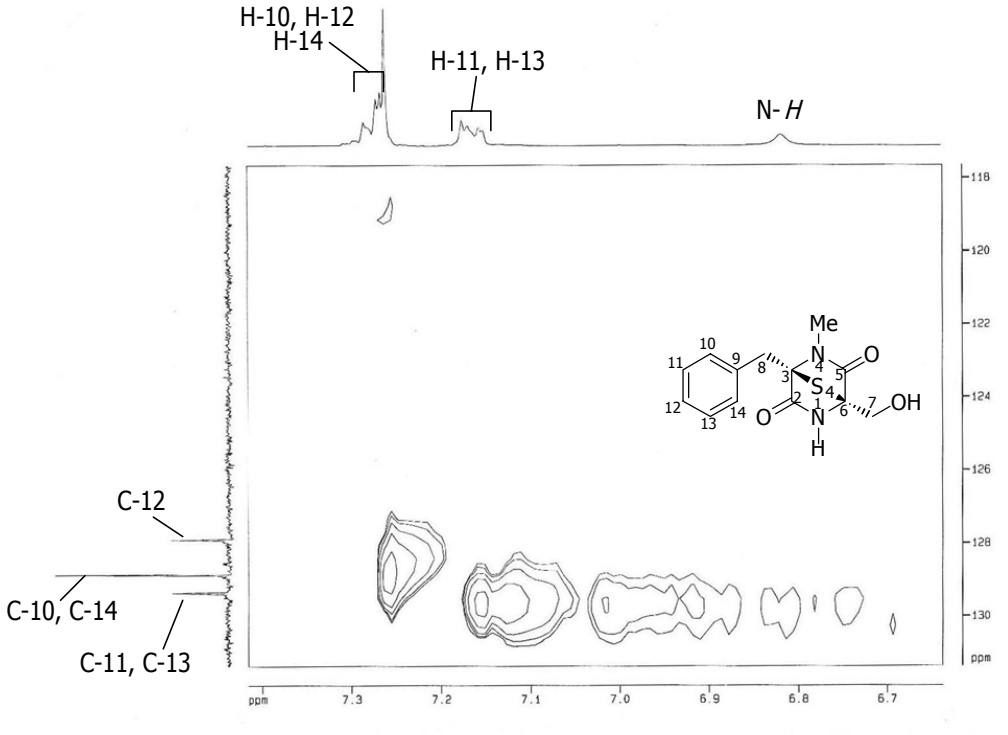

Figure 70. Expansion B of HMQC spectrum of compound **52**

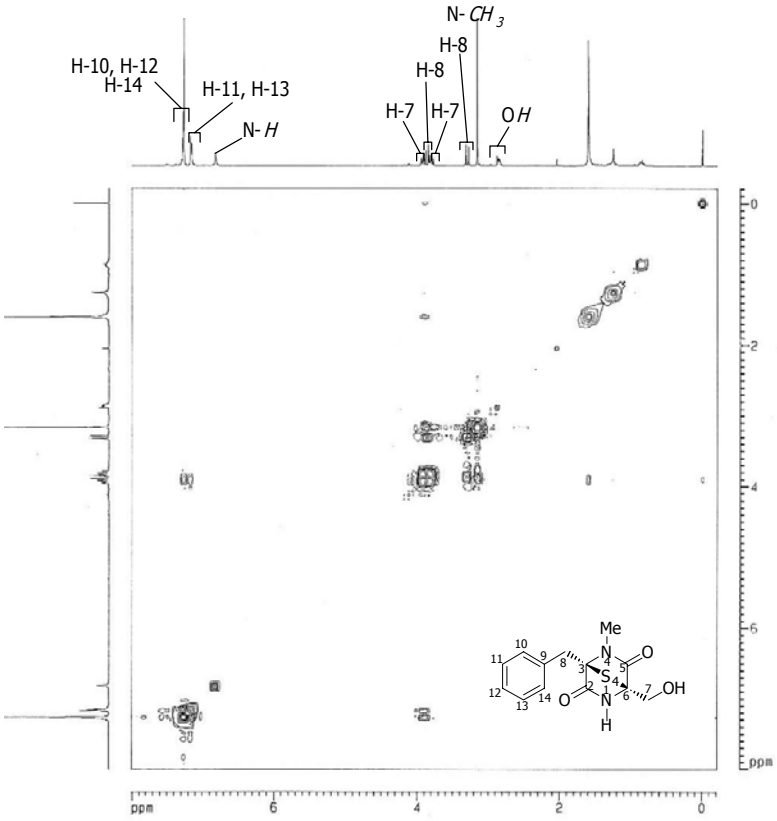

Figure 71. COSY spectrum of compound **52**

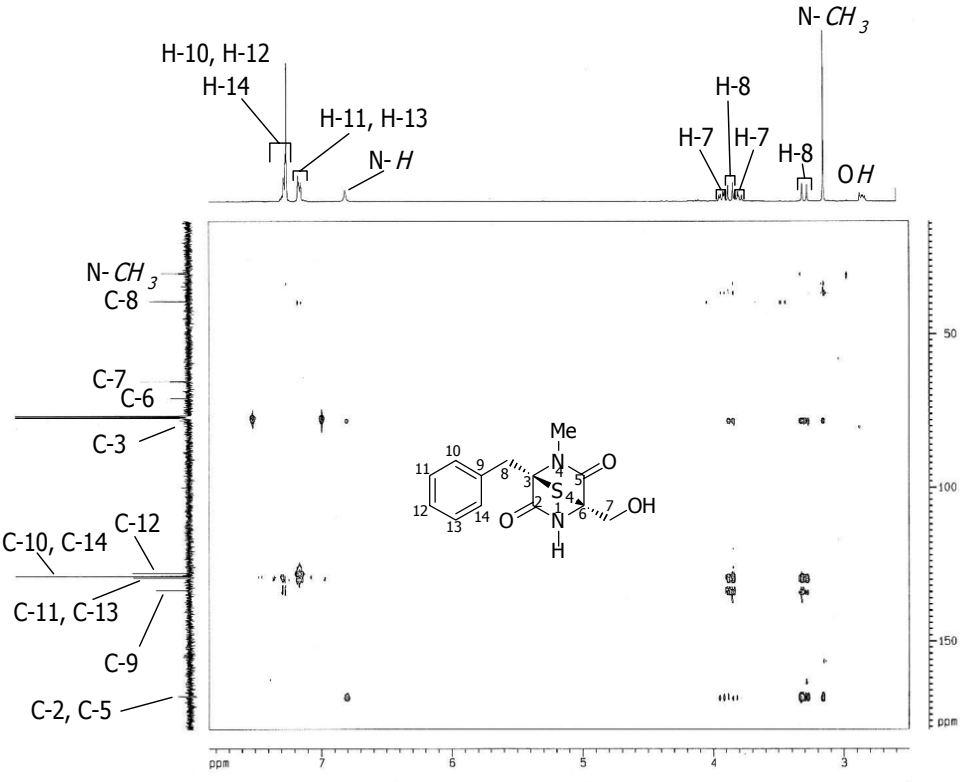

Figure 72. HMBC spectrum (d6=50 msec) of compound **52**

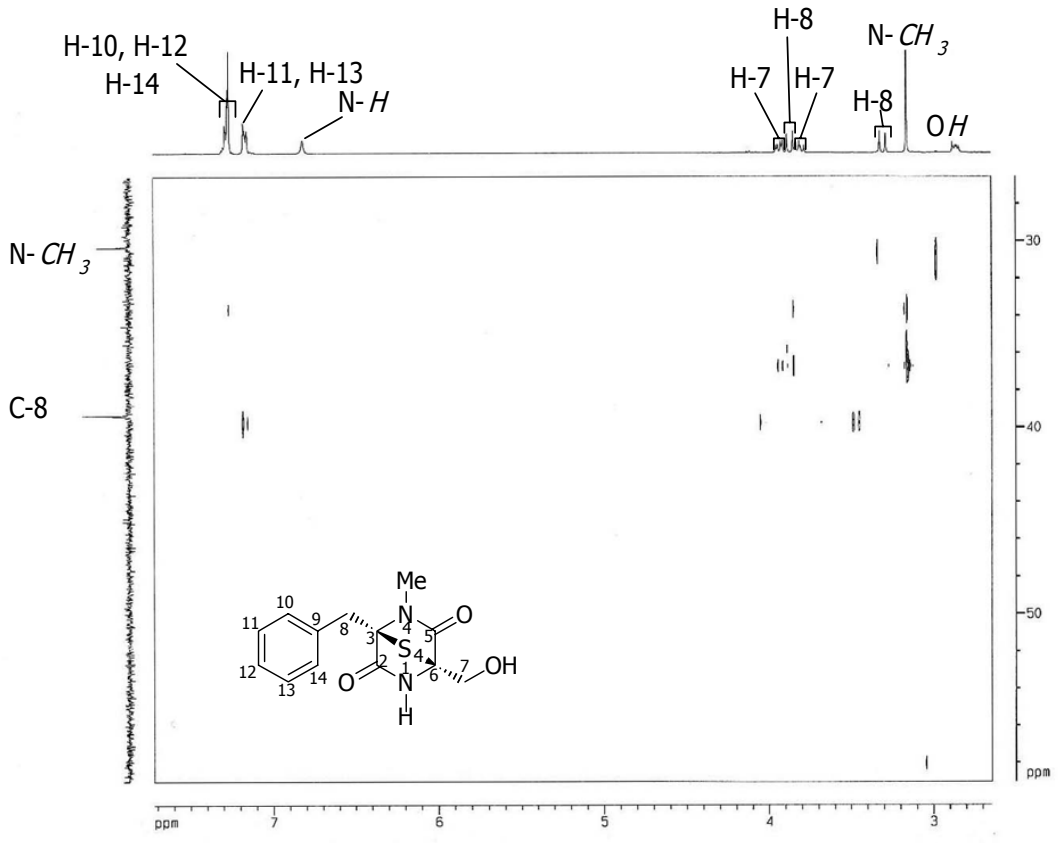

Figure 73. Expansion A of HMBC spectrum (d6=50 msec) of compound **52**

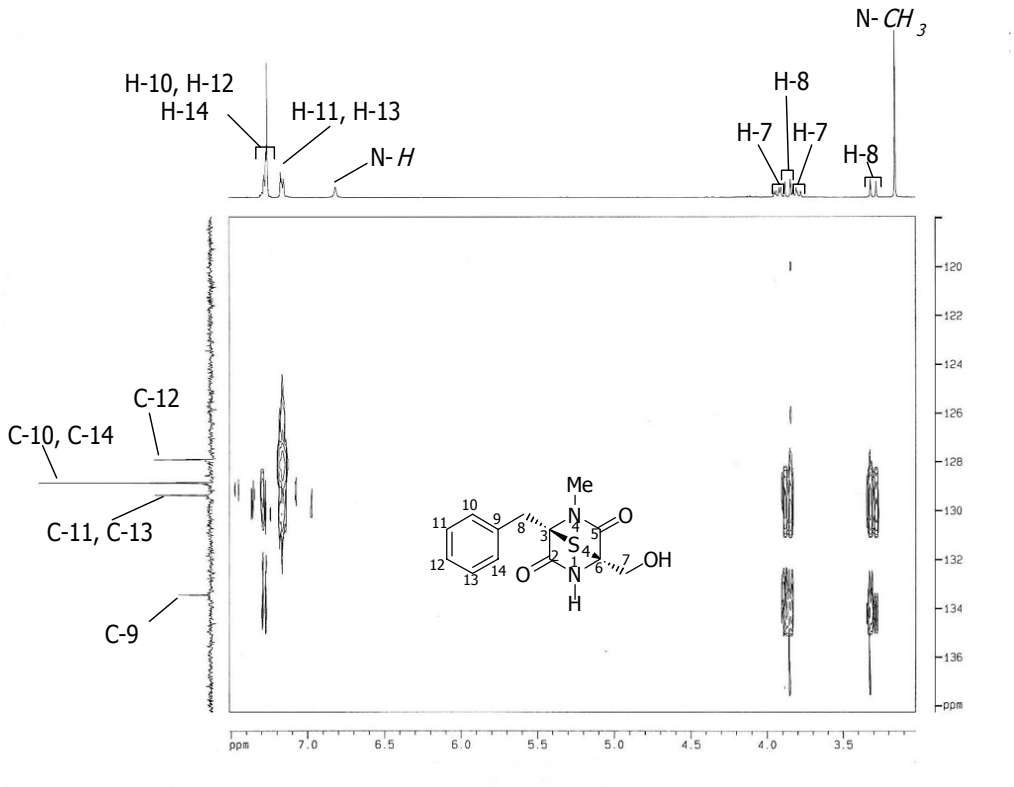

Figure 74. Expansion B of HMBC spectrum (d6=50 msec) of compound **52**

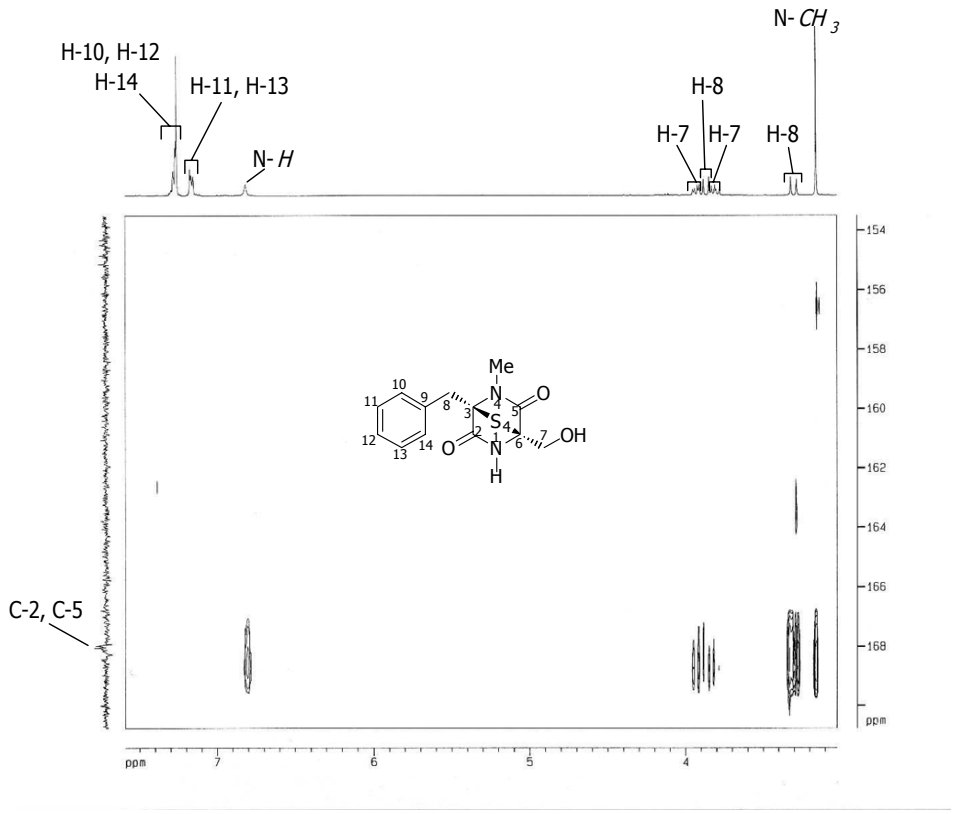

Figure 75. Expansion C of HMBC spectrum (d6=50 msec) of compound **52**

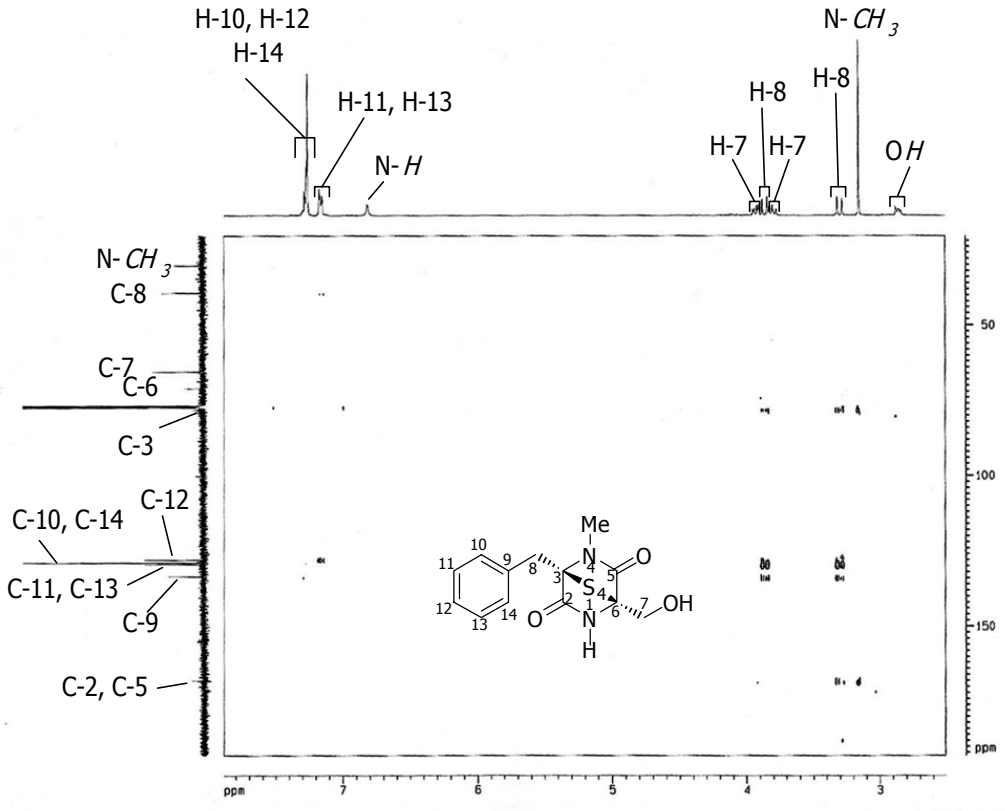

Figure 76. HMBC spectrum (d6=100 msec) of compound **52**

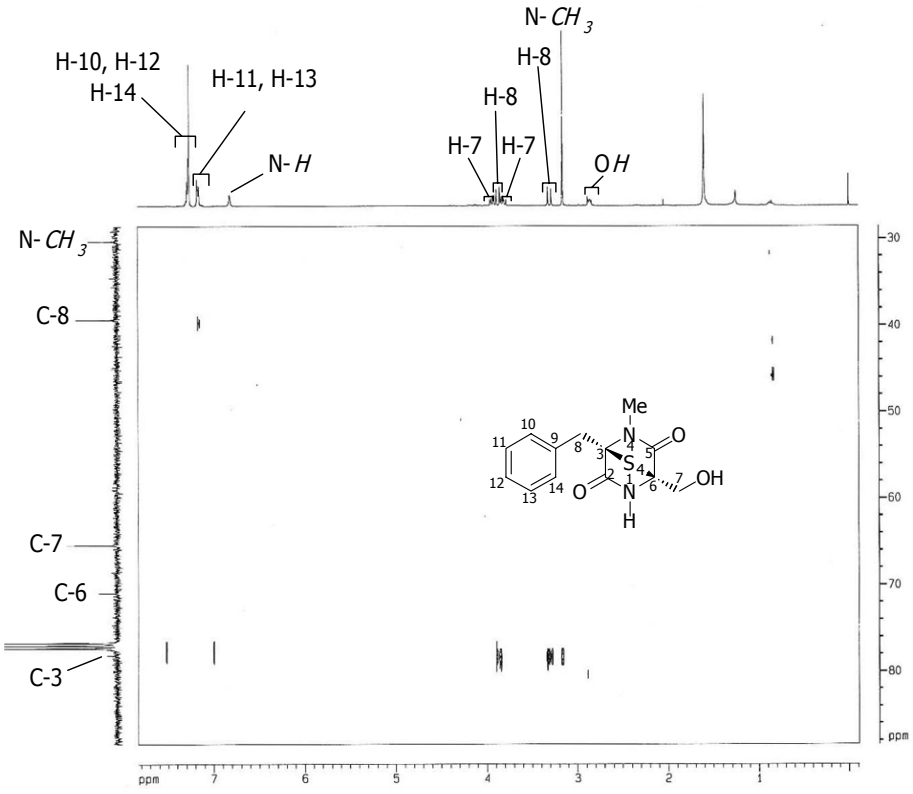

Figure 77. Expansion A of HMBC spectrum (d6=100 msec) of compound **52**

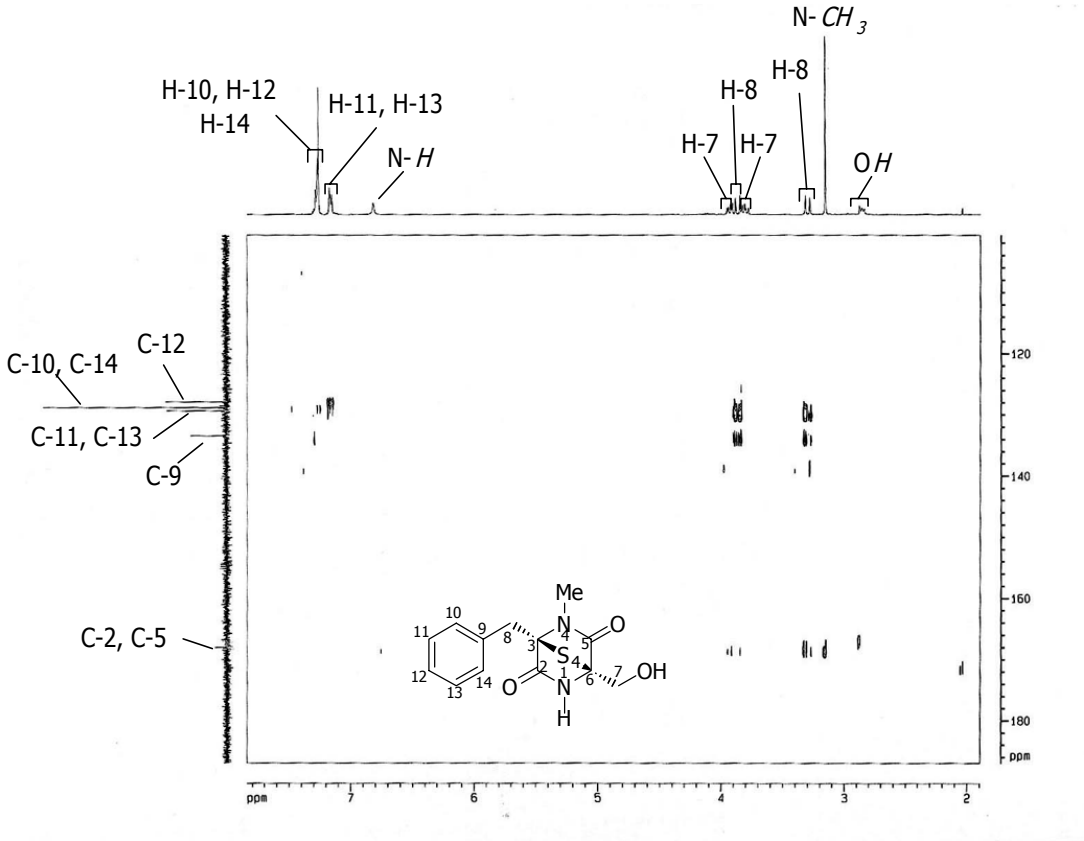

Figure 78. Expansion B of HMBC spectrum (d6=100 msec) of compound **52**

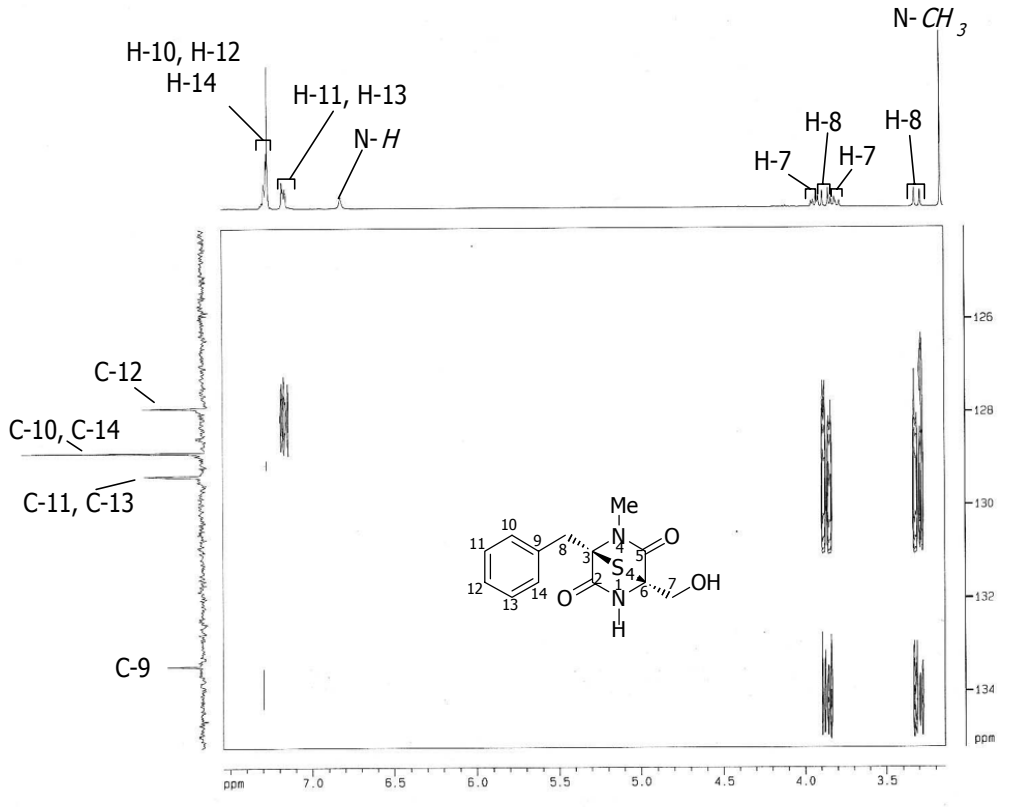

Figure 79. Expansion C of HMBC spectrum (d6=100 msec) of compound **52**

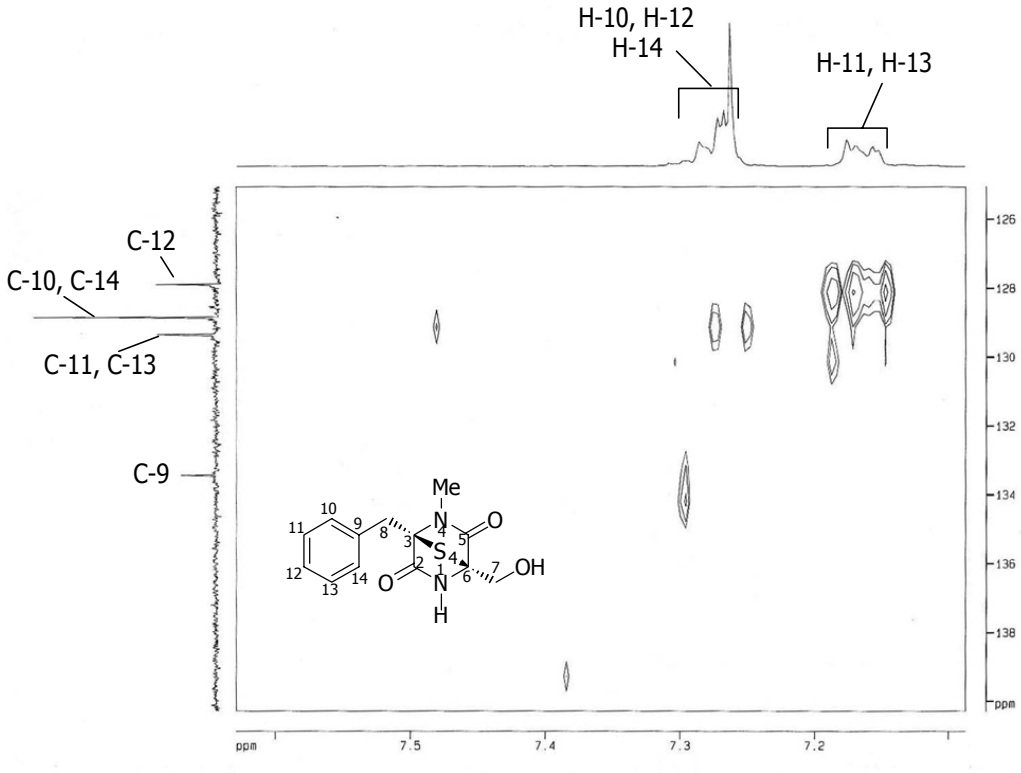

Figure 80. Expansion D of HMBC spectrum (d6=100 msec) of compound **52**

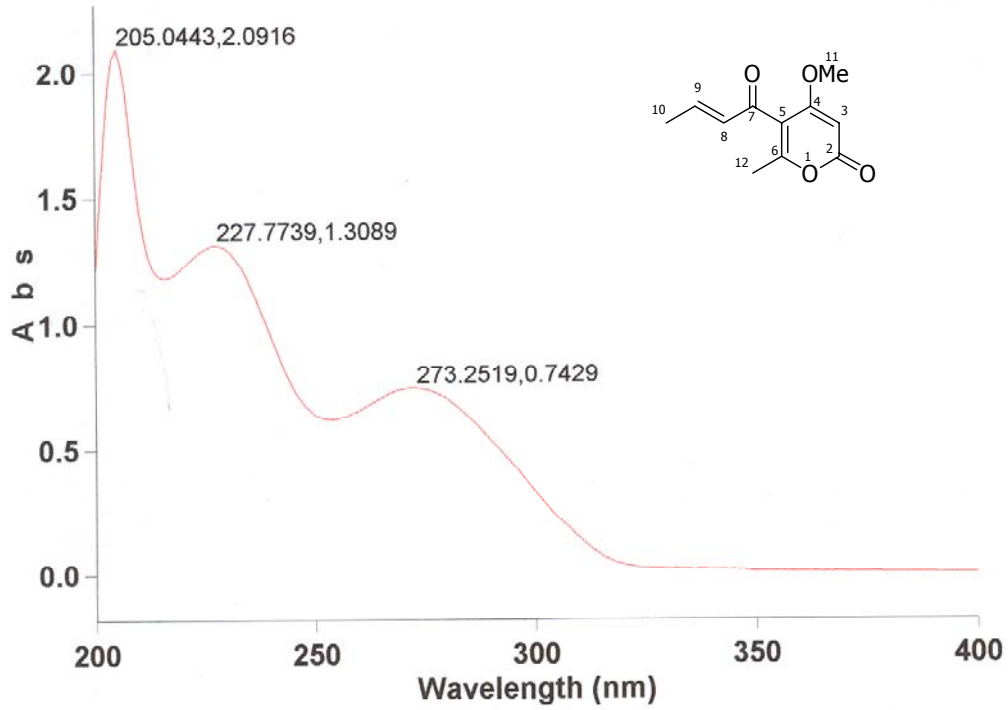

Figure 81. UV spectrum of pyrenocine A **(53)**

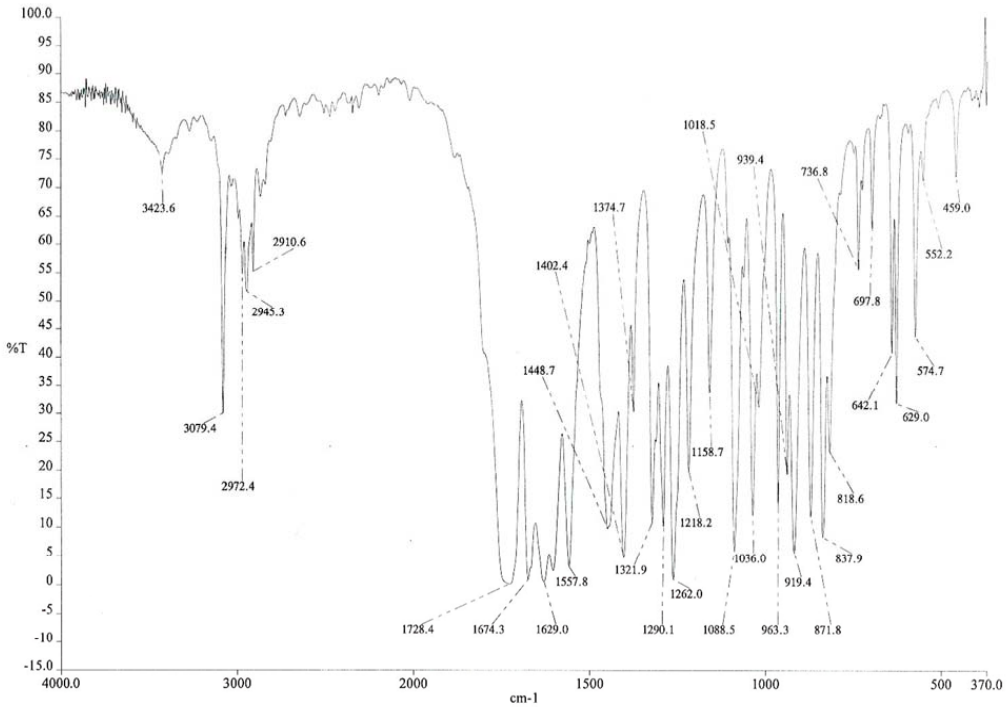

Figure 82. IR spectrum of pyrenocine A **(53)**

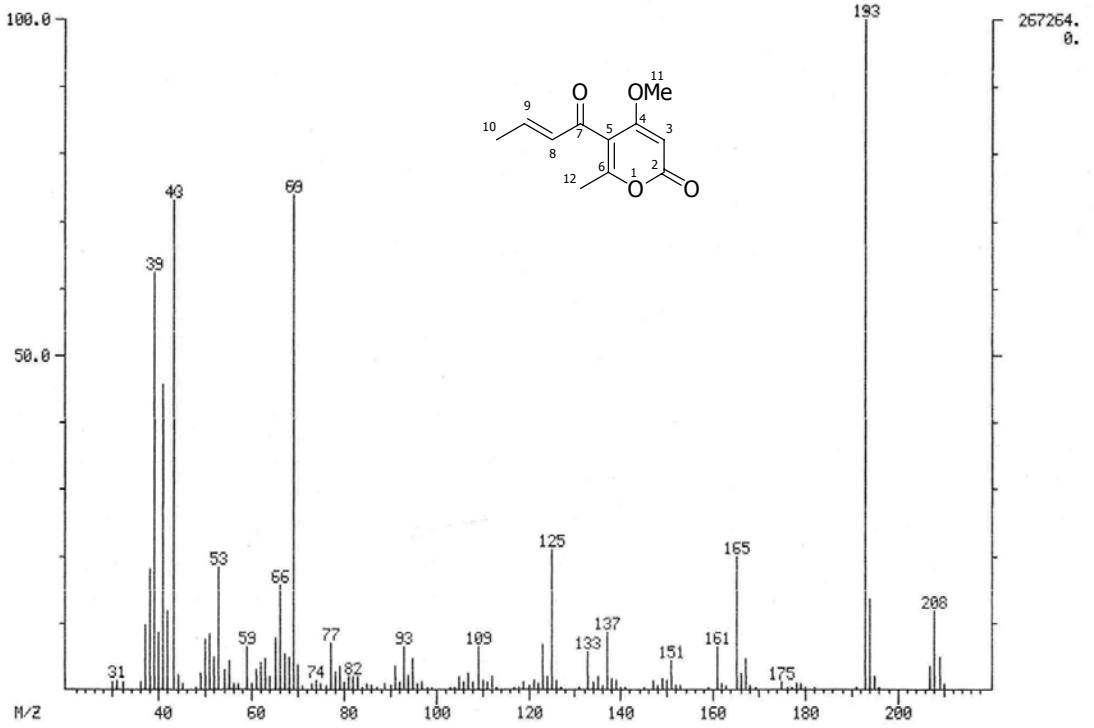

Figure 83. EIMS spectrum of pyrenocine A **(53)**

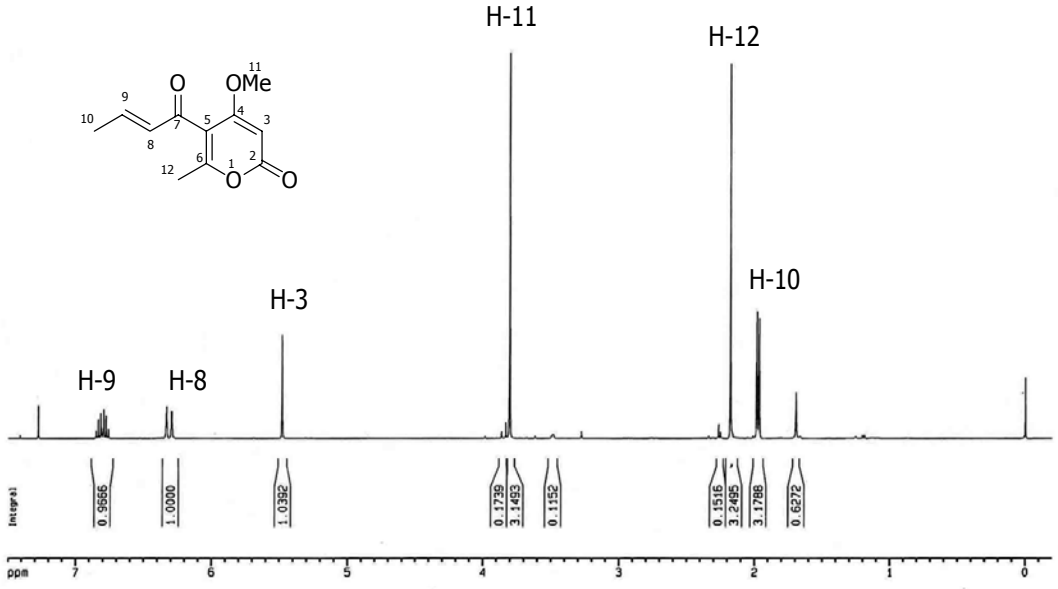

Figure 84. ^{1}H-NMR ($CDCl_3$) spectrum of pyrenocine A **(53)**

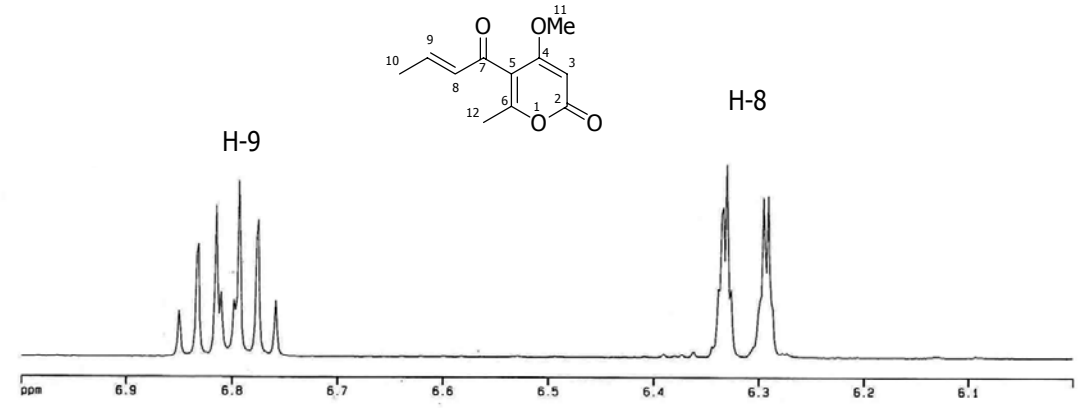

Figure 85. Expansion of ^{1}H-NMR ($CDCl_3$) spectrum of pyrenocine A **(53)**

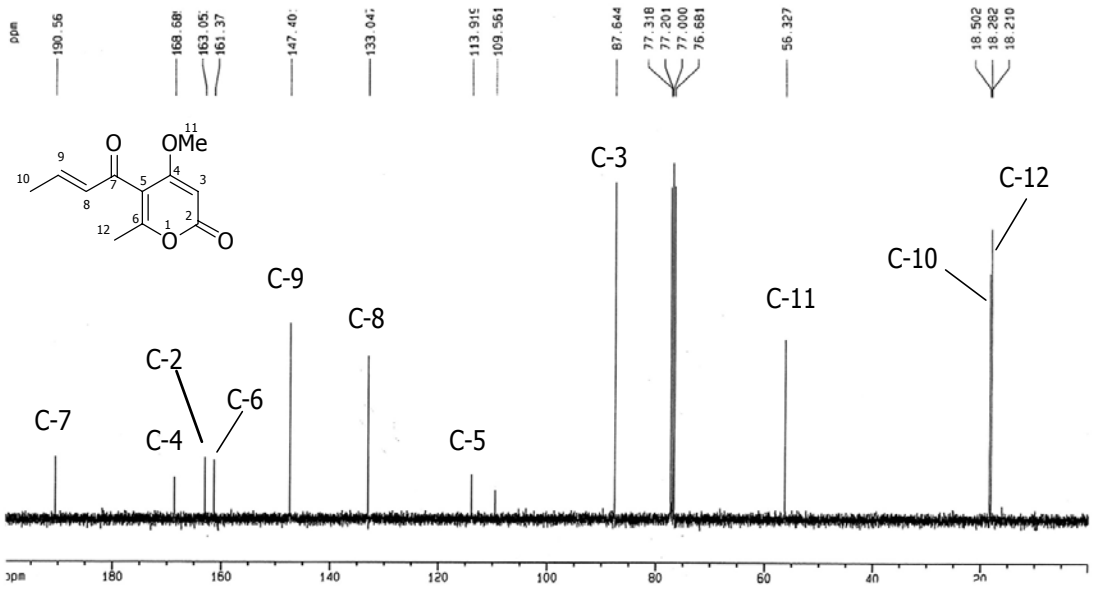

Figure 86. ^{13}C-NMR spectrum of pyrenocine A **(53)**

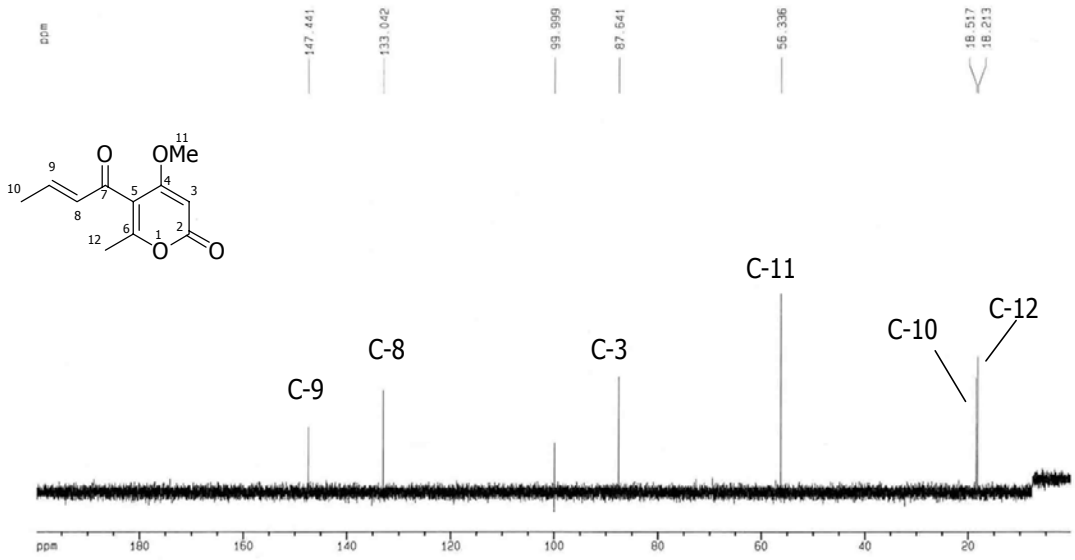

Figure 87. DEPT 45 spectrum of pyrenocine A **(53)**

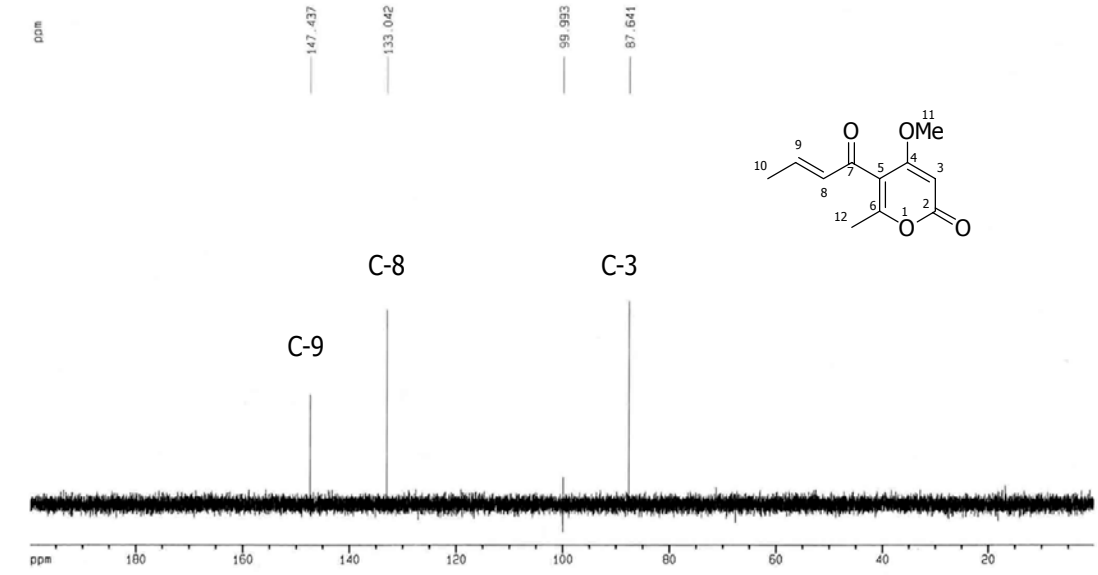

Figure 88. DEPT 90 spectrum of pyrenocine A **(53)**

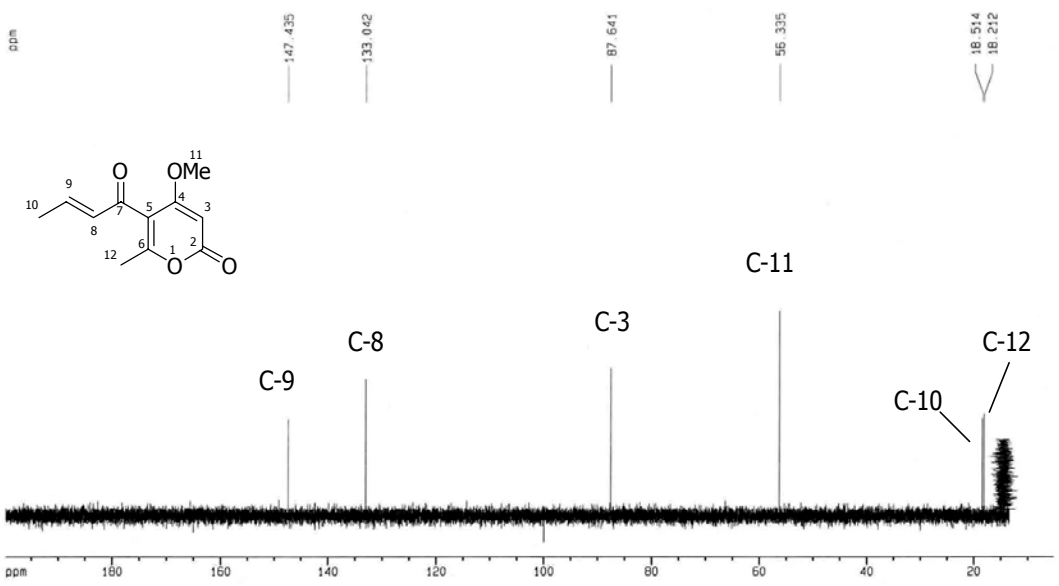

Figure 89. DEPT 135 spectrum of pyrenocine A **(53)**

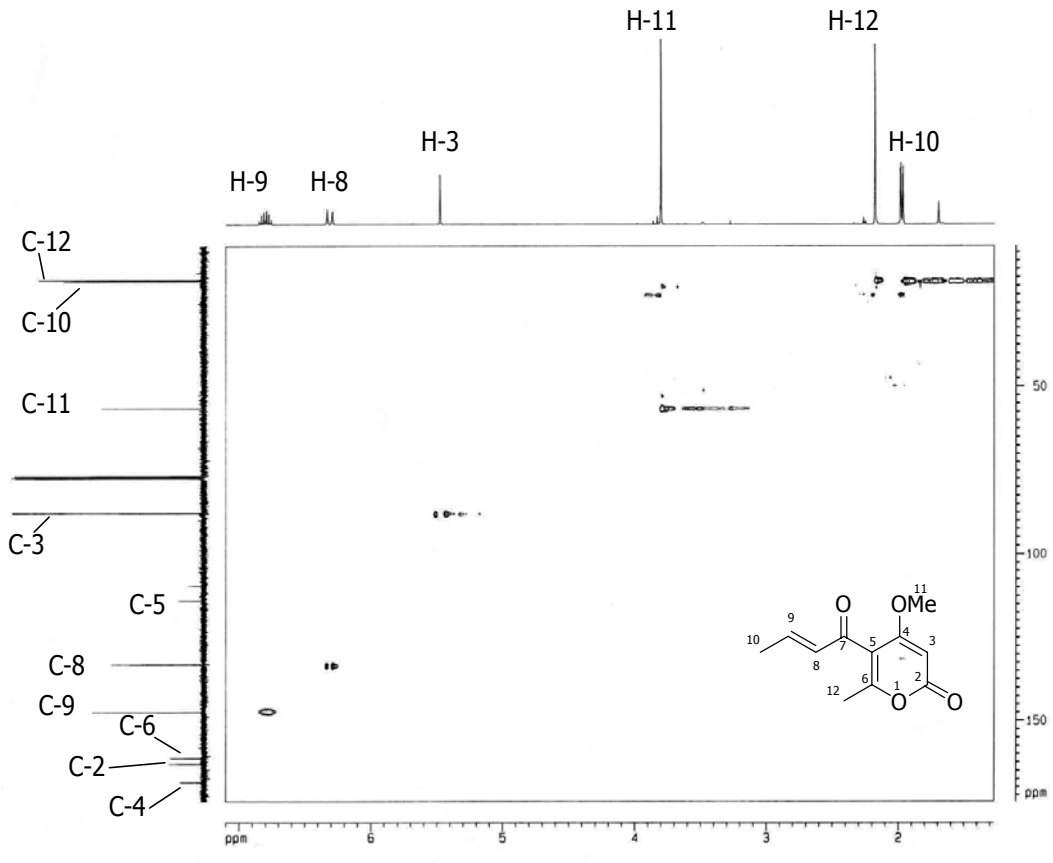

Figure 90. HMQC spectrum of pyrenocine A **(53)**

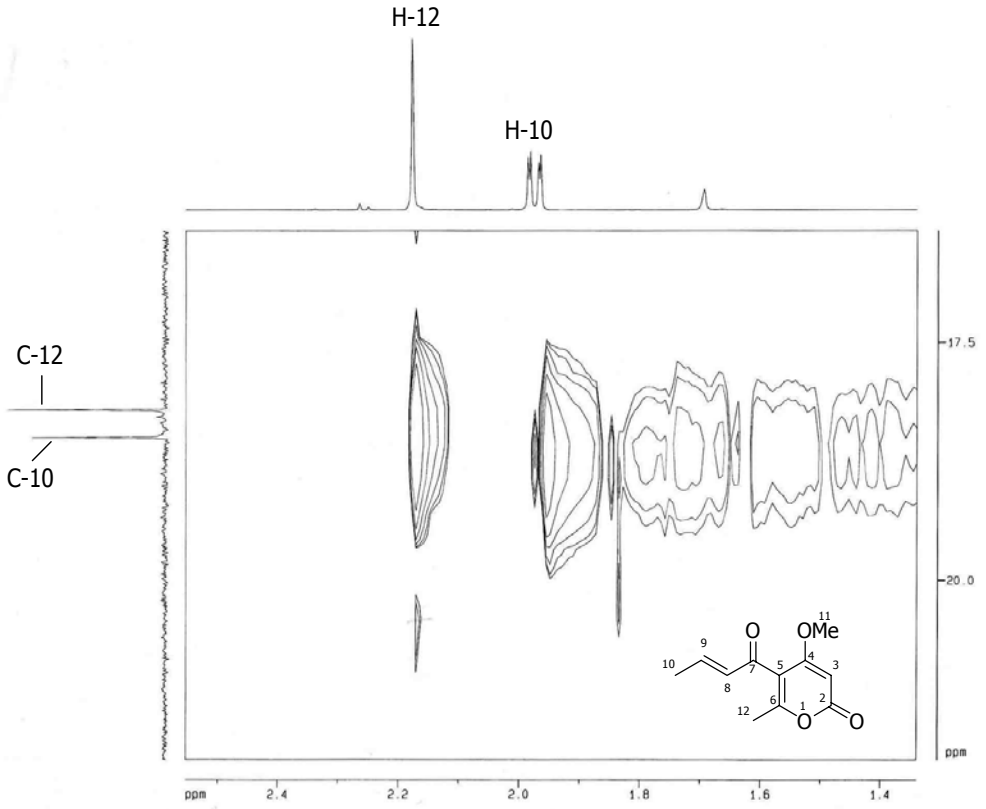

Figure 91. Expansion of HMQC spectrum of pyrenocine A **(53)**

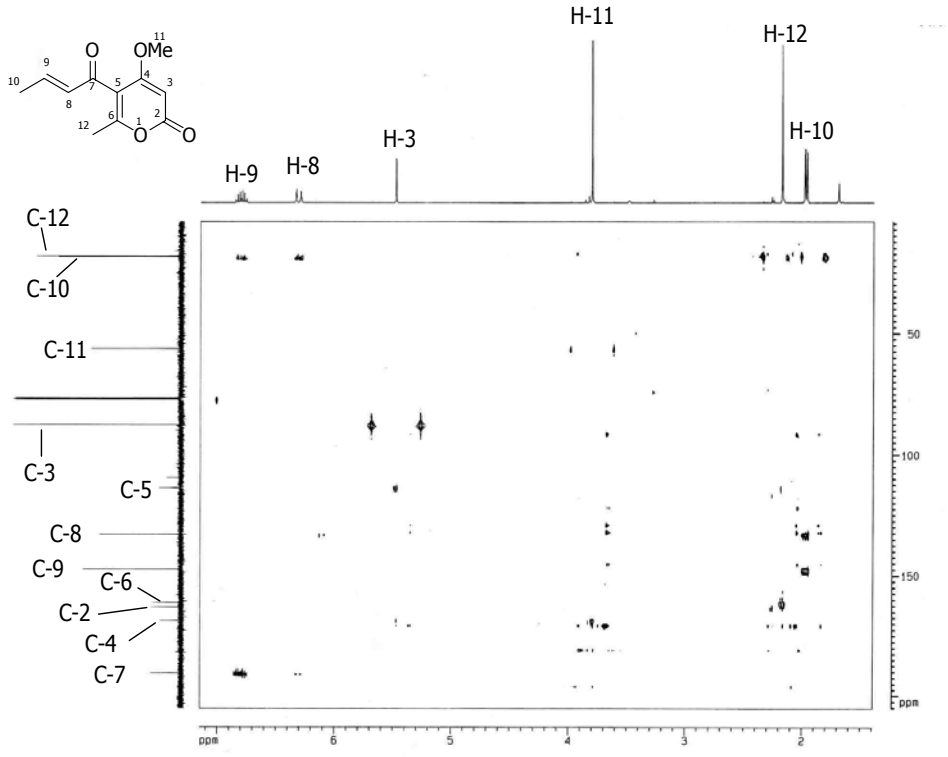

Figure 92. HMBC spectrum (d6 = 100 msec) of pyrenocine A **(53)**

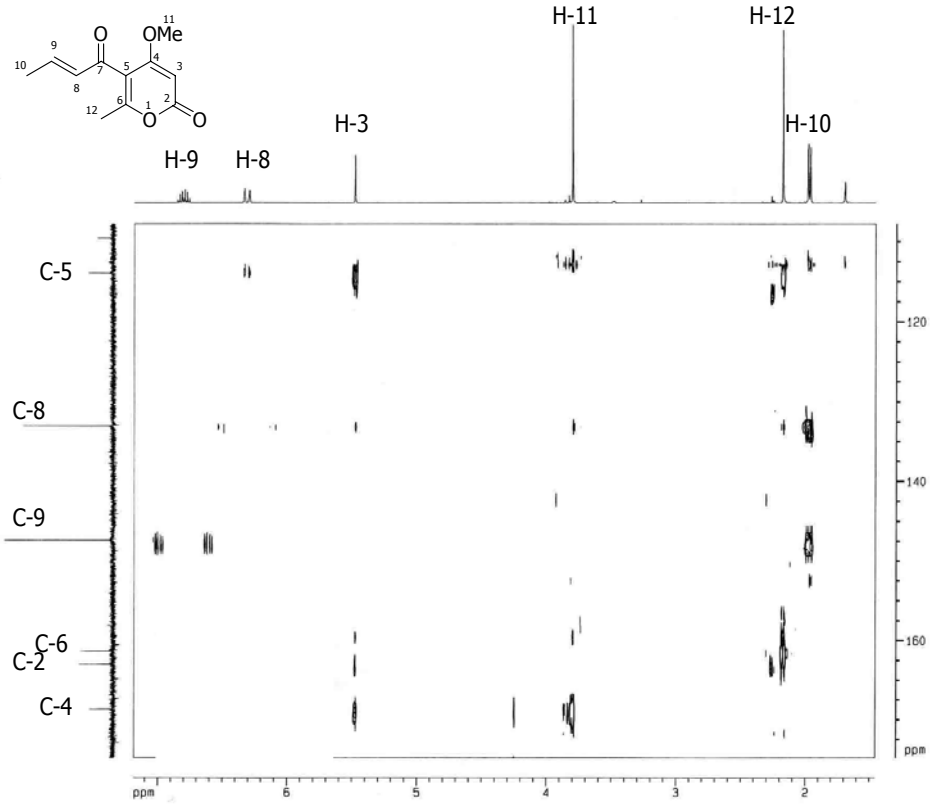

Figure 93. Expansion A of HMBC spectrum (d6 = 100 msec) of pyrenocine A **(53)**

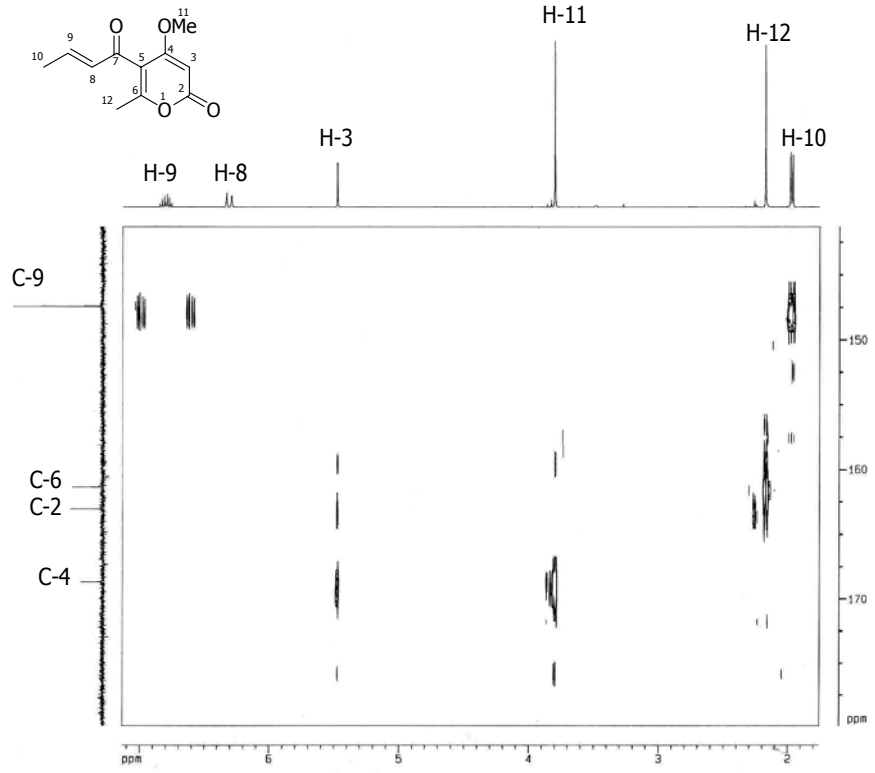

Figure 94. Expansion B of HMBC spectrum (d6 = 100 msec) of pyrenocine A **(53)**

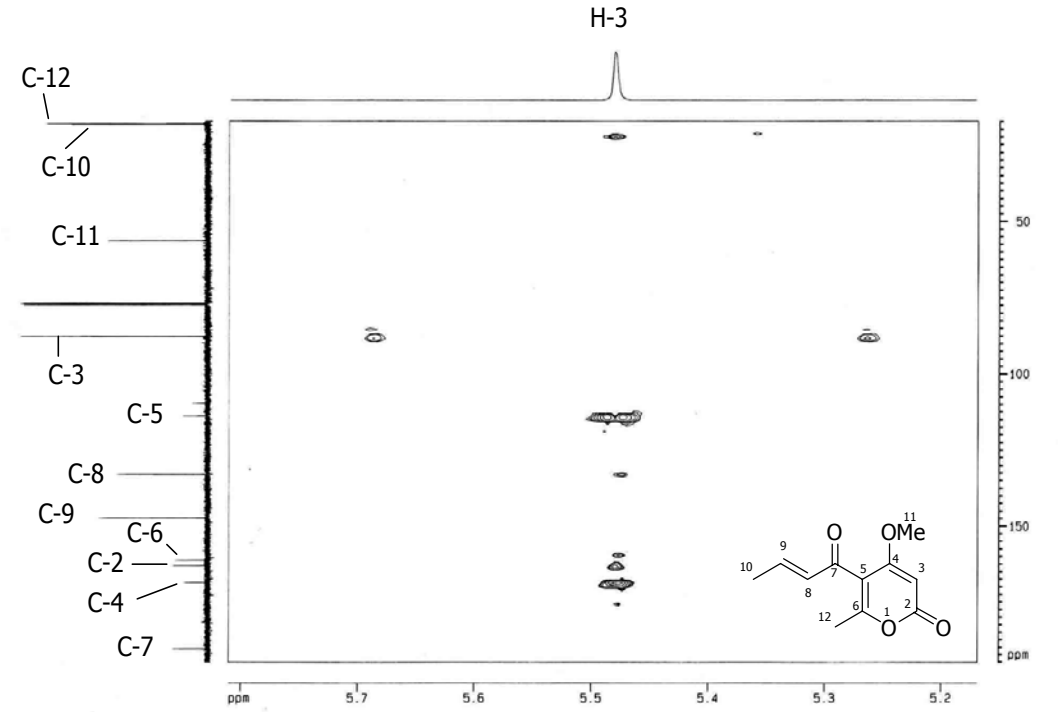

Figure 95. Expansion C of HMBC spectrum (d6 = 100 msec) of pyrenocine A **(53)**

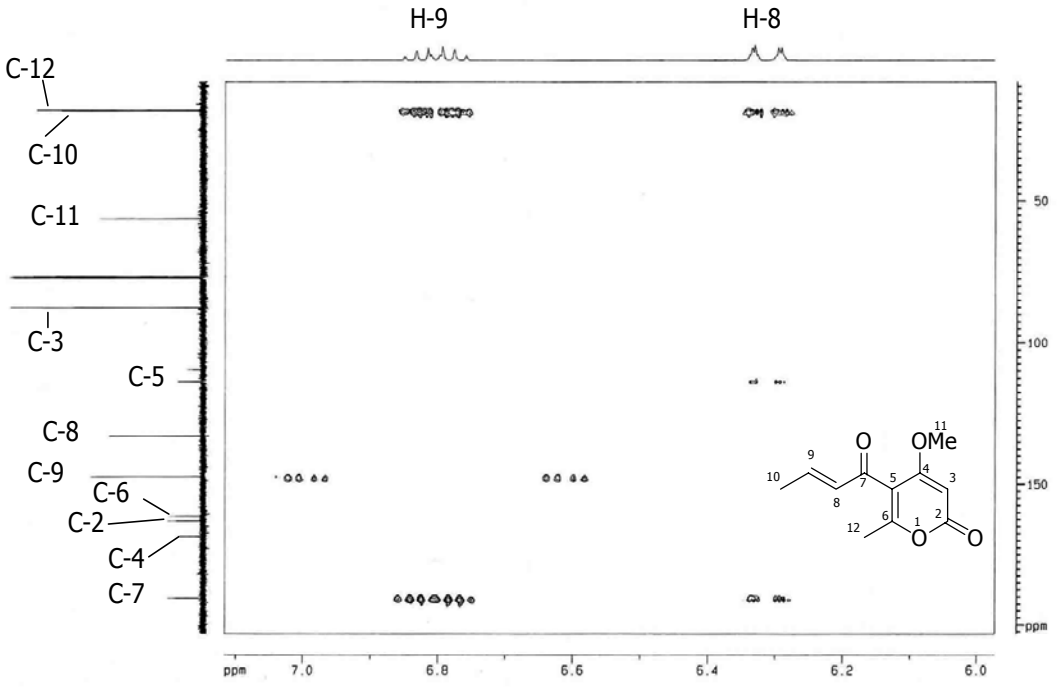

Figure 96. Expansion D of HMBC spectrum (d6 = 100 msec) of pyrenocine A **(53)**

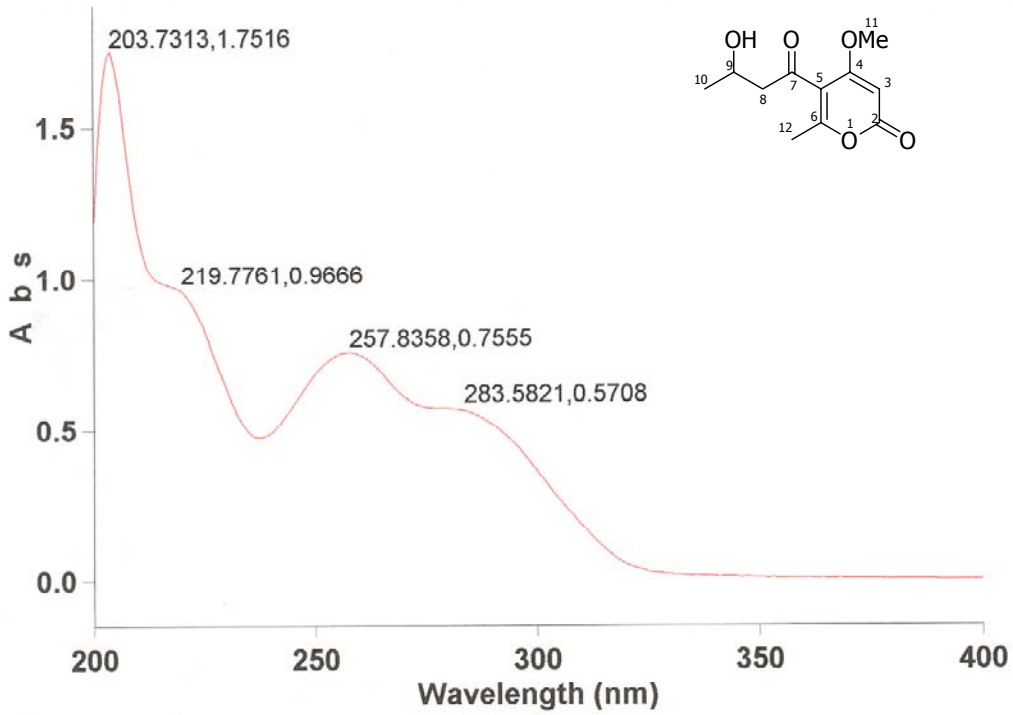

Figure 97. UV spectrum of pyrenocine B **(54)**

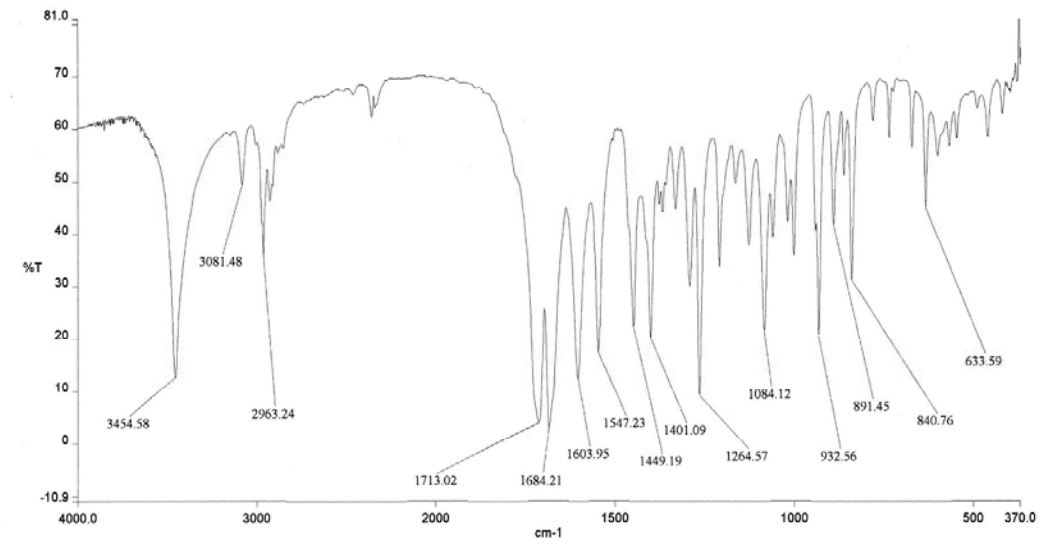

Figure 98. IR spectrum of pyrenocine B **(54)**

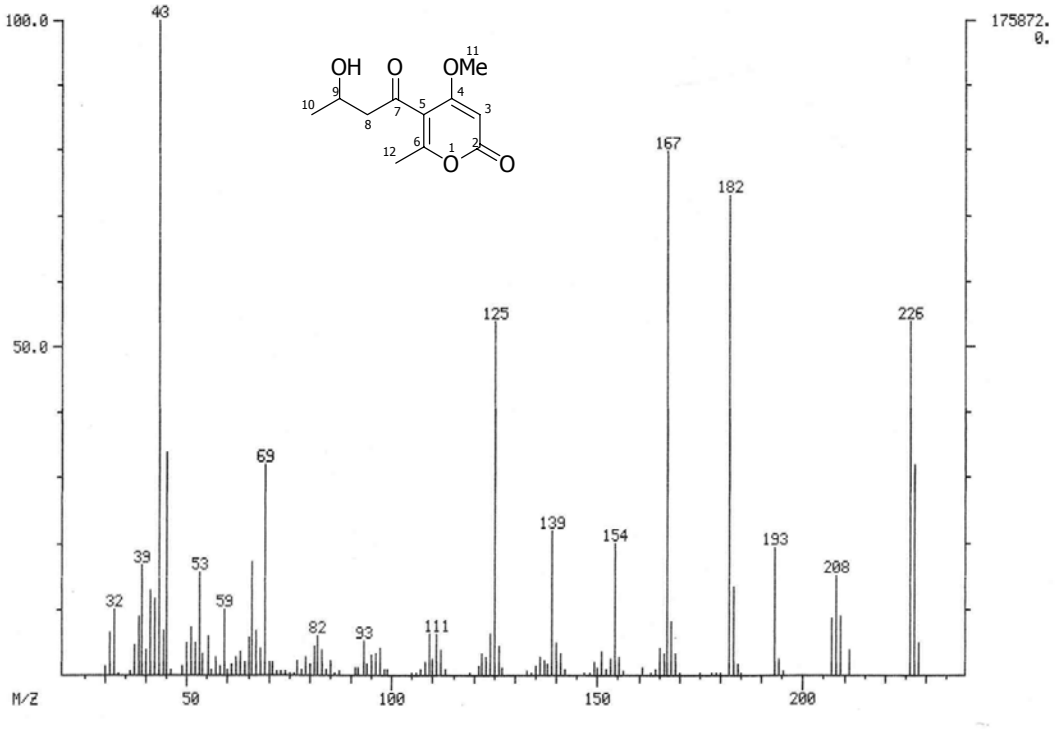

Figure 99. EIMS spectrum of pyrenocine B **(54)**

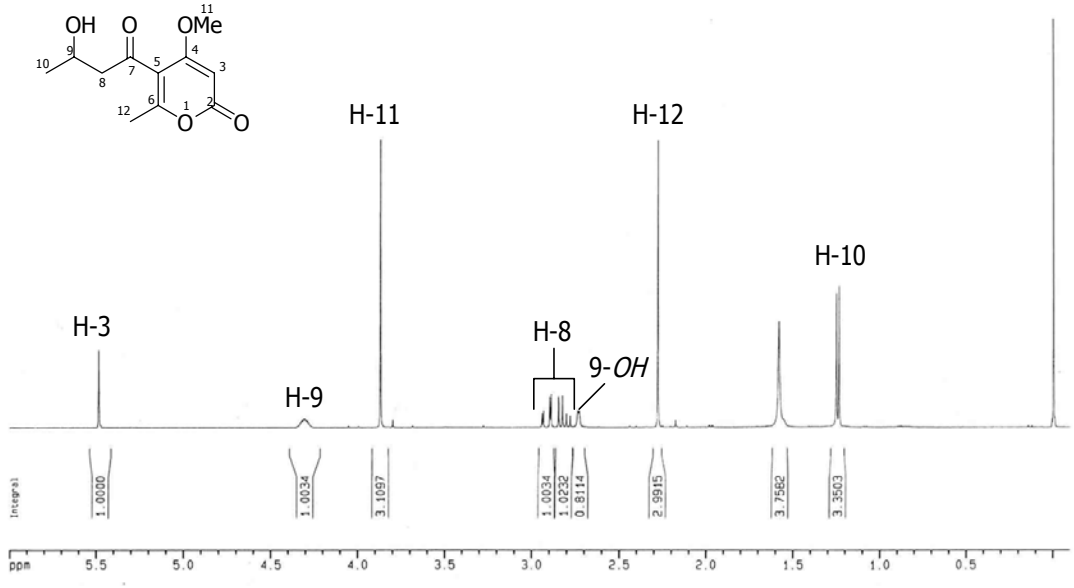

Figure 100. ^{1}H-NMR ($CDCl_3$) spectrum of pyrenocine B **(54)**

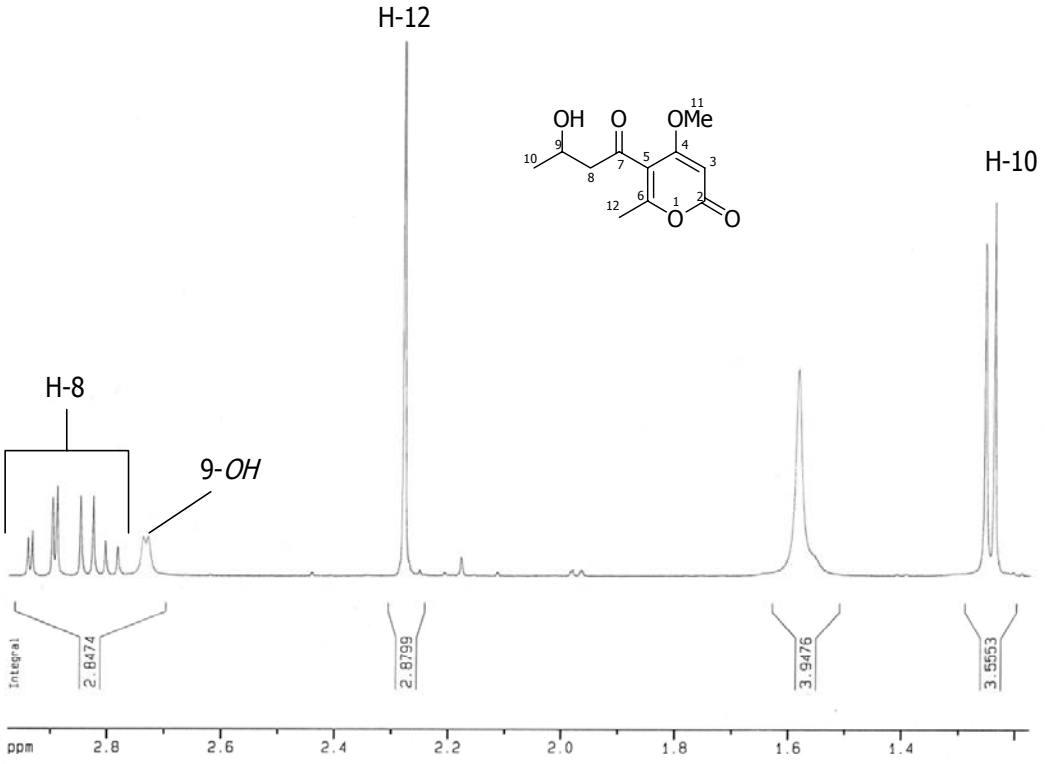

Figure 101. Expansion A of ^{1}H-NMR ($CDCl_3$) spectrum of pyrenocine B **(54)**

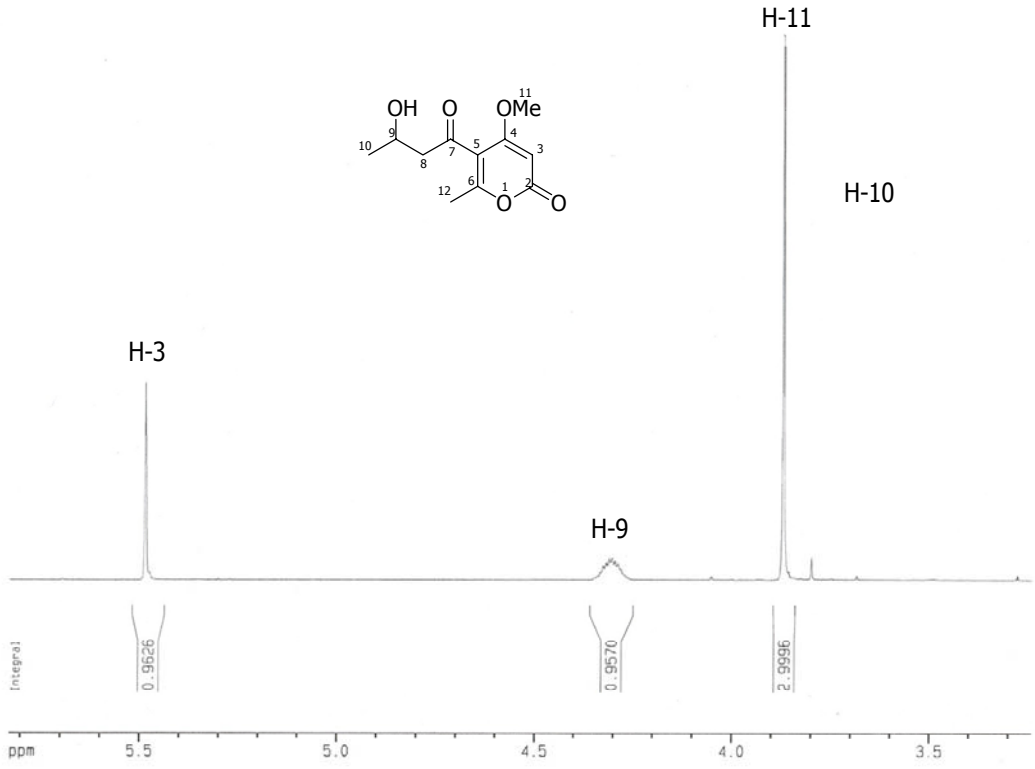

Figure 102. Expansion B of ^{1}H-NMR ($CDCl_3$) spectrum of pyrenocine B **(54)**

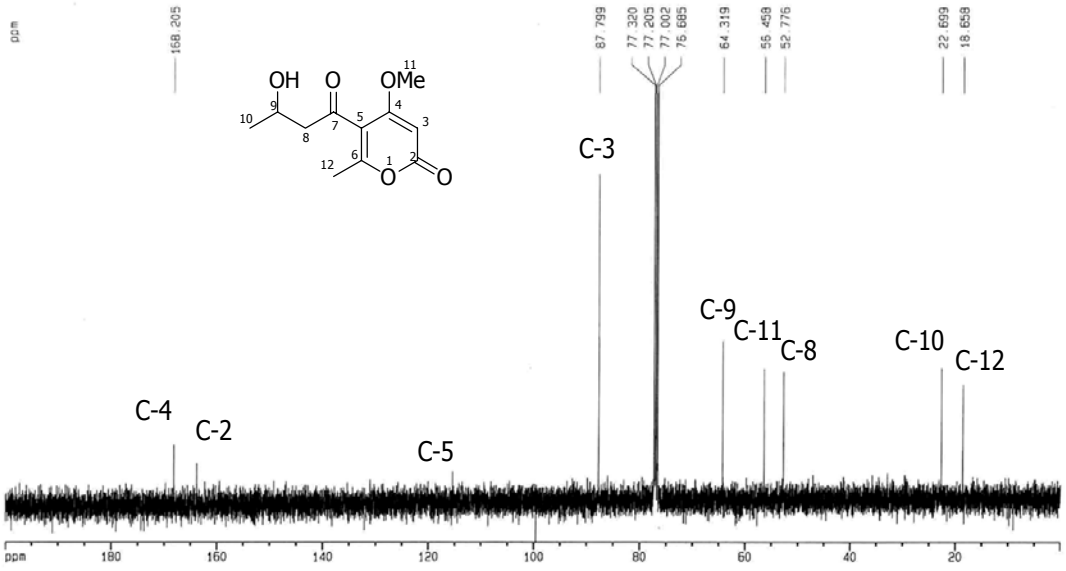

Figure 103. ^{13}C-NMR ($CDCl_3$) spectrum of pyrenocine B **(54)**

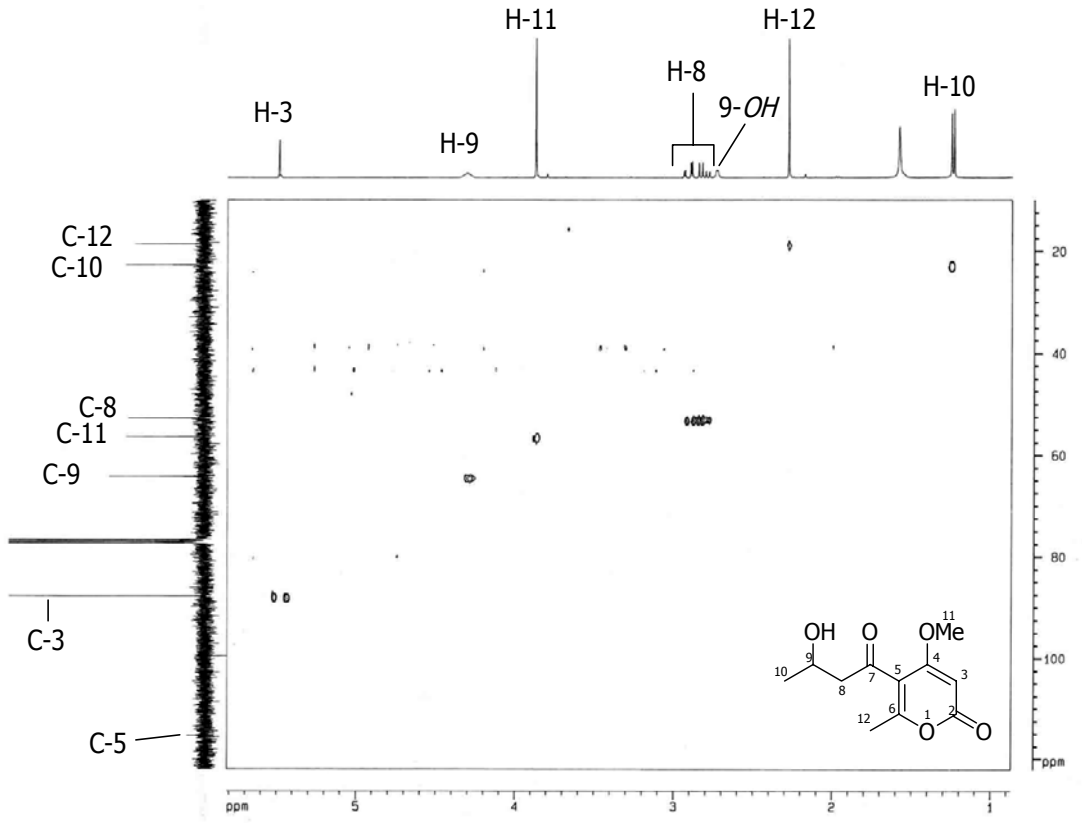

Figure 104. HMQC spectrum of pyrenocine B **(54)**

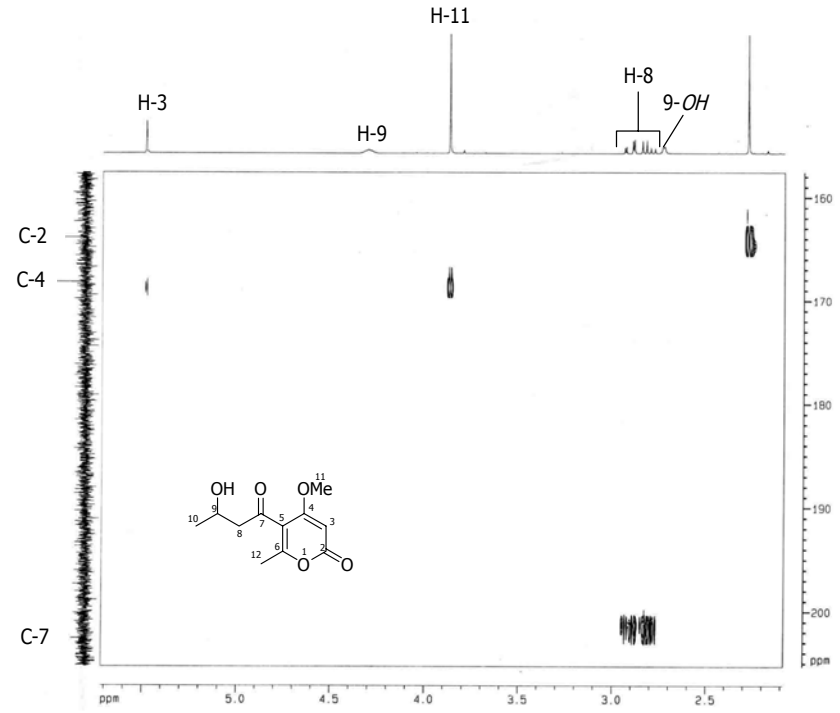

Figure 105. Expansion of HMQC spectrum of pyrenocine B **(54)**

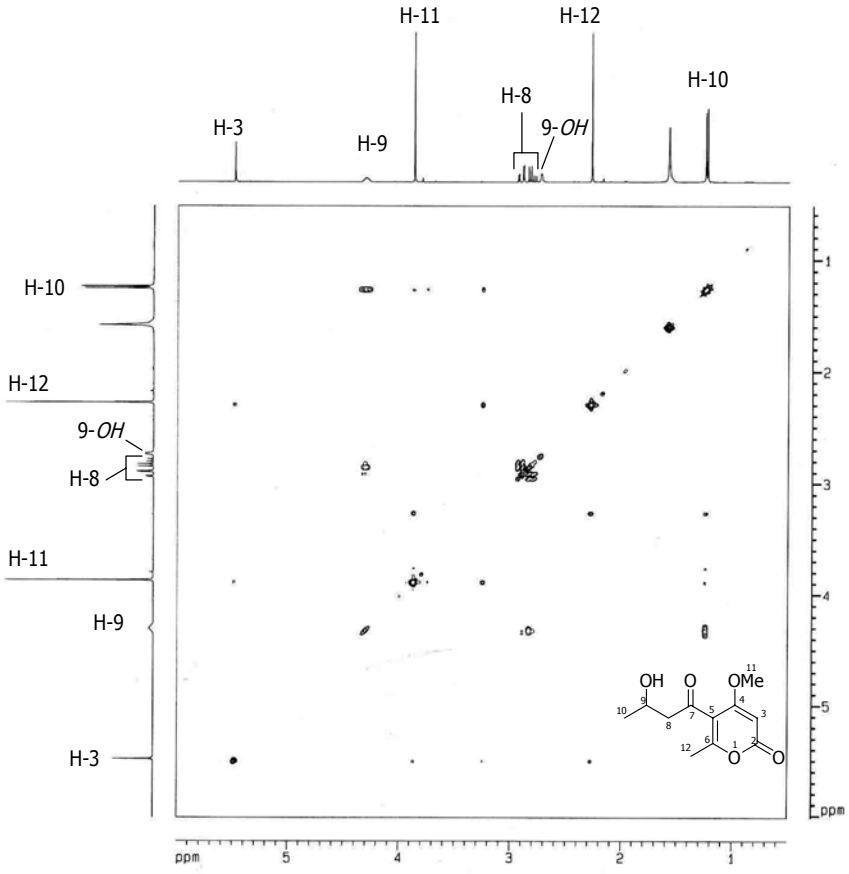

Figure 106. COSY spectrum of pyrenocine B **(54)**

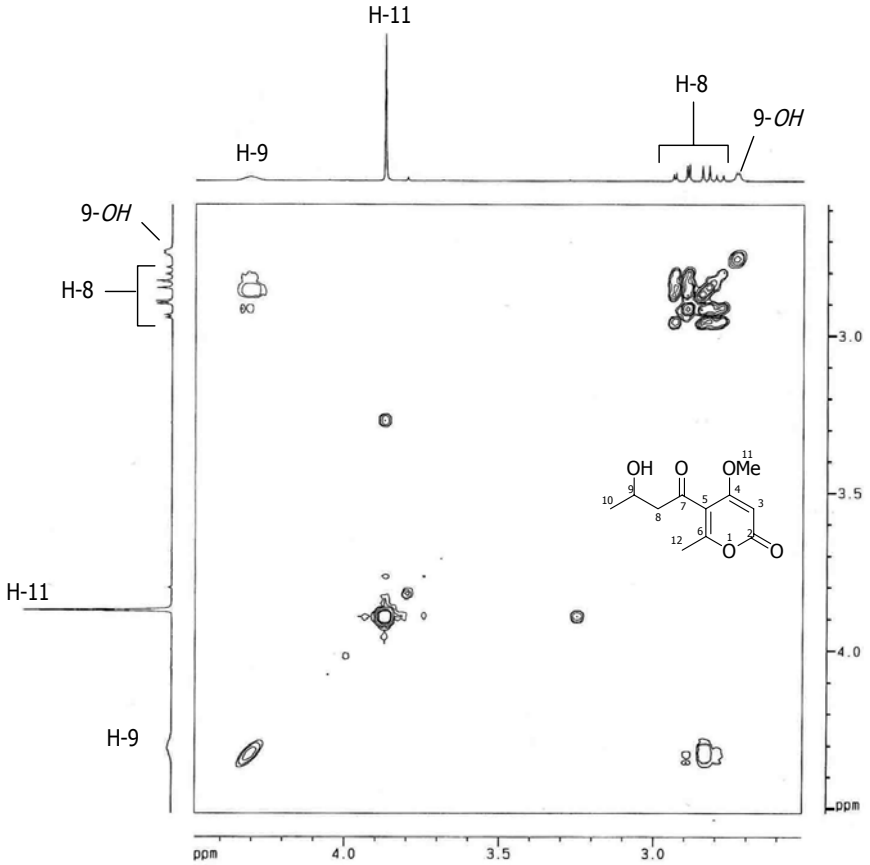

Figure 107. Expansion of COSY spectrum of pyrenocine B **(54)**

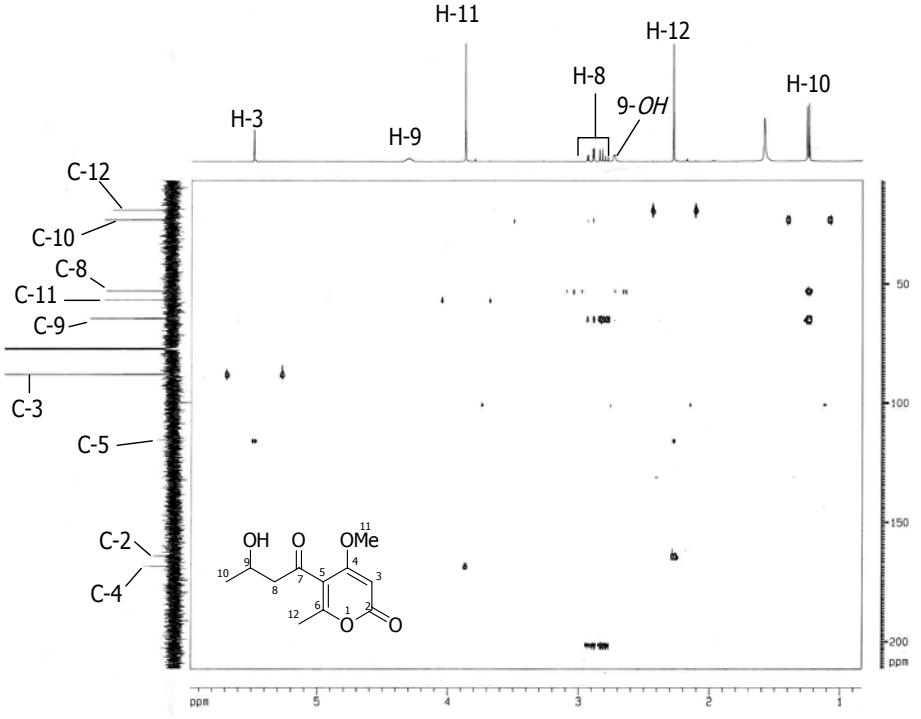

Figure 108. HMBC spectrum of pyrenocine B **(54)**

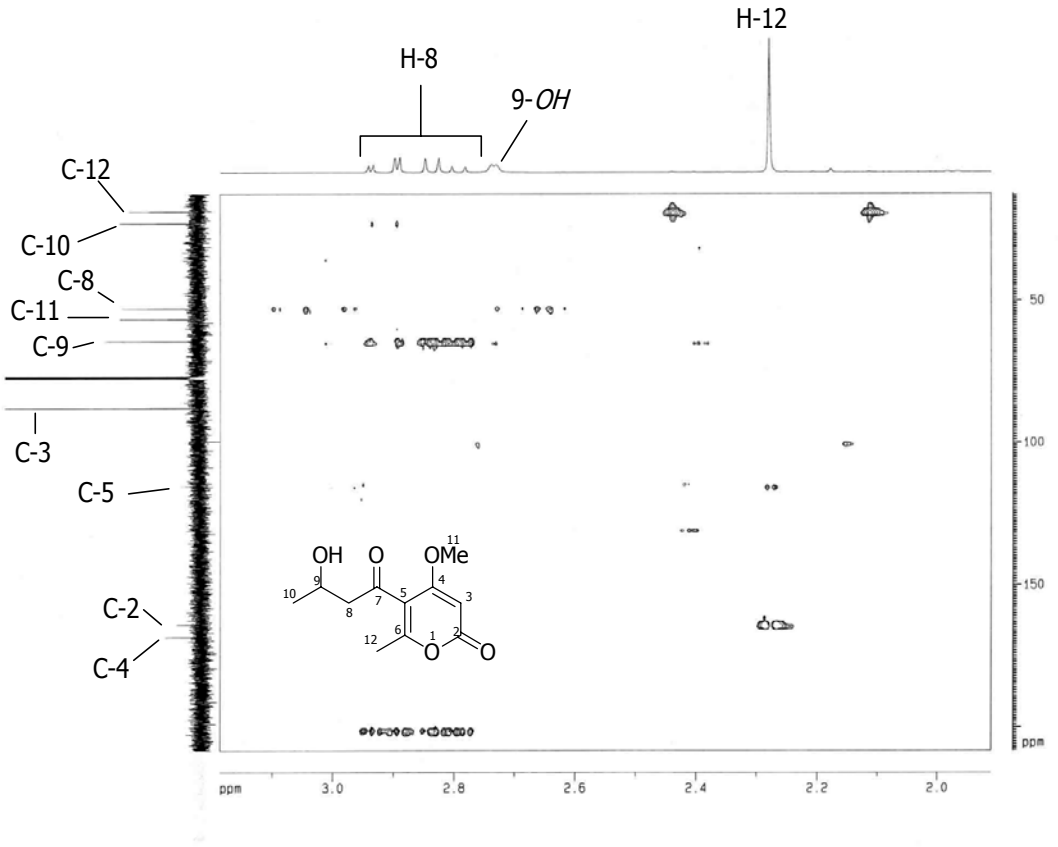

Figure 109. Expansion of HMBC spectrum of pyrenocine B **(54)**

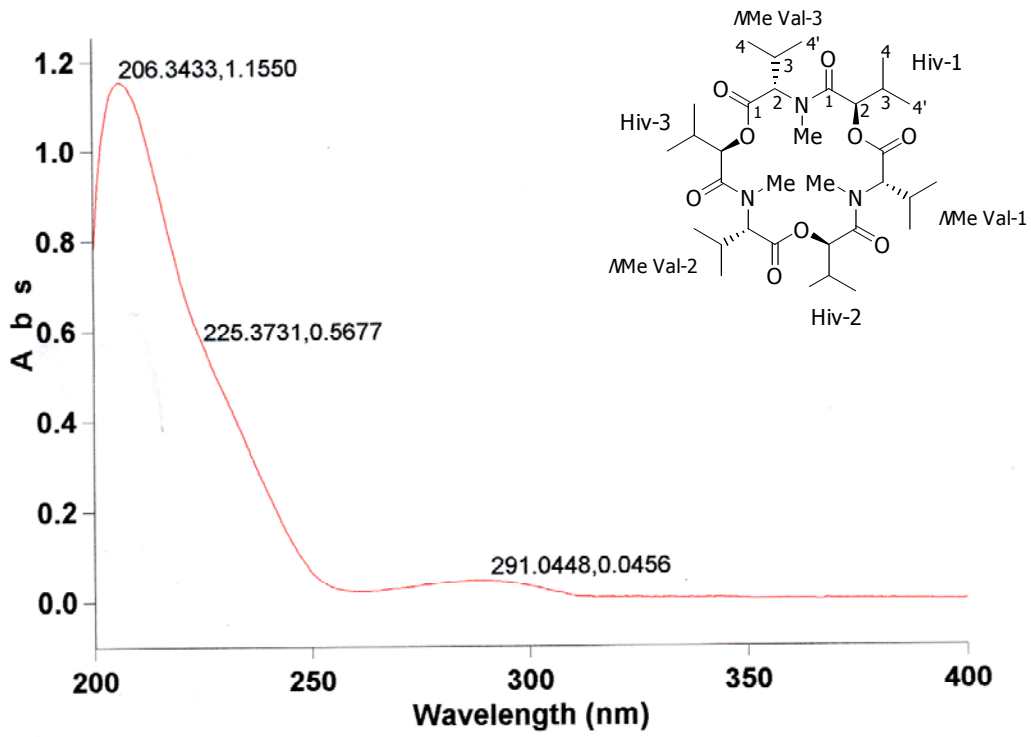

Figure 110. UV spectrum of enniatin B **(55)**

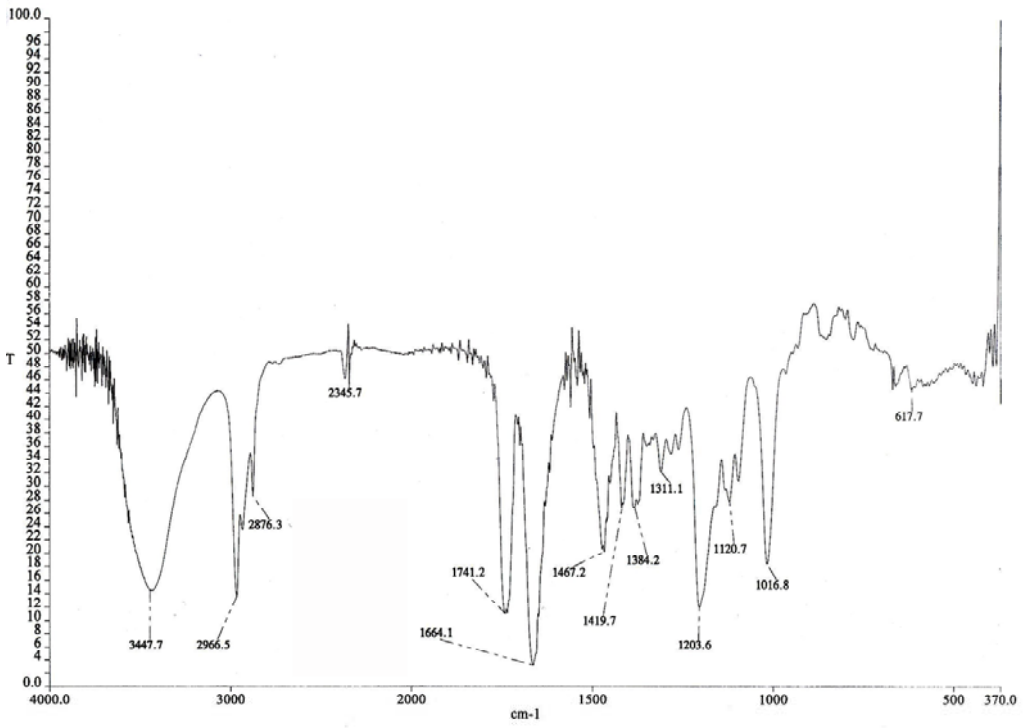

Figure 111. IR spectrum of enniatin B **(55)**

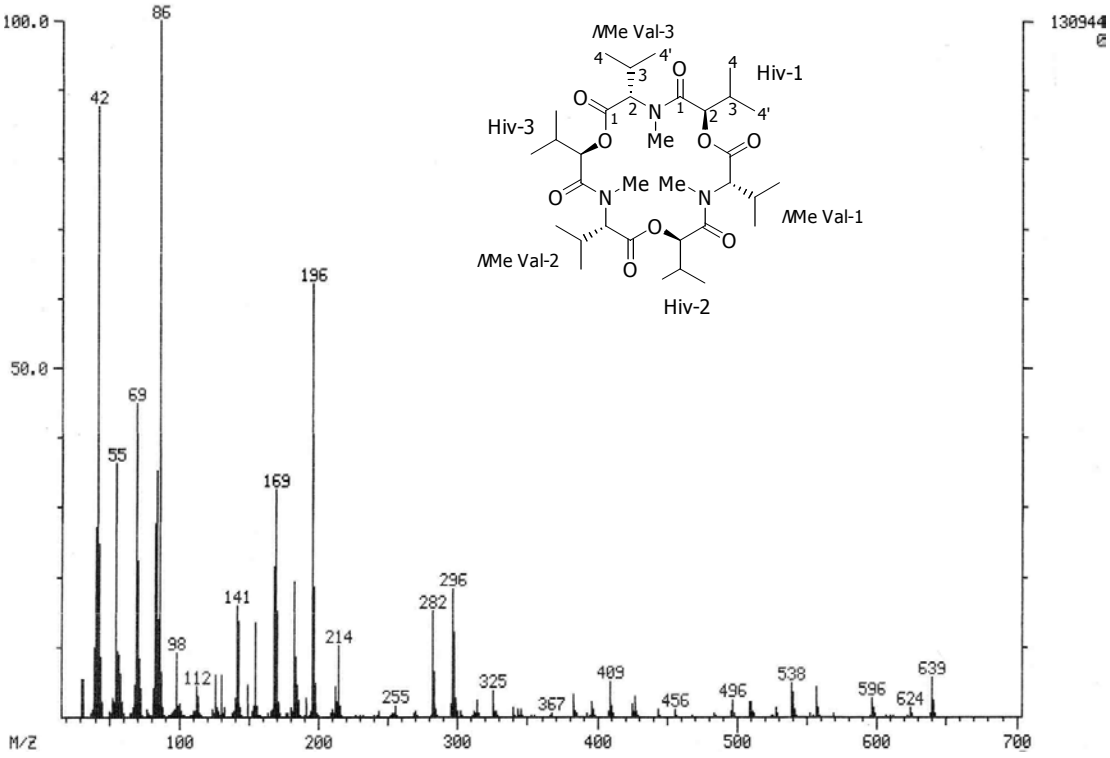

Figure 112. EIMS spectrum of enniatin B **(55)**

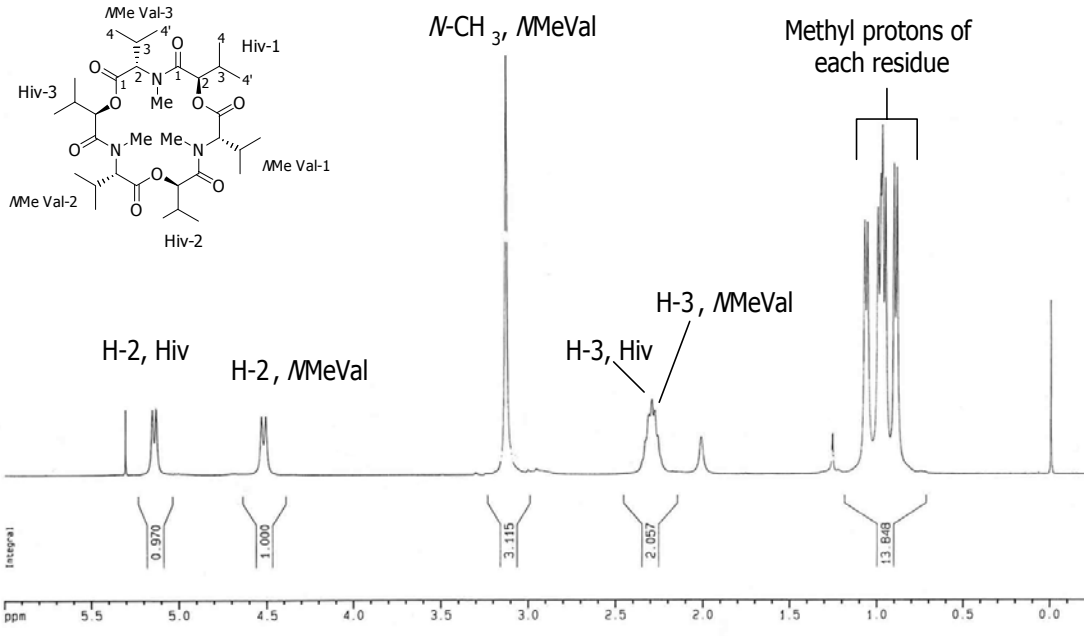

Figure 113. ^{1}H-NMR ($CDCl_3$) spectrum of enniatin B **(55)**

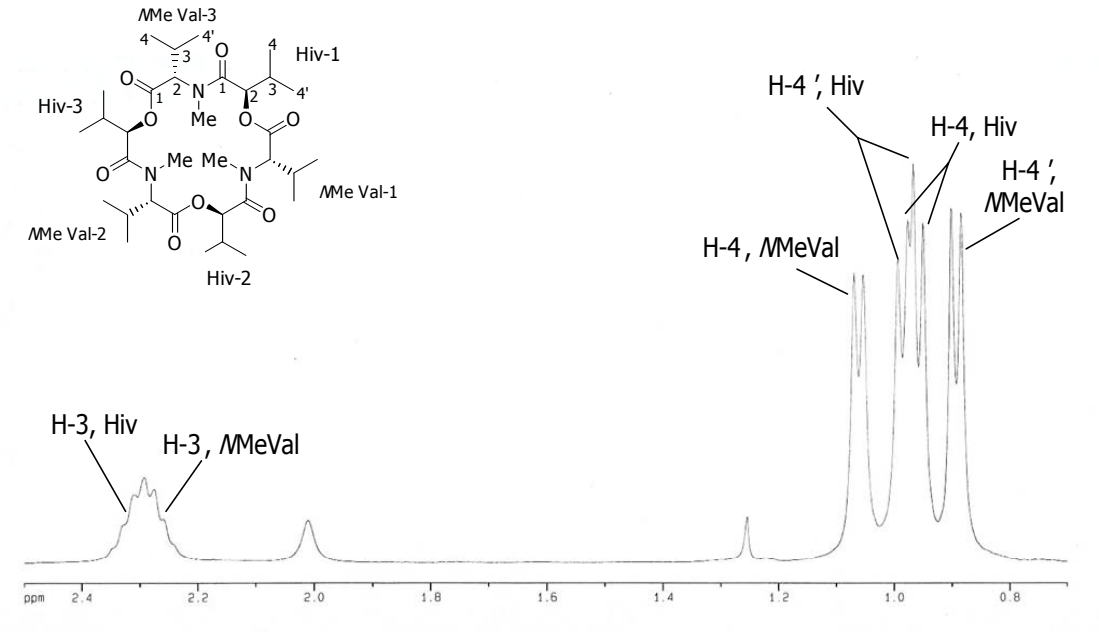

Figure 114. Expansion of ^{1}H-NMR ($CDCl_3$) spectrum of enniatin B **(55)**

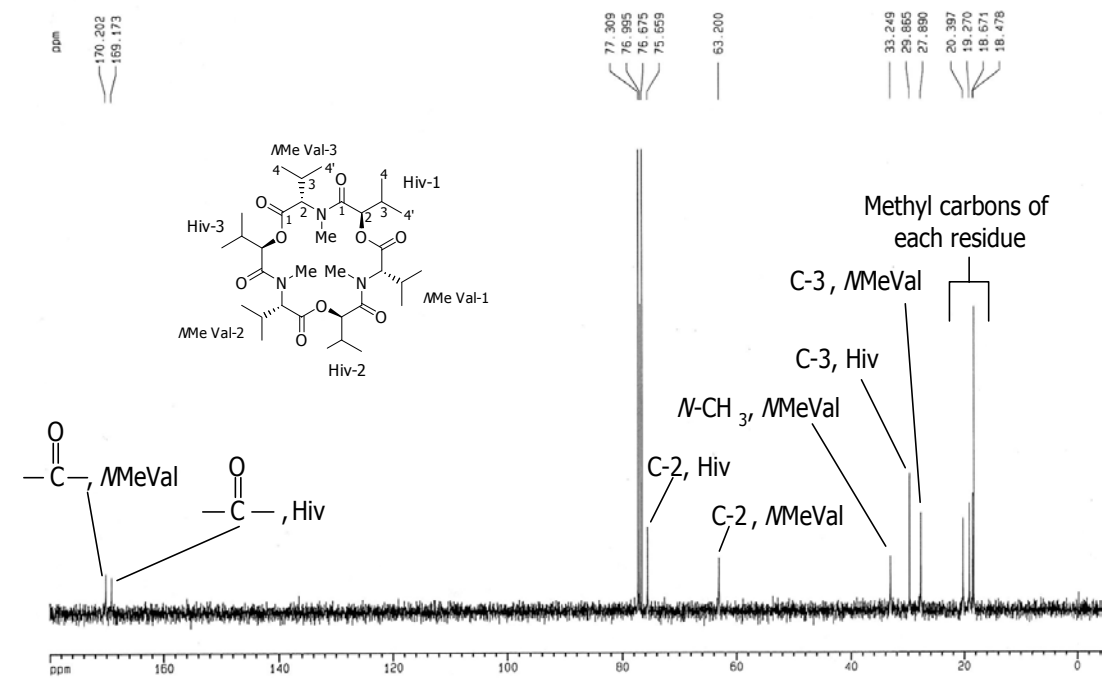

Figure 115. ^{13}C-NMR spectrum of enniatin B **(55)**

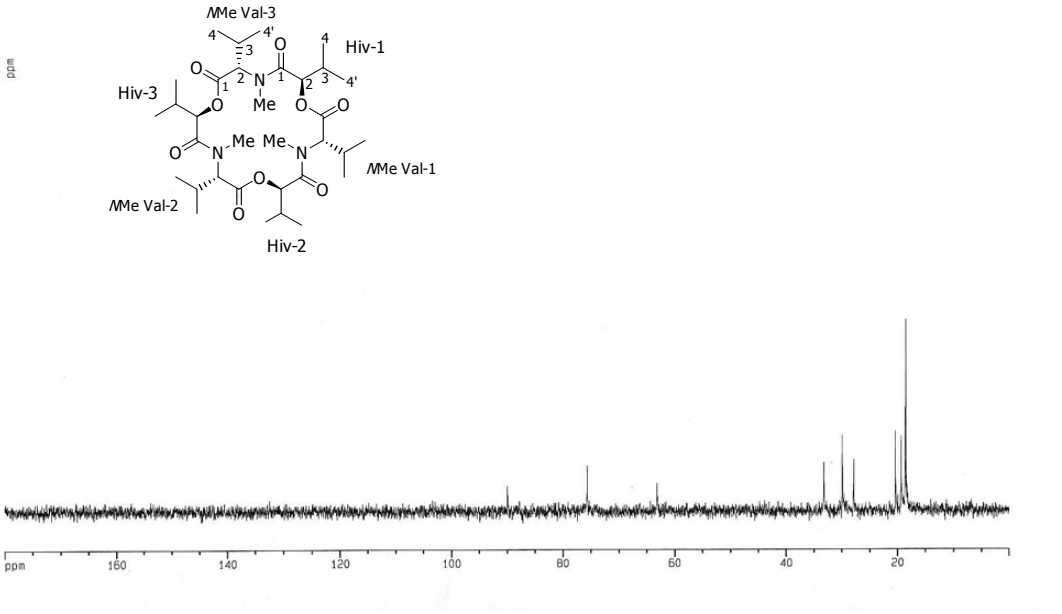

Figure 116. DEPT 45 spectrum of enniatin B **(55)**

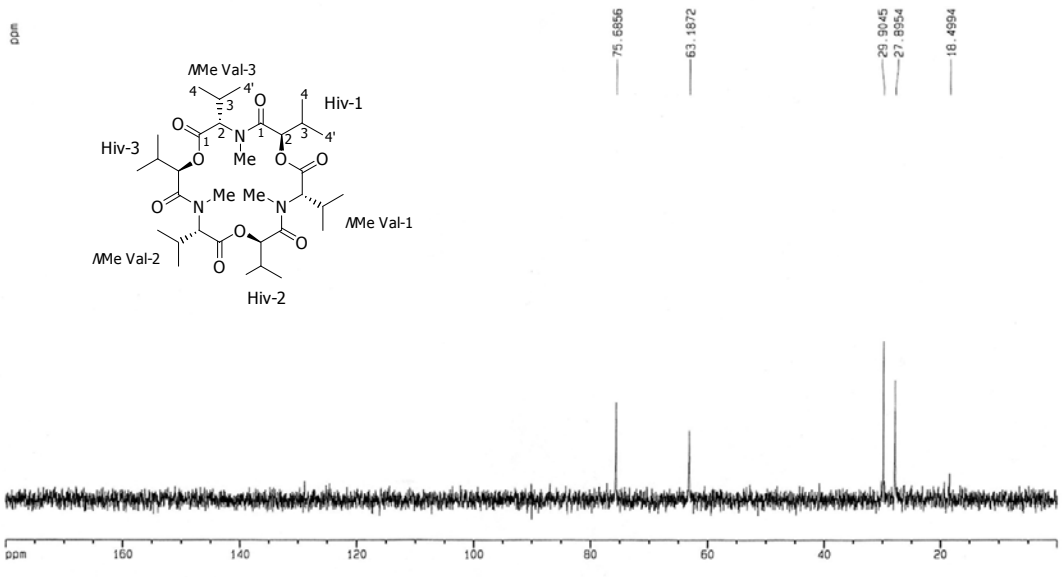

Figure 117. DEPT 90 spectrum of enniatin B **(55)**

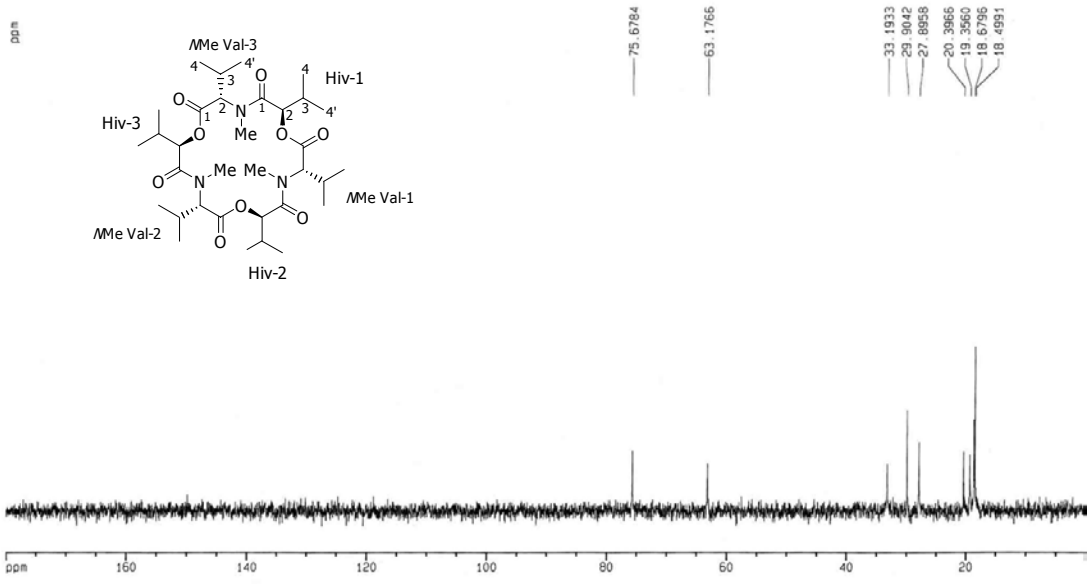

Figure 118. DEPT 135 spectrum of enniatin B **(55)**

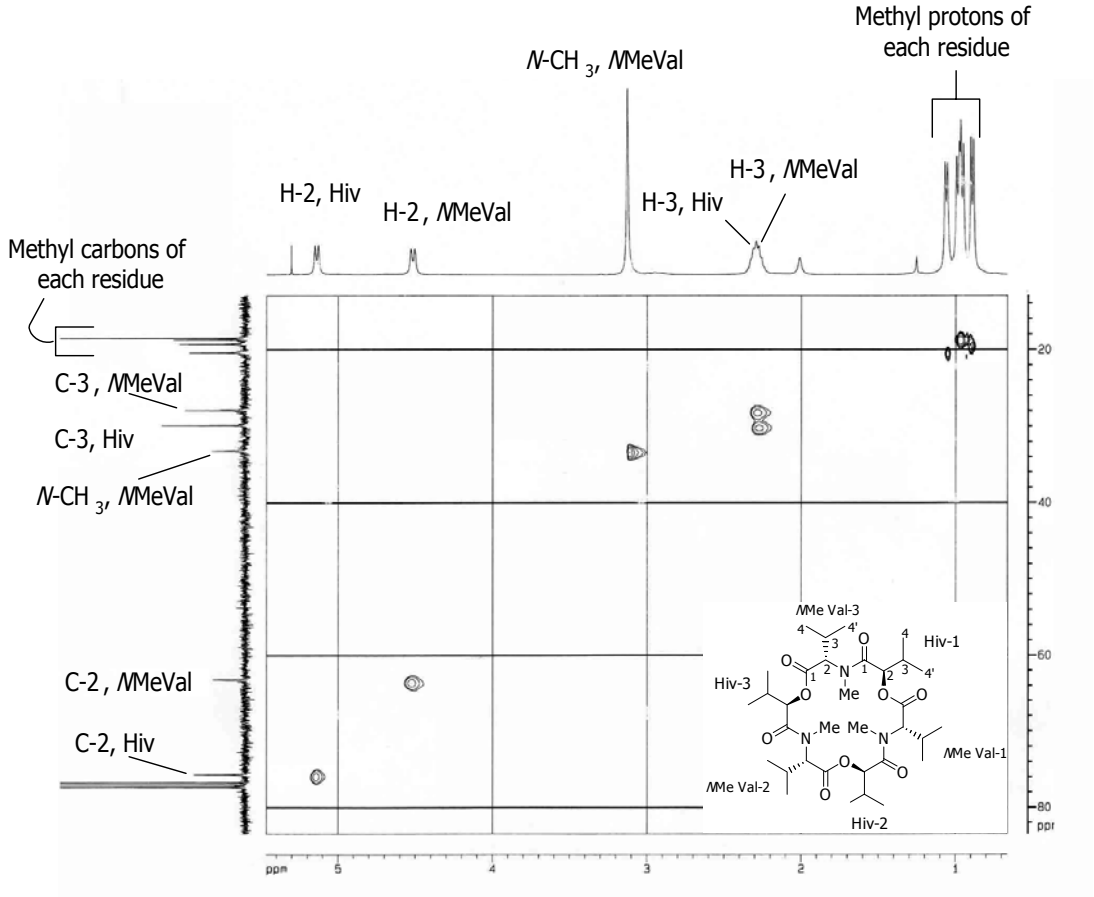

Figure 119. HMQC spectrum of enniatin B **(55)**

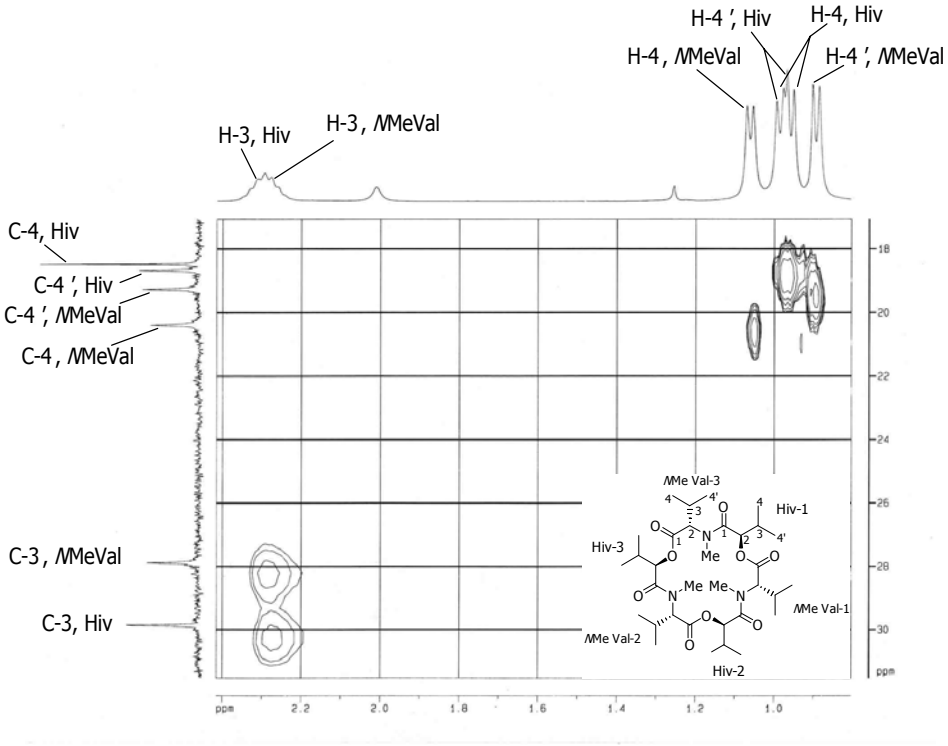

Figure 120. Expansion of HMQC spectrum of enniatin B **(55)**

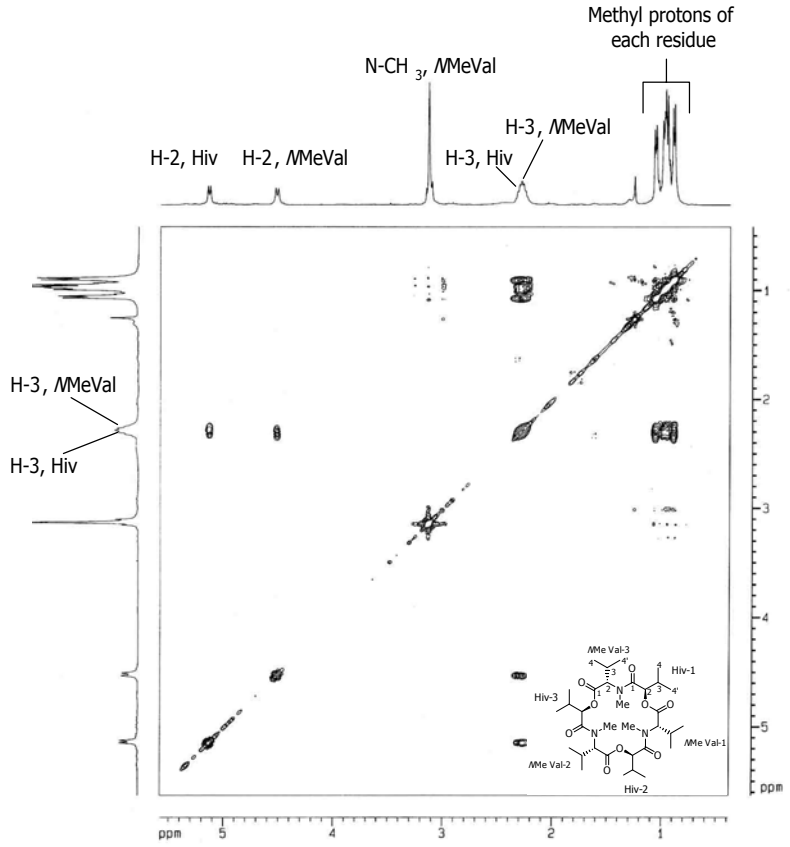

Figure 121. COSY spectrum of enniatin B **(55)**

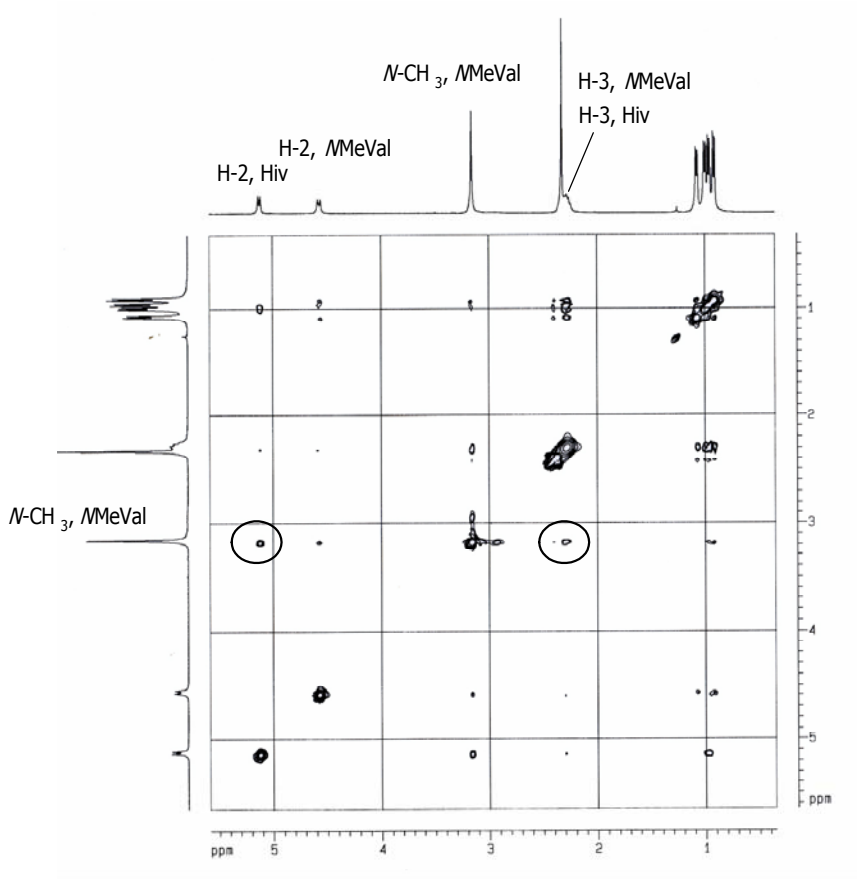

Figure 122. NOESY spectrum of enniatin B **(55)**

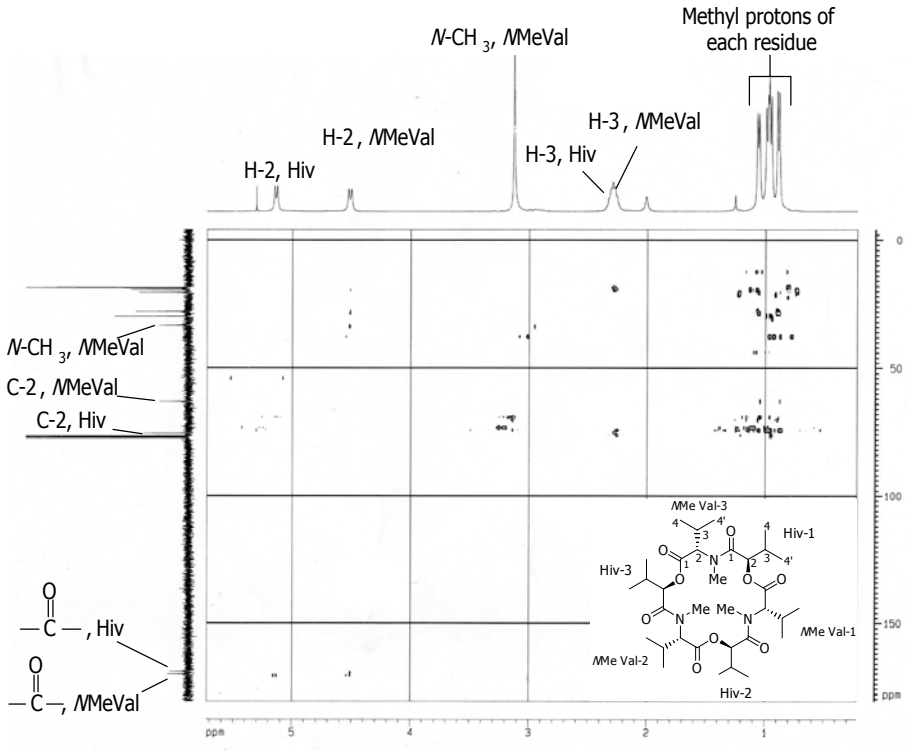

Figure 123. HMBC spectrum of enniatin B **(55)**

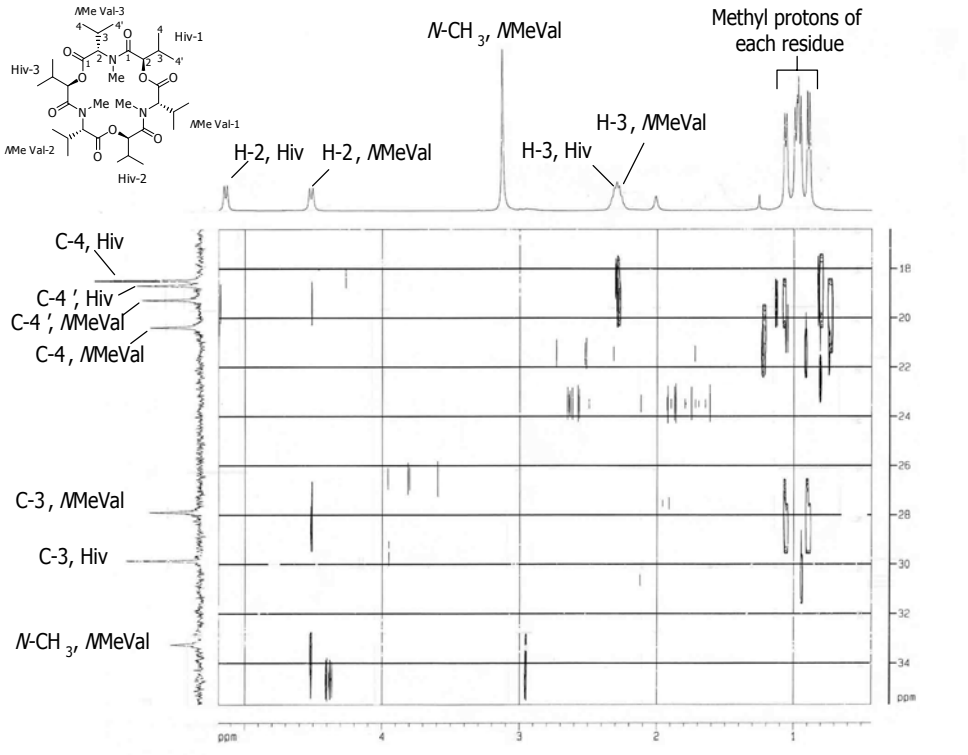

Figure 124. Expansion A of HMBC spectrum of enniatin B **(55)**

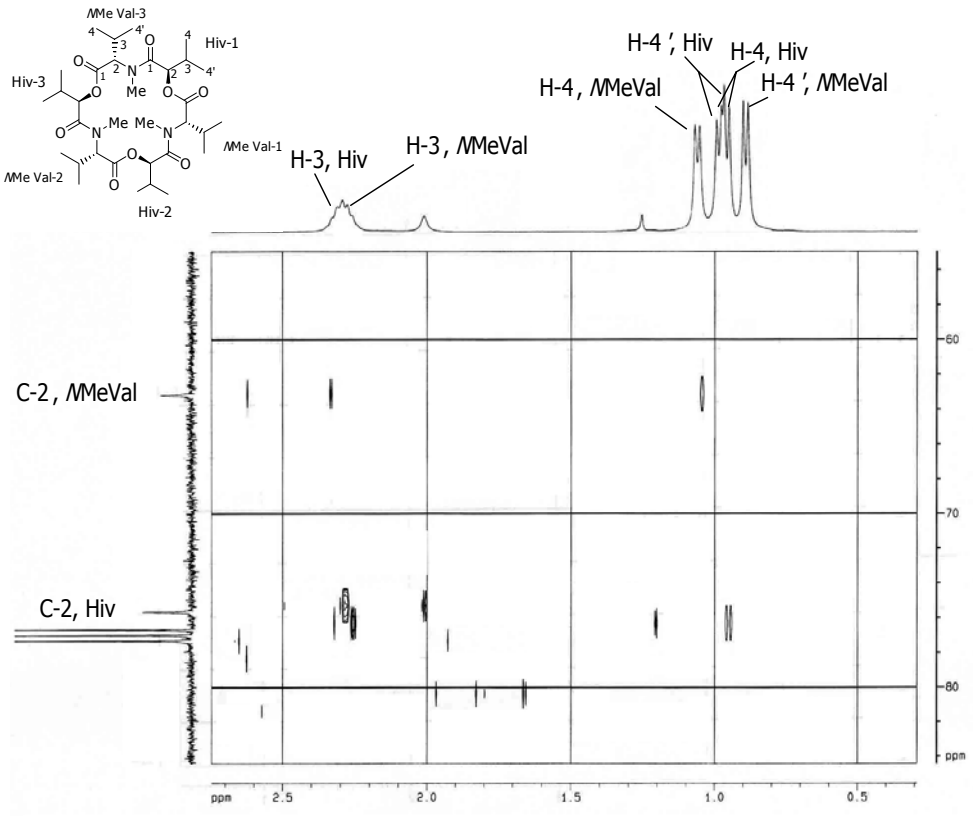

Figure 125. Expansion B of HMBC spectrum of enniatin B **(55)**

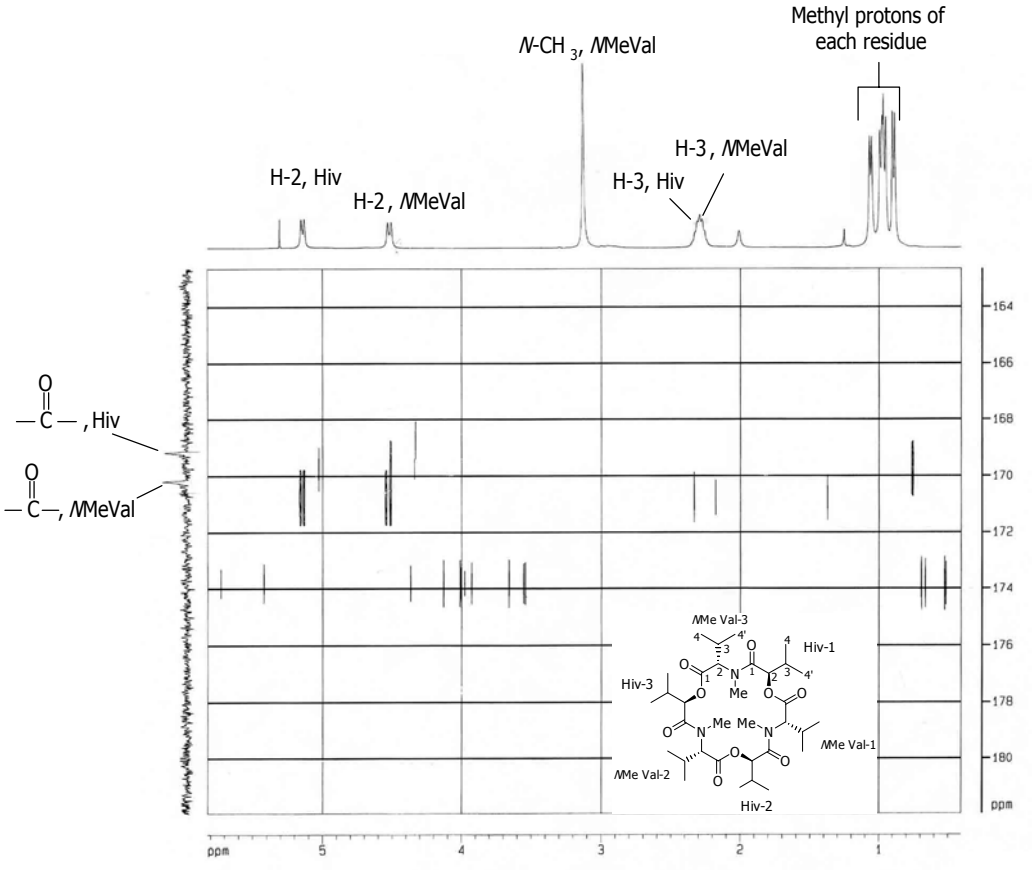

Figure 126. Expansion C of HMBC spectrum of enniatin B **(55)**

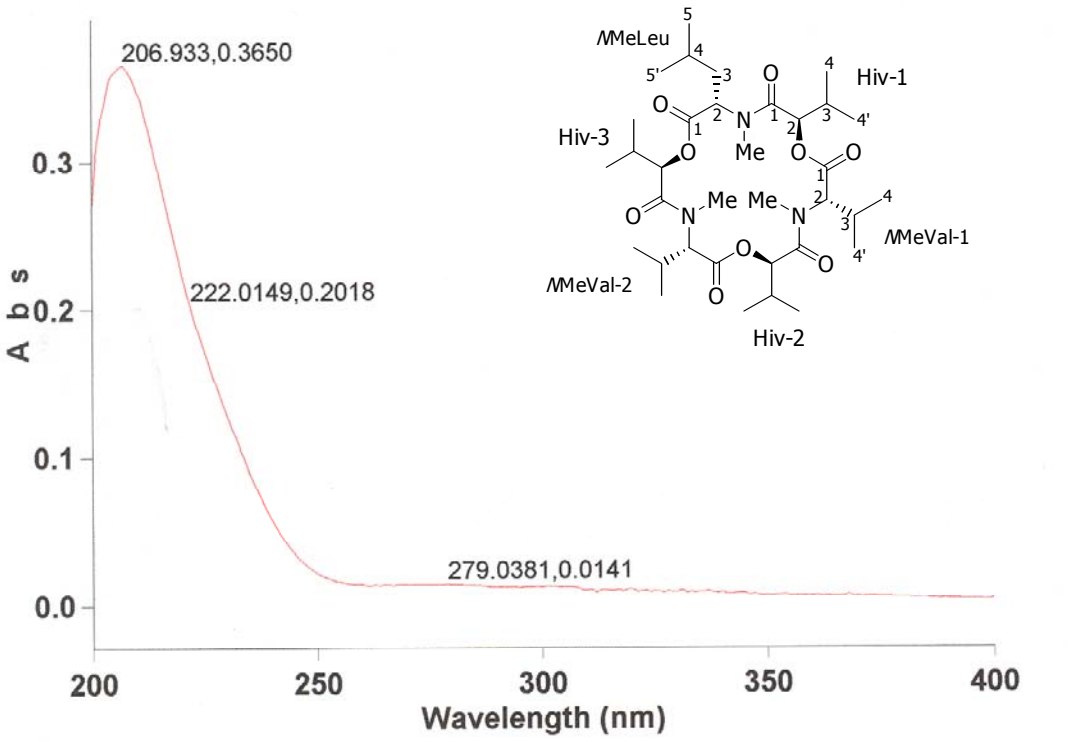

Figure 127. UV spectrum of enniatin B_4 **(56)**

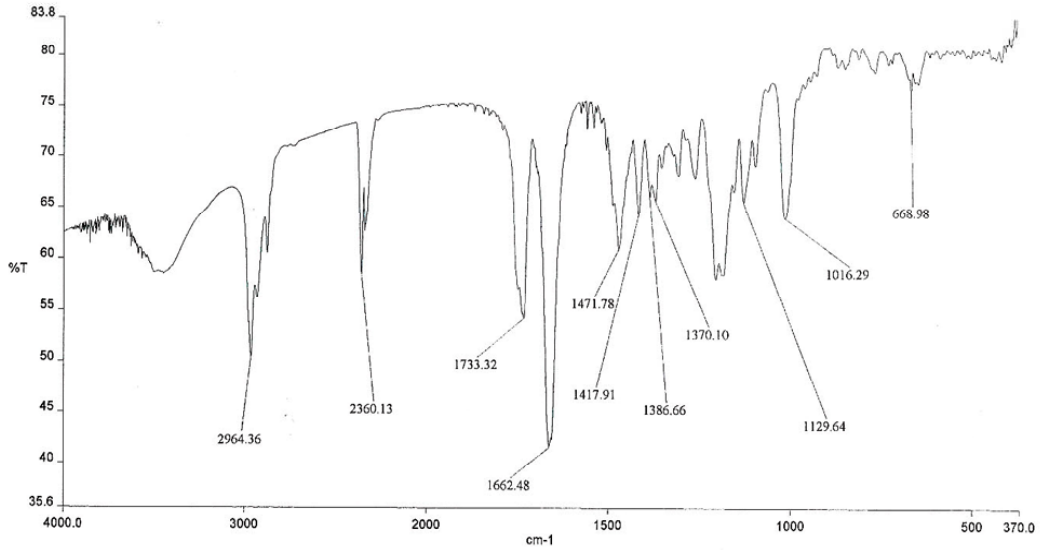

Figure 128. IR spectrum of enniatin B_4 **(56)**

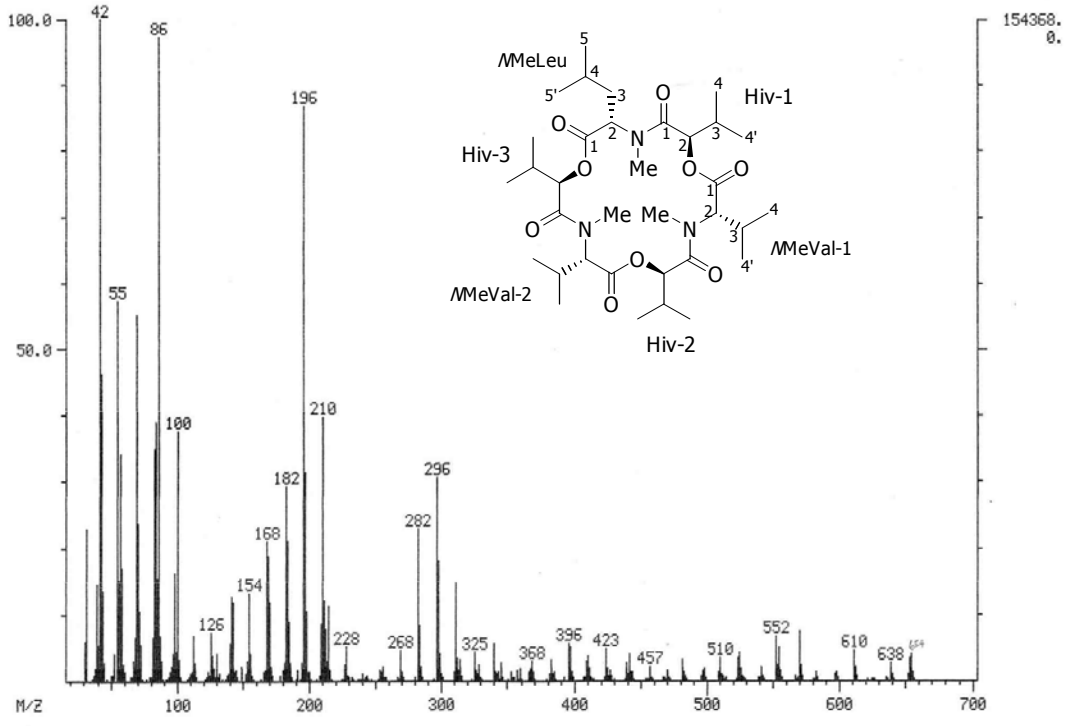

Figure 129. EIMS spectrum of enniatin B_4 **(56)**

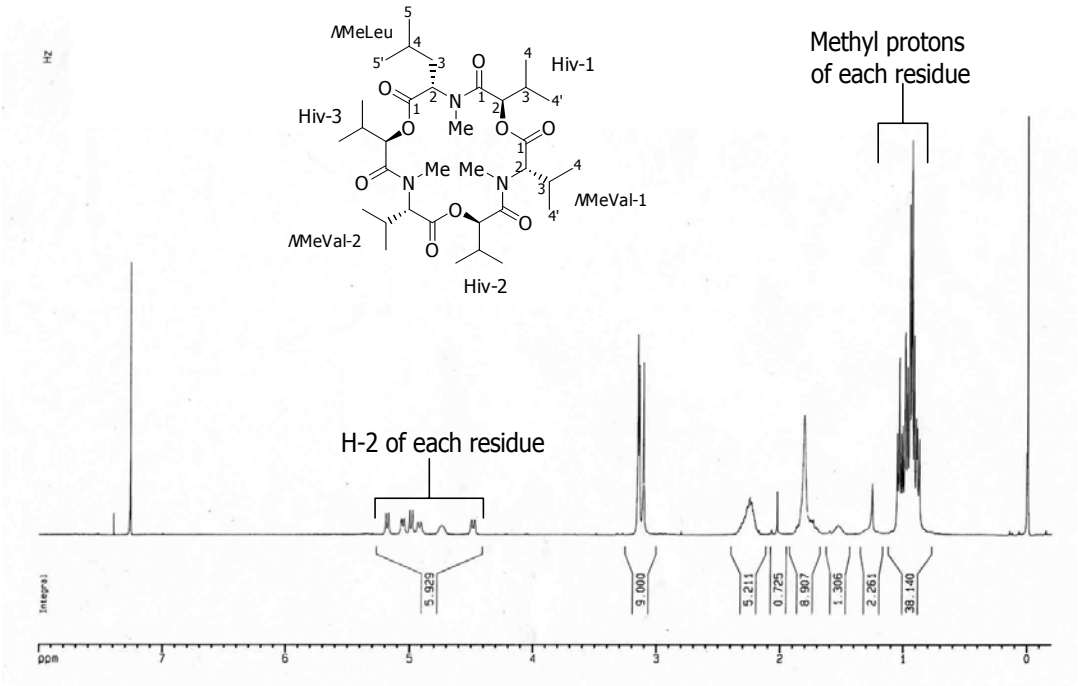

Figure 130. ^{1}H NMR spectrum ($CDCl_3$) of enniatin B_4 **(56)**

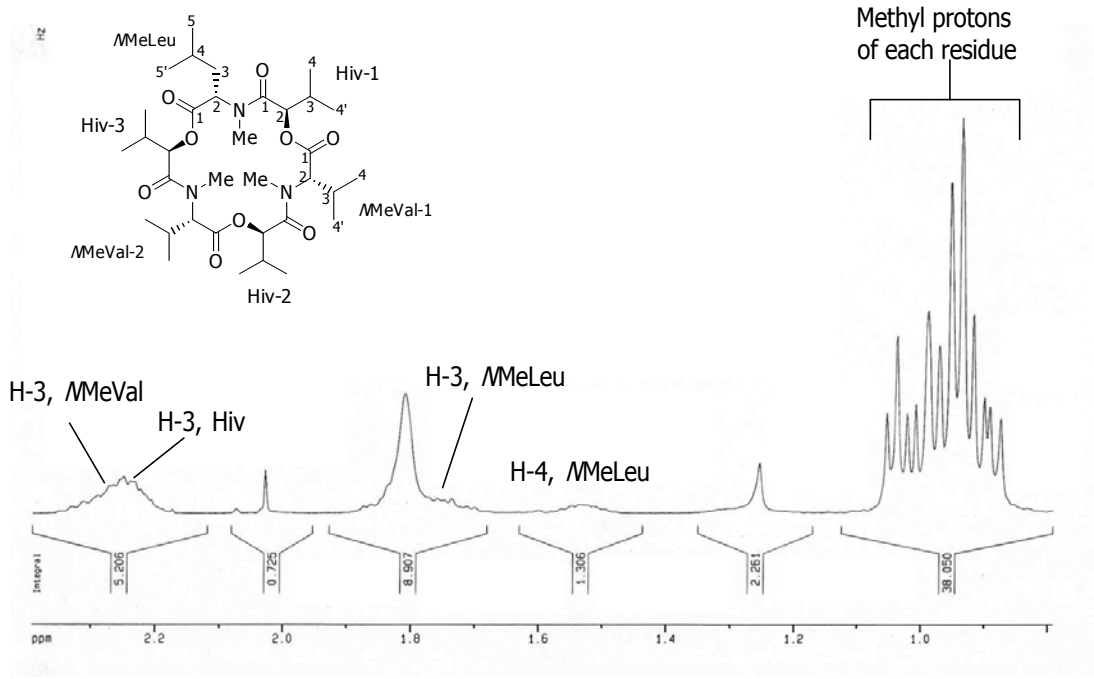

Figure 131. Expansion A of ^{1}H NMR ($CDCl_3$) spectrum of enniatin B_4 **(56)**

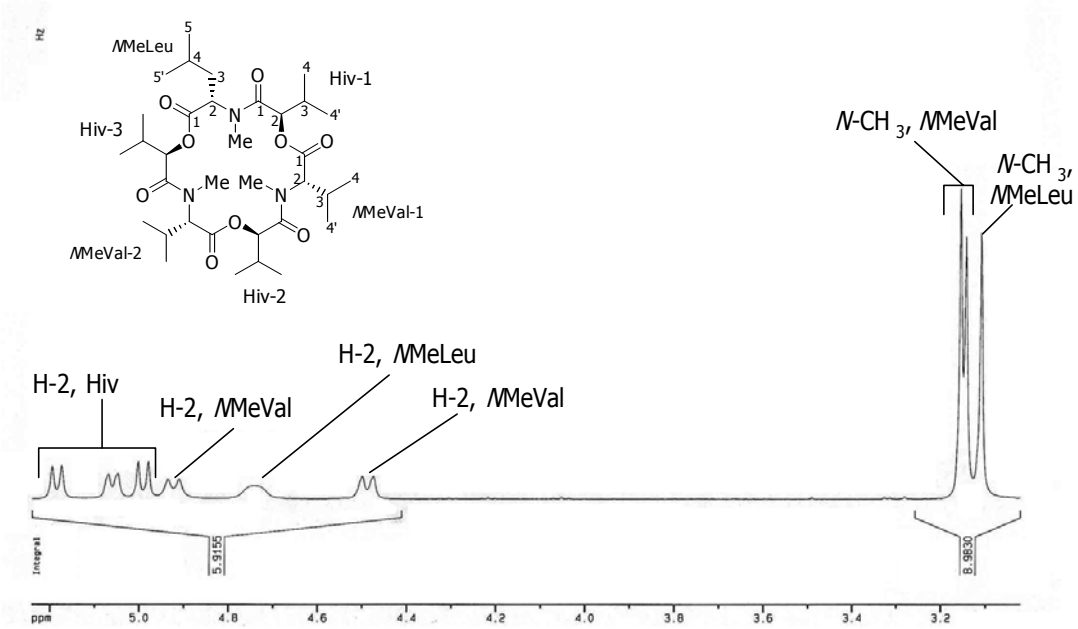

Figure 132. Expansion B of ^{1}H NMR ($CDCl_3$) spectrum of enniatin B_4 **(56)**

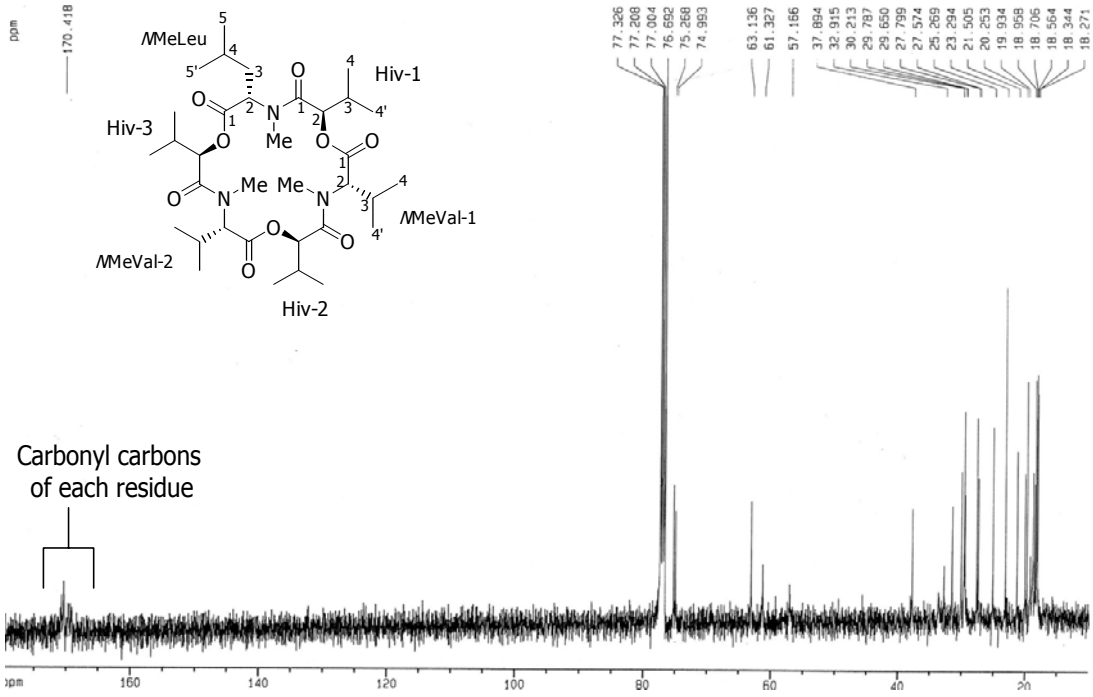

Figure 133. ^{13}C NMR spectrum of enniatin B_4 **(56)**

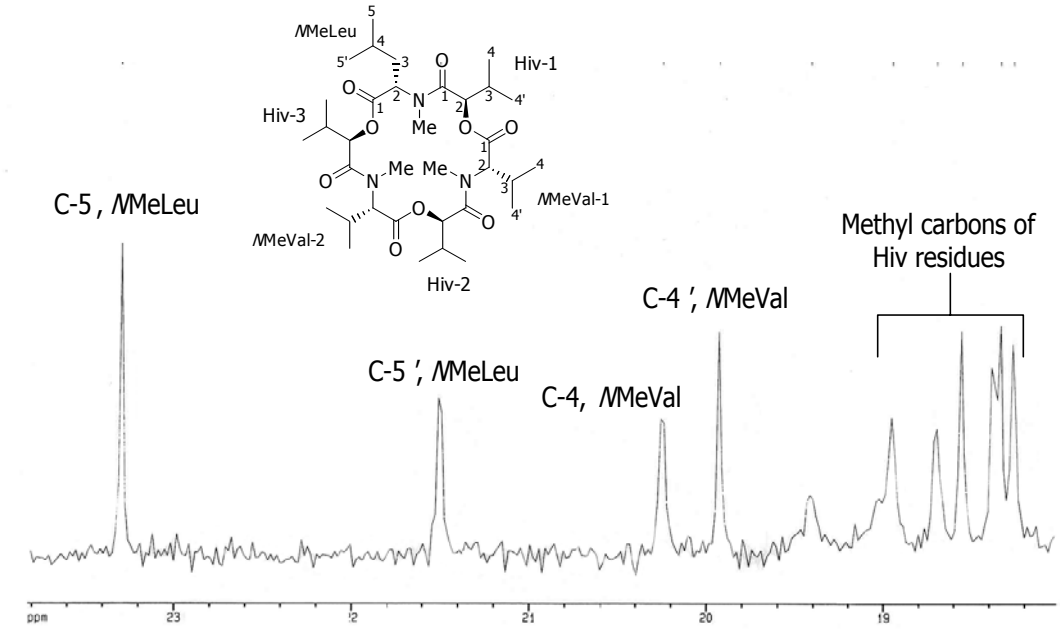

Figure 134. Expansion A of ^{13}C NMR spectrum of enniatin B_4 **(56)**

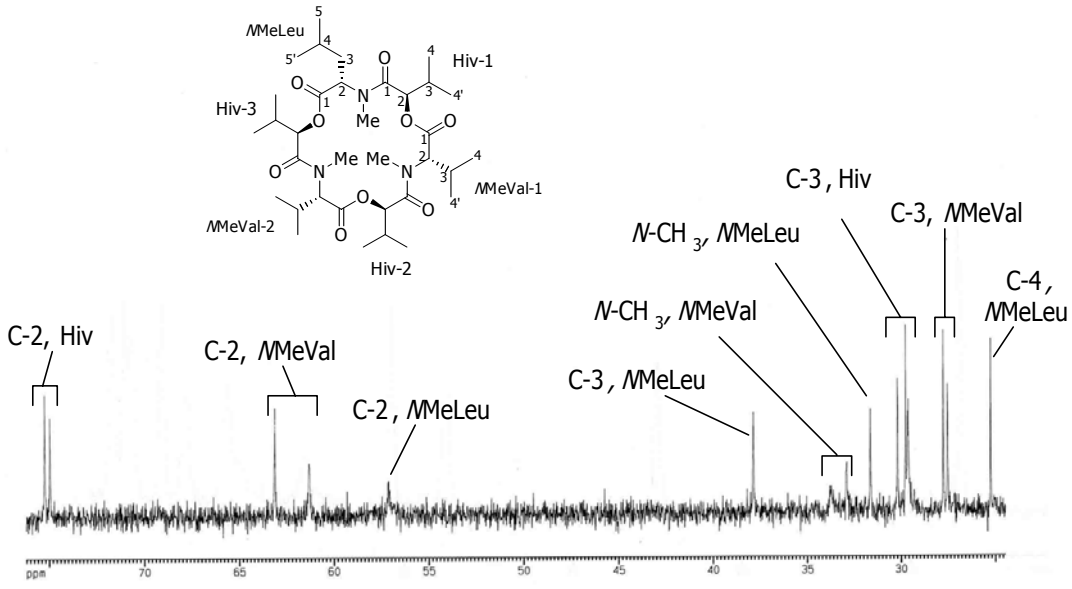

Figure 135. Expansion B of ^{13}C NMR spectrum of enniatin B_4 **(56)**

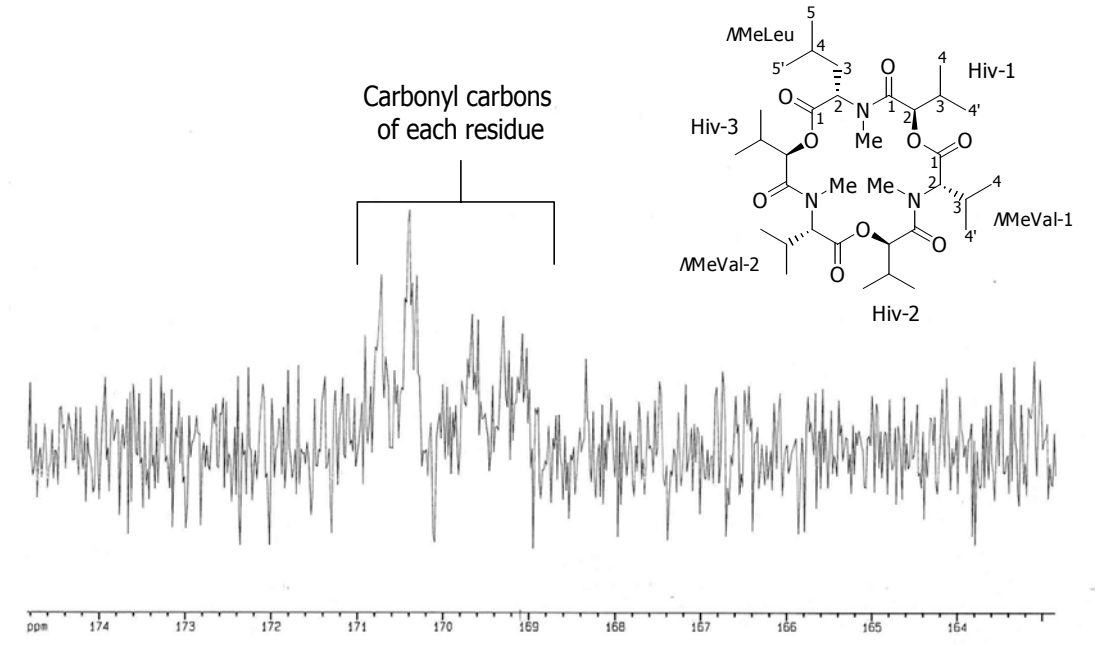

Figure 136. Expansion C of ^{13}C NMR spectrum of enniatin B_4 **(56)**

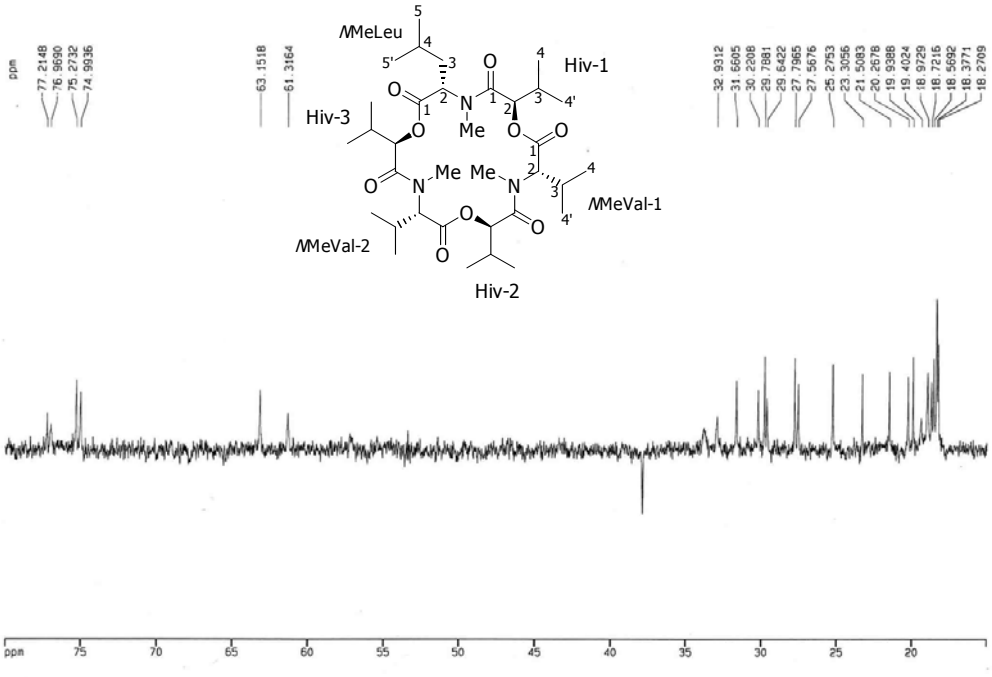

Figure 137. DEPT 135 spectrum of enniatin B_4 **(56)**

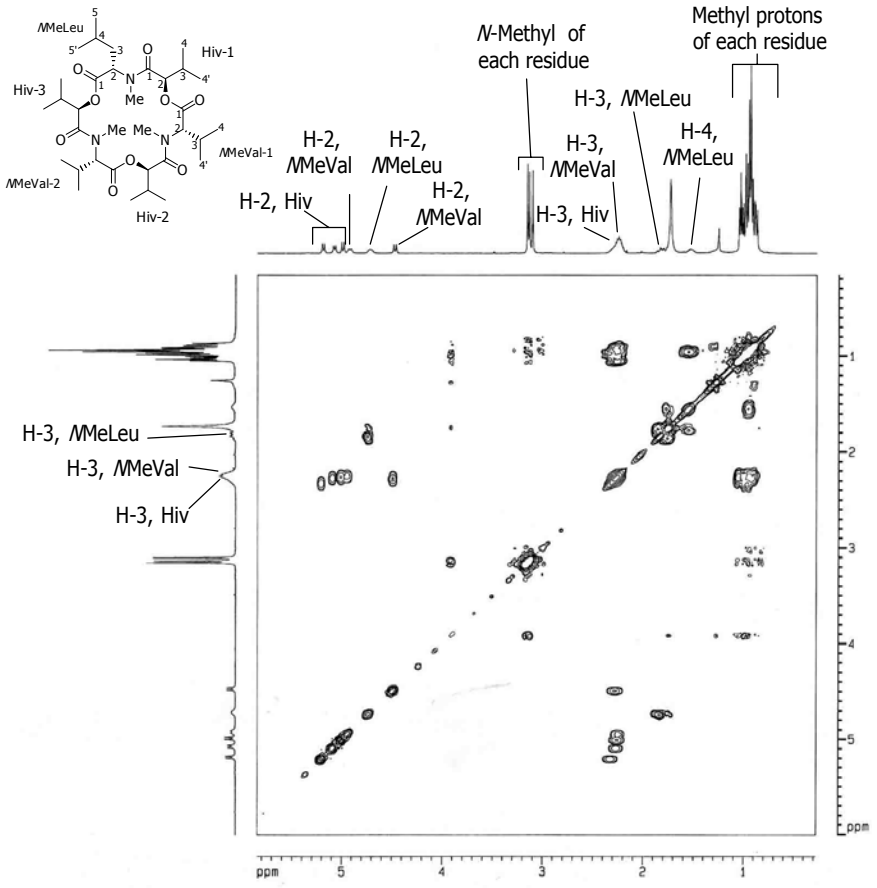

Figure 138. COSY spectrum of enniatin B_4 **(56)**

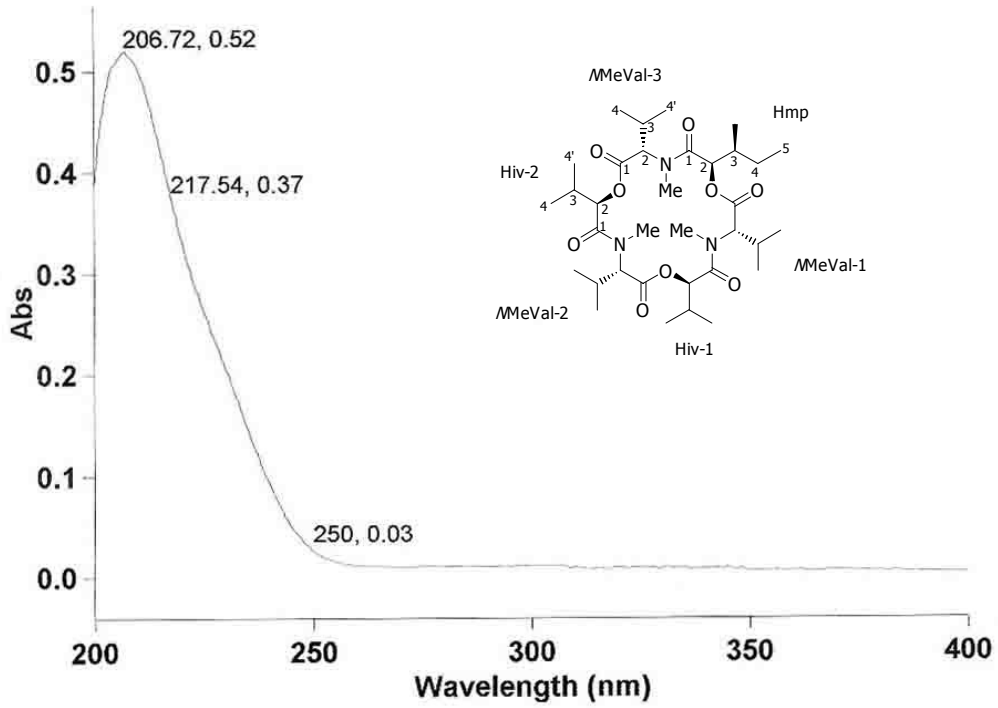

Figure 139. UV spectrum of enniatin H **(57)**

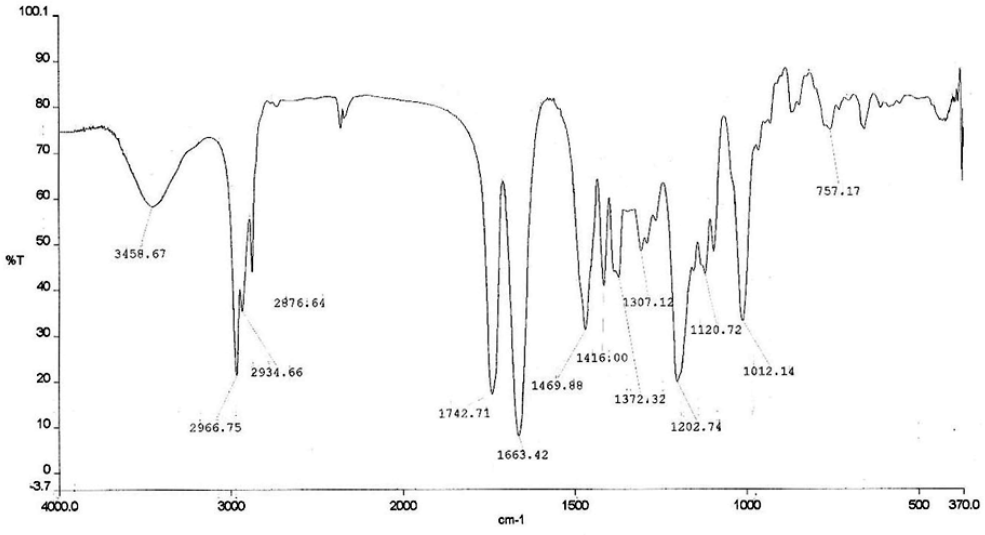

Figure 140. IR spectrum of enniatin H **(57)**

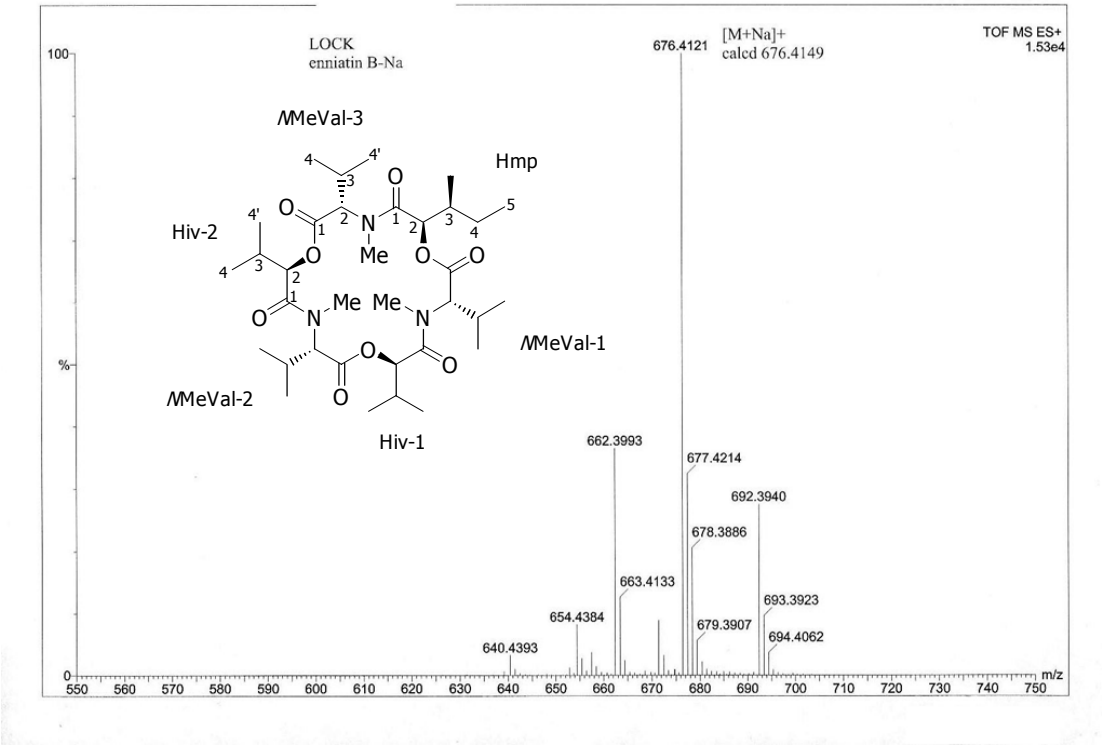

Figure 141. HRMS spectrum of enniatin H **(57)**

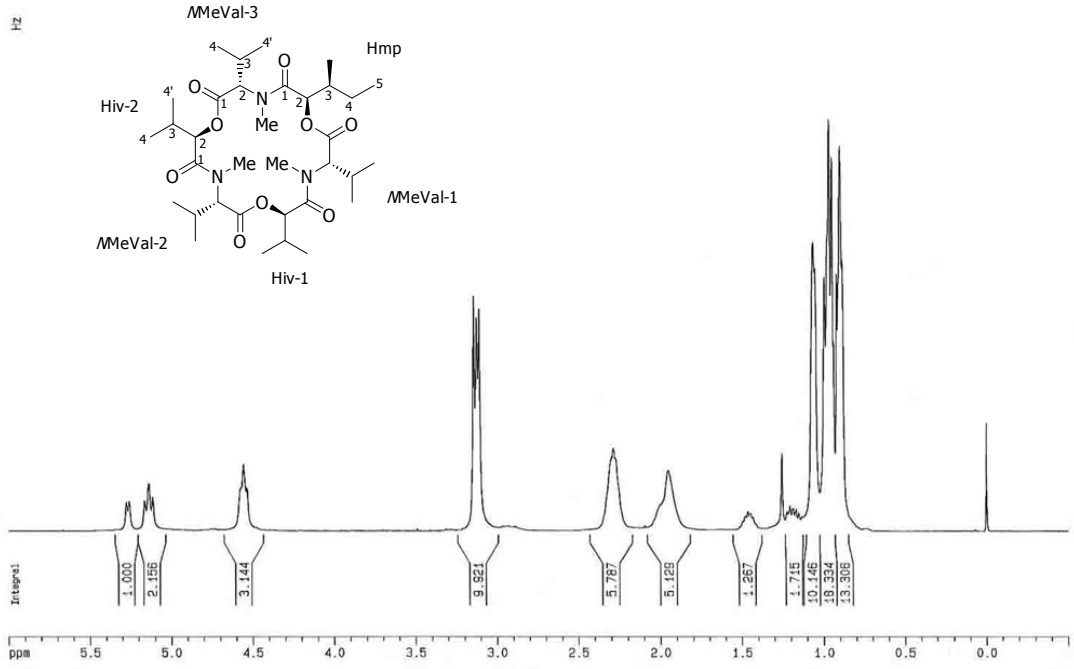

Figure 142. ^{1}H NMR ($CDCl_3$) spectrum of enniatin H **(57)**

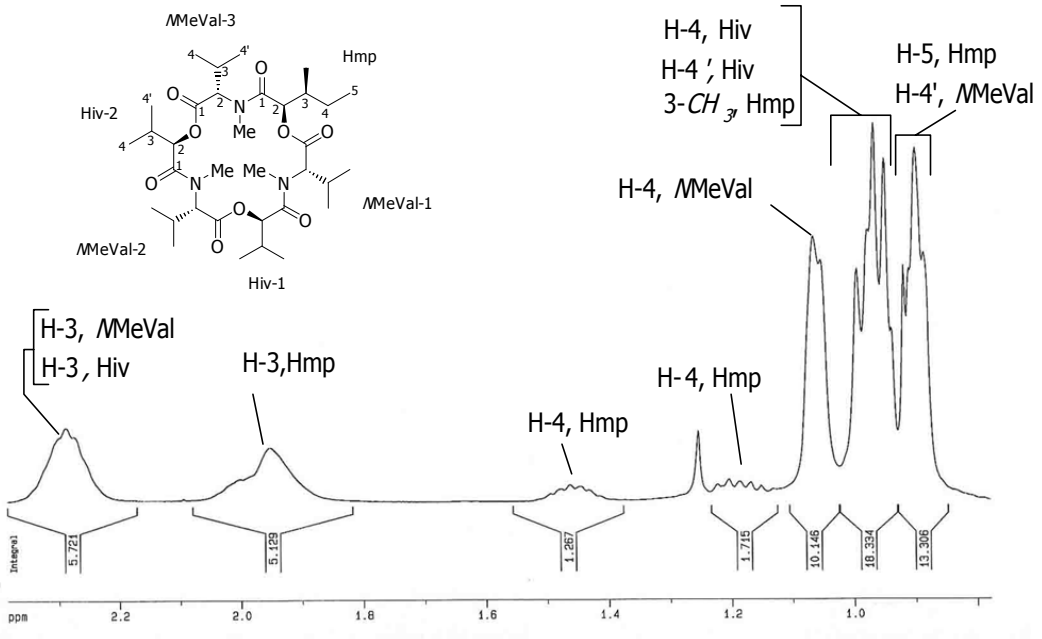

Figure 143. Expansion A of ^{1}H NMR ($CDCl_3$) spectrum of enniatin H **(57)**

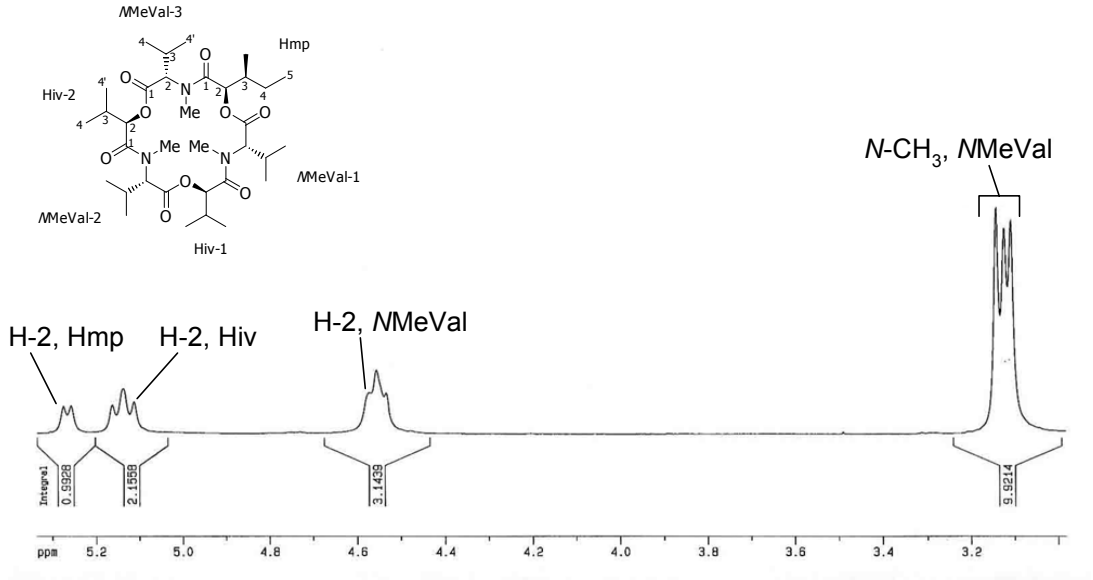

Figure 144. Expansion B of ^{1}H NMR ($CDCl_3$) spectrum of enniatin H **(57)**

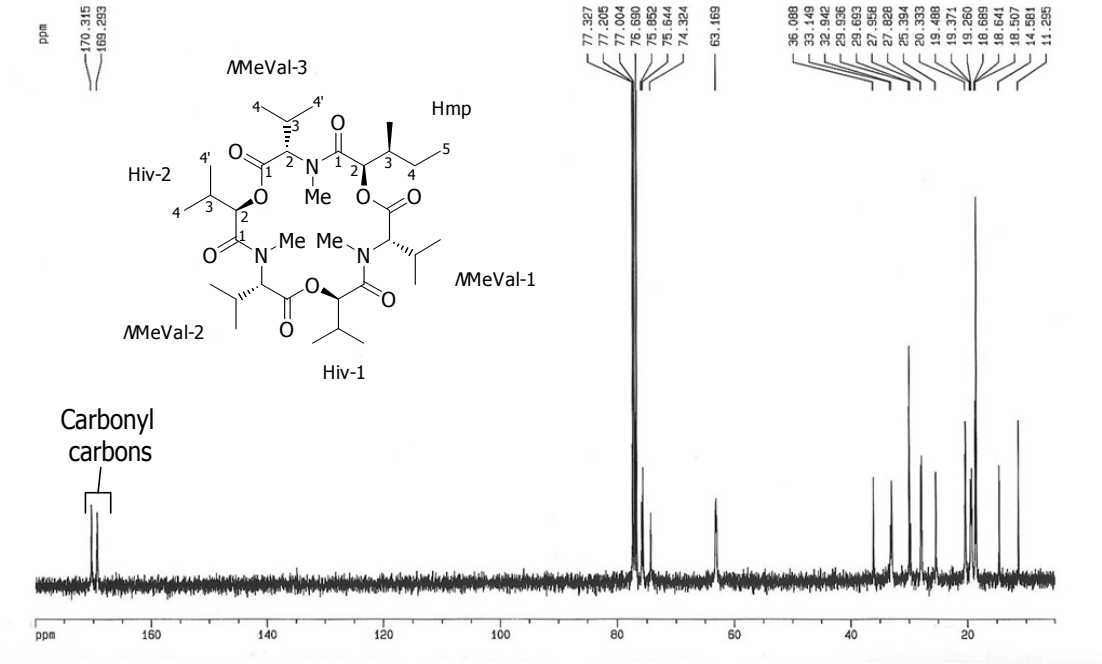

Figure 145. ^{13}C NMR spectrum of enniatin H **(57)**

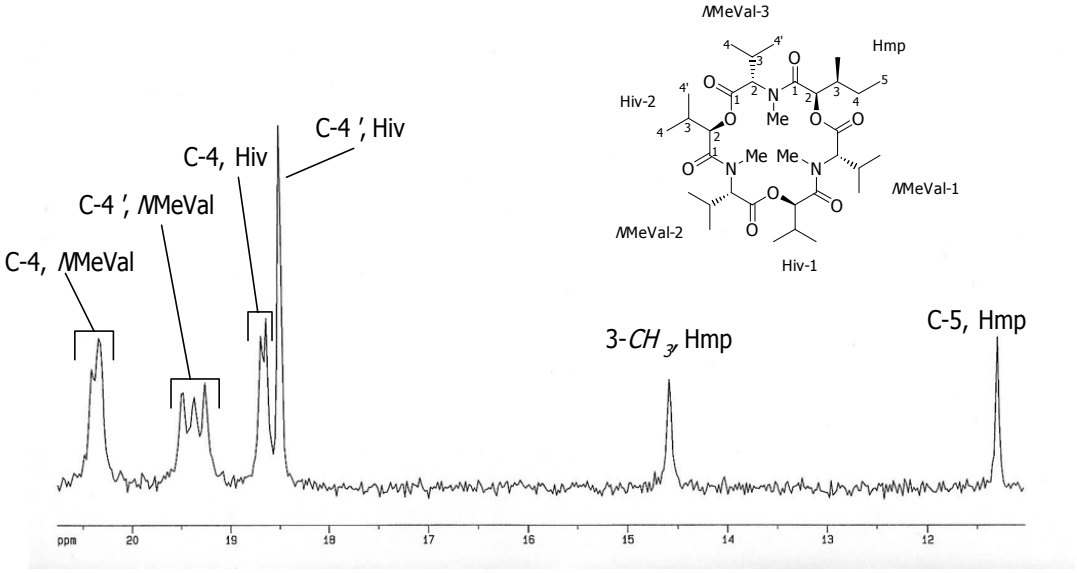

Figure 146. Expansion A of ^{13}C NMR spectrum of enniatin H **(57)**

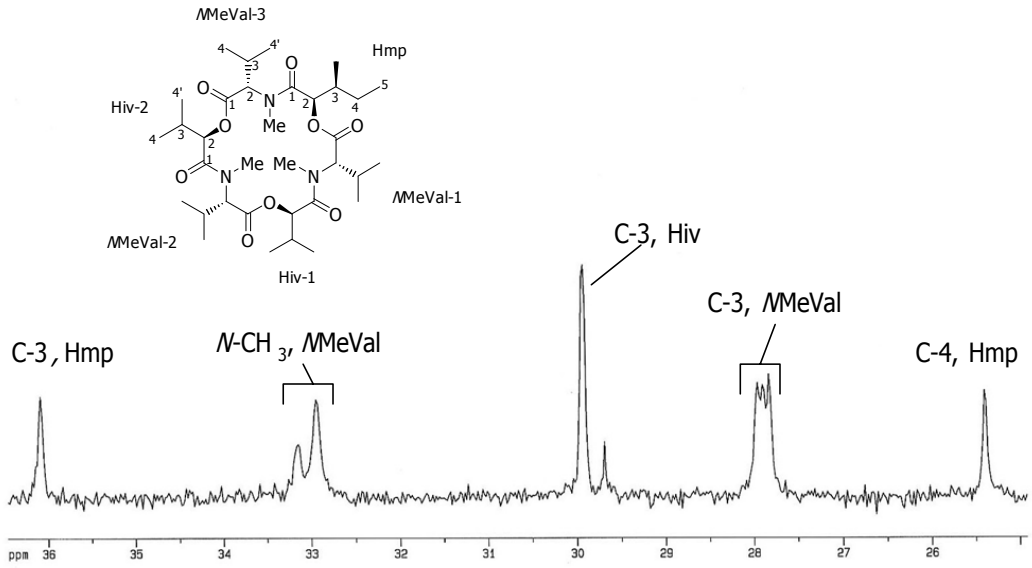

Figure 147. Expansion B of ^{13}C NMR spectrum of enniatin H **(57)**

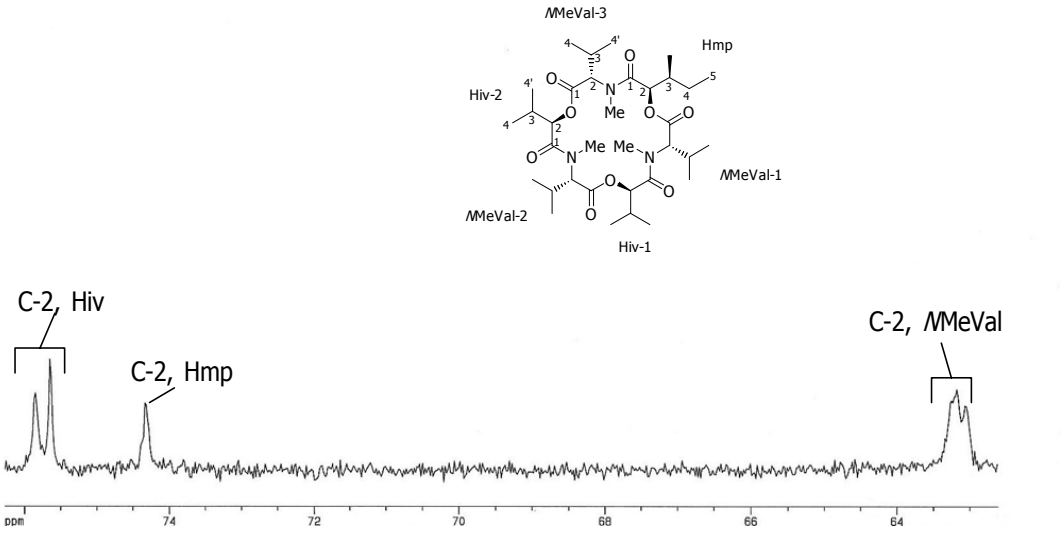

Figure 148. Expansion C of ^{13}C NMR spectrum of enniatin H **(57)**

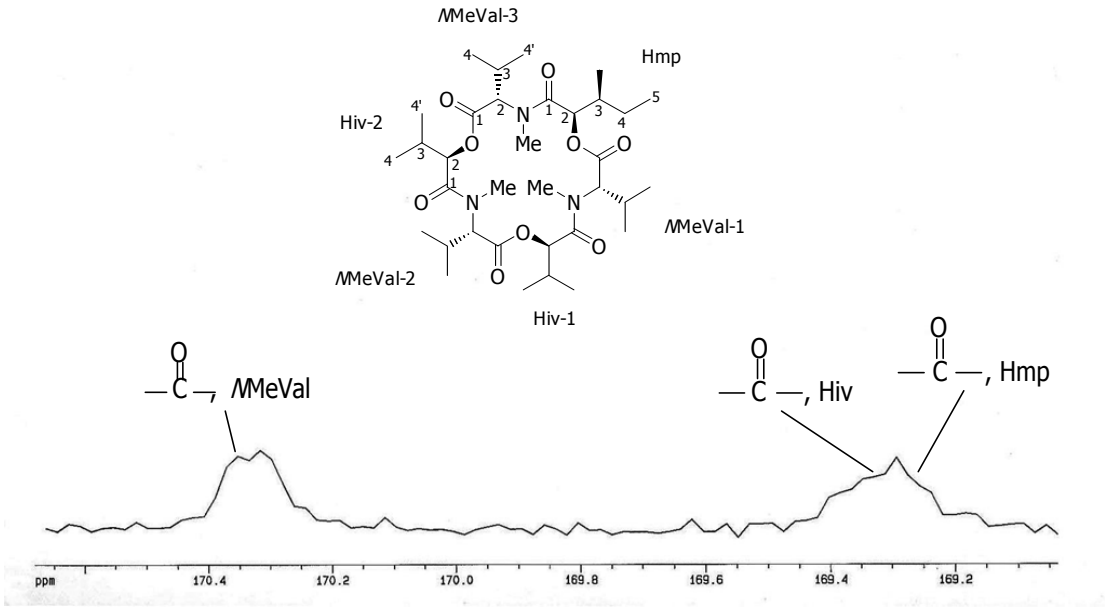

Figure 149. Expansion D of ^{13}C NMR spectrum of enniatin H **(57)**

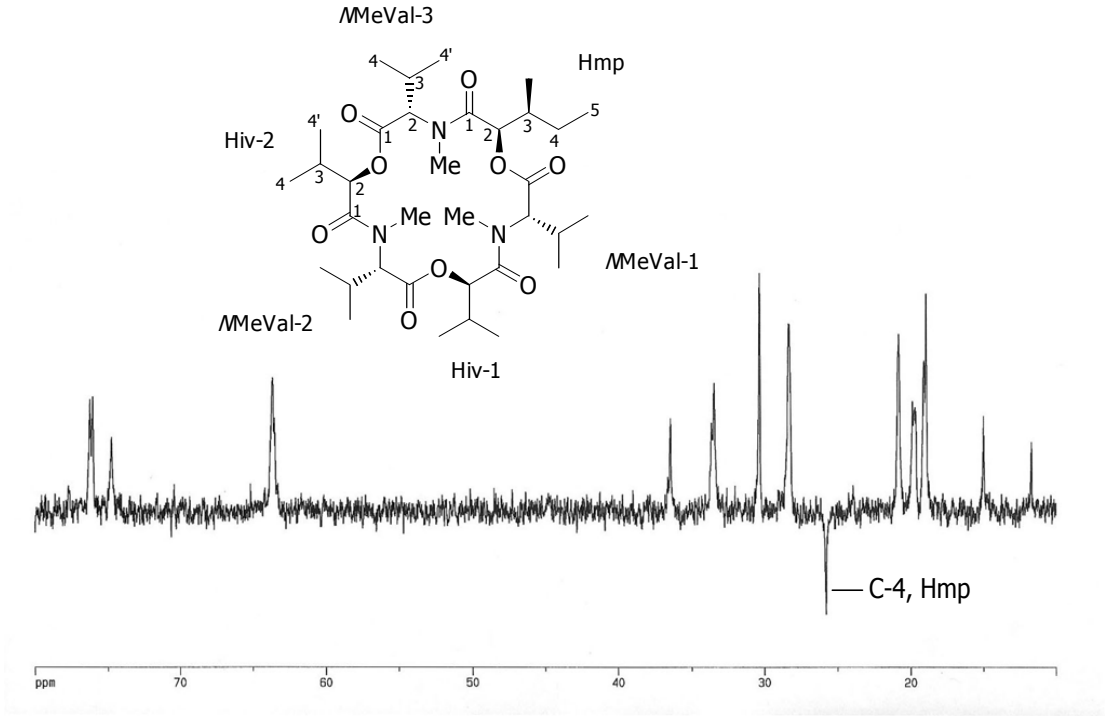

Figure 150. DEPT 135 spectrum of enniatin H **(57)**

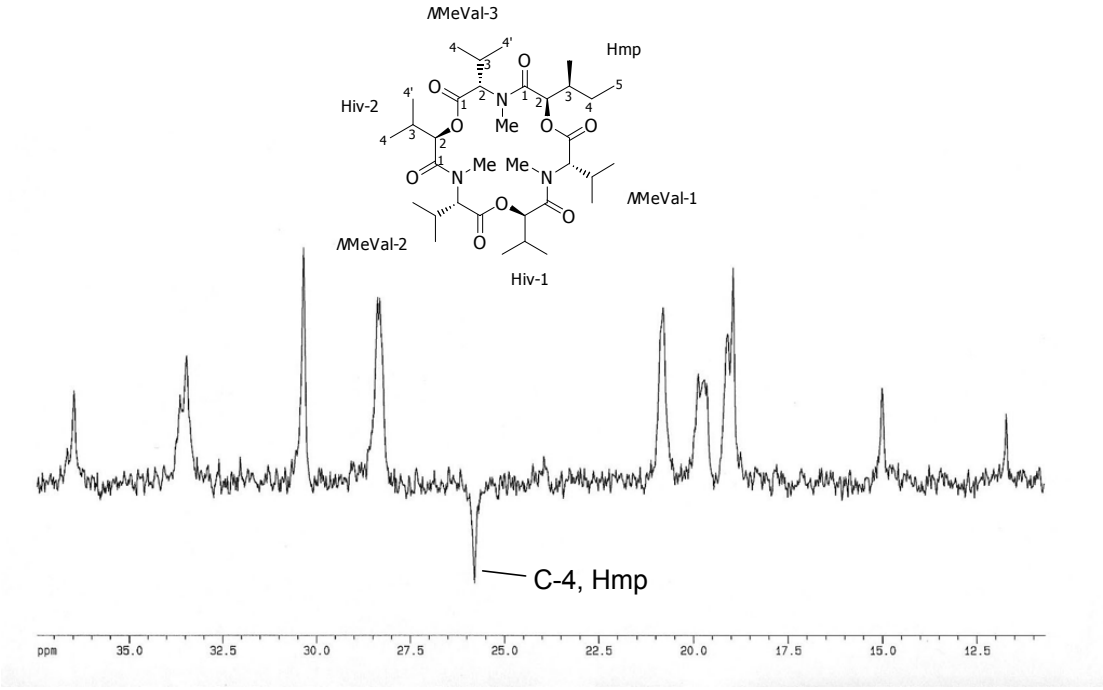

Figure 151. Expansion A of DEPT 135 spectrum of enniatin H **(57)**

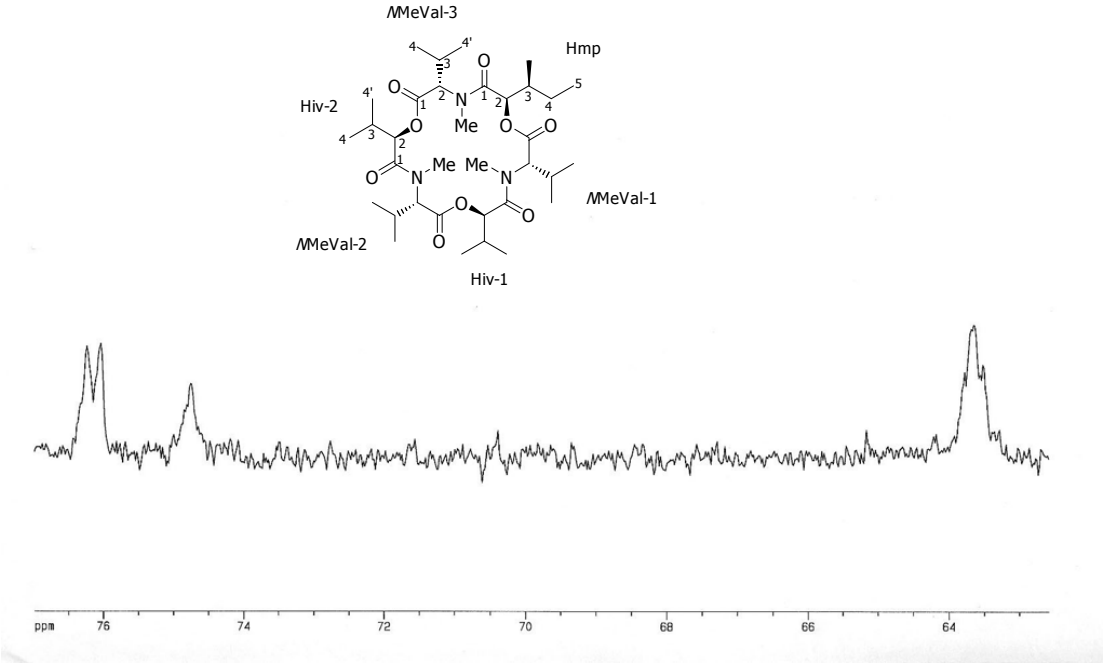

Figure 152. Expansion B of DEPT 135 spectrum of enniatin H **(57)**

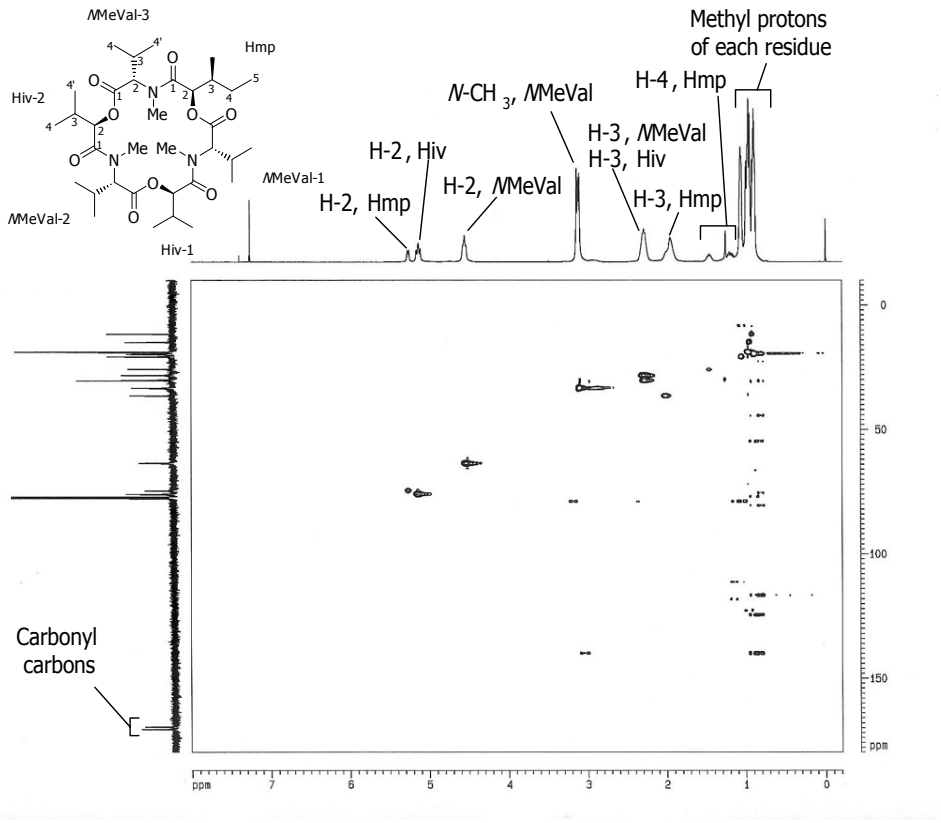

Figure 153. HMQC spectrum of enniatin H **(57)**

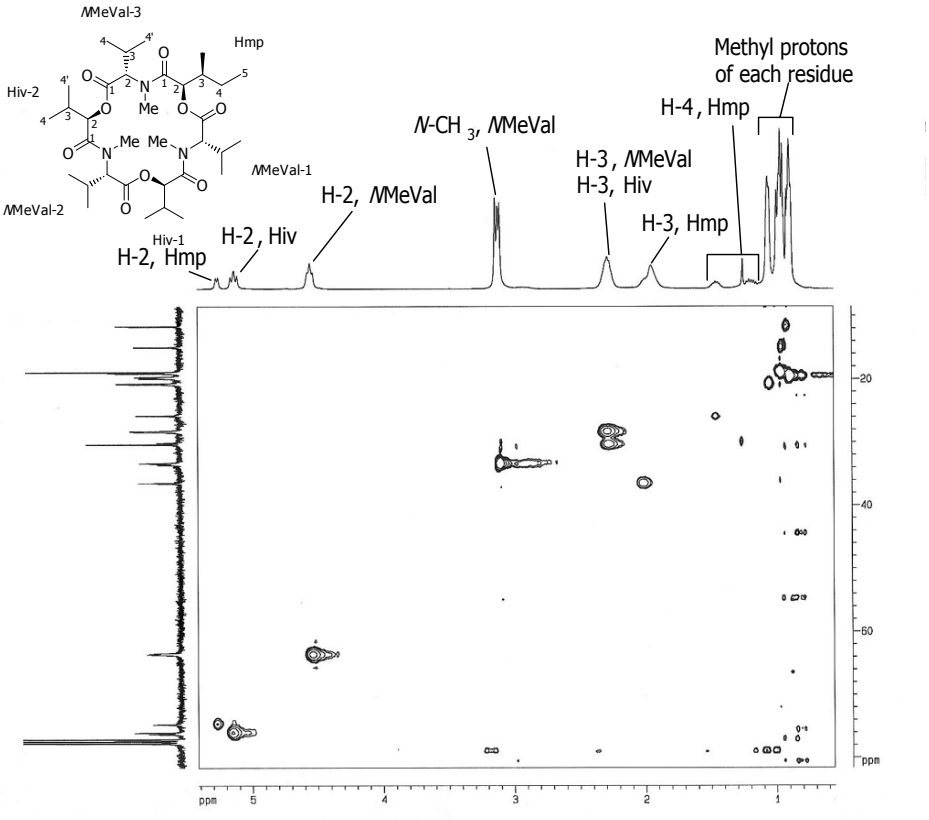

Figure 154. Expansion A of HMQC spectrum of enniatin H **(57)**

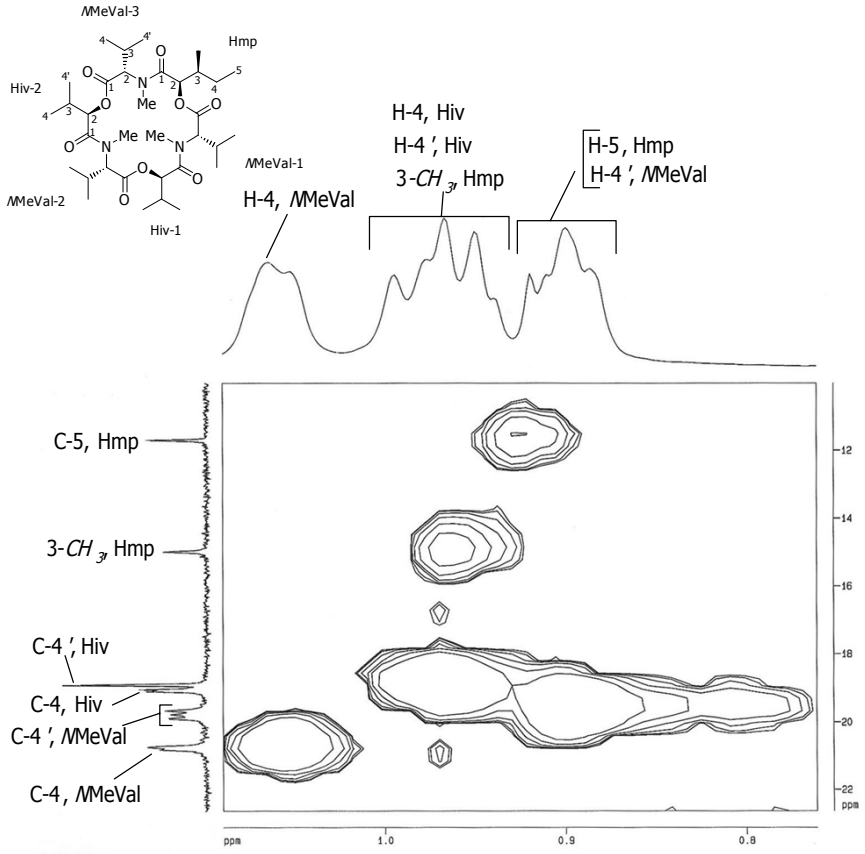

Figure 155. Expansion B of HMQC spectrum of enniatin H **(57)**

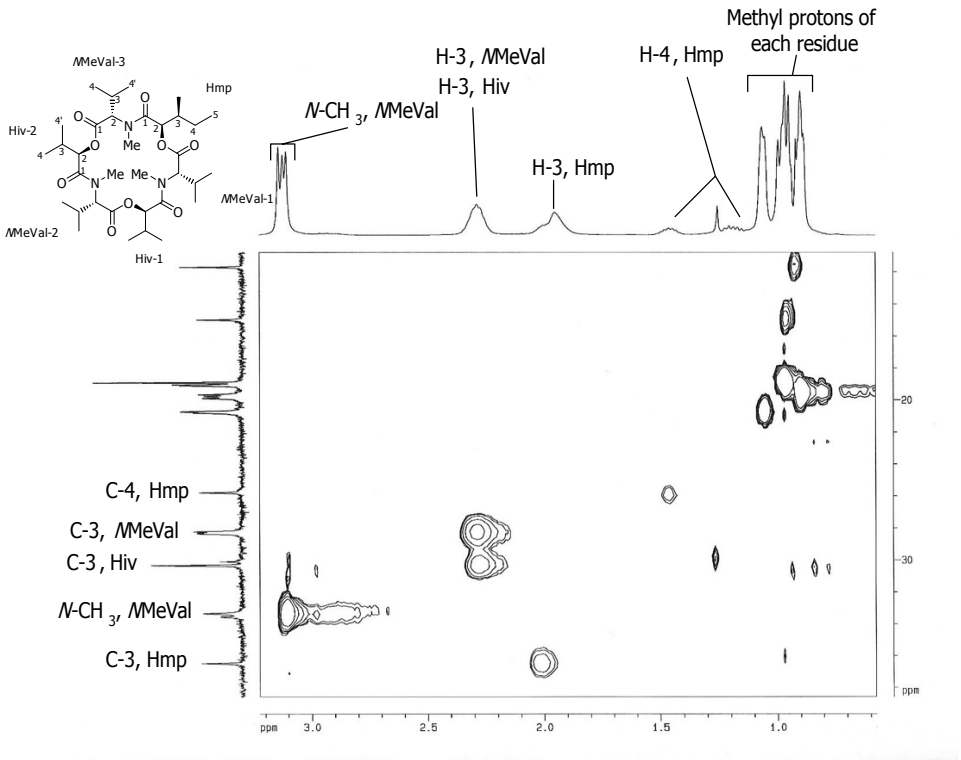

Figure 156. Expansion C of HMQC spectrum of enniatin H **(57)**

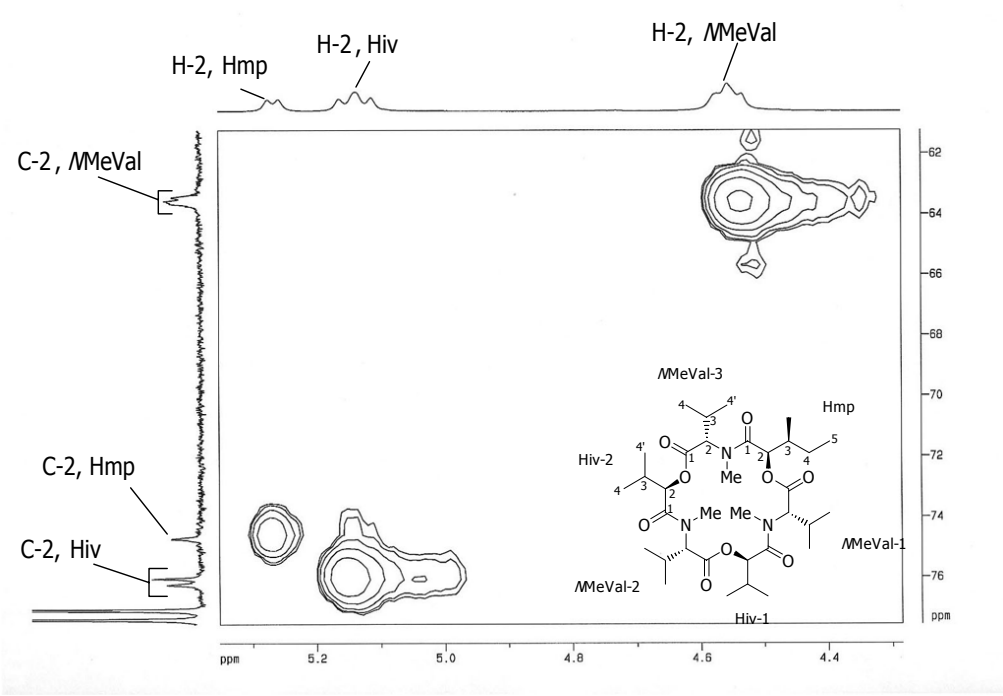

Figure 157. Expansion D of HMQC spectrum of enniatin H **(57)**

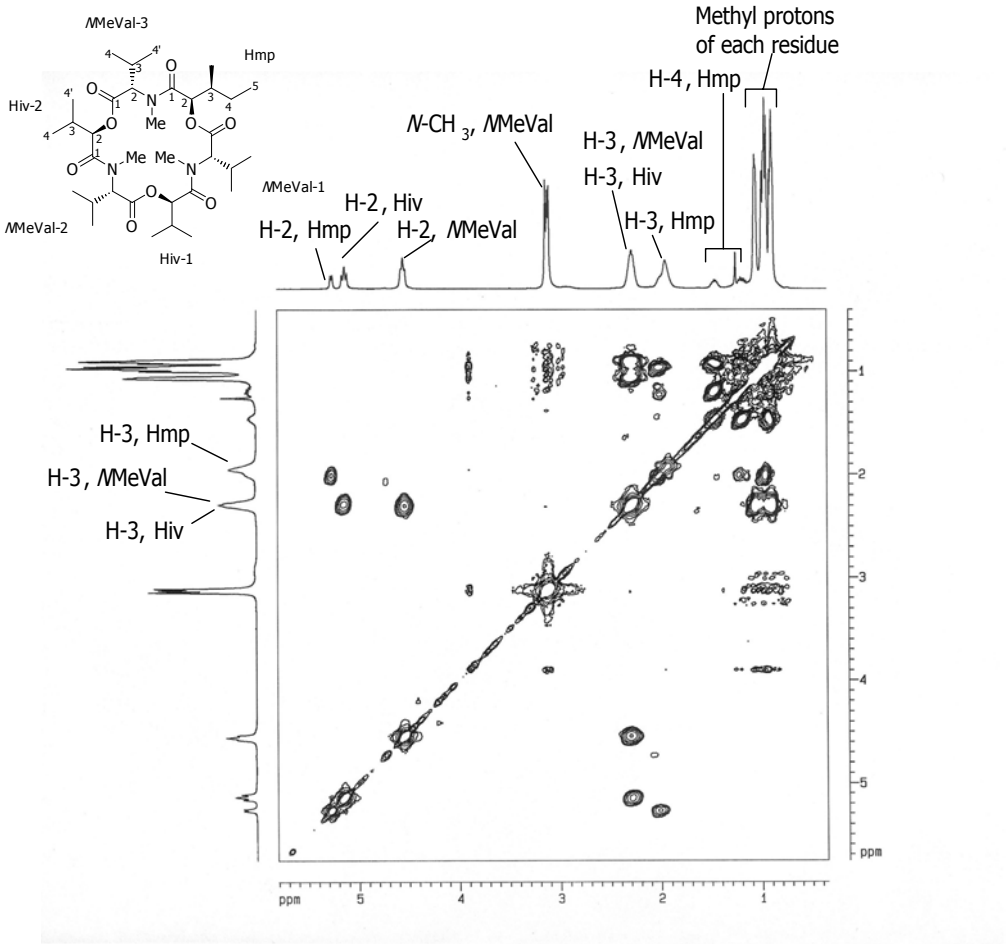

Figure 158. COSY spectrum of enniatin H **(57)**

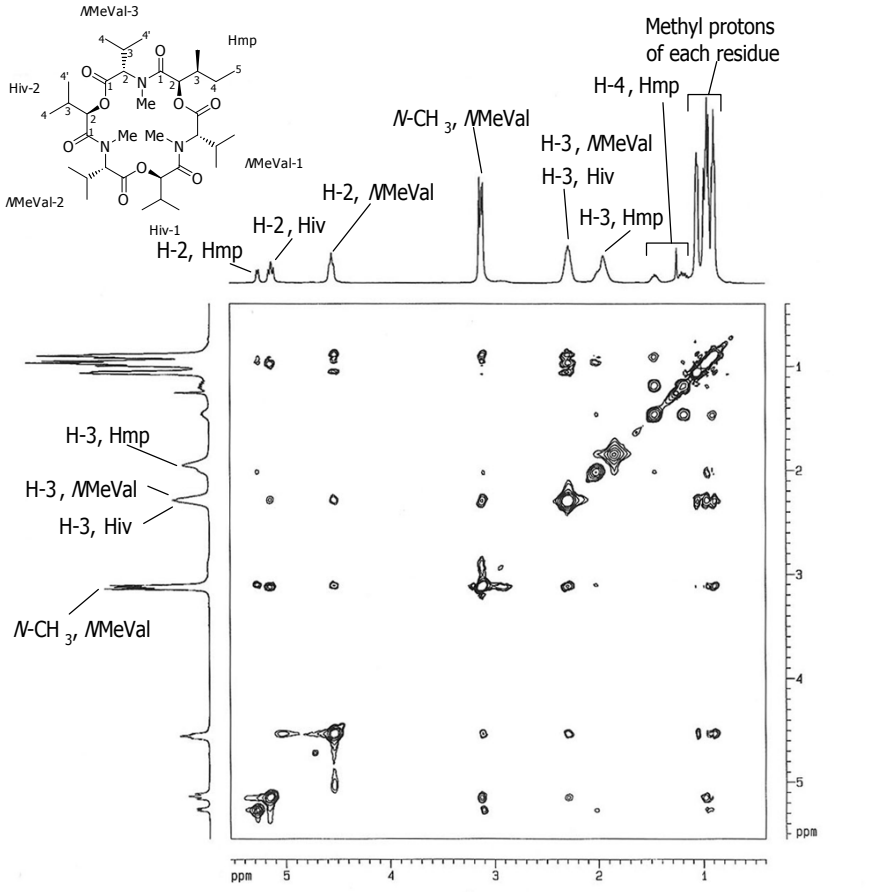

Figure 159. NOESY spectrum of enniatin H **(57)**

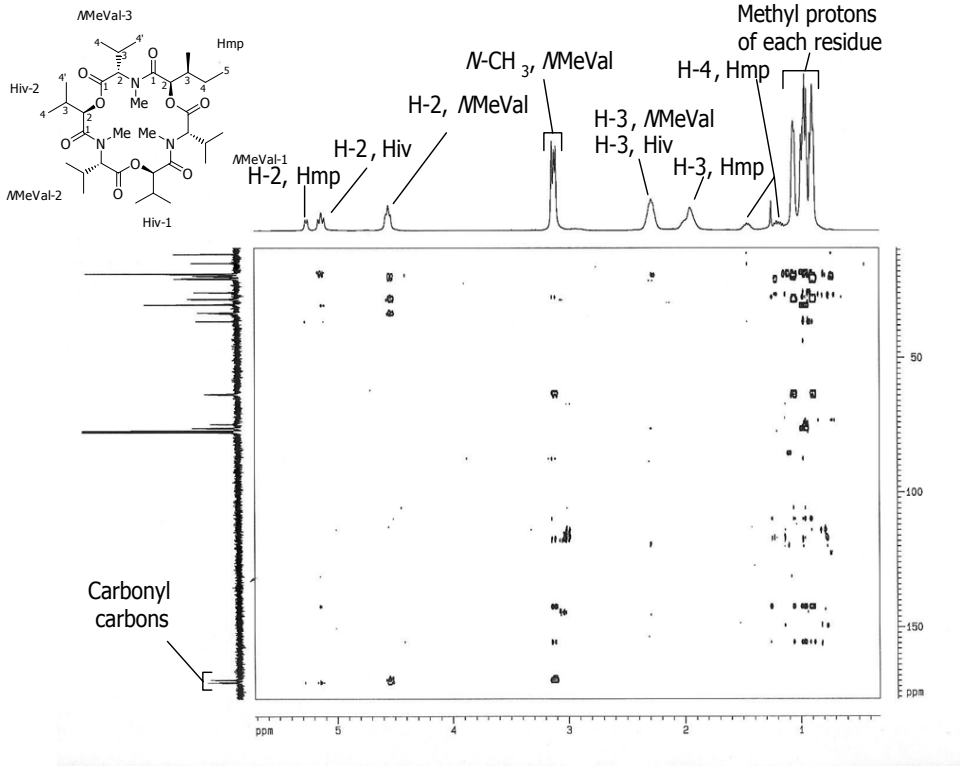

Figure 160. HMBC (d6 = 100 msec) spectrum of enniatin H **(57)**

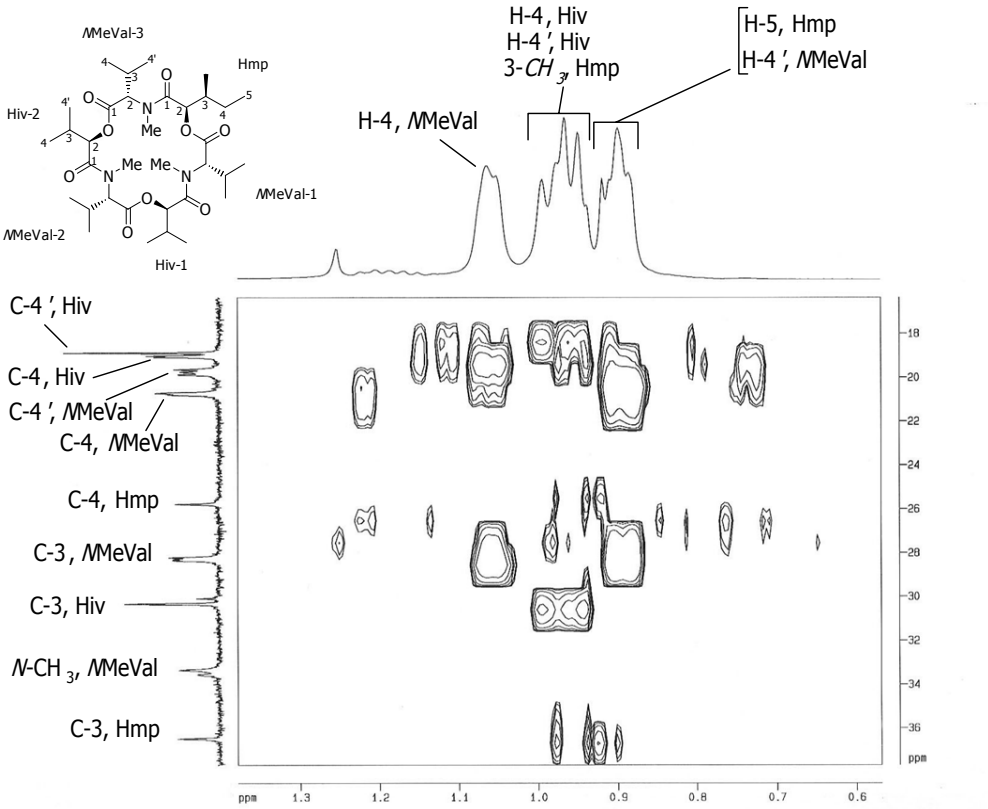

Figure 161. Expansion A of HMBC (d6 = 100 msec) spectrum of enniatin H **(57)**

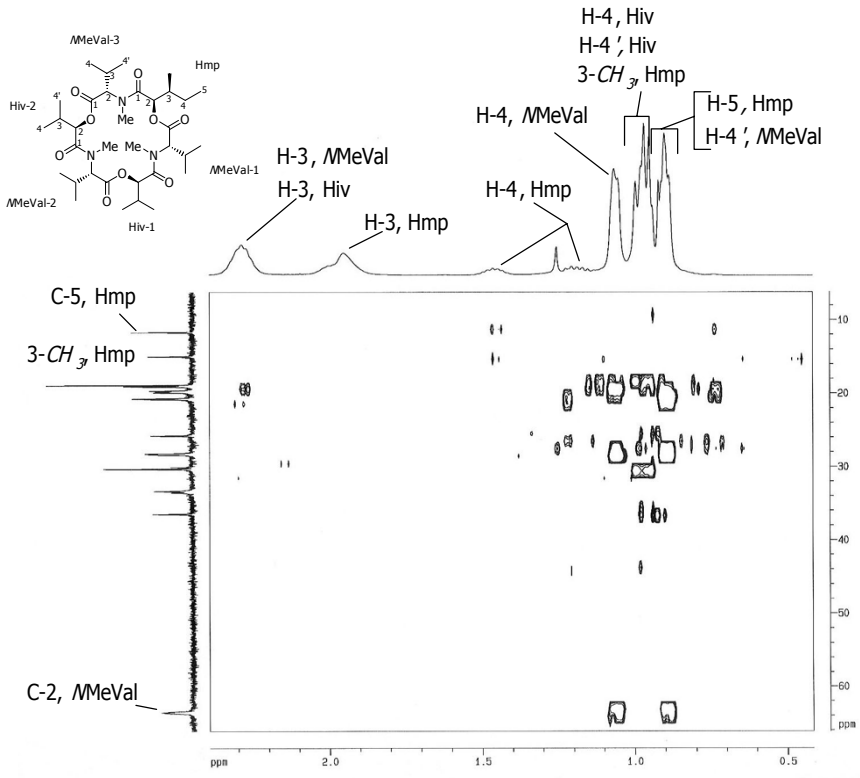

Figure 162. Expansion B of HMBC (d6 = 100 msec) spectrum of enniatin H **(57)**

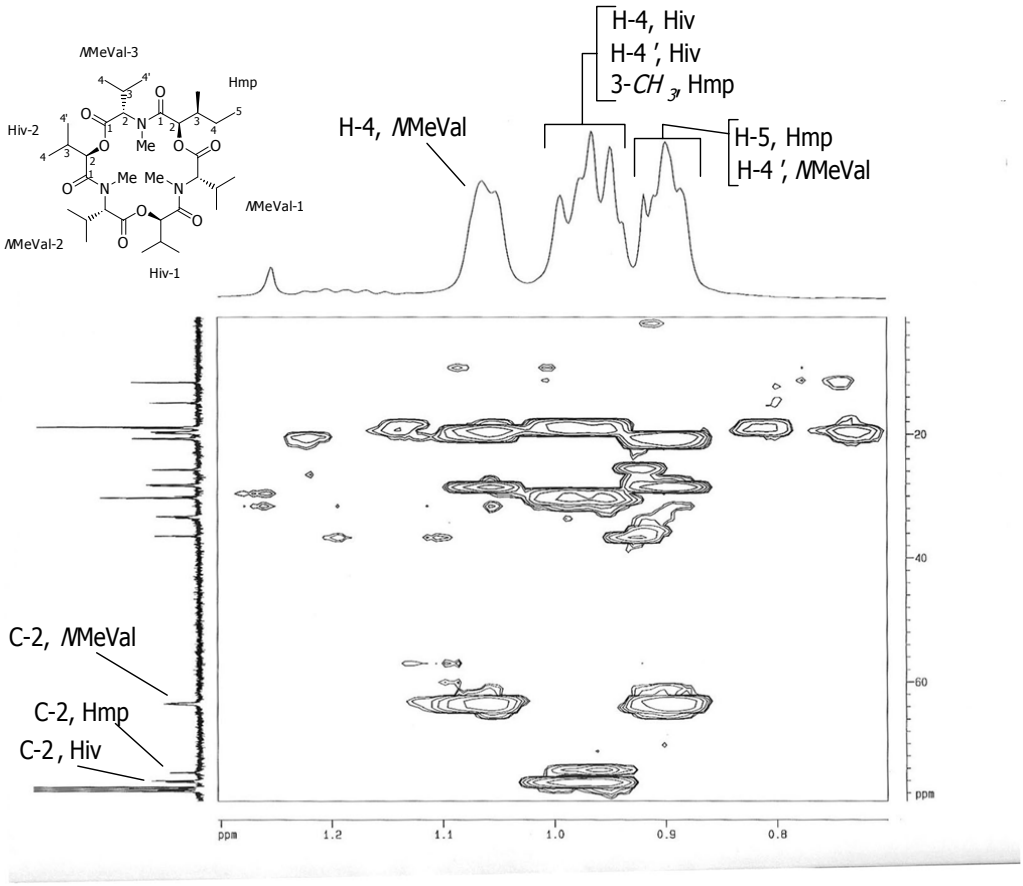

Figure 163. Expansion C of HMBC (d6 = 100 msec) spectrum of enniatin H **(57)**

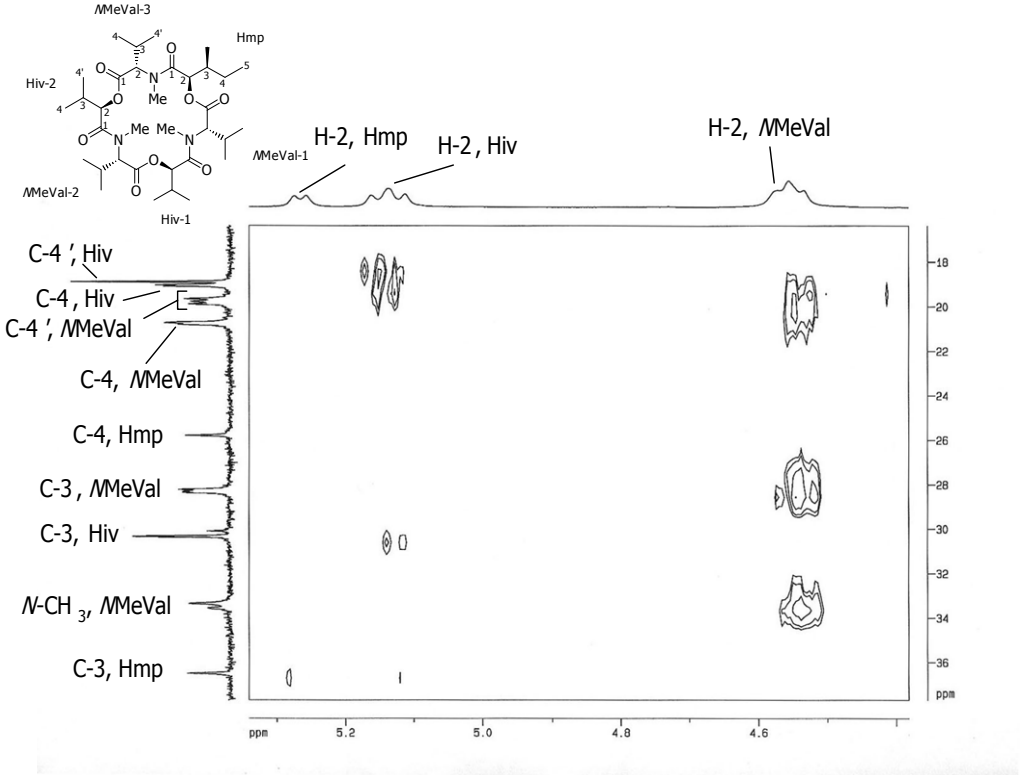

Figure 164. Expansion D of HMBC (d6 = 100 msec) spectrum of enniatin H **(57)**

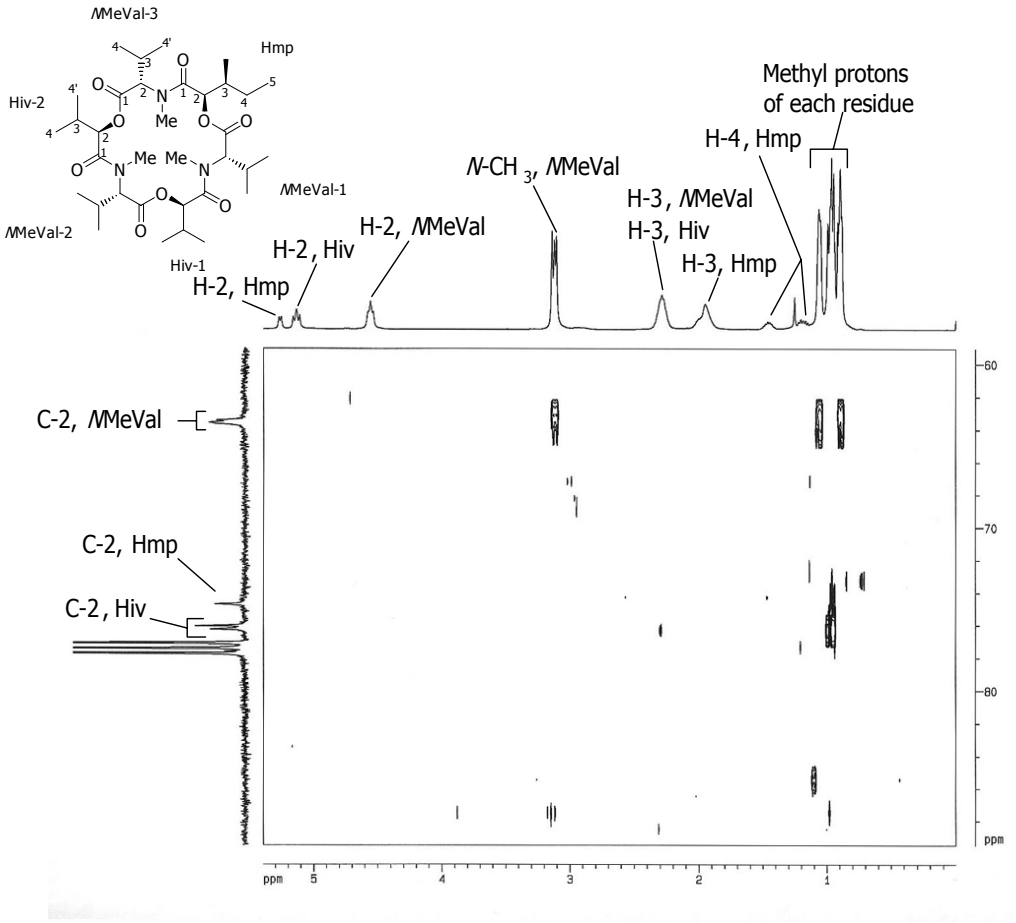

Figure 165. Expansion E of HMBC (d6 = 100 msec) spectrum of enniatin H **(57)**

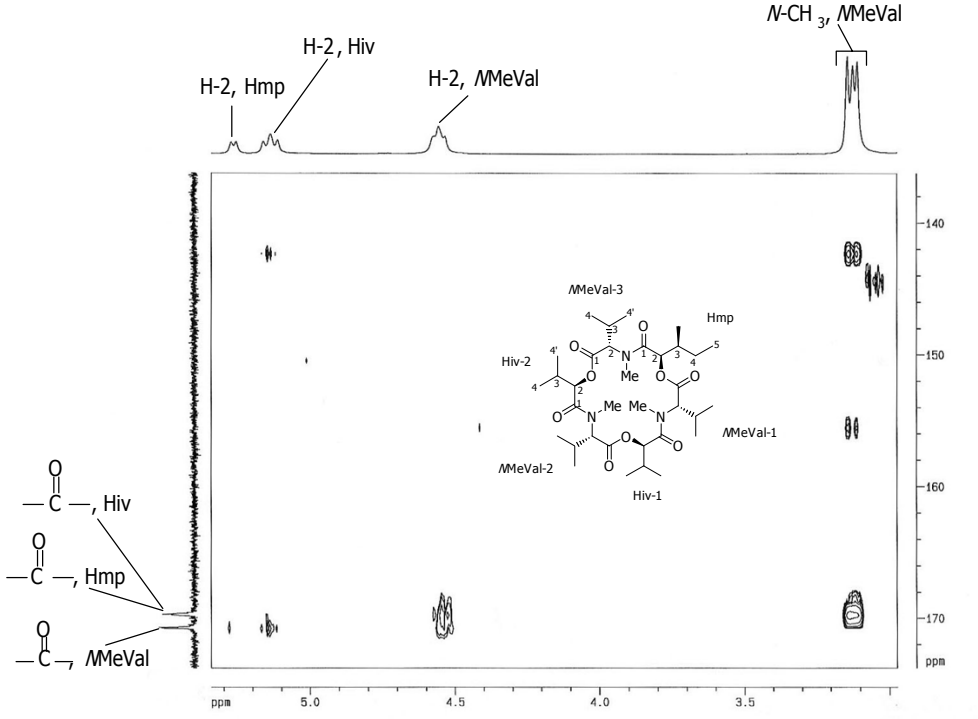

Figure 166. Expansion F of HMBC (d6 = 100 msec) spectrum of enniatin H **(57)**

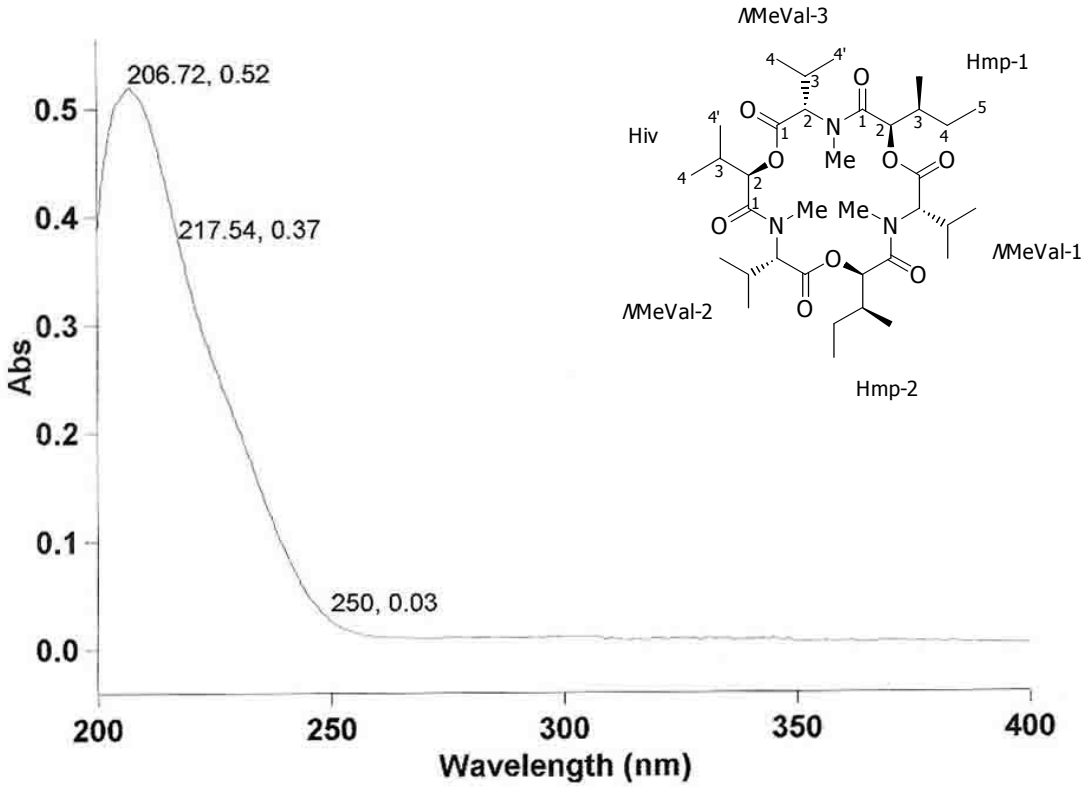

Figure 167. UV spectrum of enniatin I **(58)**

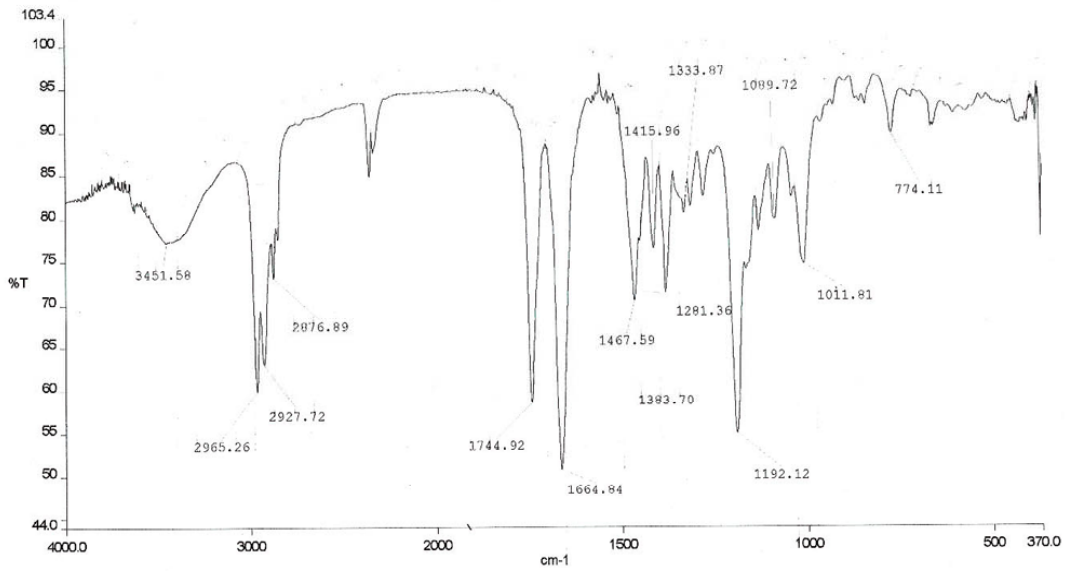

Figure 168. IR spectrum of enniatin I **(58)**

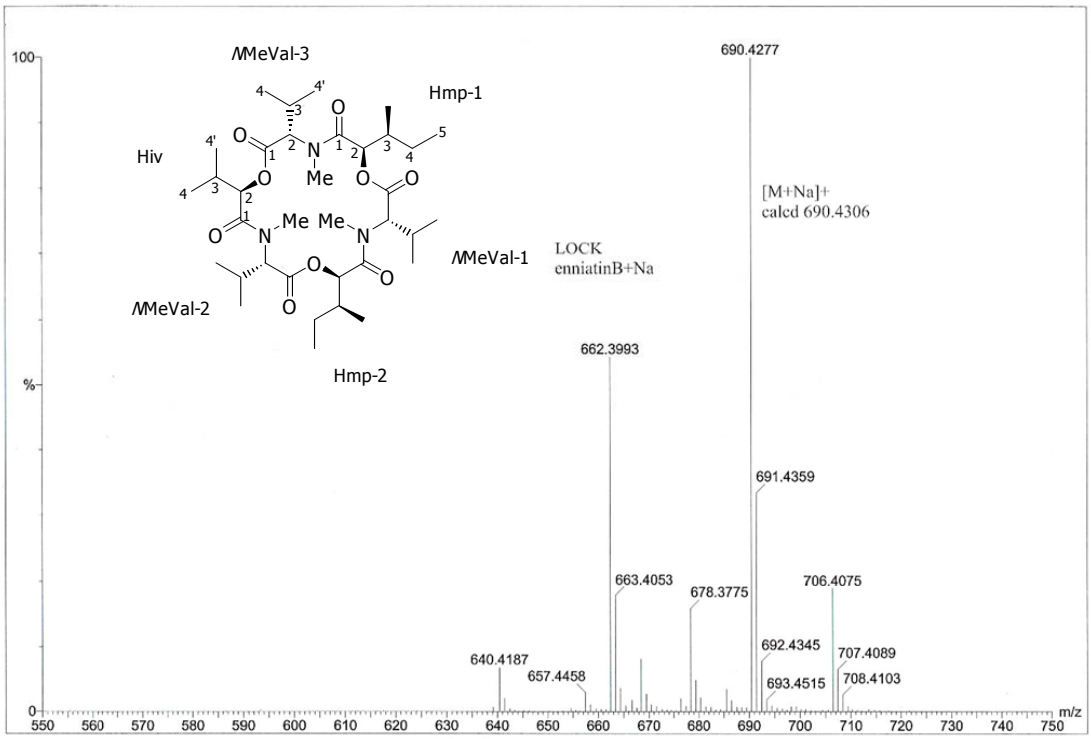

Figure 169. HRMS spectrum of enniatin I **(58)**

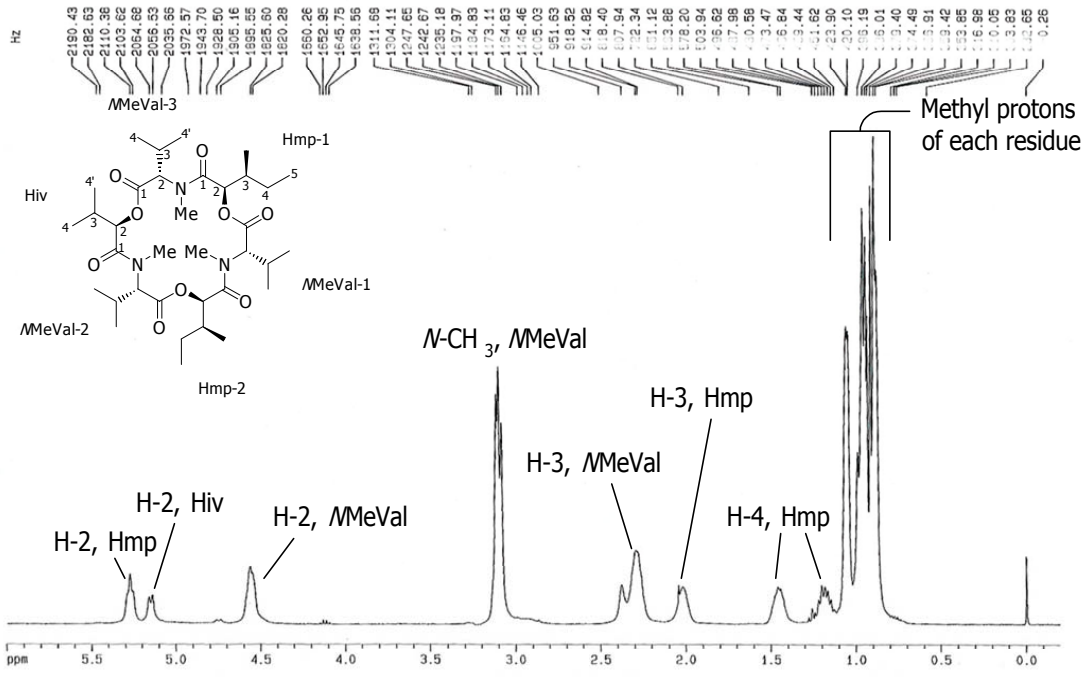

Figure 170. ^{1}H NMR ($CDCl_3$) spectrum of enniatin I **(58)**

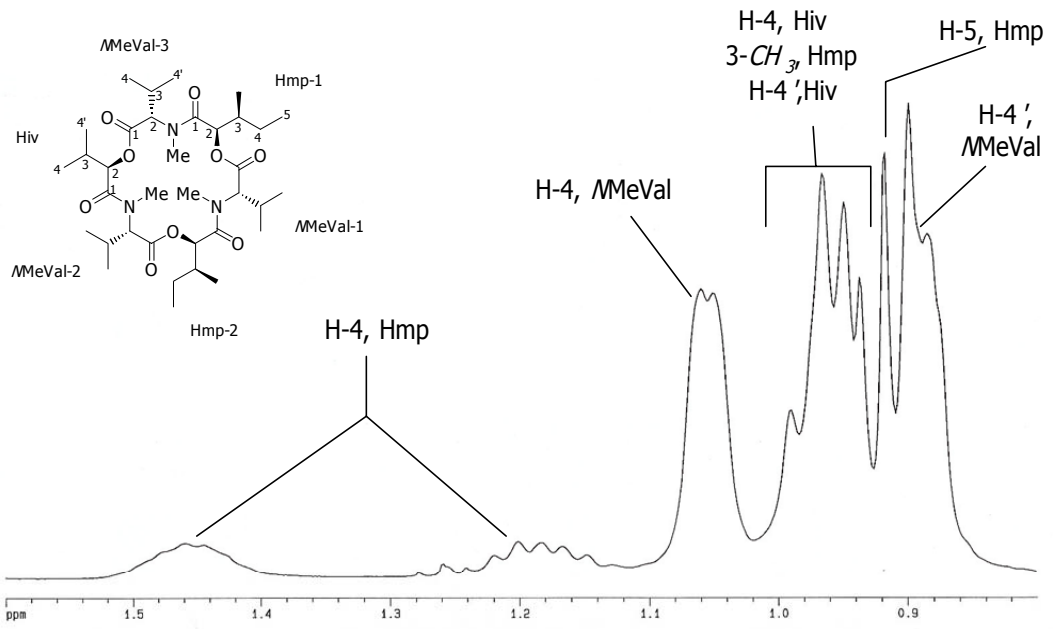

Figure 171. Expansion A of ^{1}H NMR ($CDCl_3$) spectrum of enniatin I **(58)**

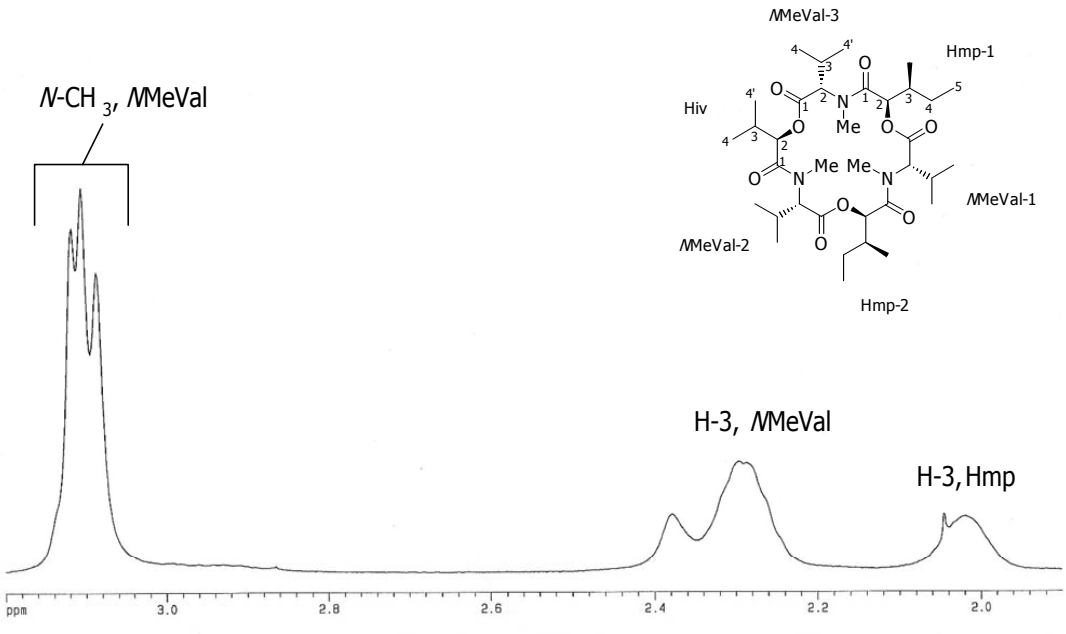

Figure 172. Expansion B of ^{1}H NMR ($CDCl_3$) spectrum of enniatin I **(58)**

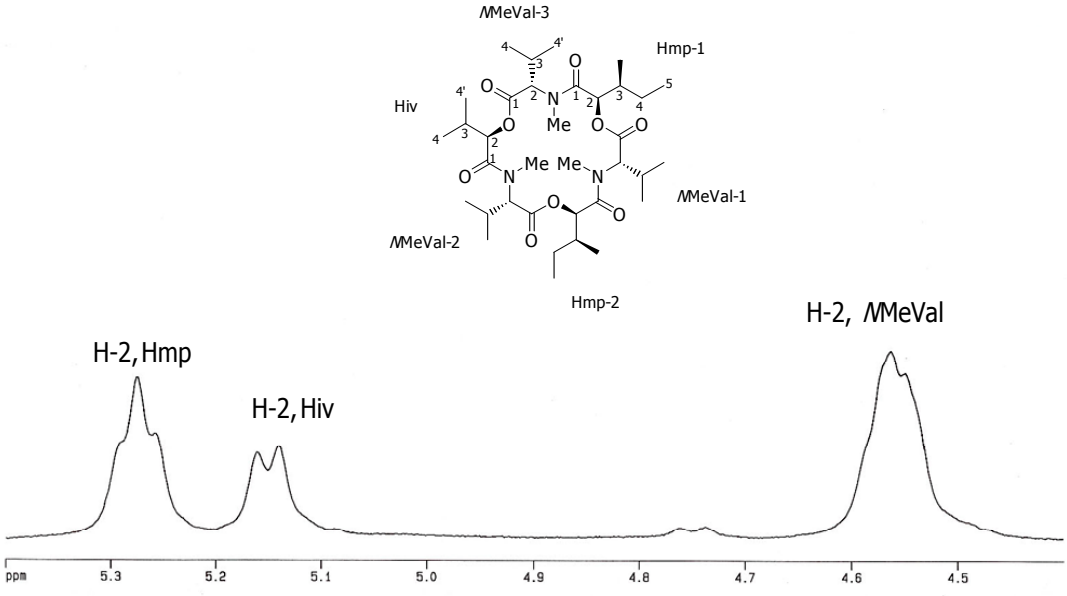

Figure 173. Expansion C of ^{1}H NMR ($CDCl_3$) spectrum of enniatin I **(58)**

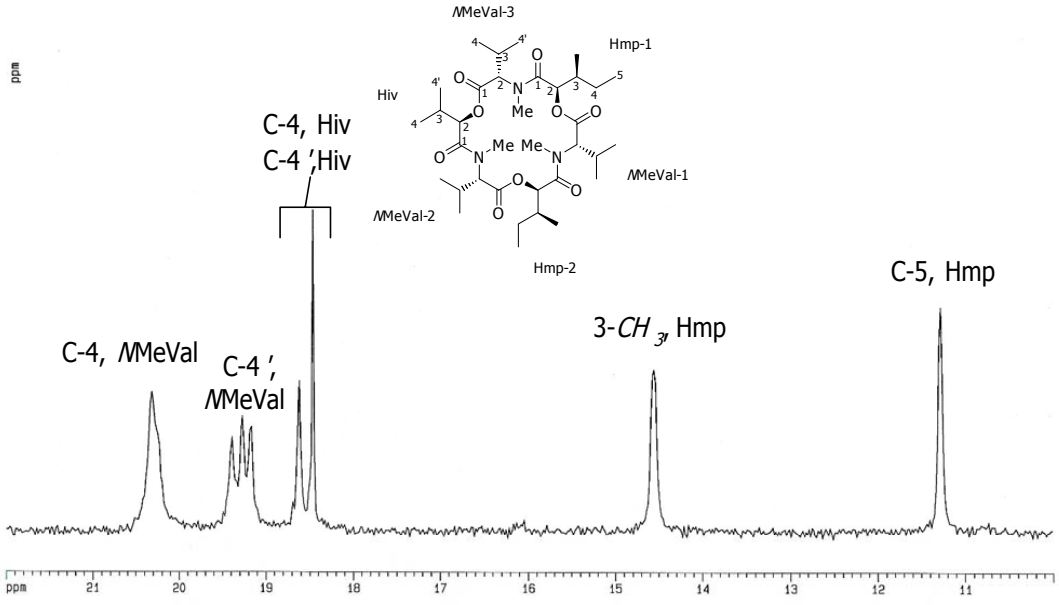

Figure 174. Expansion A of ^{13}C NMR spectrum of enniatin I **(58)**

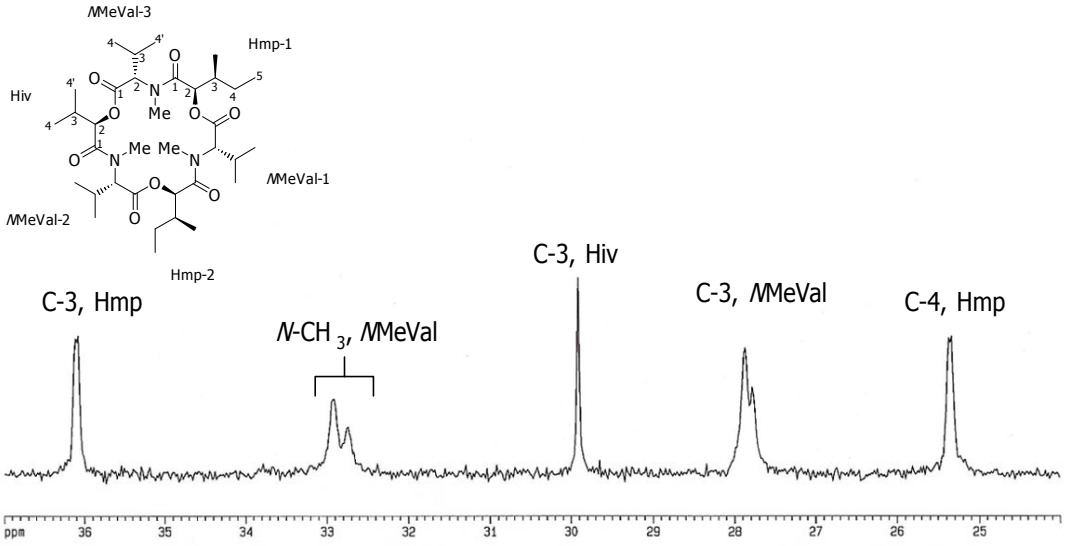

Figure 175. Expansion B of ^{13}C NMR spectrum of enniatin I **(58)**

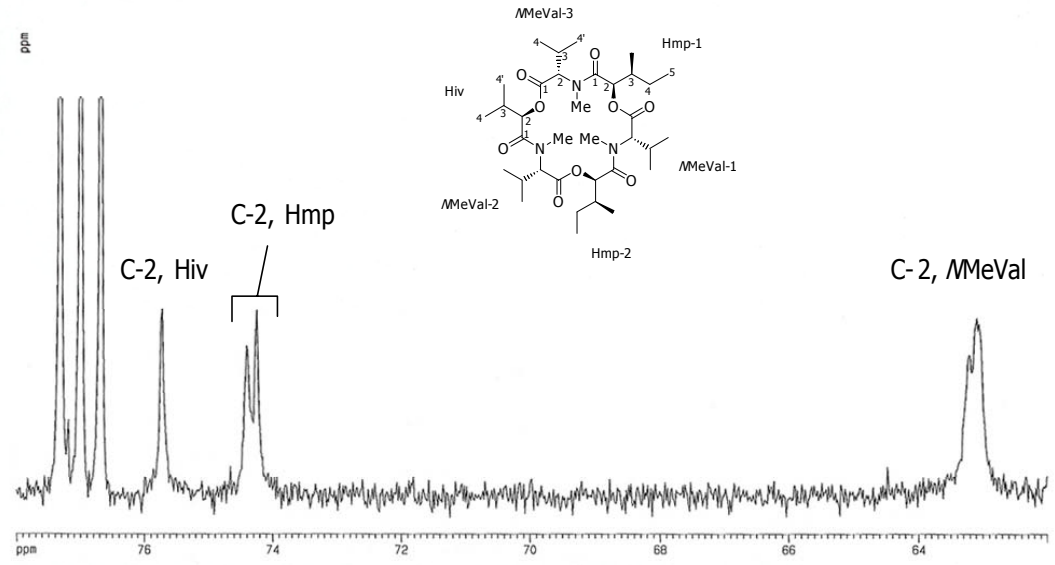

Figure 176. Expansion C of ^{13}C NMR spectrum of enniatin I **(58)**

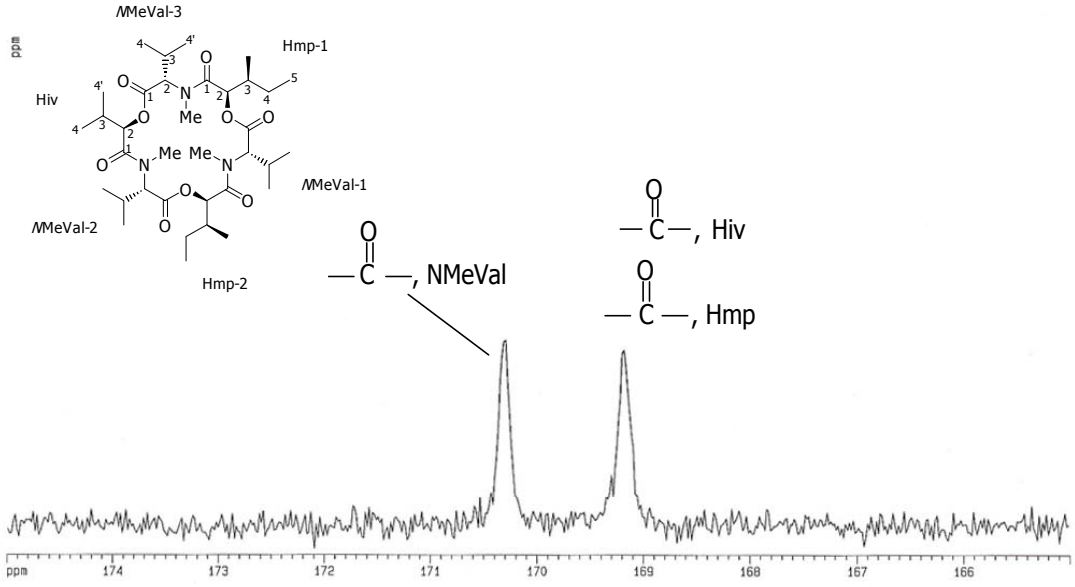

Figure 177. Expansion D of ^{13}C NMR spectrum of enniatin I **(58)**

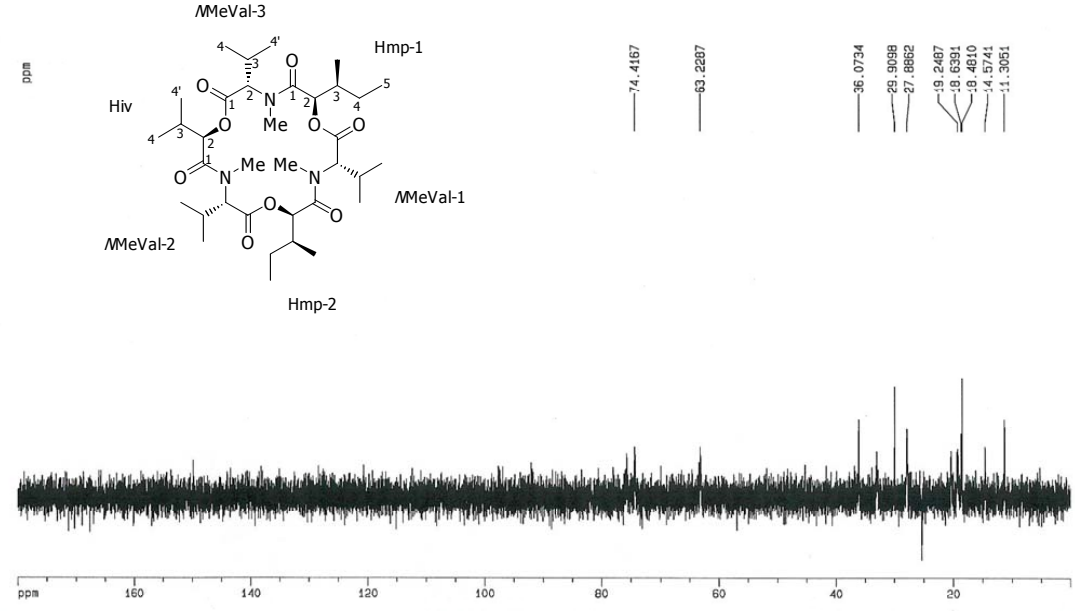

Figure 178. DEPT 135 spectrum of enniatin I **(58)**

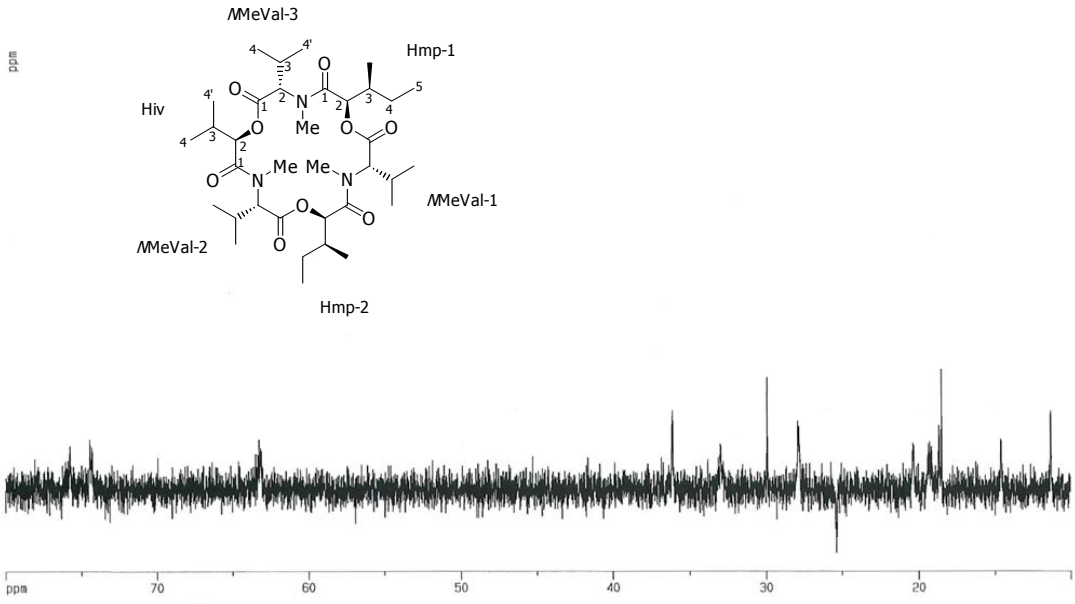

Figure 179. Expansion of DEPT 135 spectrum of enniatin I **(58)**

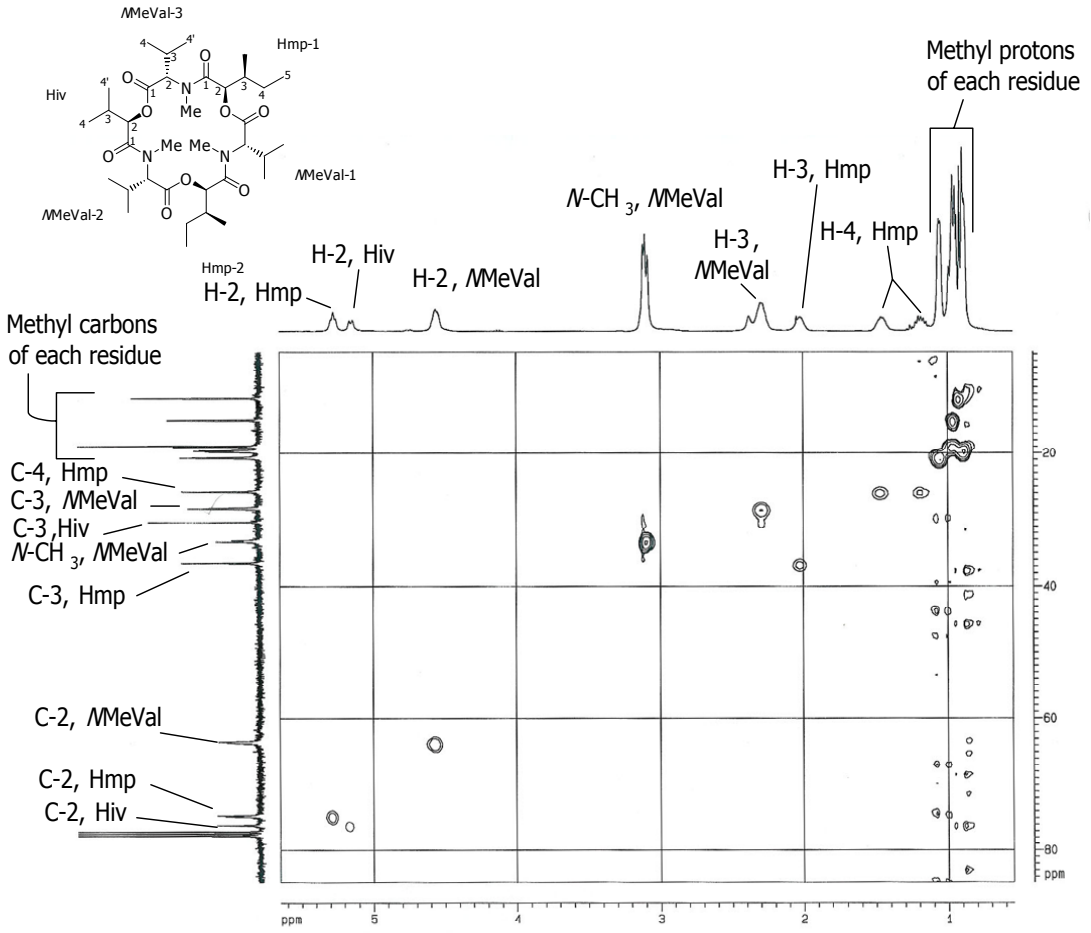

Figure 180. HMQC spectrum of enniatin I **(58)**

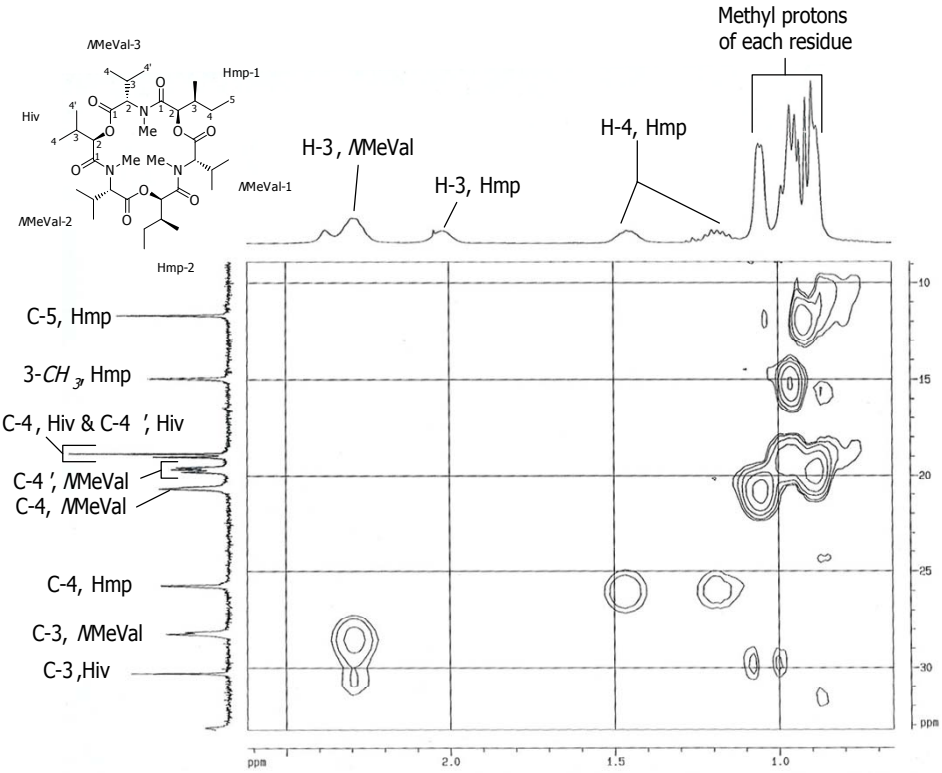

Figure 181. Expansion A of HMQC spectrum of enniatin I **(58)**

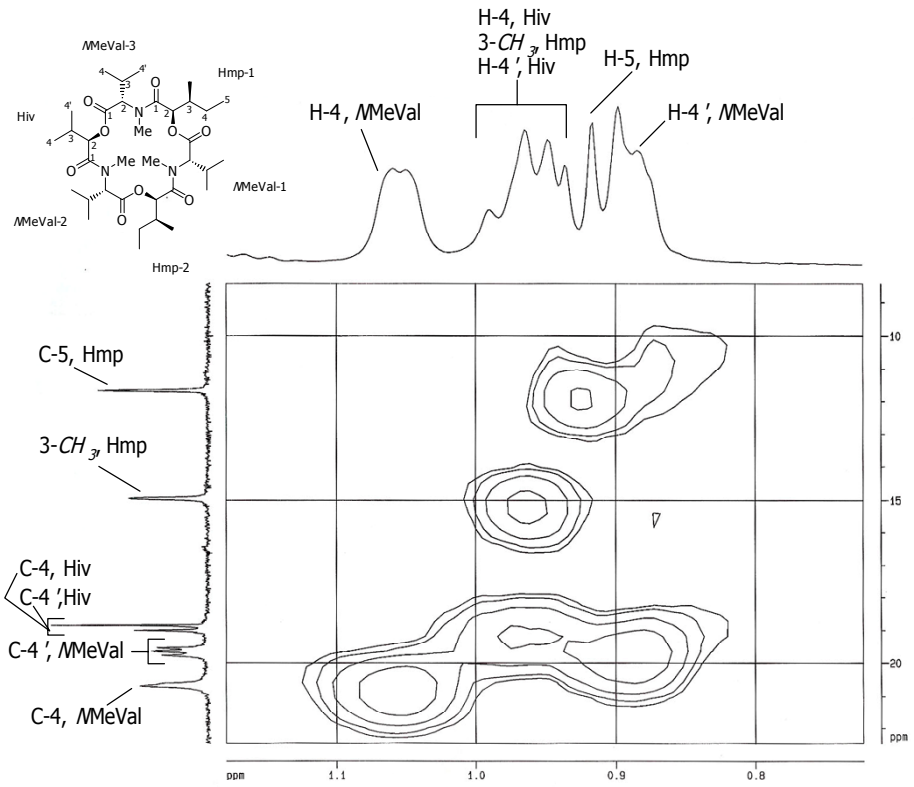

Figure 182. Expansion B of HMQC spectrum of enniatin I **(58)**

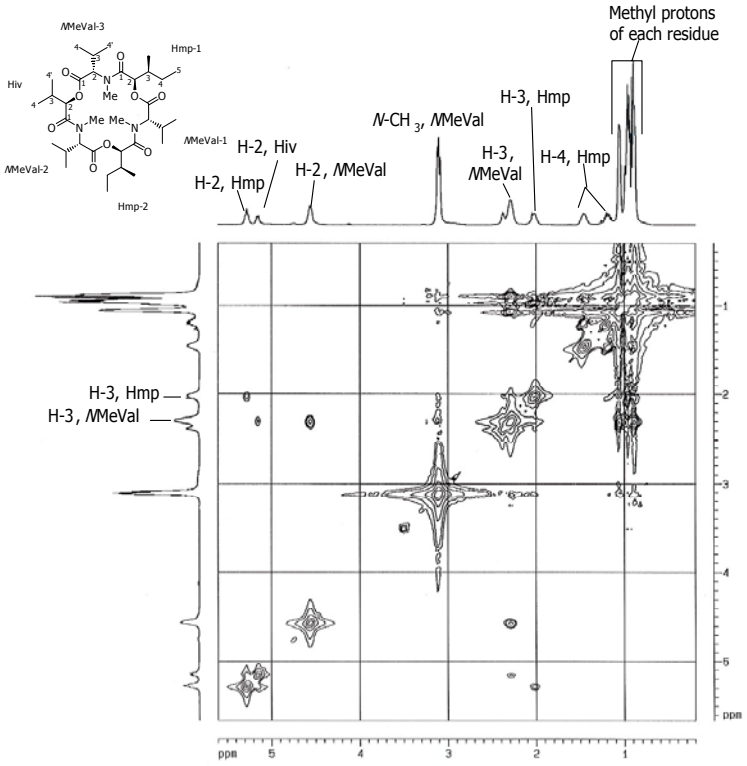

Figure 183. COSY spectrum of enniatin I **(58)**

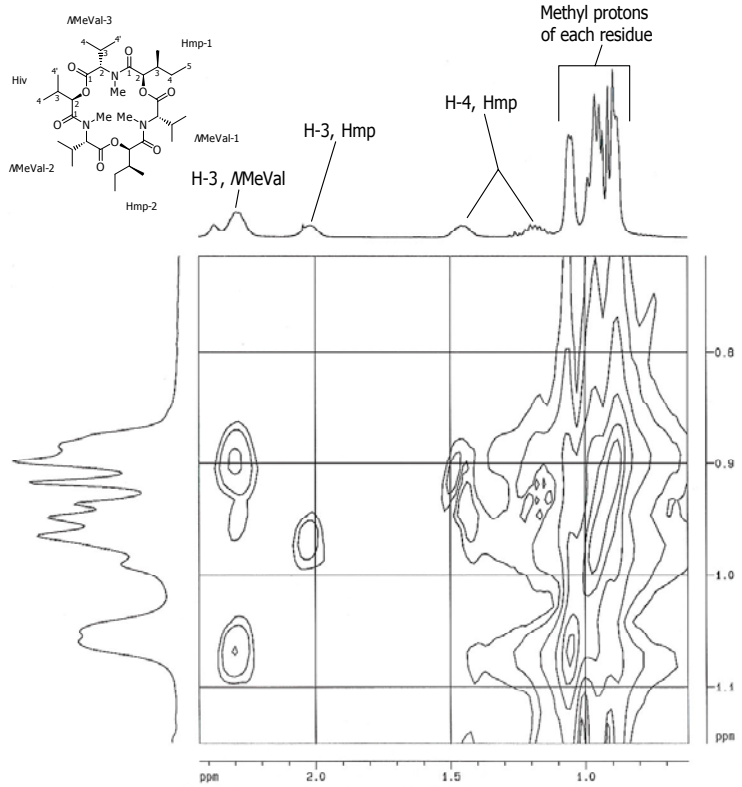

Figure 184. Expansion of COSY spectrum of enniatin I **(58)**

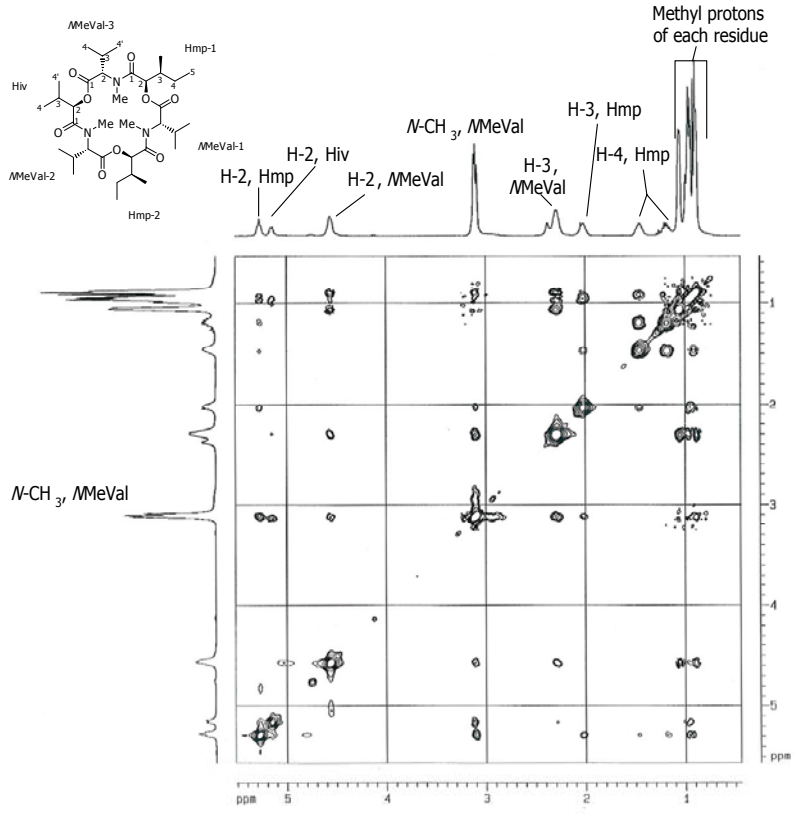

Figure 185. NOESY spectrum of enniatin I **(58)**

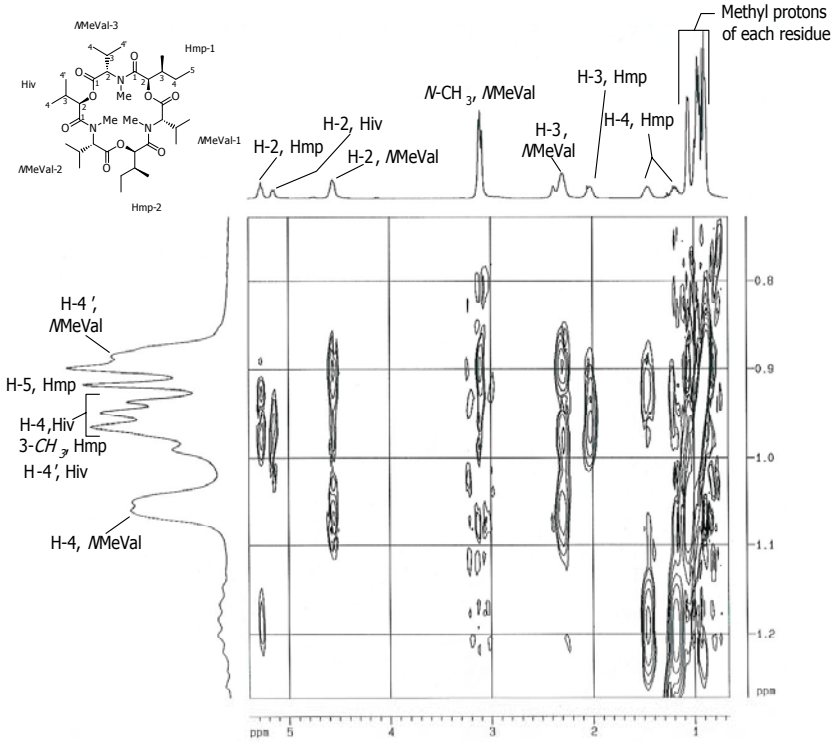

Figure 186. Expansion A of NOESY spectrum of enniatin I **(58)**

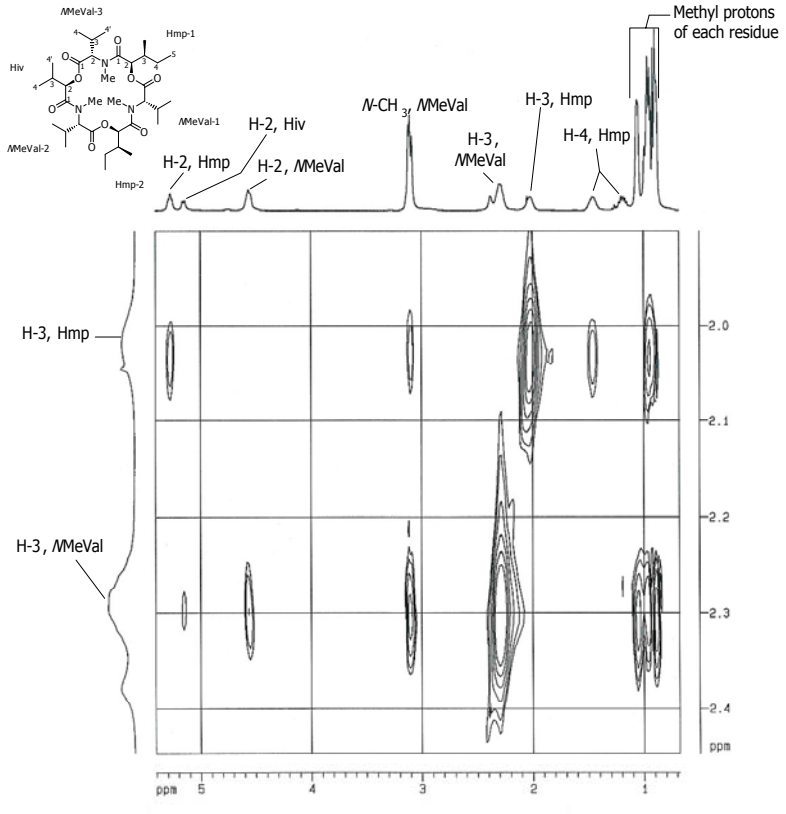

Figure 187. Expansion B of NOESY spectrum of enniatin I **(58)**

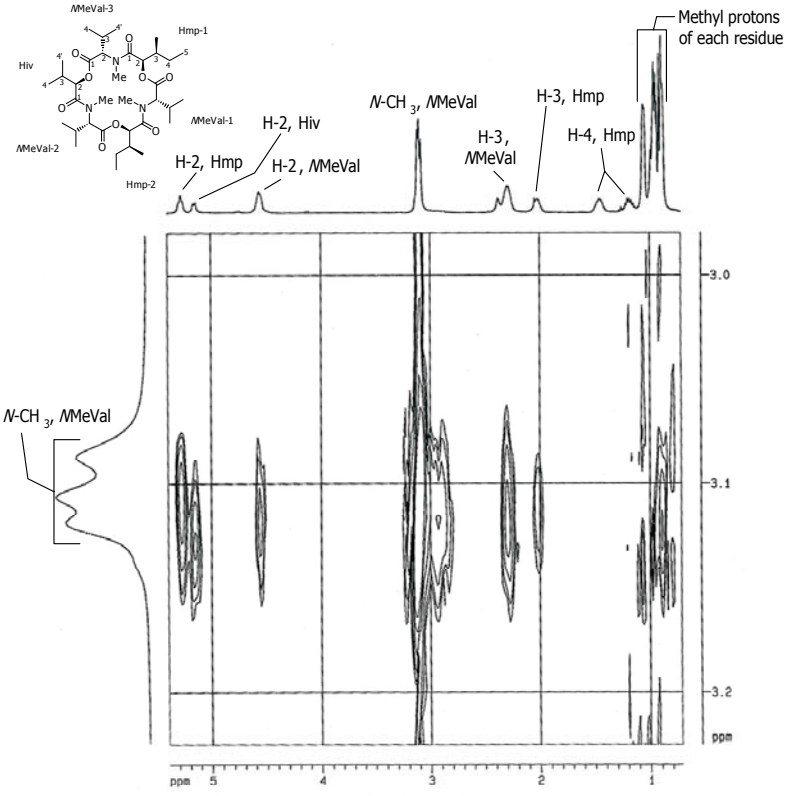

Figure 188. Expansion C of NOESY spectrum of enniatin I **(58)**

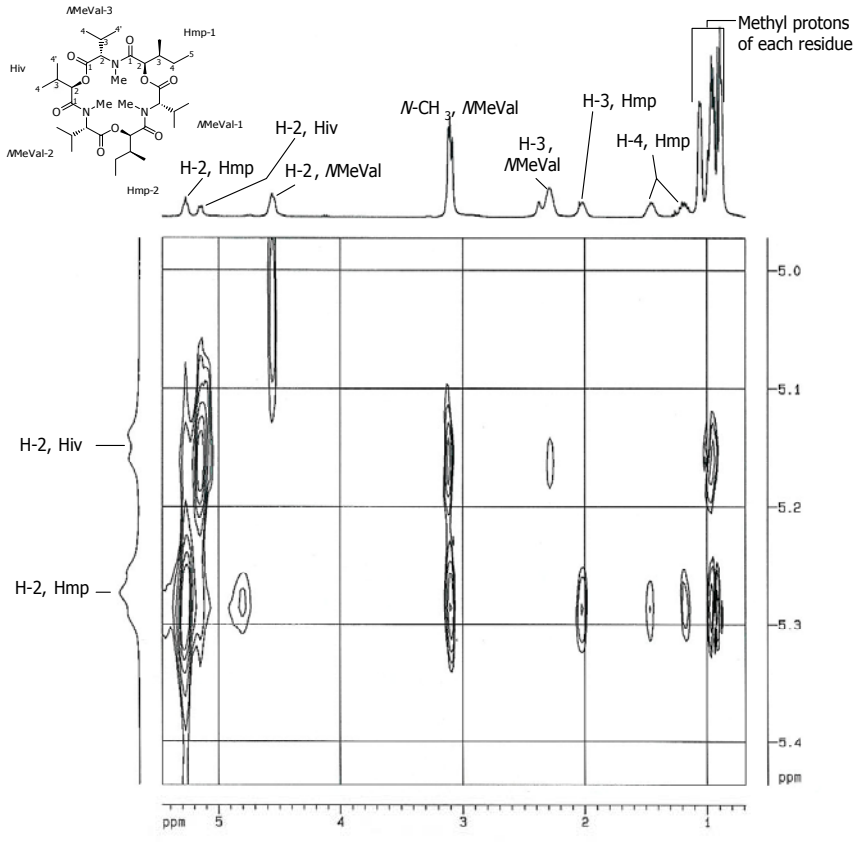

Figure 189. Expansion D of NOESY spectrum of enniatin I **(58)**

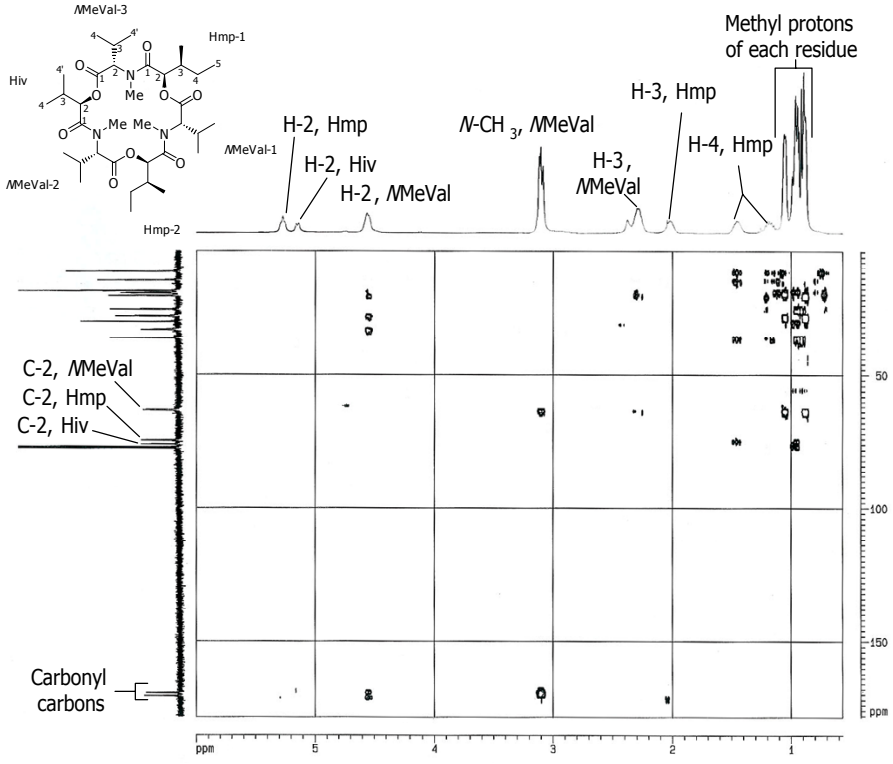

Figure 190. HMBC spectrum of enniatin I **(58)**

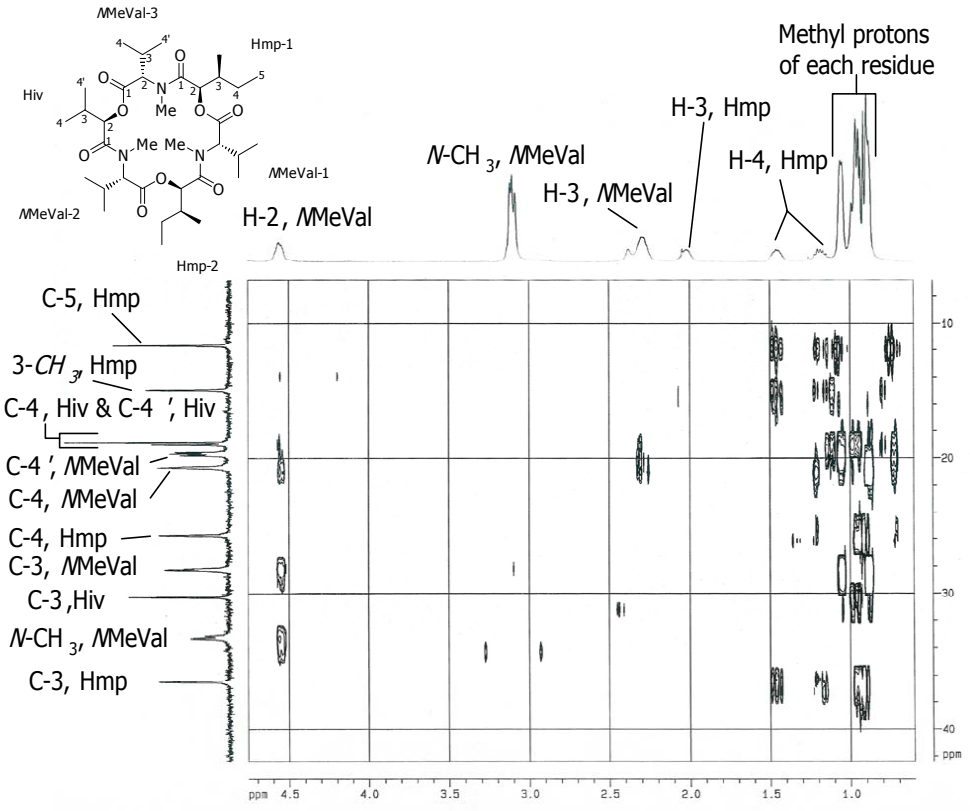

Figure 191. Expansion A of HMBC spectrum of enniatin I **(58)**

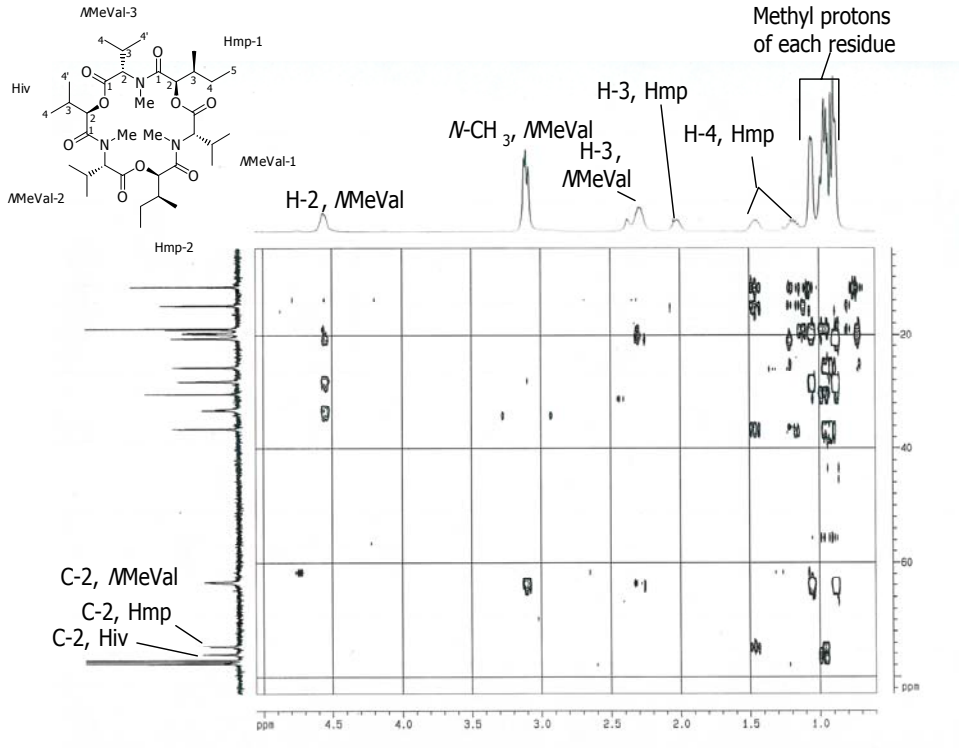

Figure 192. Expansion B of HMBC spectrum of enniatin I **(58)**

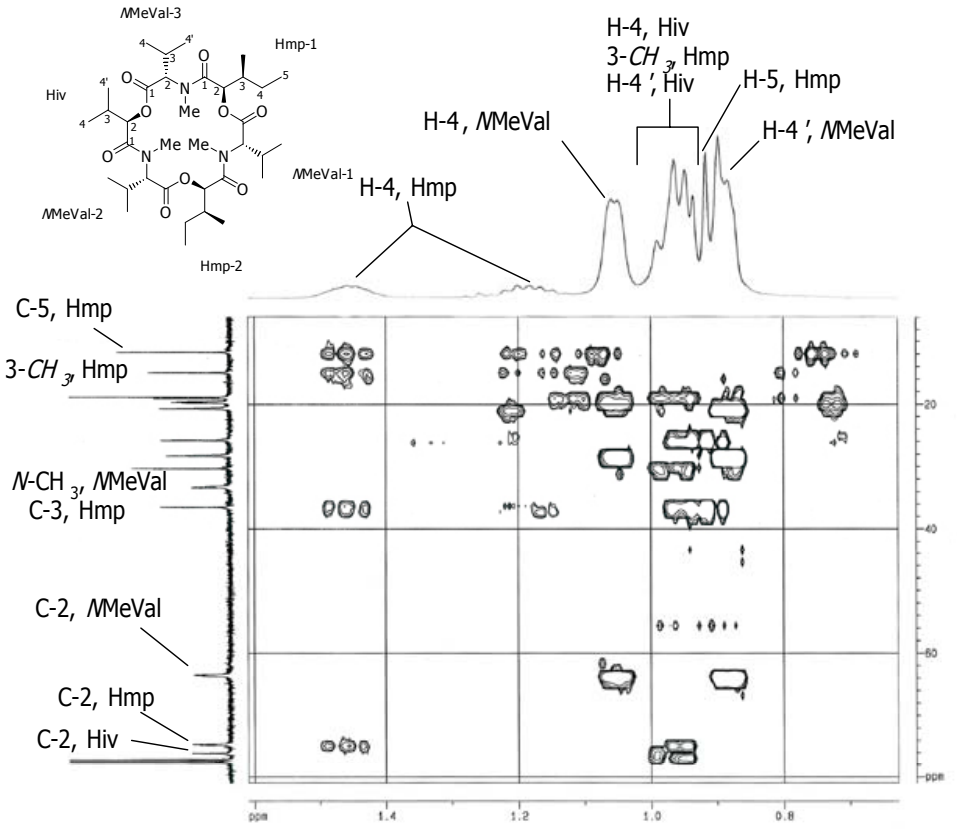

Figure 193. Expansion C of HMBC spectrum of enniatin I **(58)**

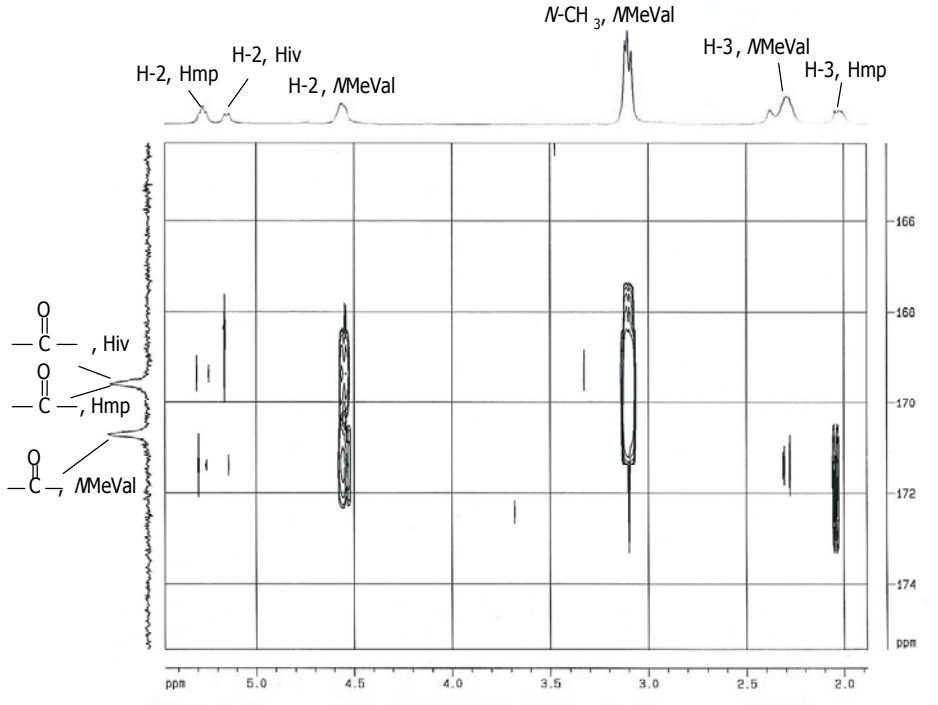

Figure 194. Expansion D of HMBC spectrum of enniatin I **(58)**

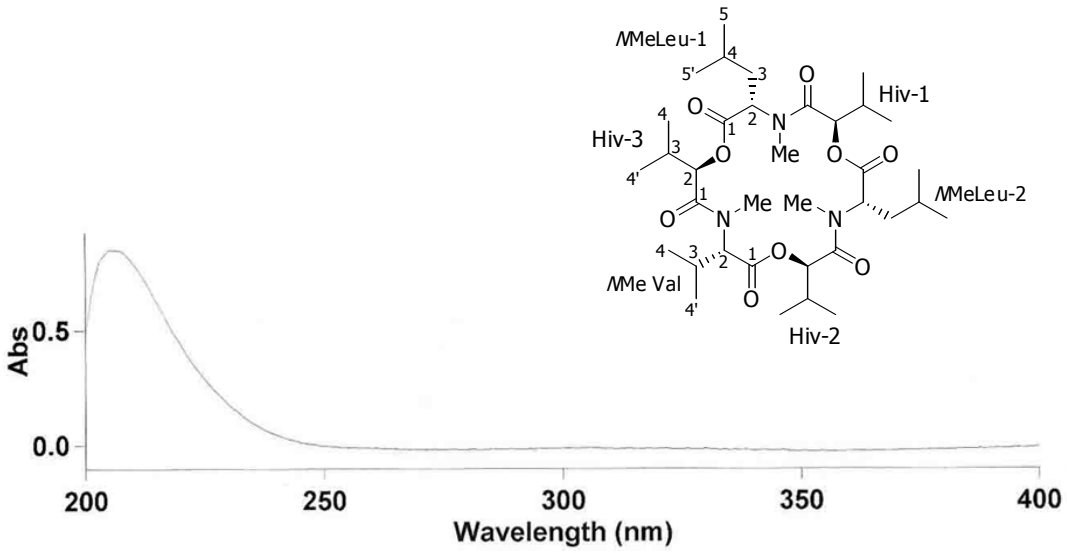

Figure 195. UV spectrum of enniatin G **(59)**

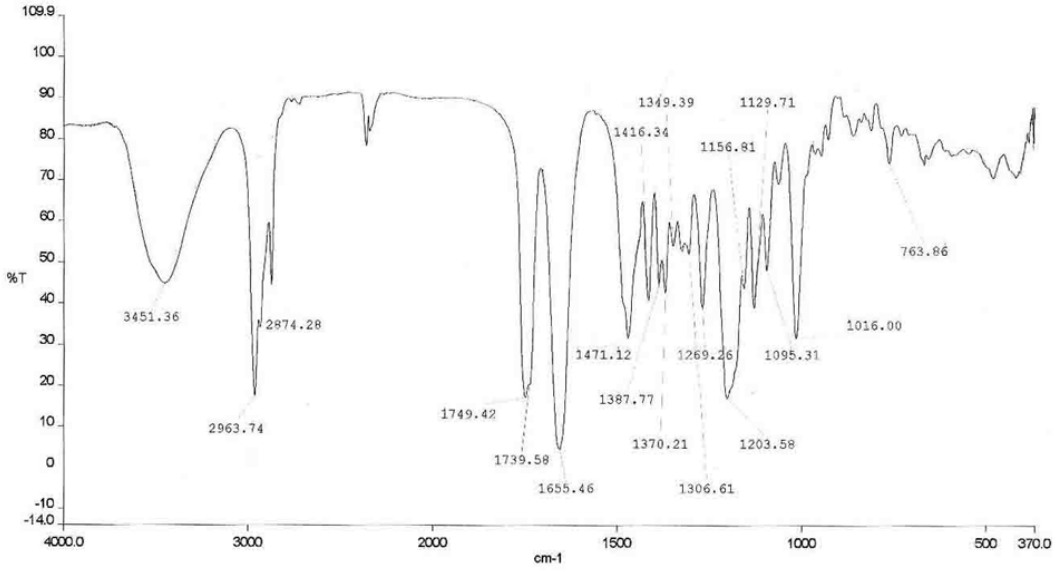

Figure 196. IR spectrum of enniatin G **(59)**

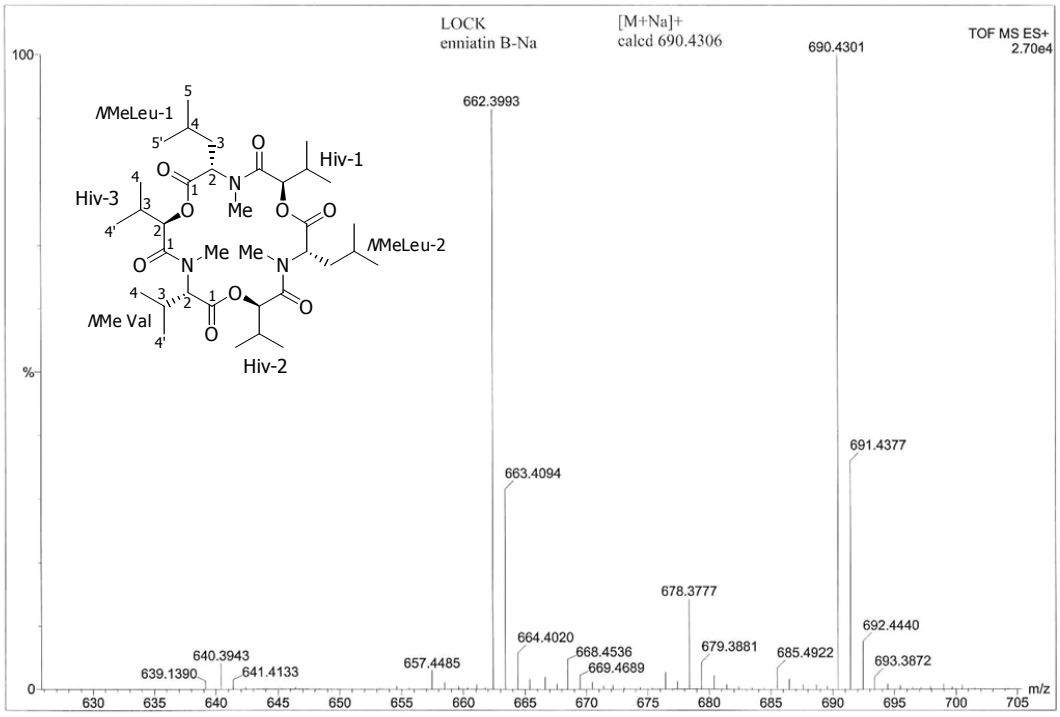

Figure 197. HRMS spectrum of enniatin G **(59)**

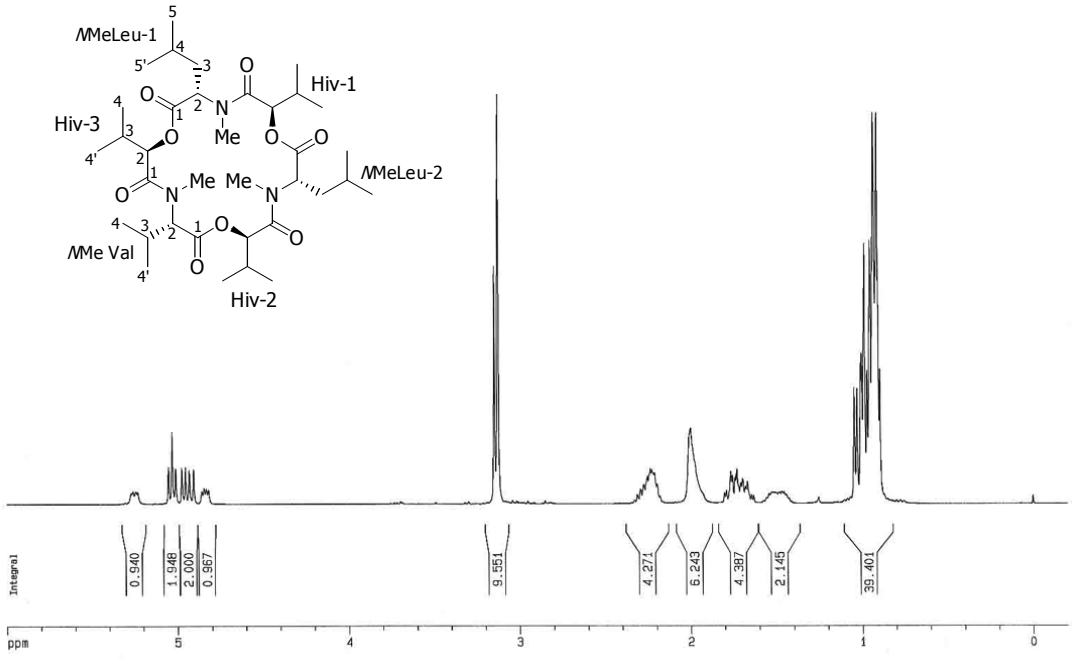

Figure 198. ^{1}H NMR ($CDCl_3$) spectrum of enniatin G **(59)**

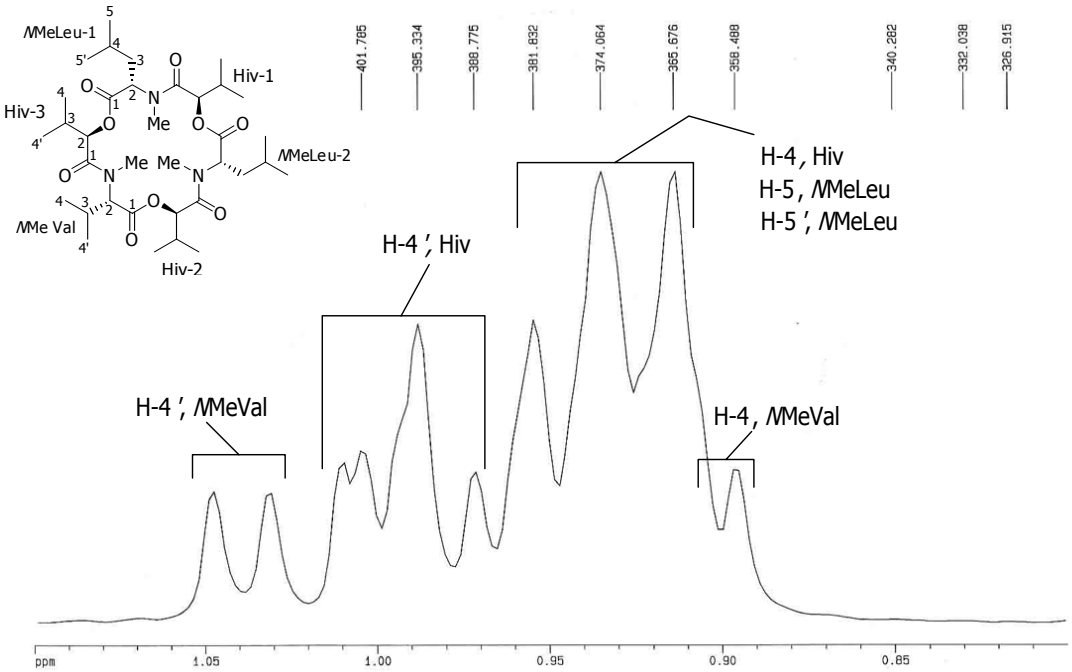

Figure 199. Expansion A of ^{1}H NMR ($CDCl_3$) spectrum of enniatin G **(59)**

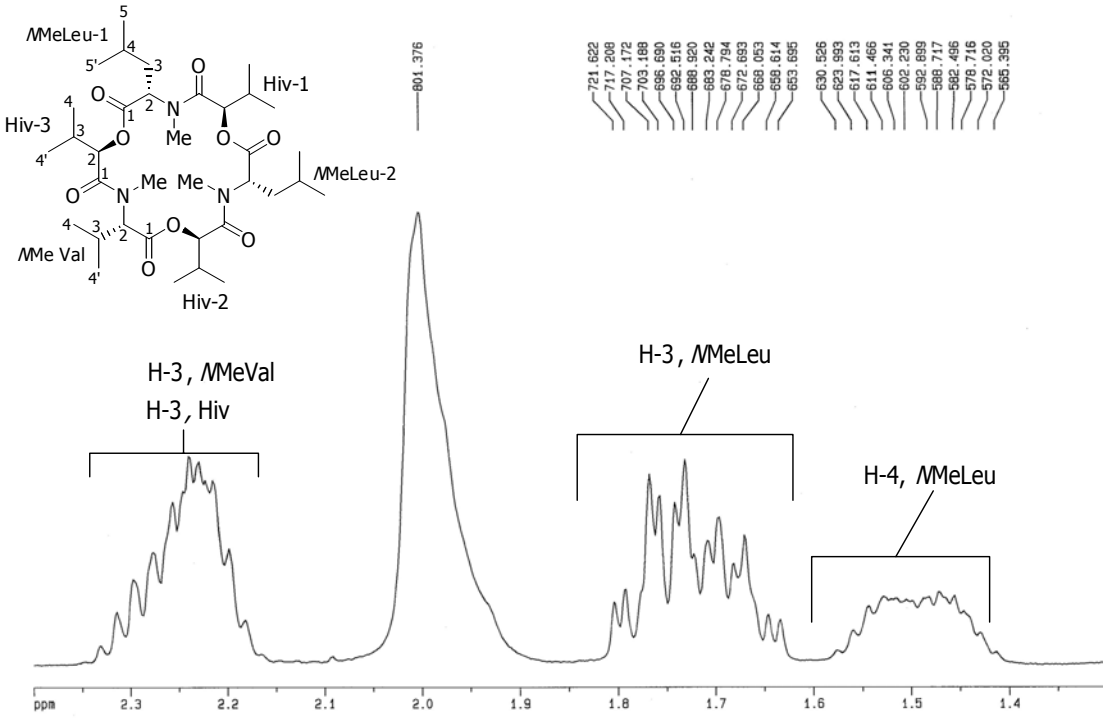

Figure 200. Expansion B of ^{1}H NMR ($CDCl_3$) spectrum of enniatin G **(59)**

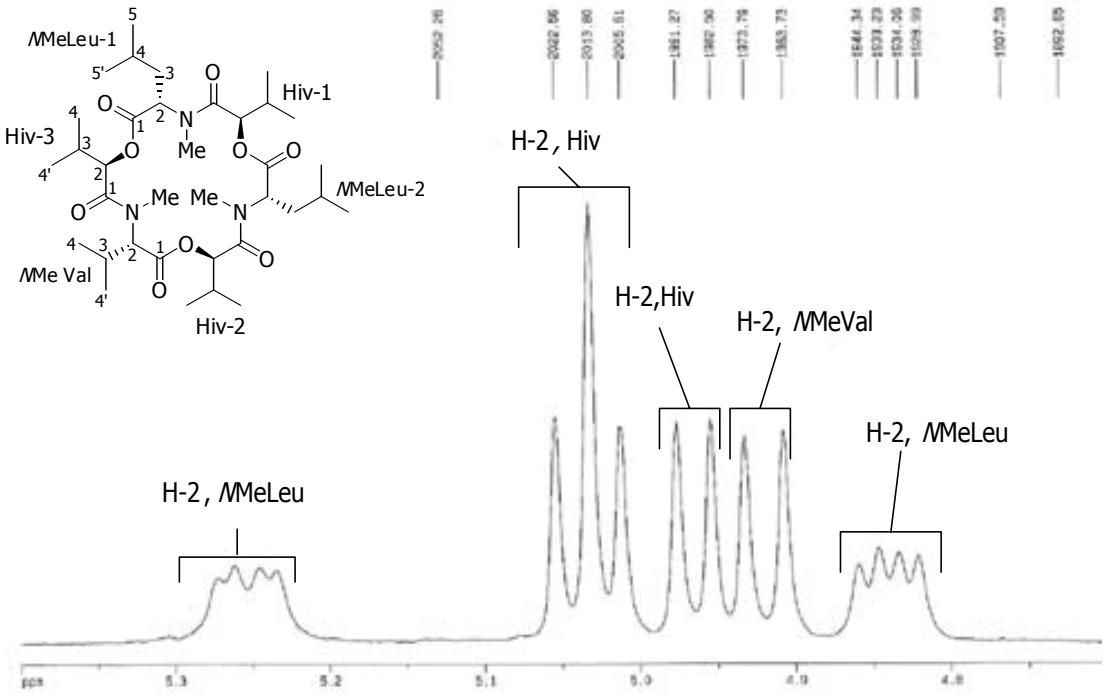

Figure 201. Expansion C of ^{1}H NMR ($CDCl_3$) spectrum of enniatin G **(59)**

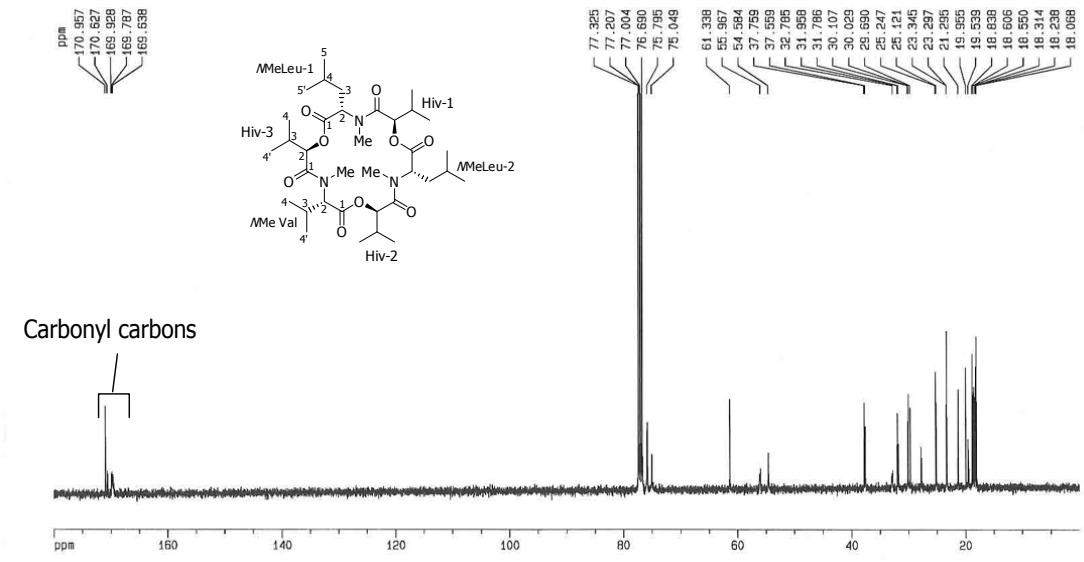

Figure 202. ^{13}C NMR spectrum of enniatin G **(59)**

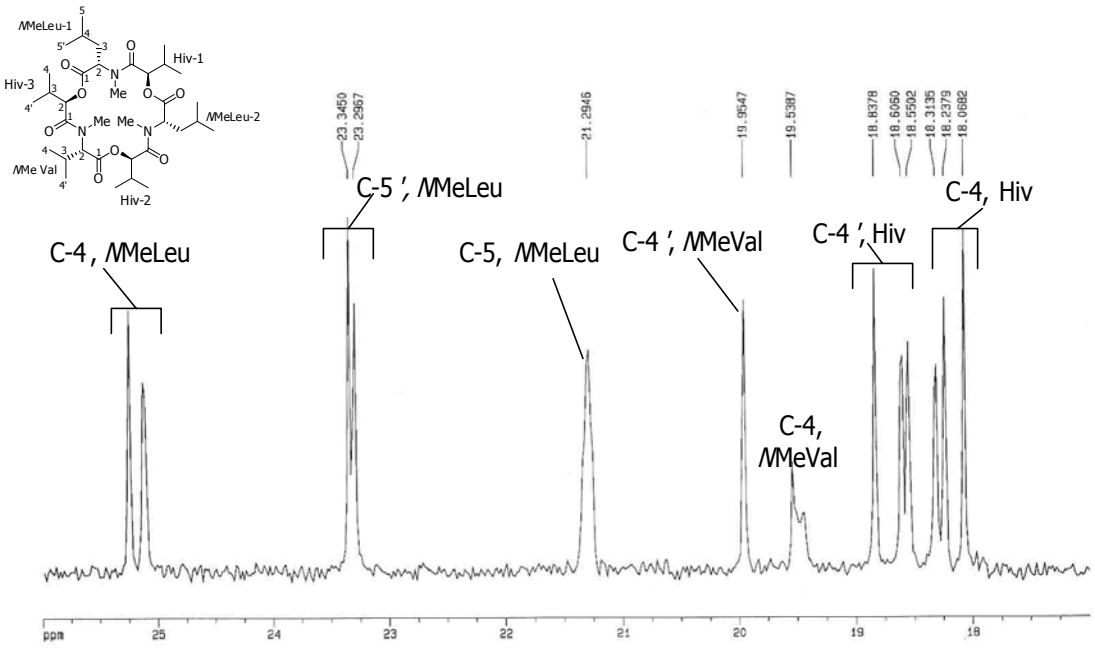

Figure 203. Expansion A of ^{13}C NMR spectrum of enniatin G **(59)**

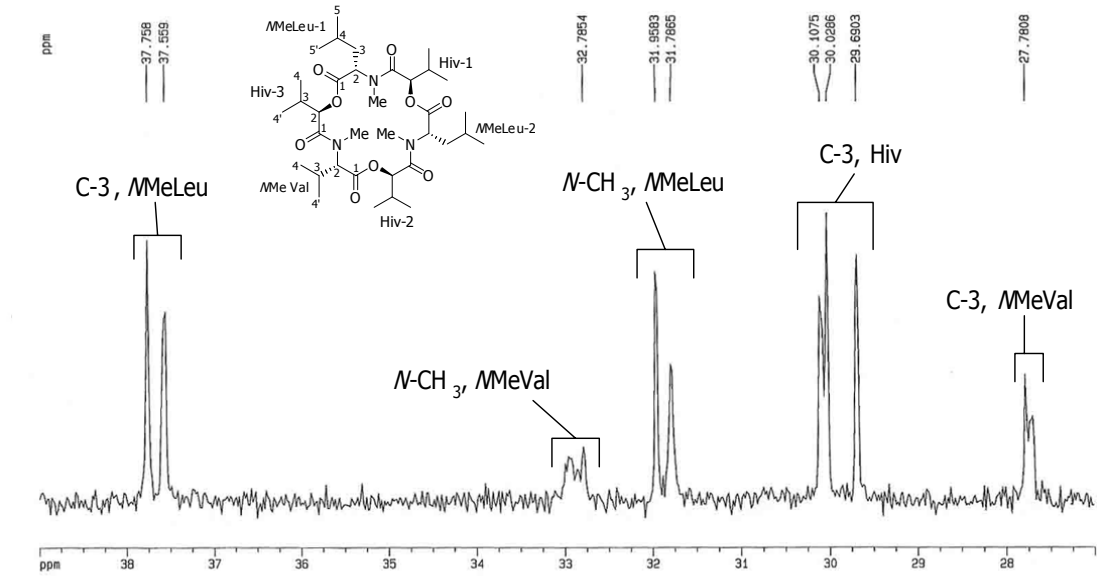

Figure 204. Expansion B of ^{13}C NMR spectrum of enniatin G **(59)**

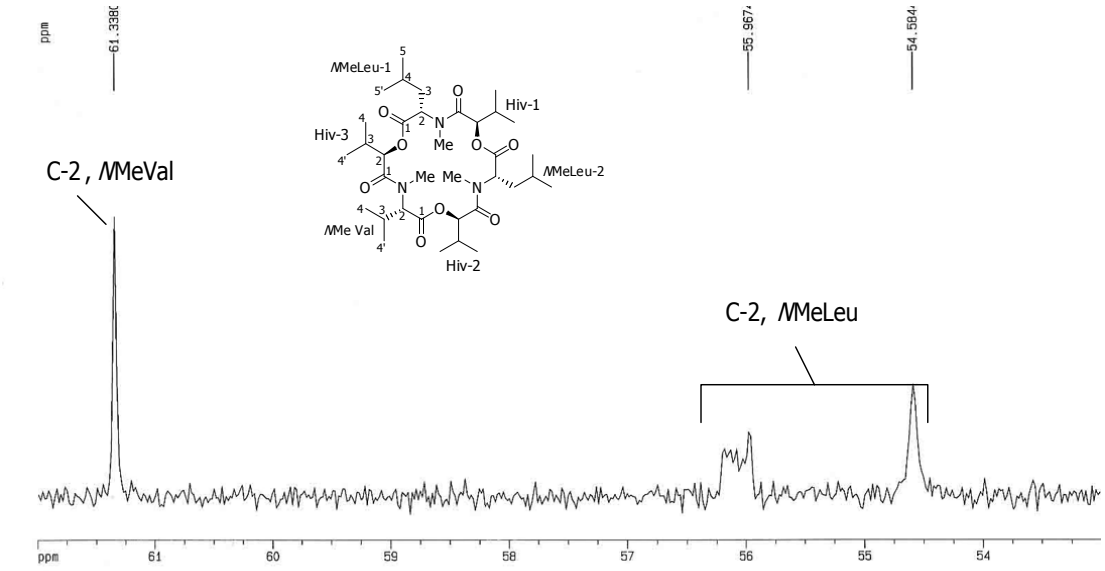

Figure 205. Expansion C of ^{13}C NMR spectrum of enniatin G **(59)**

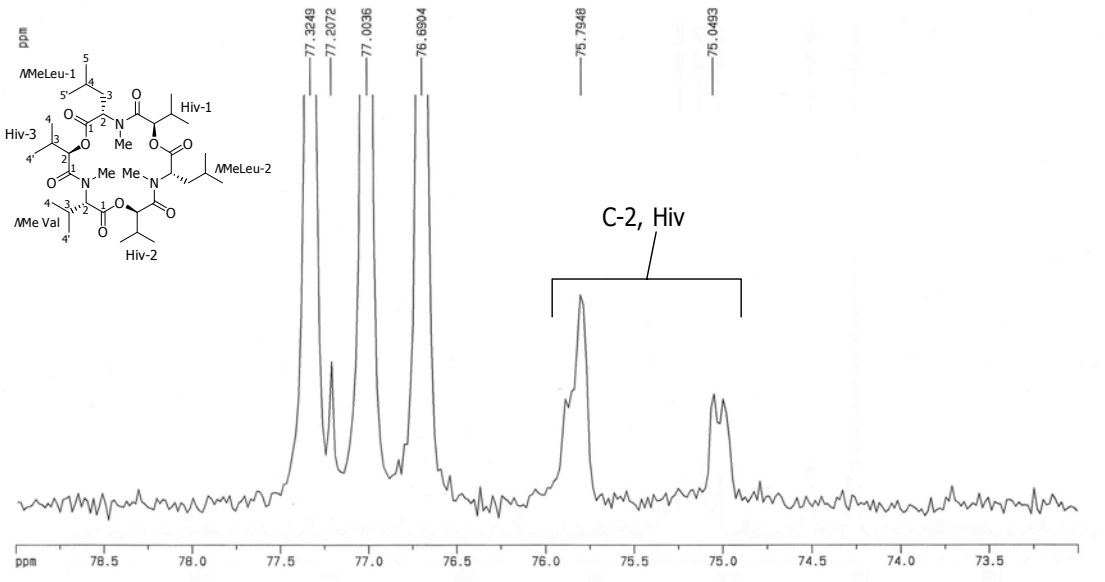

Figure 206. Expansion D of ^{13}C NMR spectrum of enniatin G **(59)**

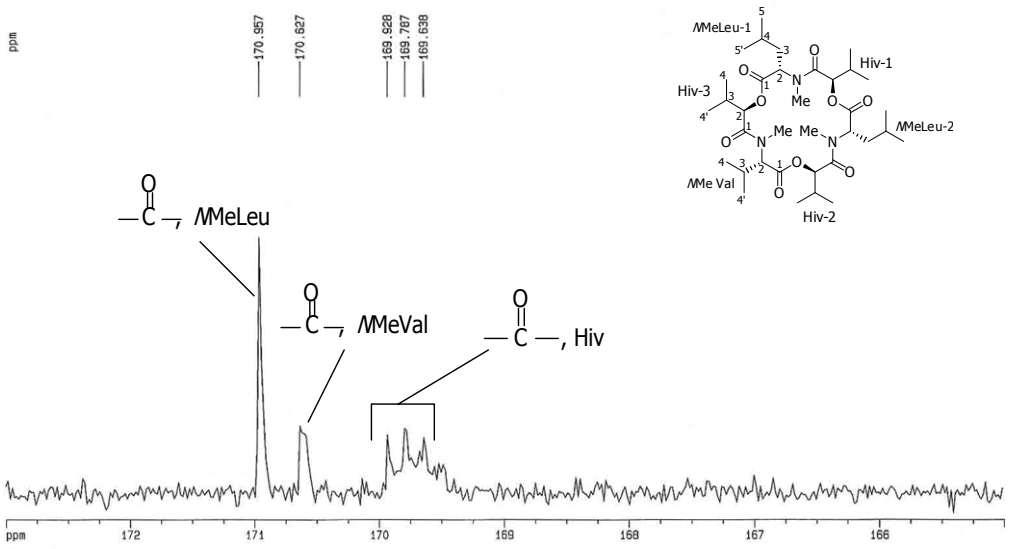

Figure 207. Expansion E of ^{13}C NMR spectrum of enniatin G **(59)**

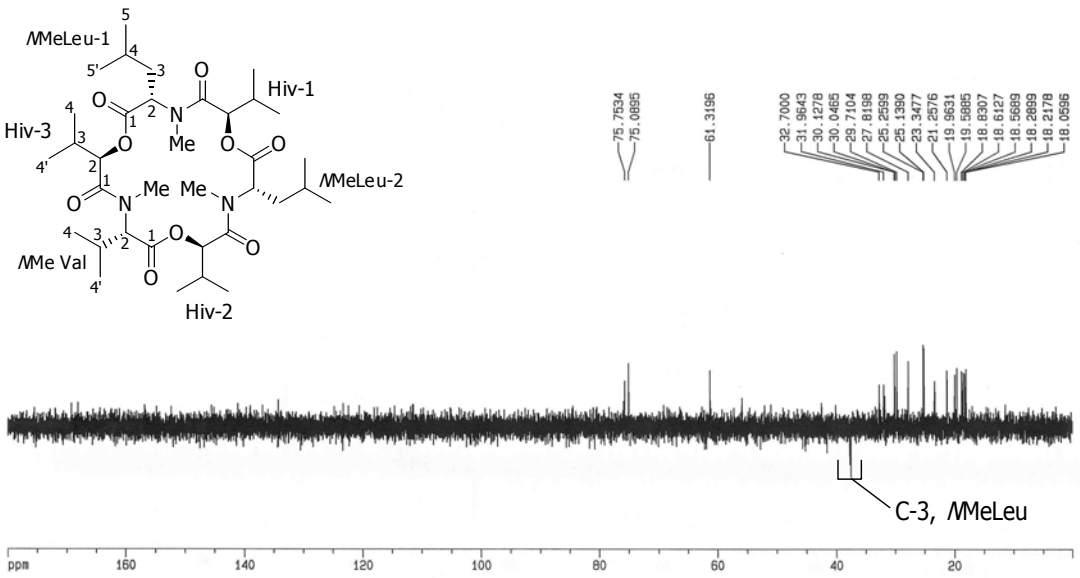

Figure 208. DEPT 135 spectrum of enniatin G **(59)**

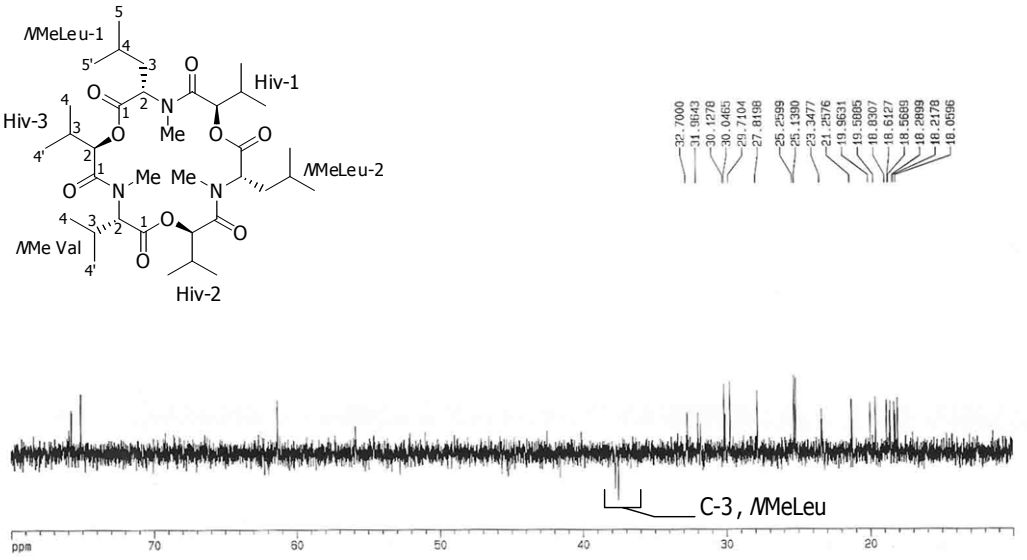

Figure 209. Expansion of DEPT 135 spectrum of enniatin G **(59)**

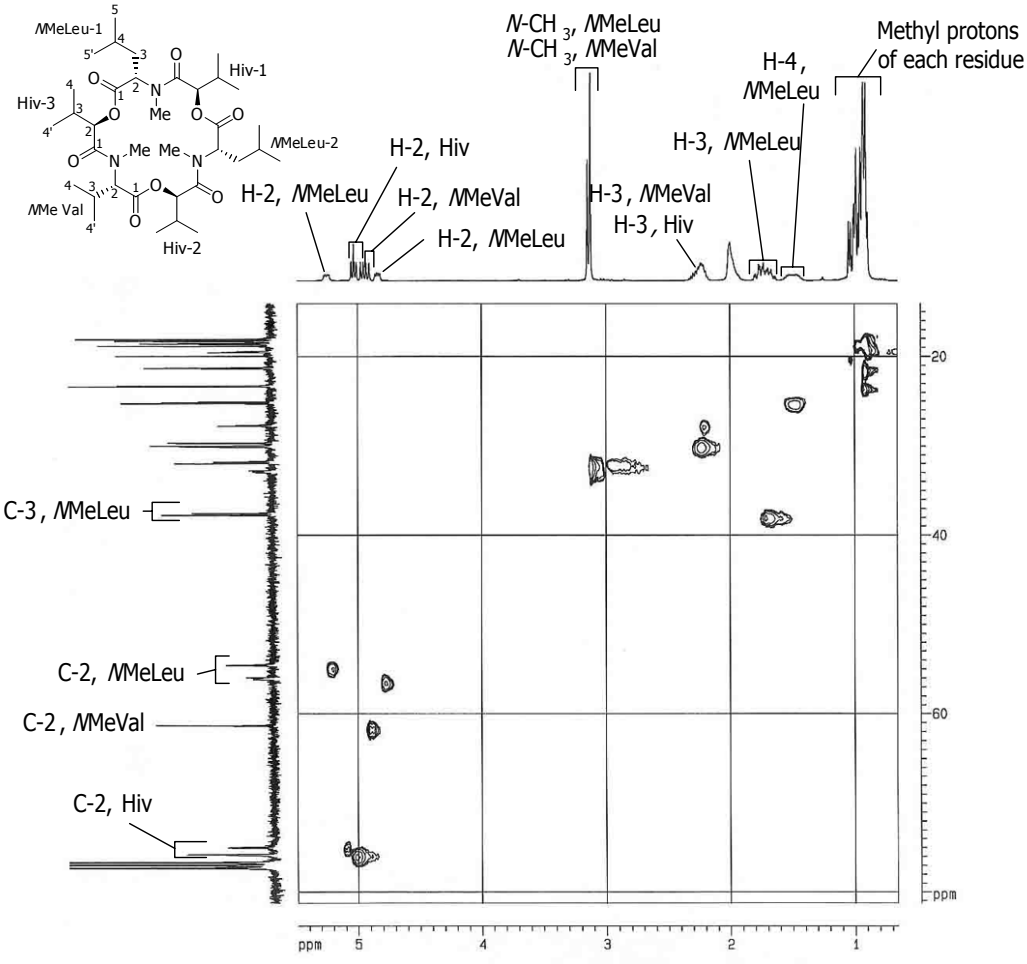

Figure 210. HMQC spectrum of enniatin G **(59)**

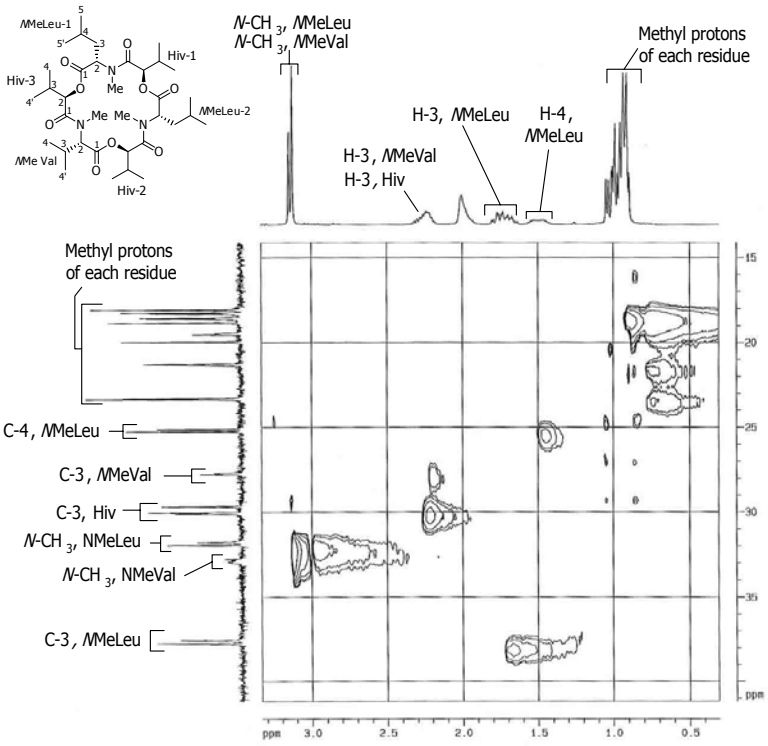

Figure 211. Expansion A of HMQC spectrum of enniatin G **(59)**

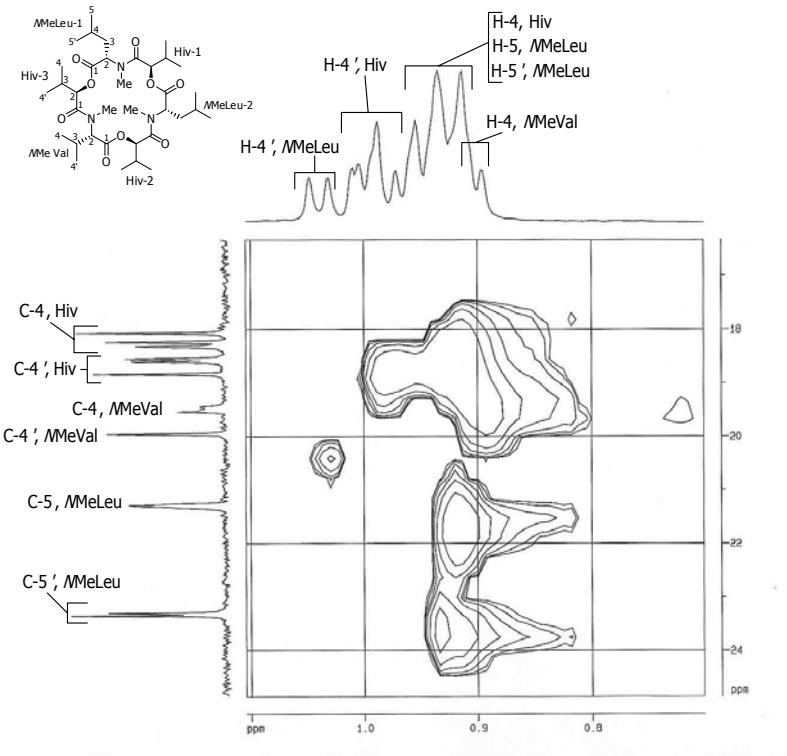

Figure 212. Expansion B of HMQC spectrum of enniatin G **(59)**

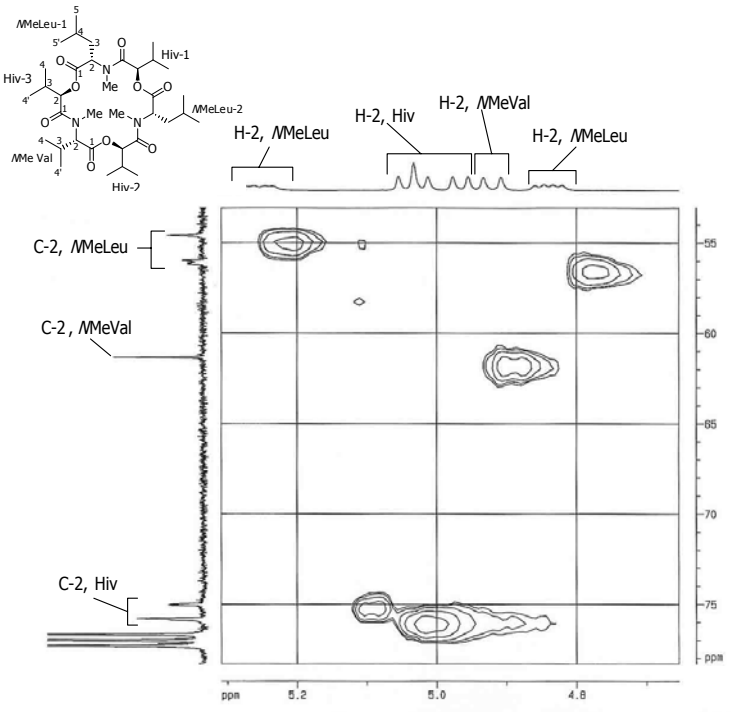

Figure 213. Expansion C of HMQC spectrum of enniatin G **(59)**

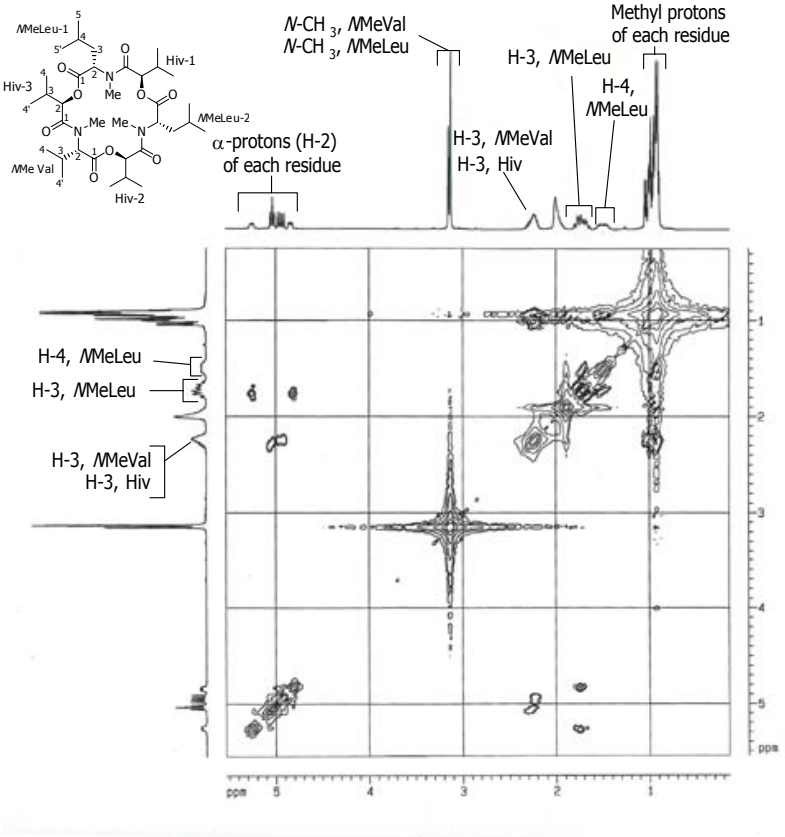

Figure 214. COSY spectrum of enniatin G **(59)**

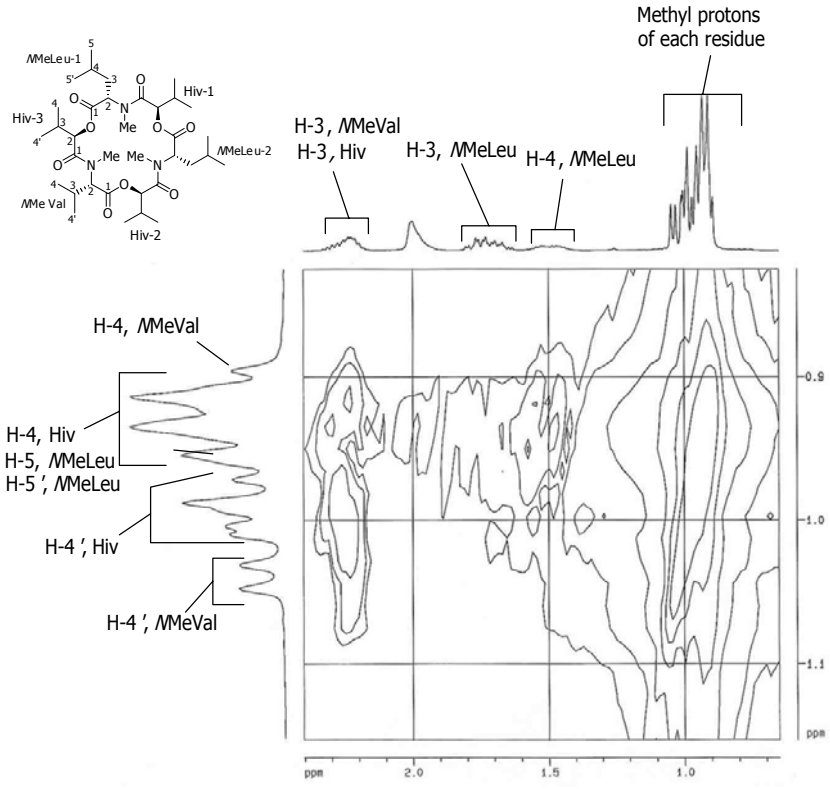

Figure 215. Expansion A of COSY spectrum of enniatin G **(59)**

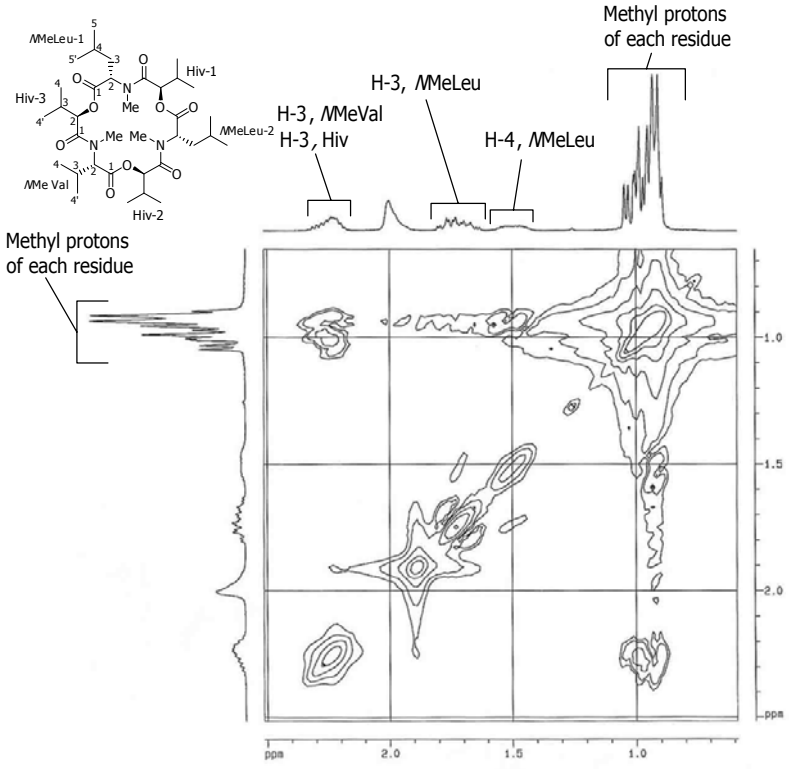

Figure 216. Expansion B of COSY spectrum of enniatin G **(59)**

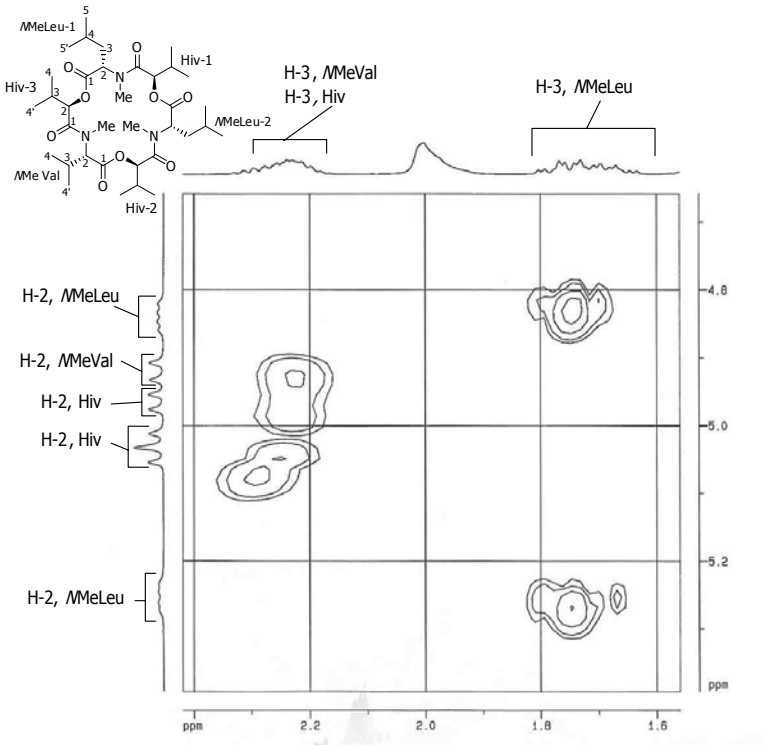

Figure 217. Expansion C of COSY spectrum of enniatin G **(59)**

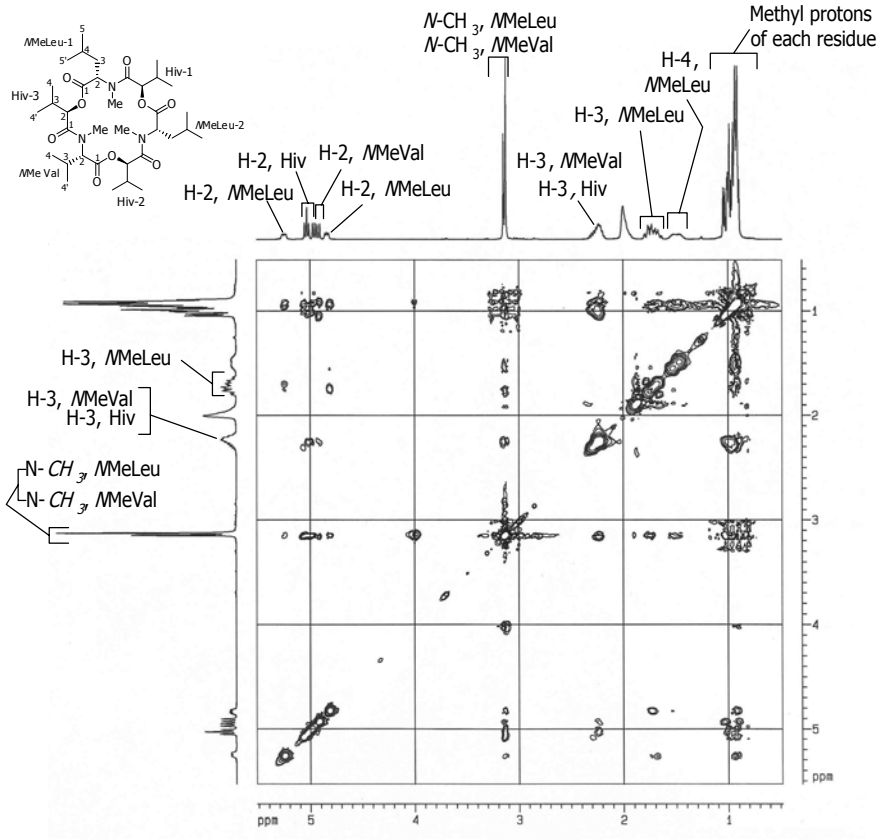

Figure 218. NOESY spectrum of enniatin G **(59)**

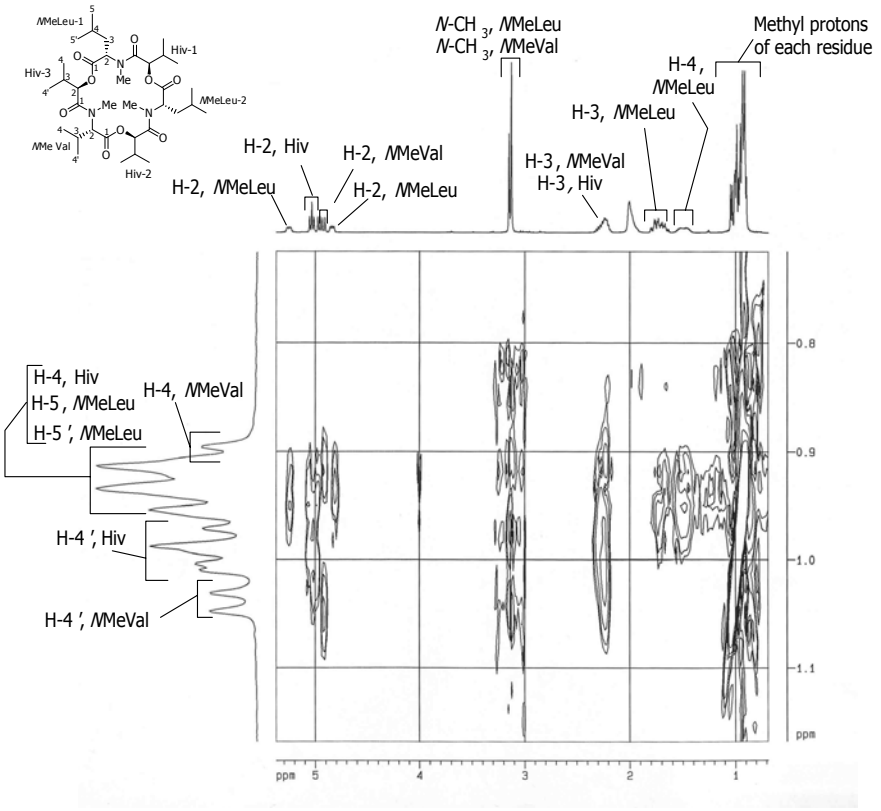

Figure 219. Expansion A of NOESY spectrum of enniatin G **(59)**

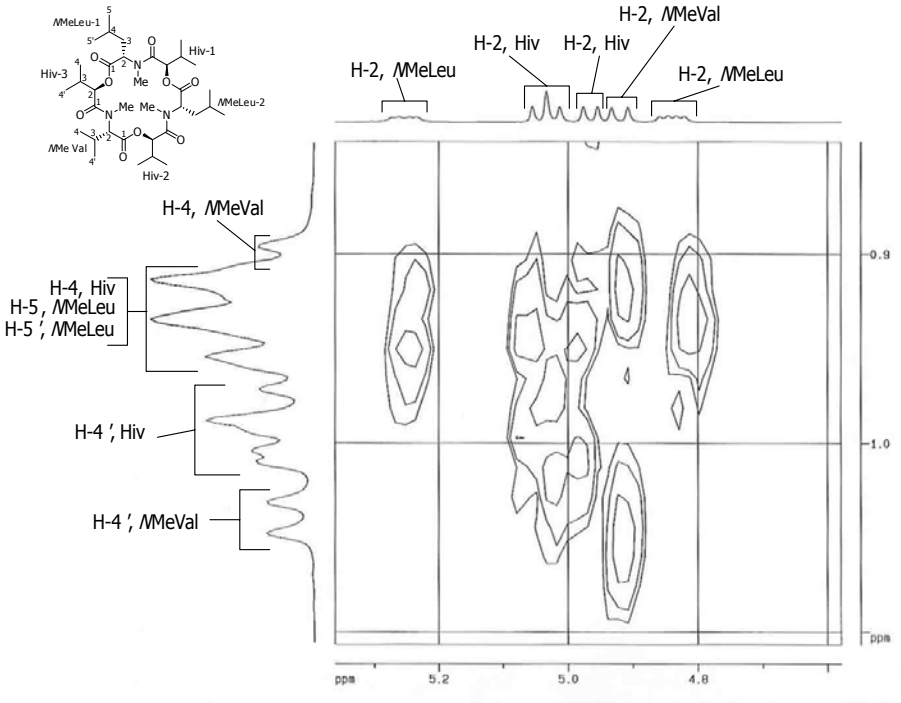

Figure 220. Expansion B of NOESY spectrum of enniatin G **(59)**

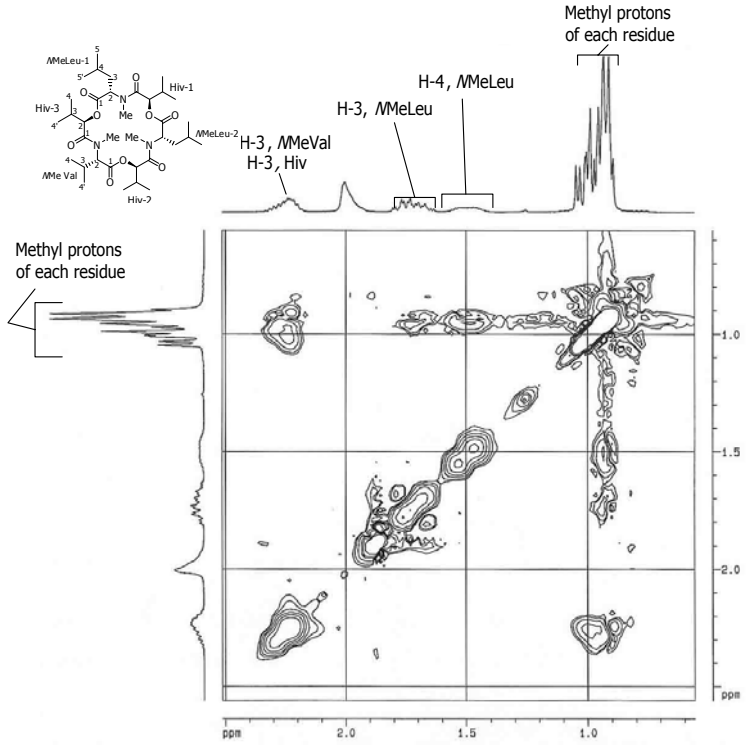

Figure 221. Expansion C of NOESY spectrum of enniatin G **(59)**

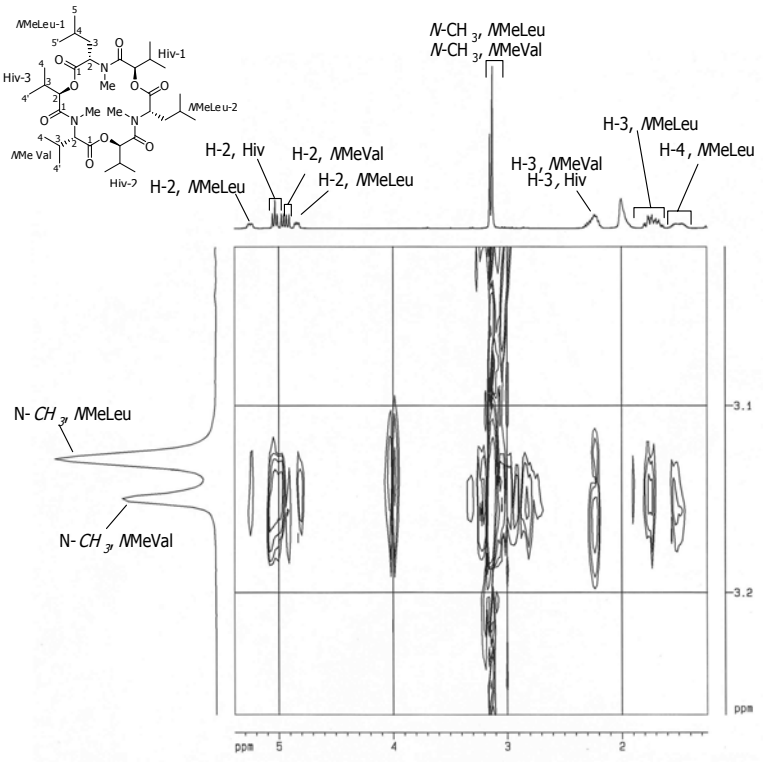

Figure 222. Expansion D of NOESY spectrum of enniatin G **(59)**

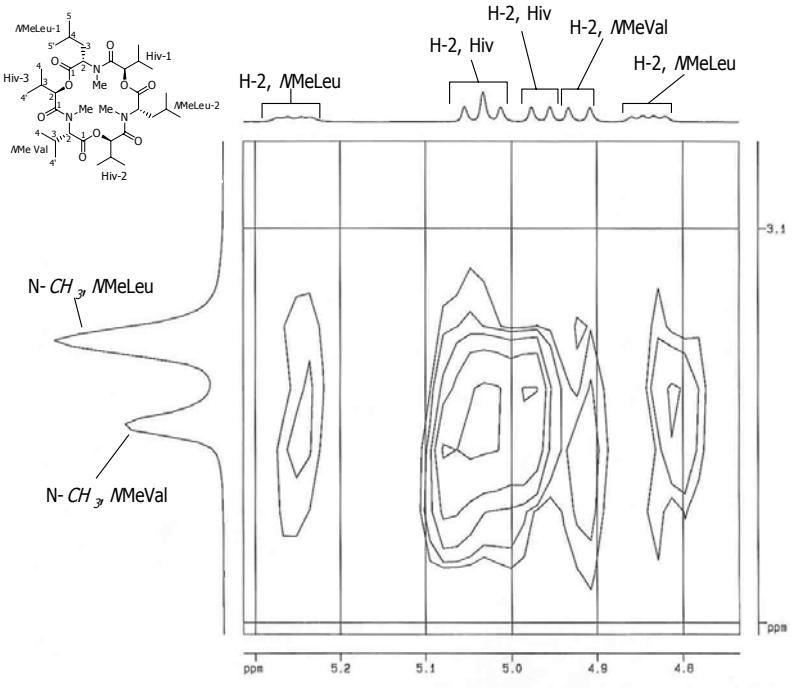

Figure 223. Expansion E of NOESY spectrum of enniatin G **(59)**

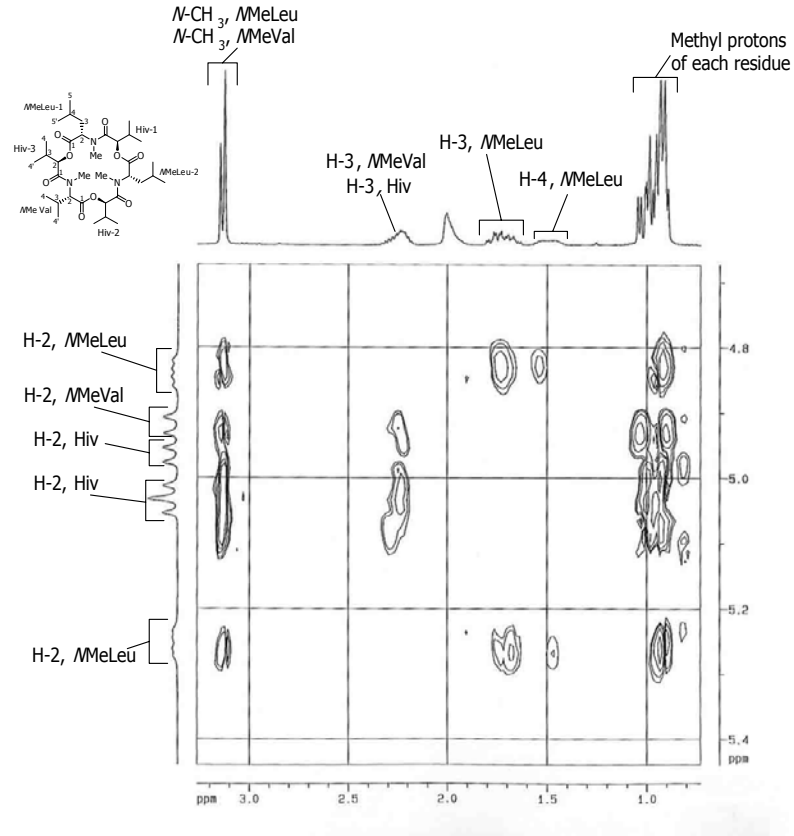

Figure 224. Expansion F of NOESY spectrum of enniatin G **(59)**

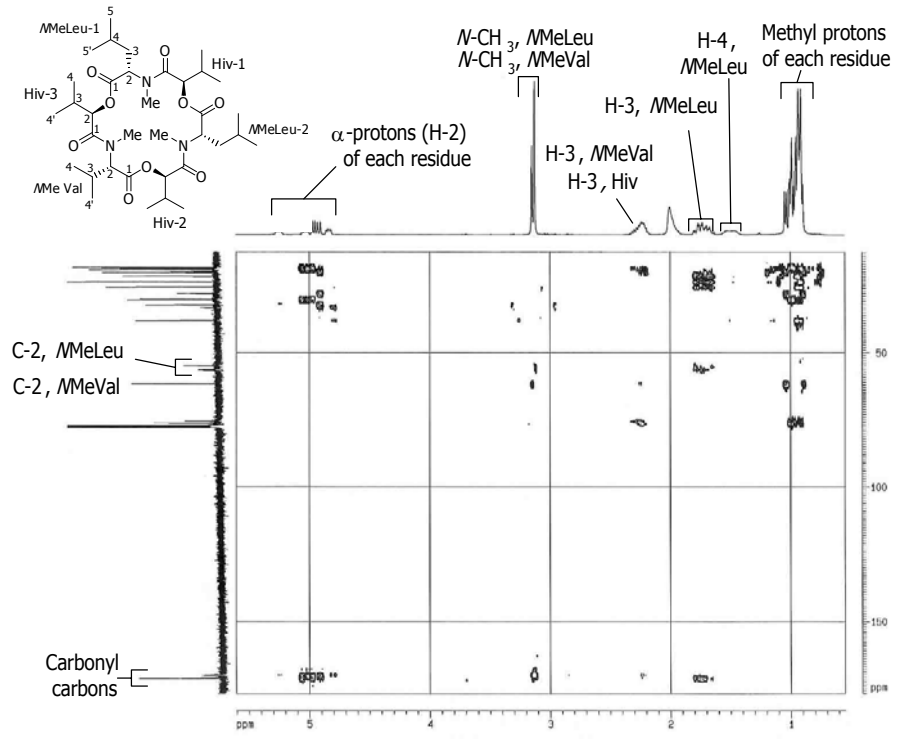

Figure 225. HMBC spectrum of enniatin G **(59)**

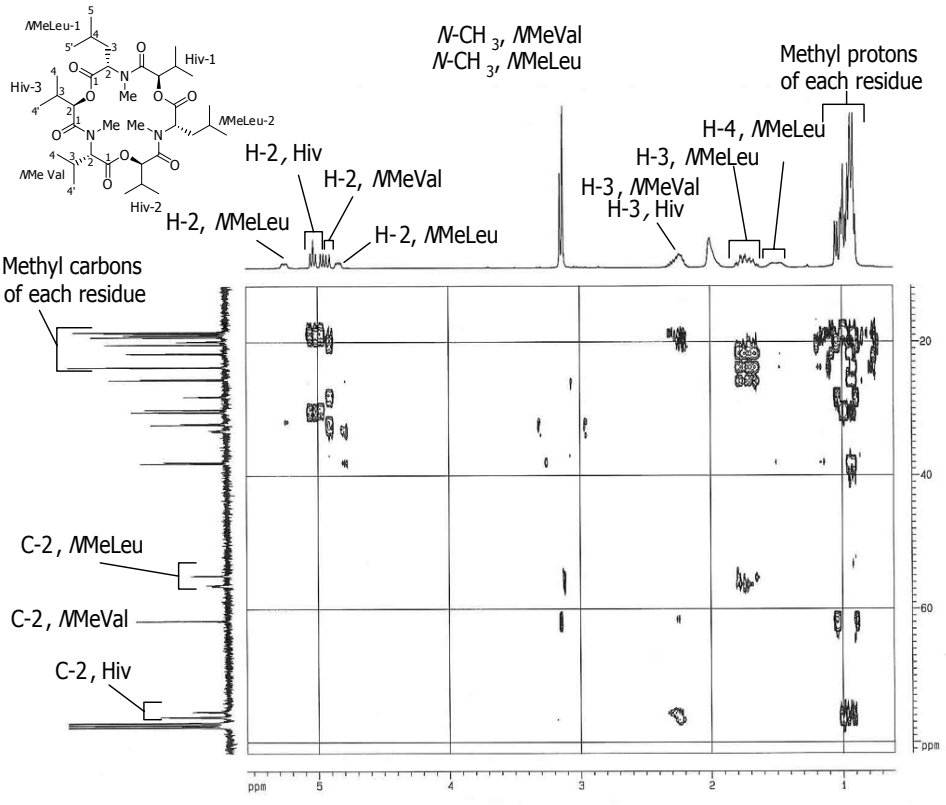

Figure 226. Expansion A of HMBC spectrum of enniatin G **(59)**

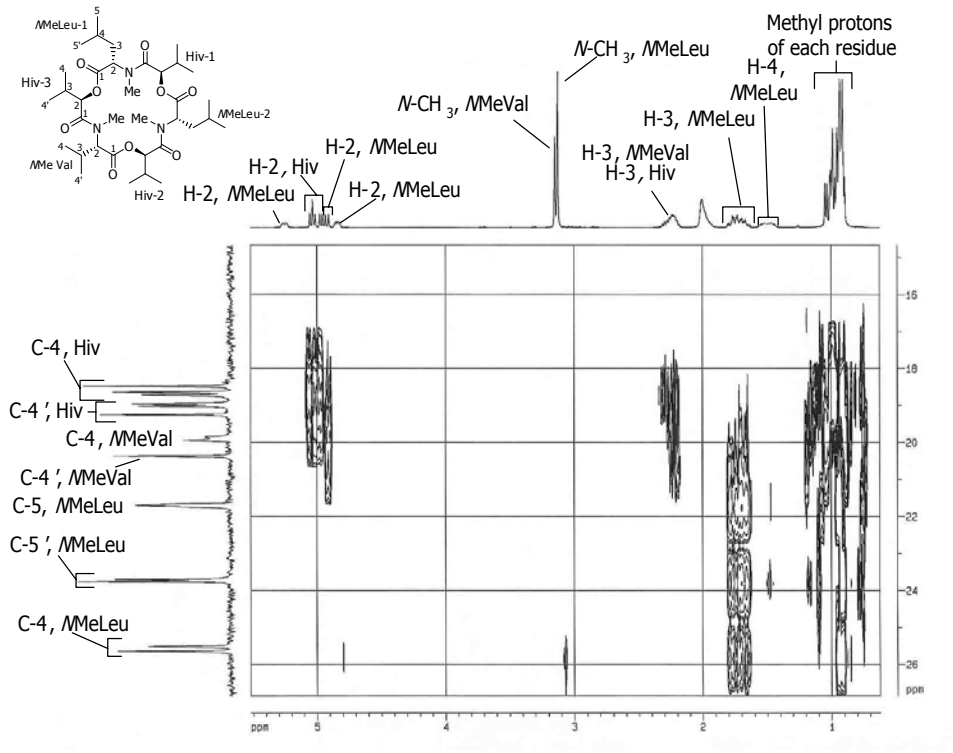

Figure 227. Expansion B of HMBC spectrum of enniatin G **(59)**

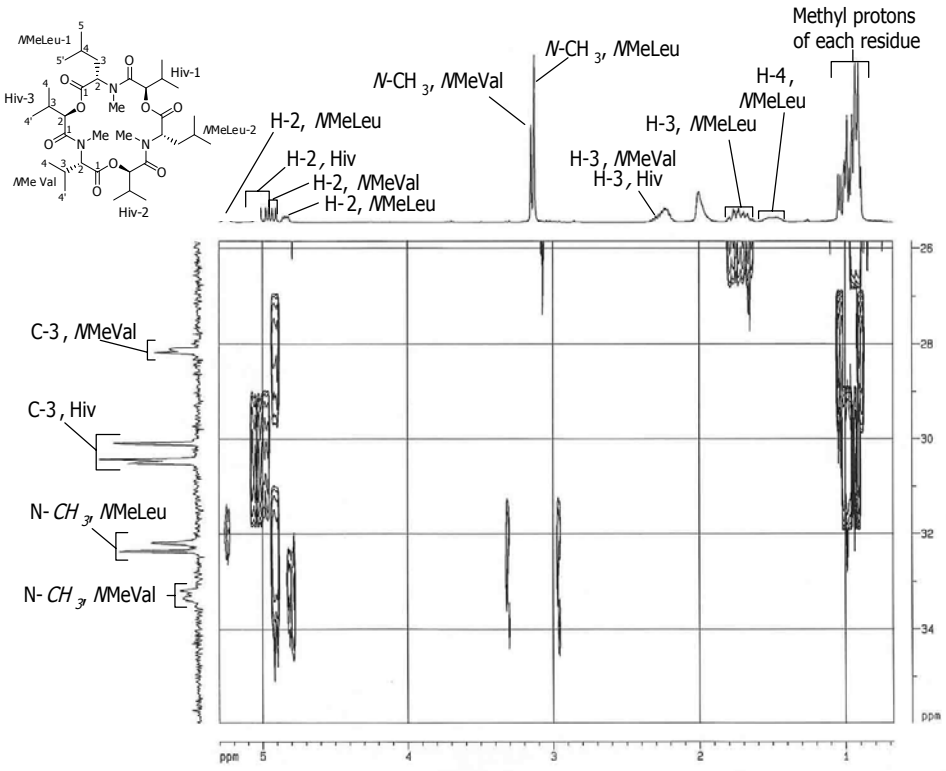

Figure 228. Expansion C of HMBC spectrum of enniatin G **(59)**

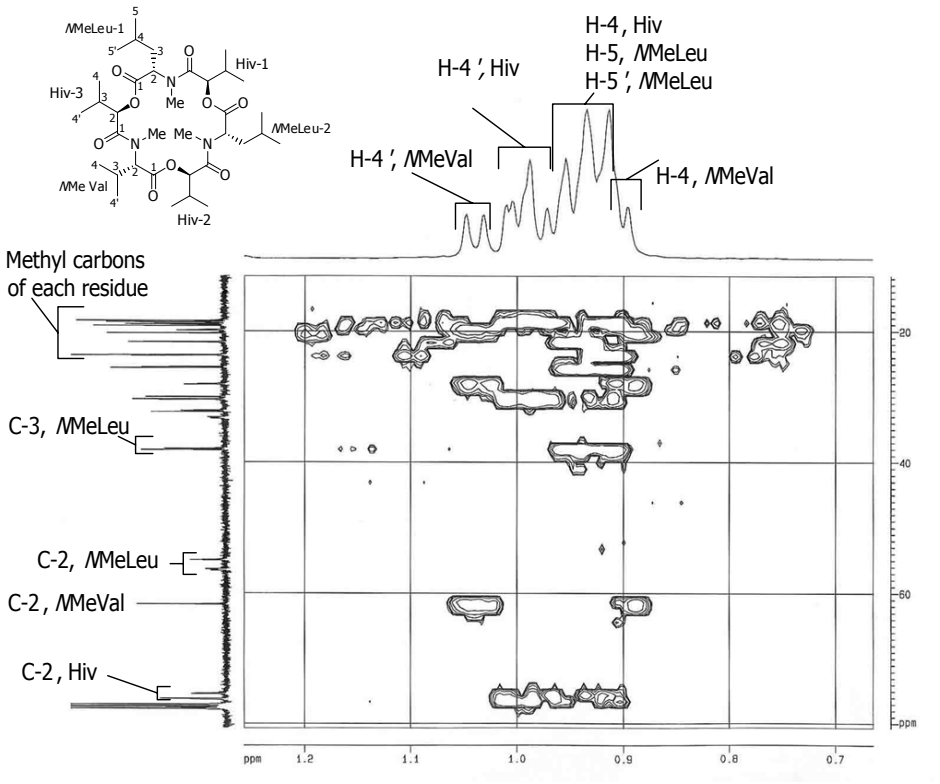

Figure 229. Expansion D of HMBC spectrum of enniatin G **(59)**

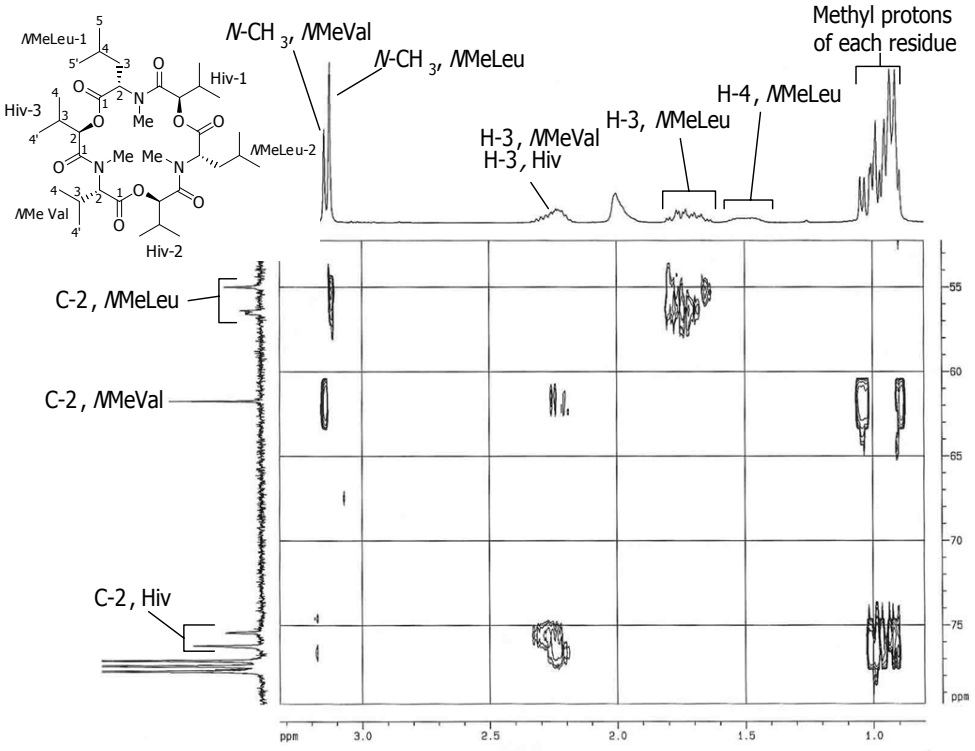

Figure 230. Expansion E of HMBC spectrum of enniatin G **(59)**

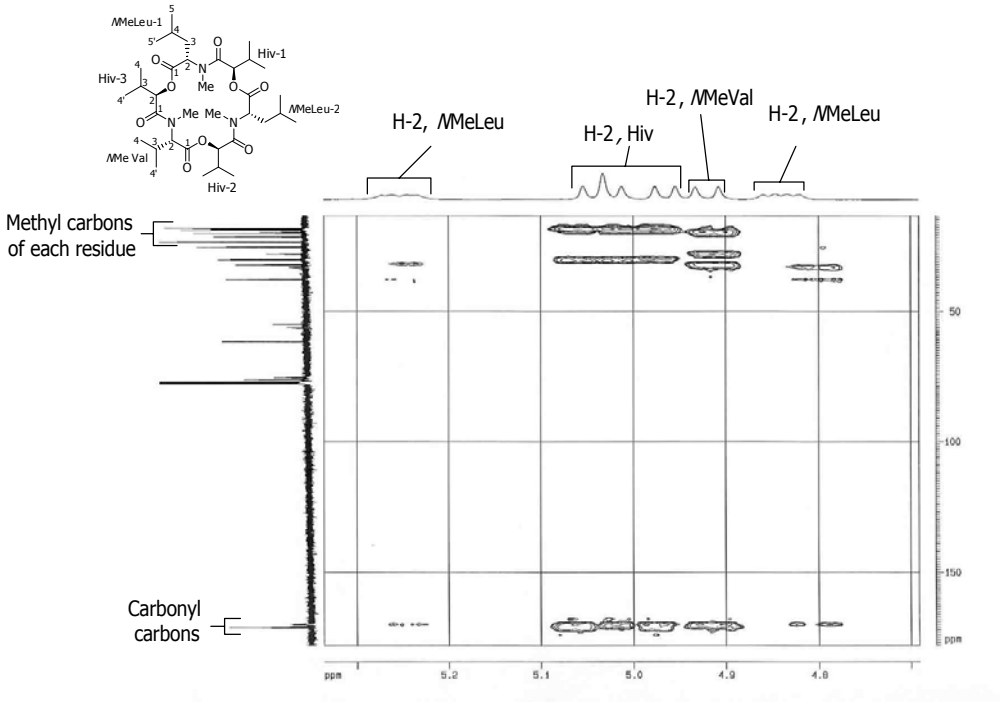

Figure 231. Expansion F of HMBC spectrum of enniatin G **(59)**

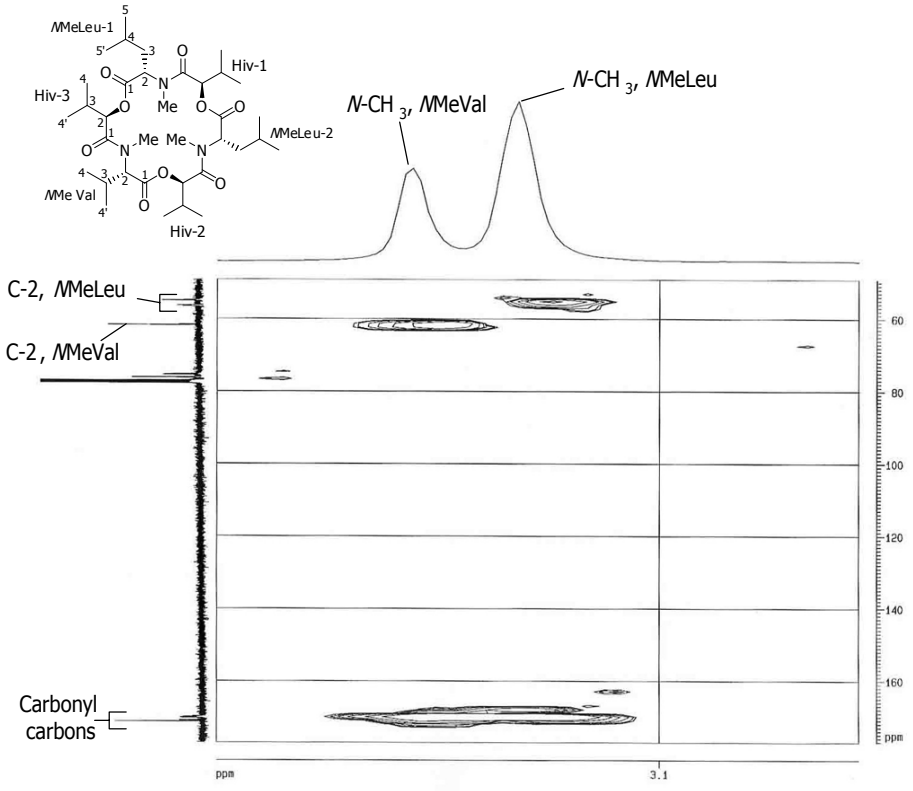

Figure 232. Expansion G of HMBC spectrum of enniatin G **(59)**

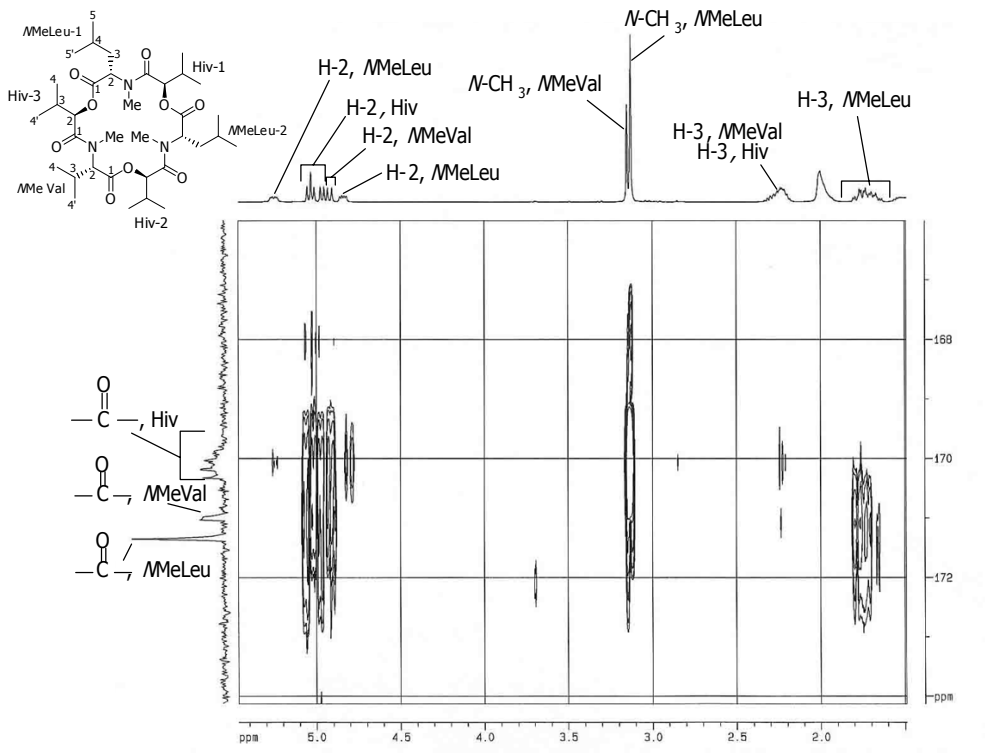

Figure 233. Expansion H of HMBC spectrum of enniatin G **(59)**

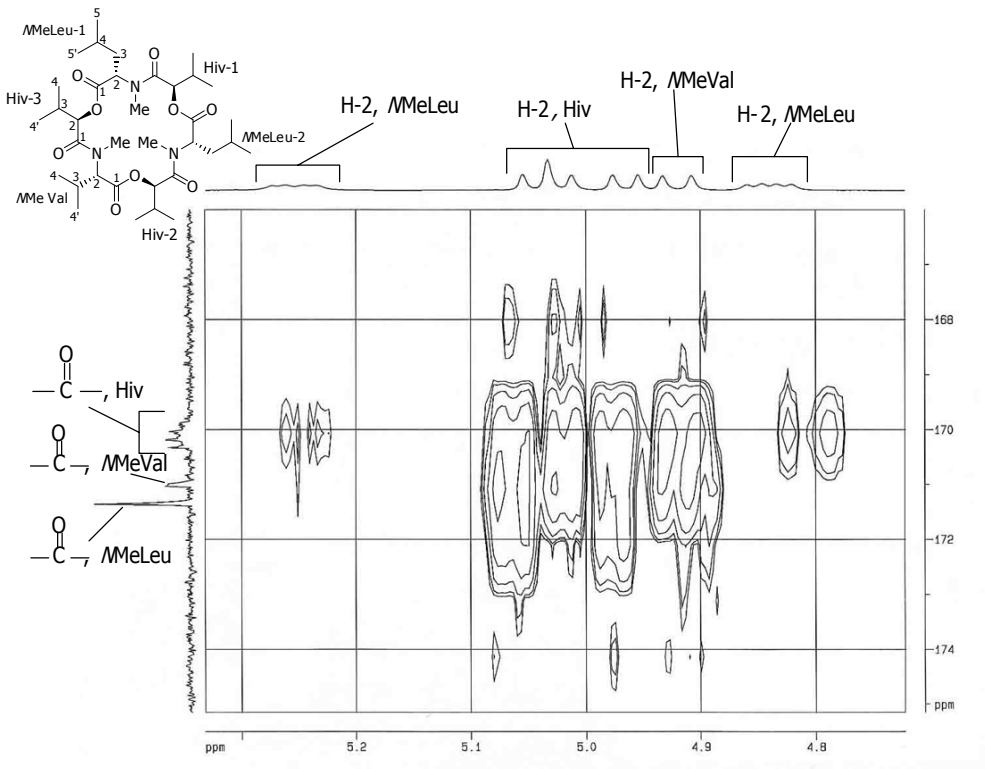

Figure 234. Expansion I of HMBC spectrum of enniatin G **(59)**

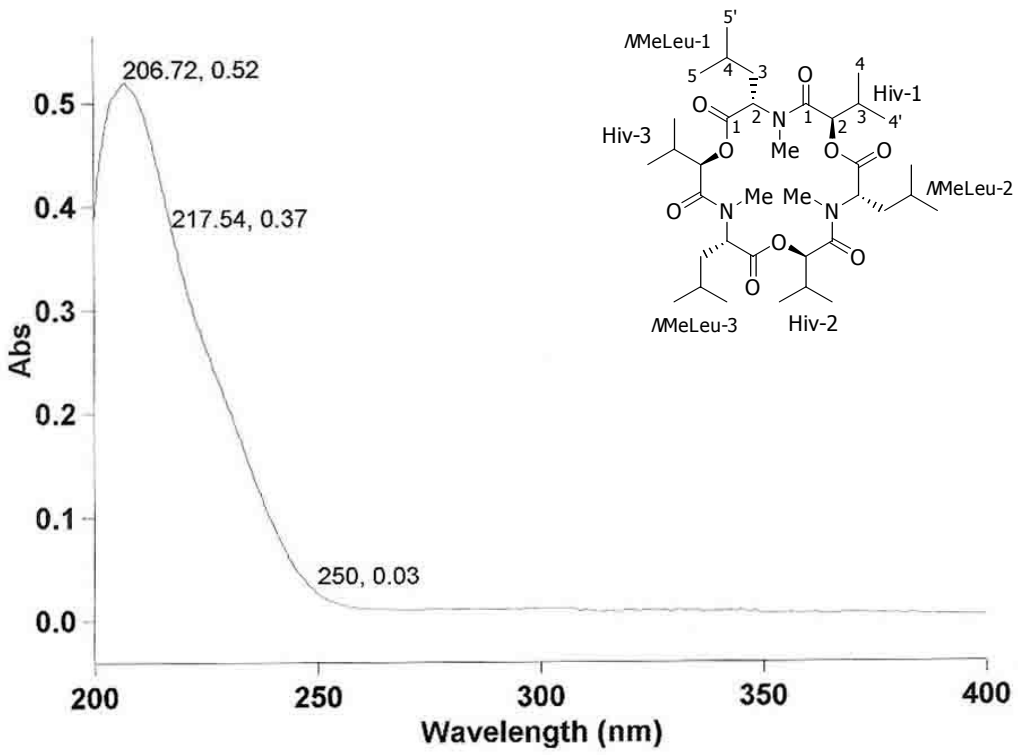

Figure 235. UV spectrum of enniatin C **(60)**

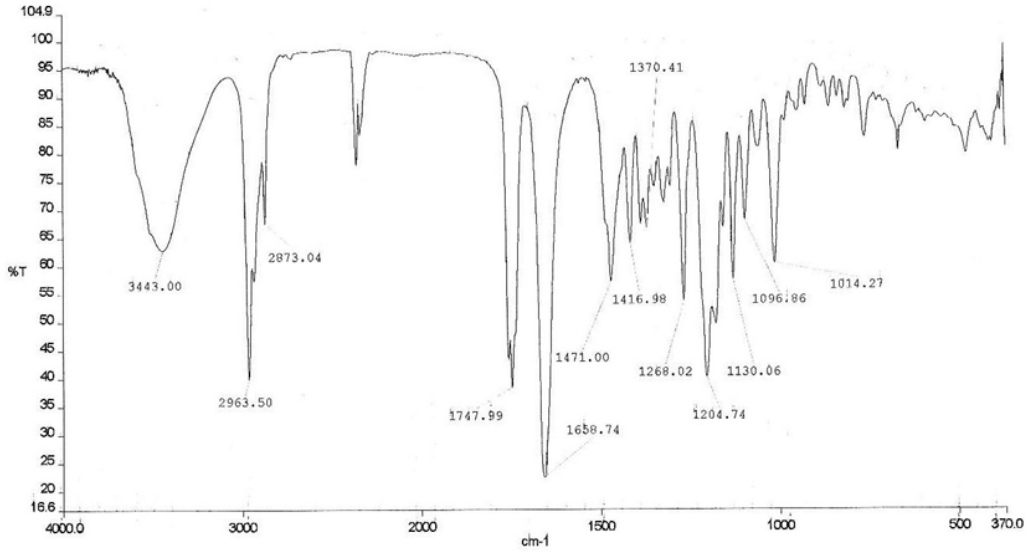

Figure 236. IR spectrum of enniatin C **(60)**

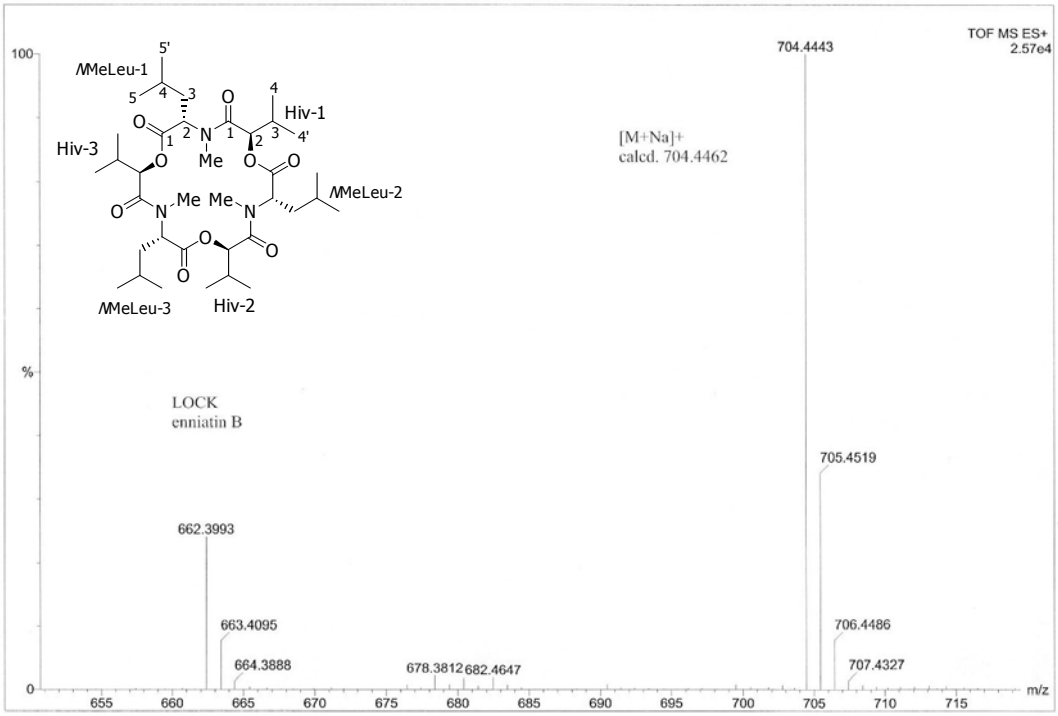

Figure 237. HRMS spectrum of enniatin C **(60)**

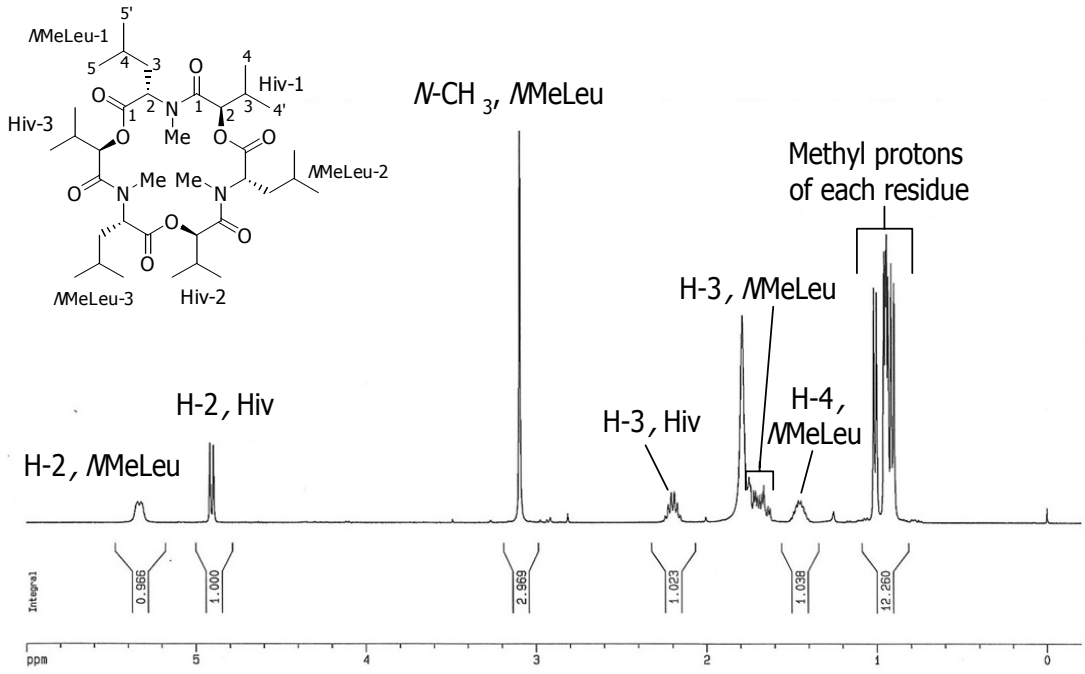

Figure 238. ^{1}H NMR ($CDCl_3$) spectrum of enniatin C **(60)**

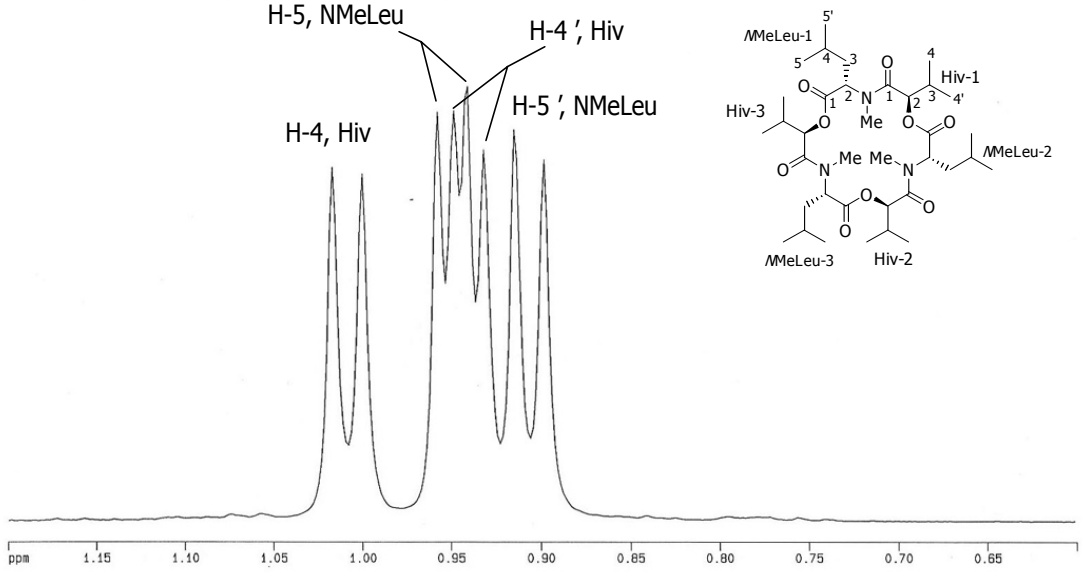

Figure 239. Expansion A of ^{1}H NMR ($CDCl_3$) spectrum of enniatin C **(60)**

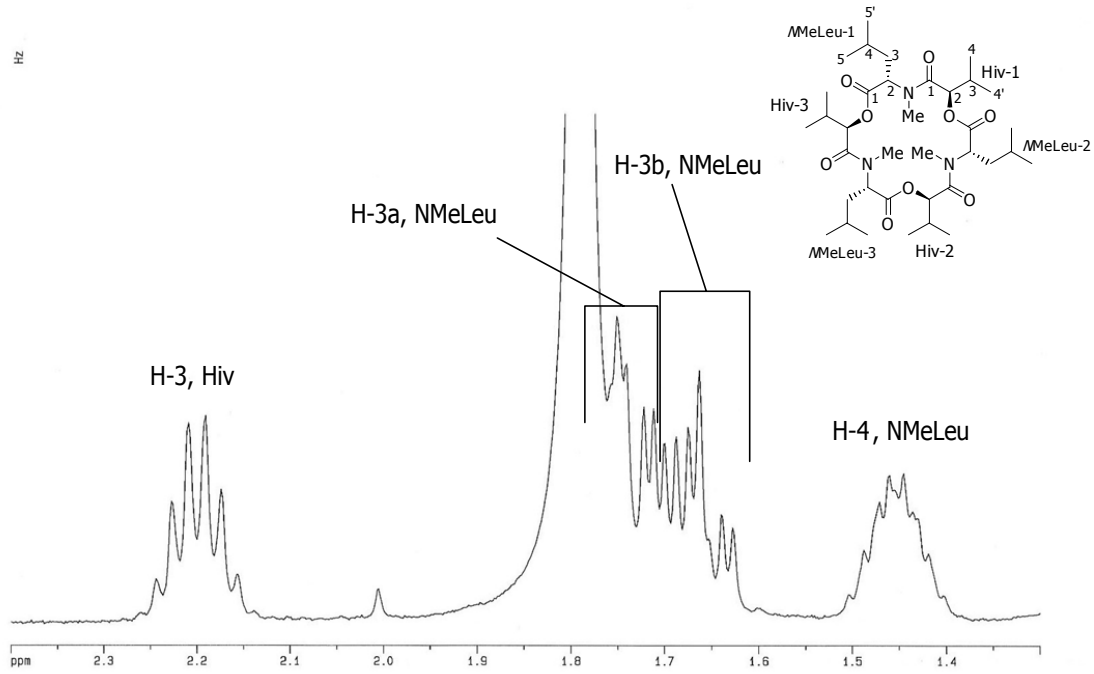

Figure 240. Expansion B of ^{1}H NMR ($CDCl_3$) spectrum of enniatin C **(60)**

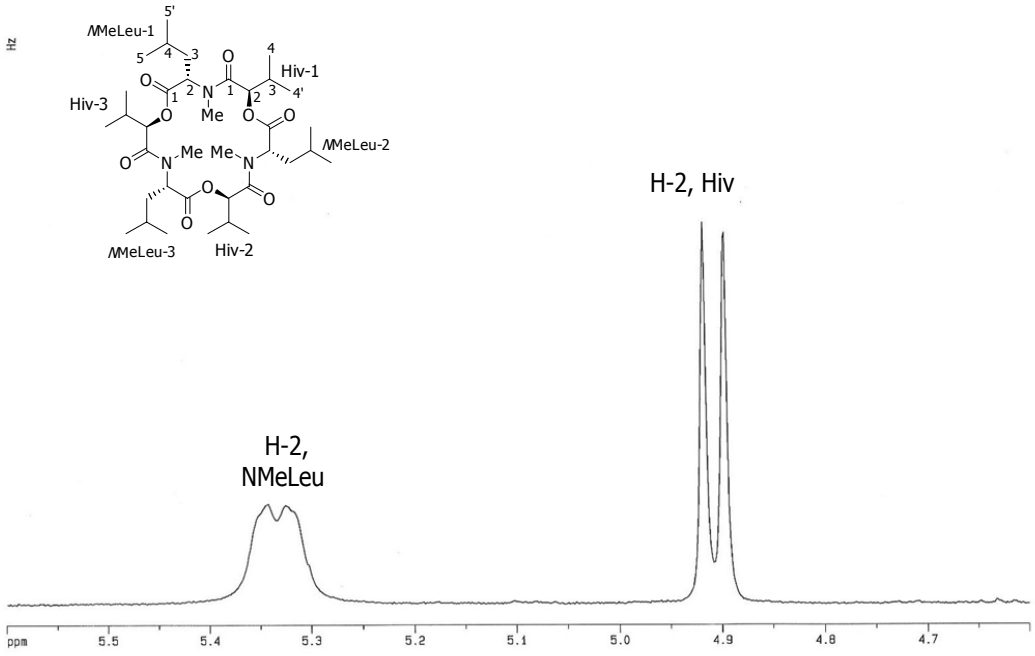

Figure 241. Expansion C of ^{1}H NMR ($CDCl_3$) spectrum of enniatin C **(60)**

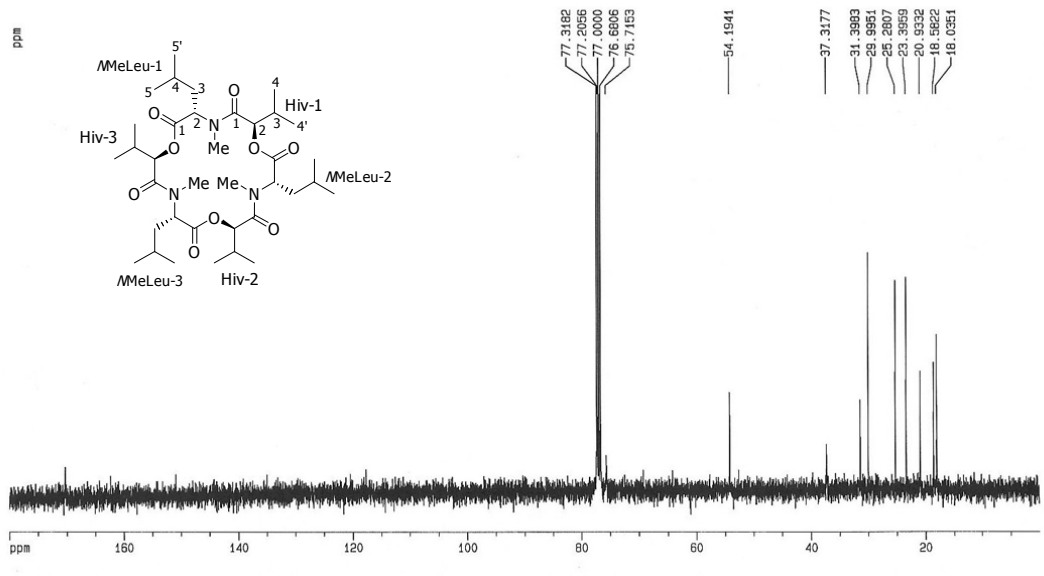

Figure 242. ^{13}C NMR spectrum of enniatin C **(60)**

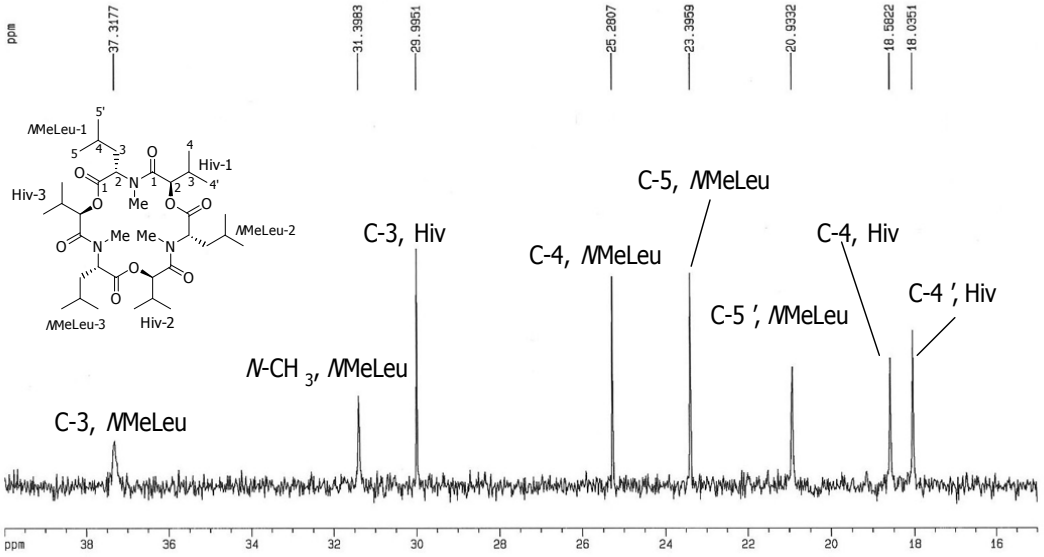

Figure 243. Expansion A of ^{13}C NMR spectrum of enniatin C **(60)**

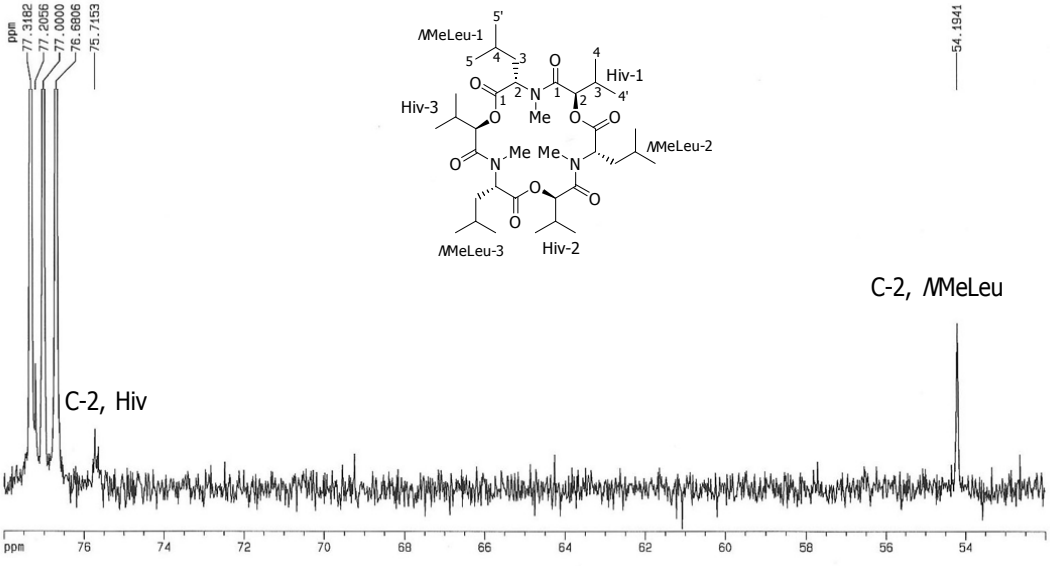

Figure 244. Expansion B of ^{13}C NMR spectrum of enniatin C **(60)**

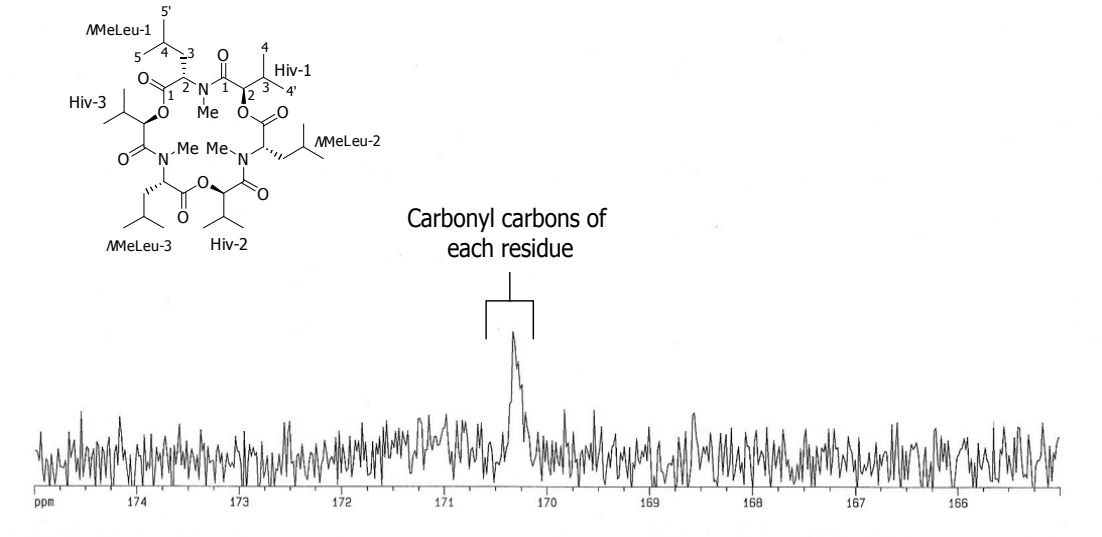

Figure 245. Expansion C of ^{13}C NMR spectrum of enniatin C **(60)**

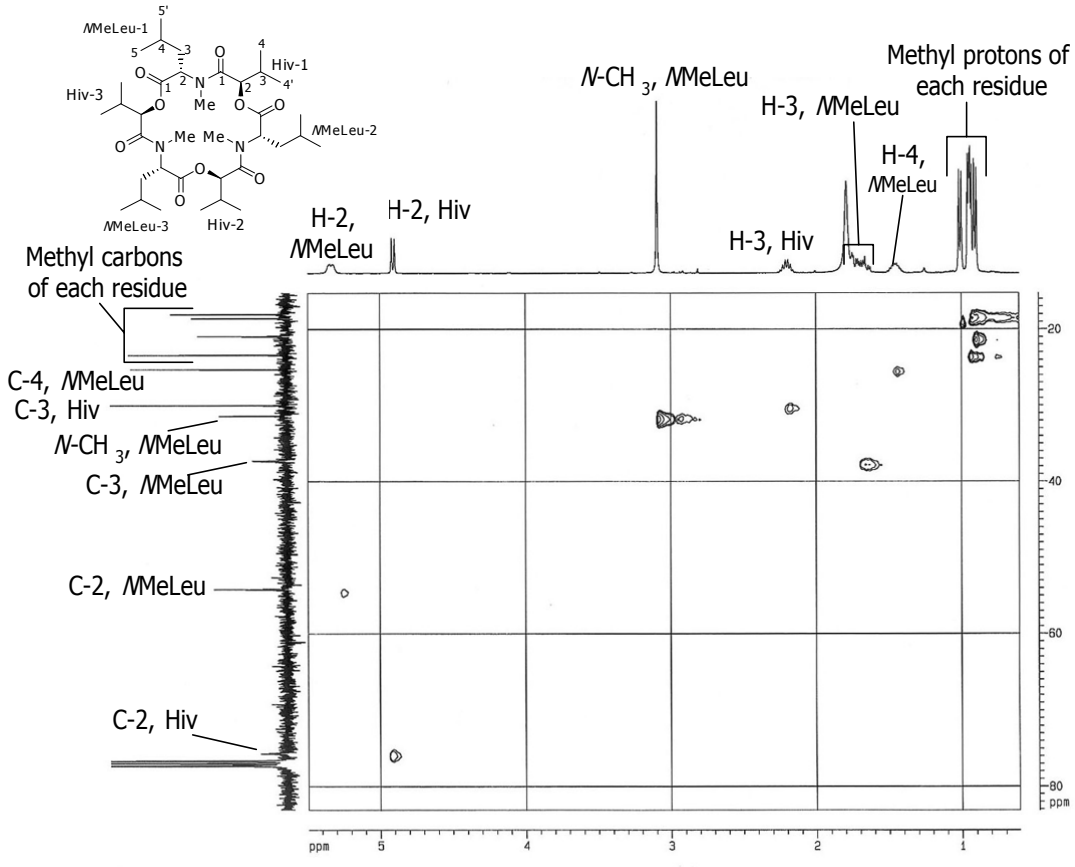

Figure 246. HMQC spectrum of enniatin C **(60)**

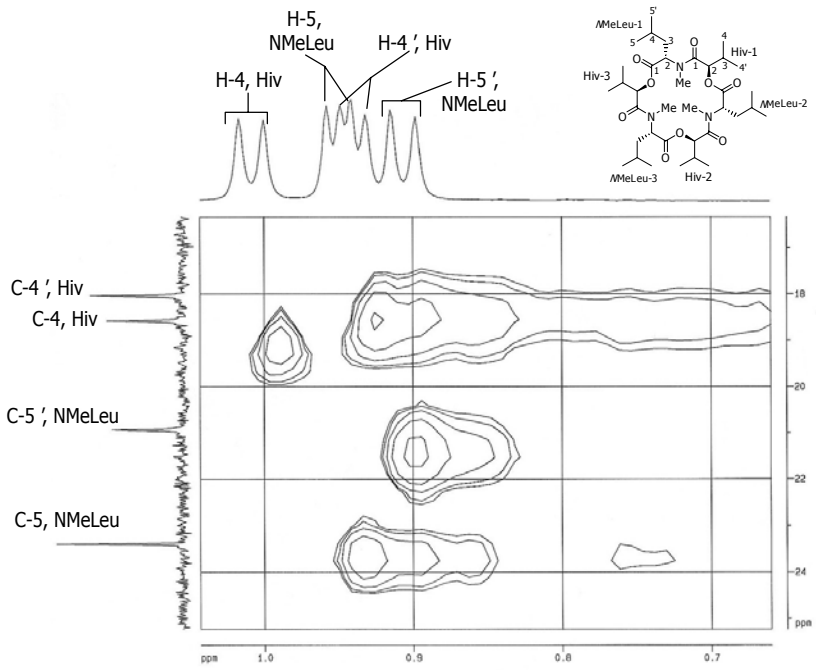

Figure 247. Expansion of HMQC spectrum of enniatin C **(60)**

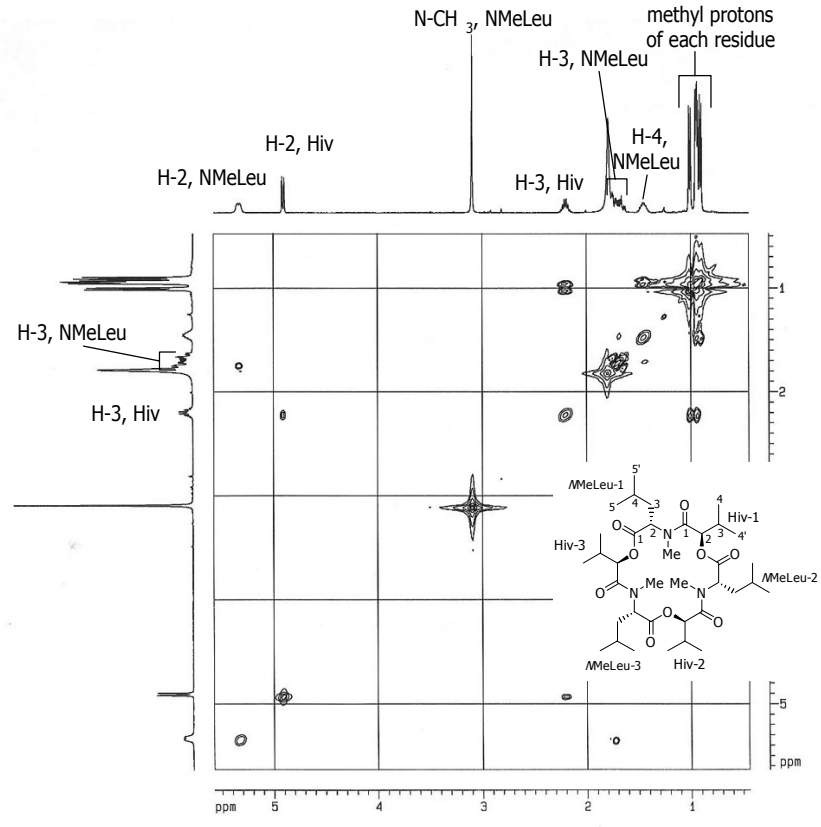

Figure 248. COSY spectrum of enniatin C **(60)**

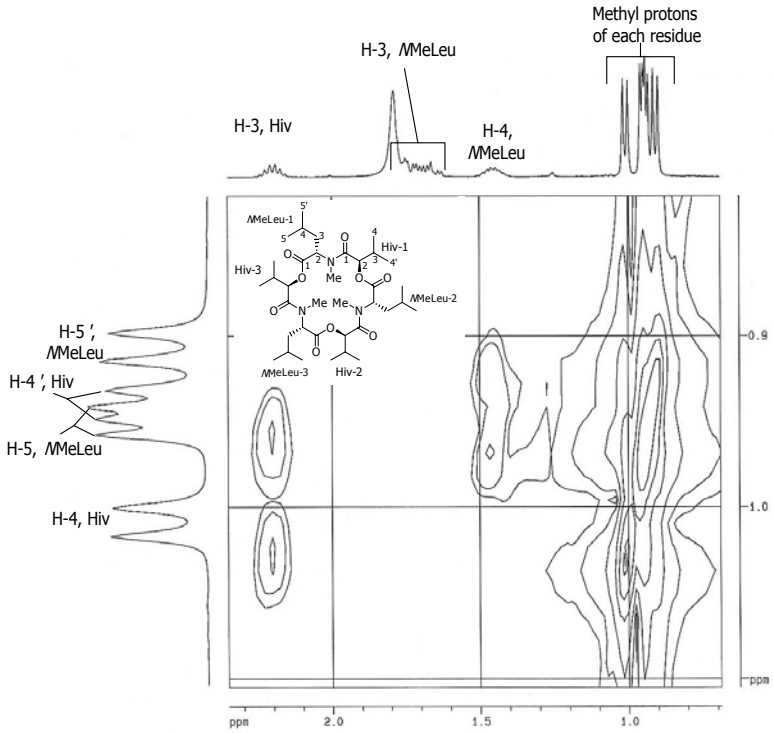

Figure 249. Expansion A of COSY spectrum of enniatin C **(60)**

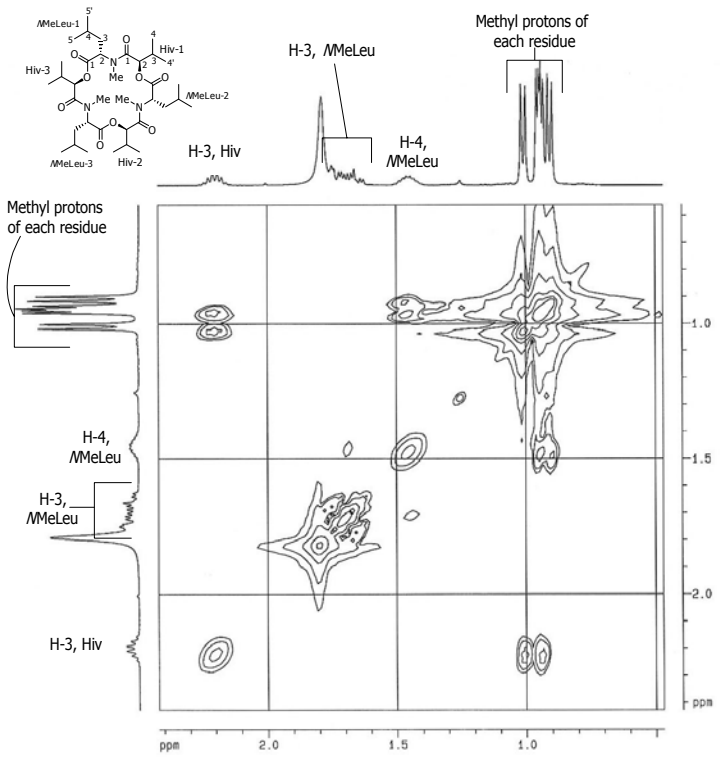

Figure 250. Expansion B of COSY spectrum of enniatin C **(60)**

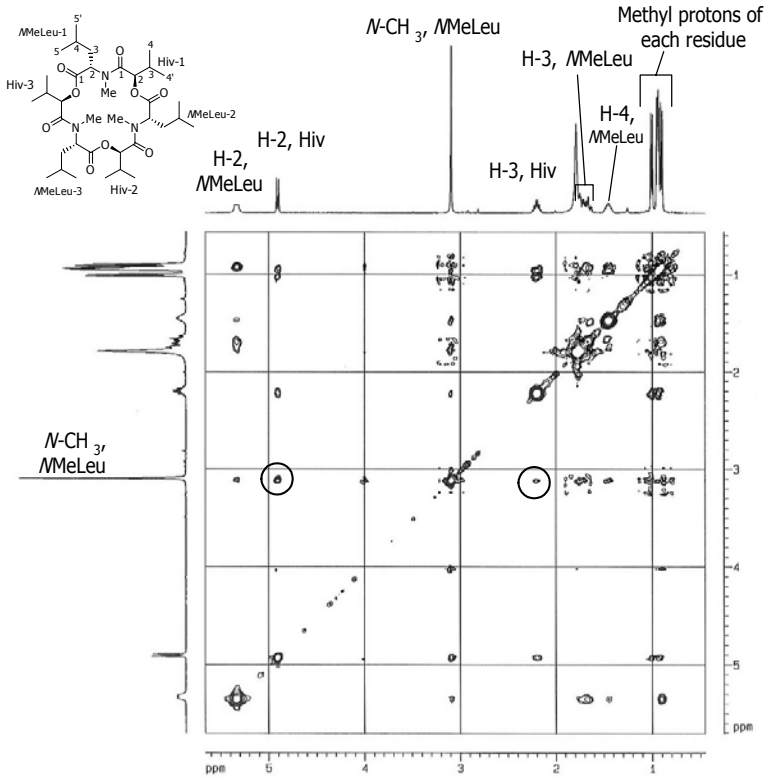

Figure 251. NOESY spectrum of enniatin C **(60)**

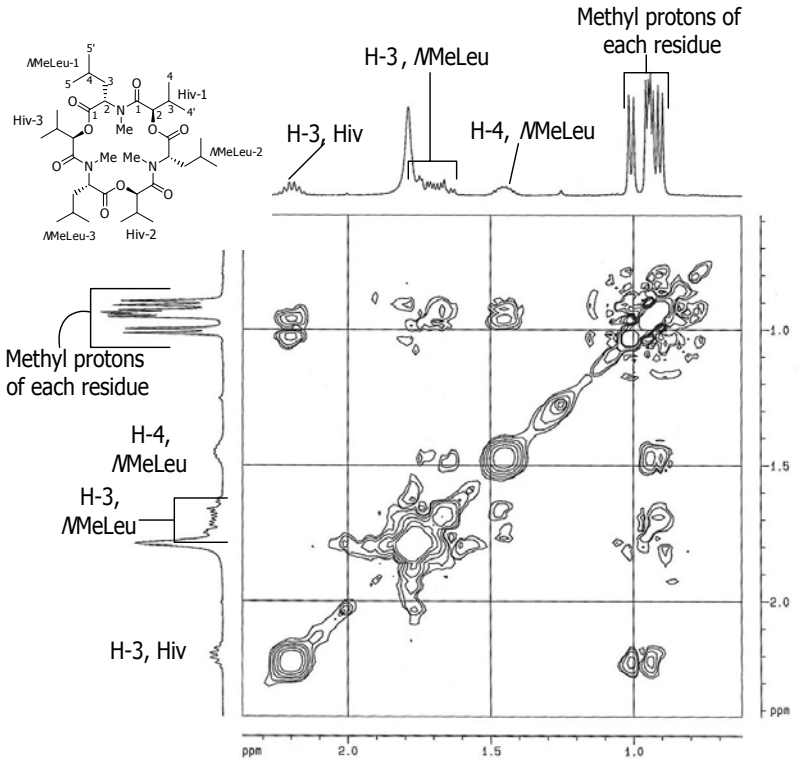

Figure 252. Expansion A of NOESY spectrum of enniatin C **(60)**

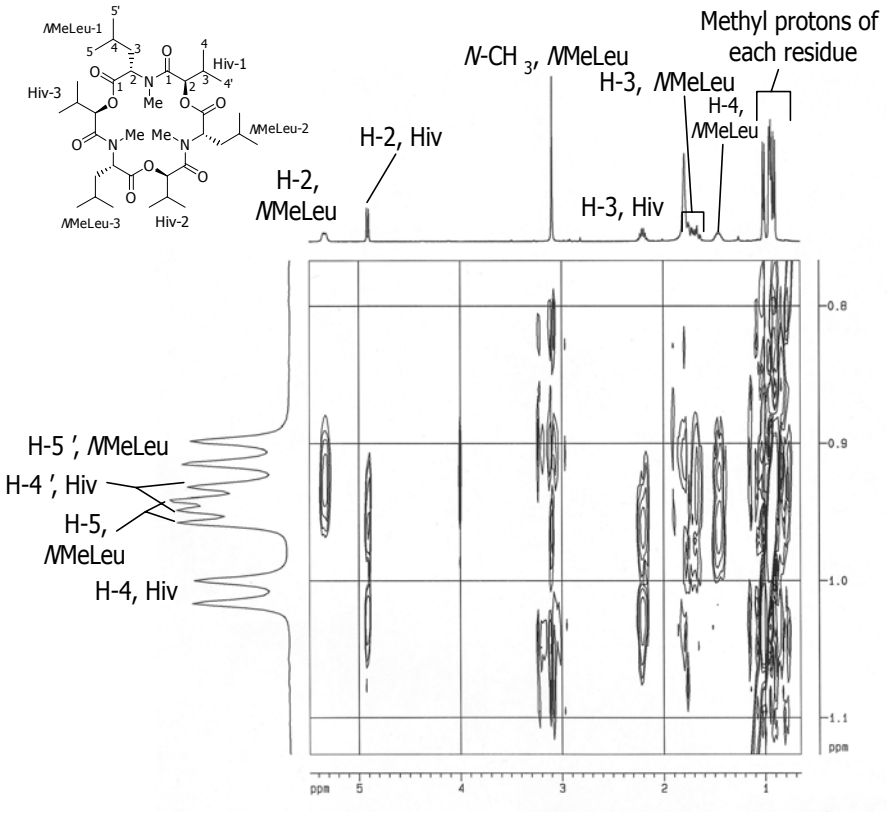

Figure 253. Expansion B of NOESY spectrum of enniatin C **(60)**

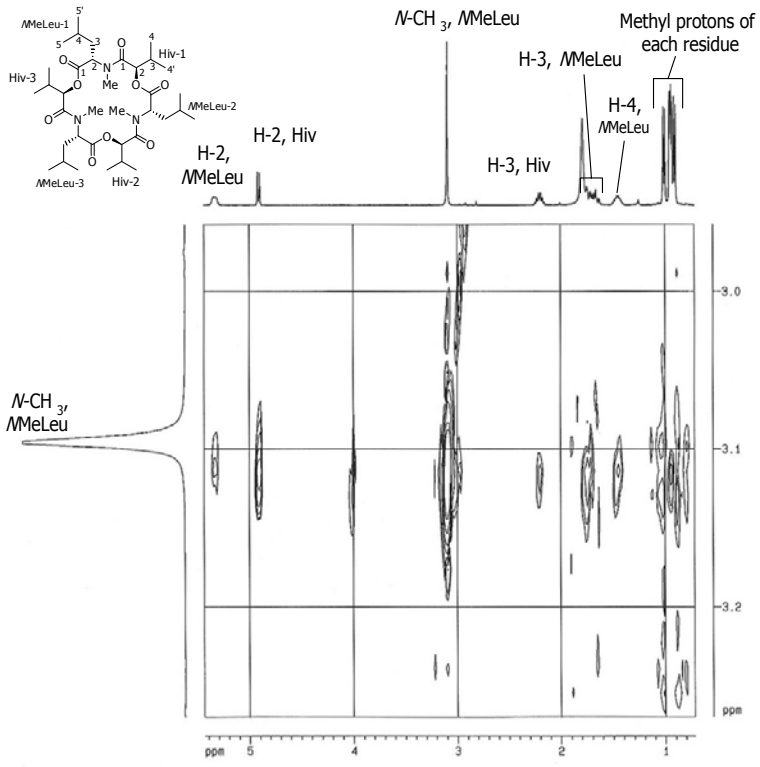

Figure 254. Expansion C of NOESY spectrum of enniatin C **(60)**

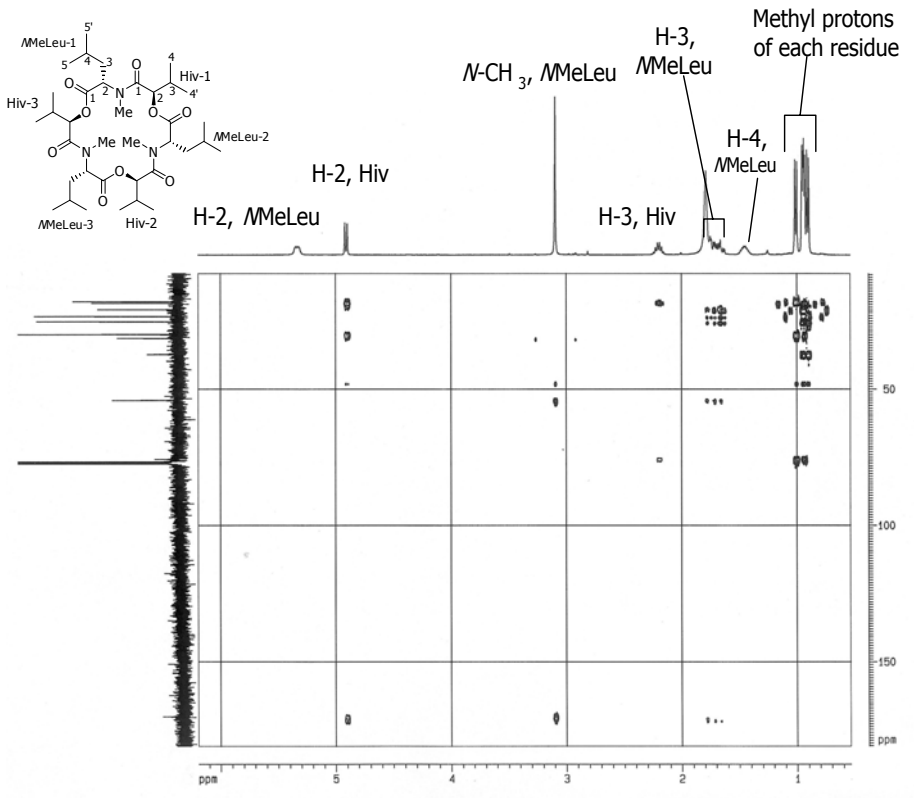

Figure 255. HMBC spectrum of enniatin C **(60)**

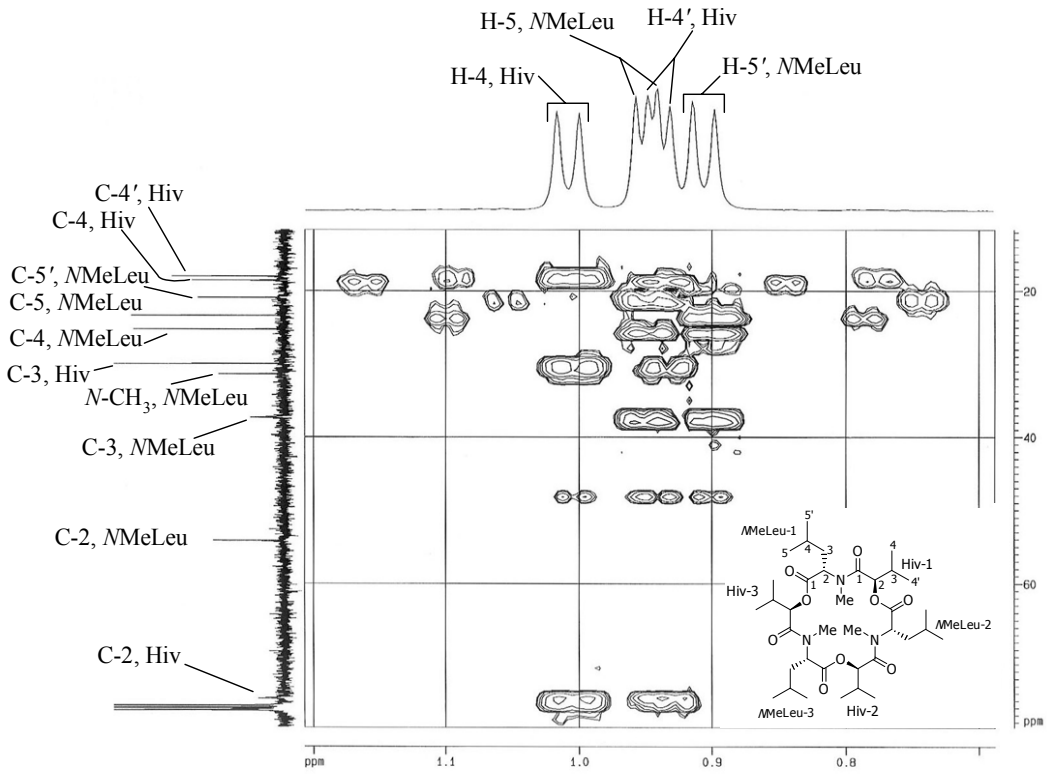

Figure 256. Expansion A of HMBC spectrum of enniatin C **(60)**

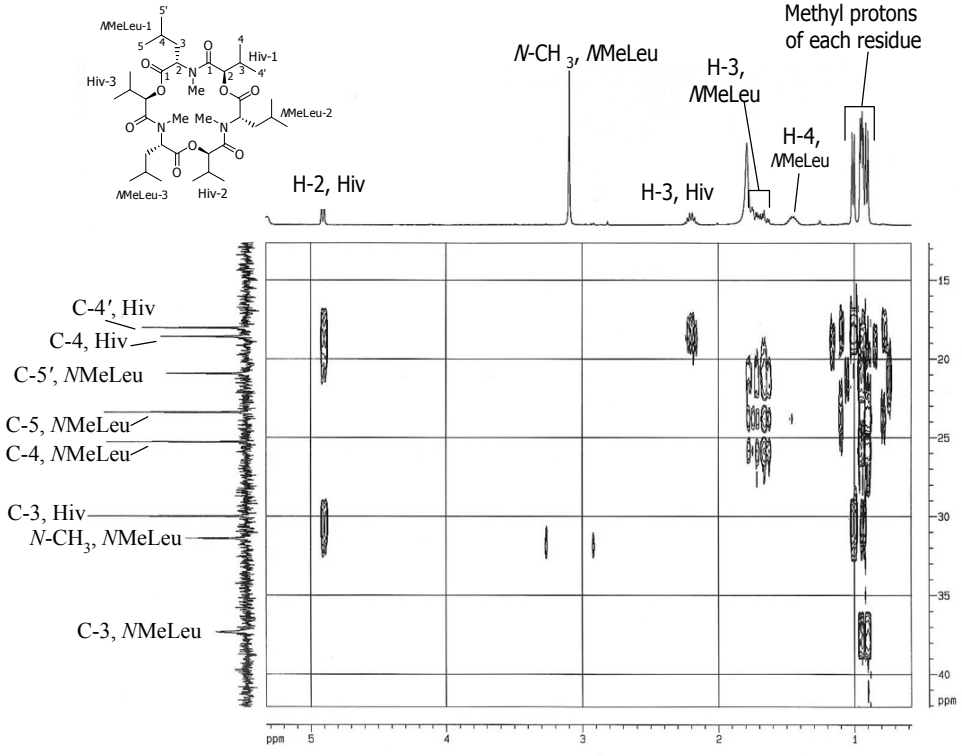

Figure 257. Expansion B of HMBC spectrum of enniatin C **(60)**

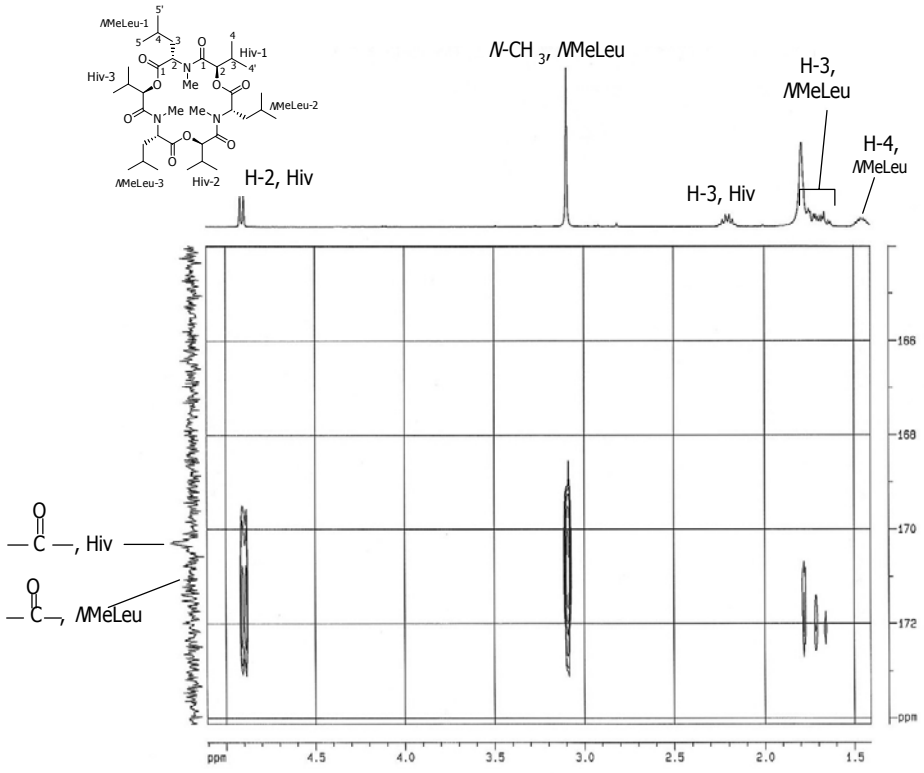

Figure 258. Expansion C of HMBC spectrum of enniatin C **(60)**

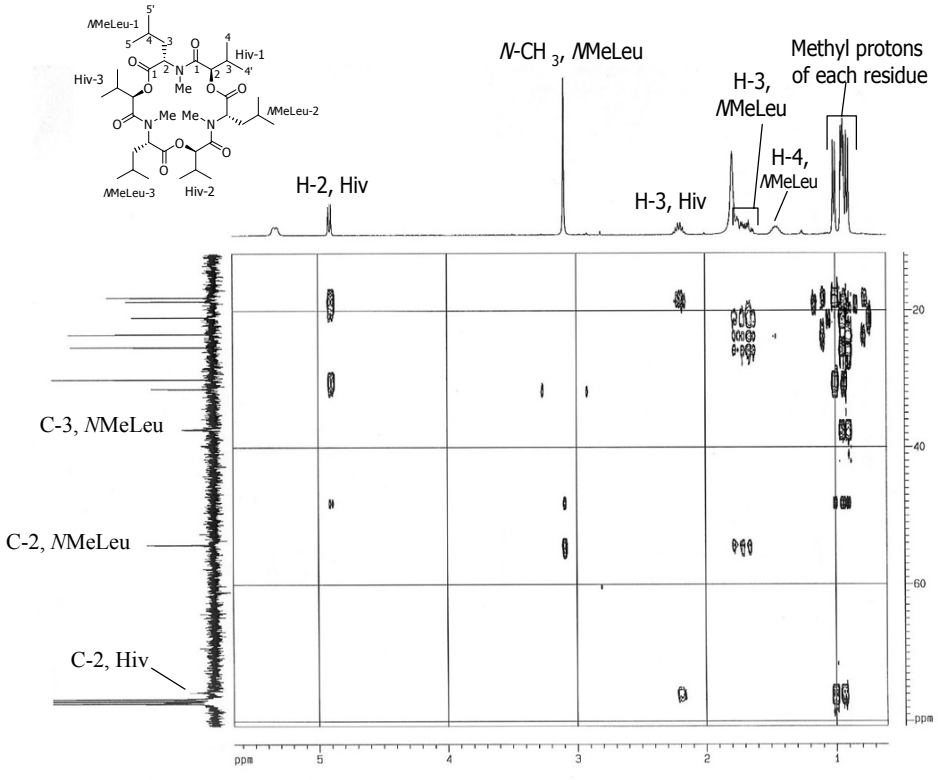

Figure 259. Expansion D of HMBC spectrum of enniatin C **(60)**

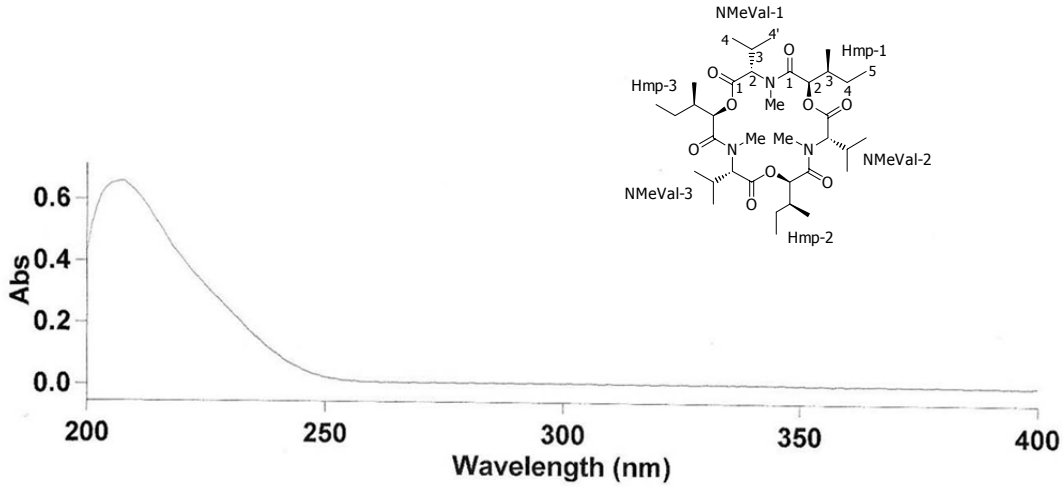

Figure 260. UV spectrum of MK 1688 **(61)**

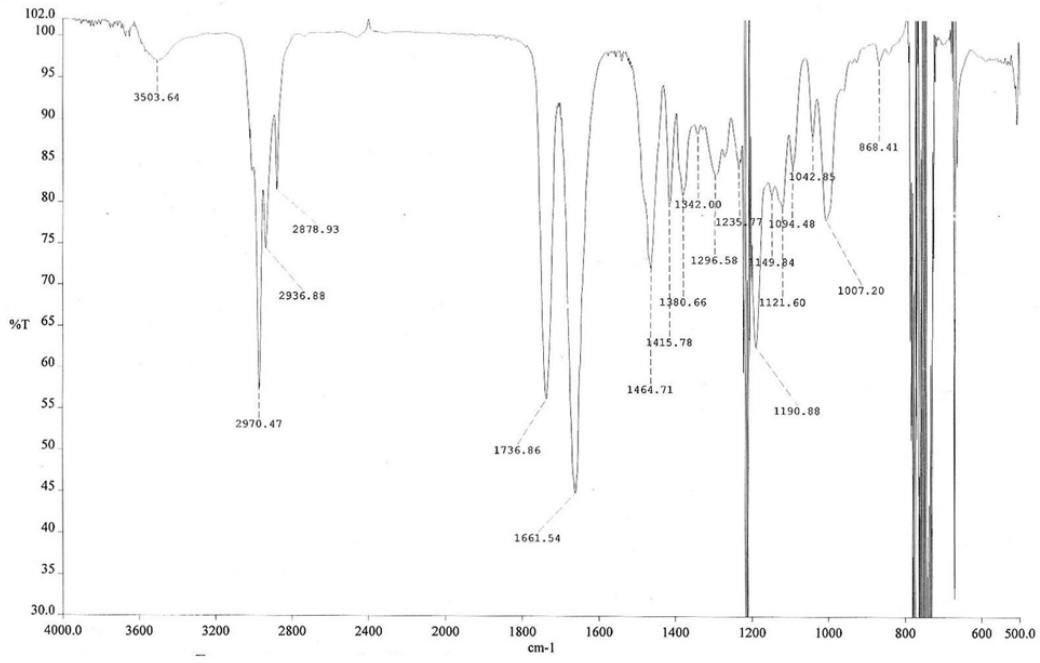

Figure 261. IR spectrum of MK 1688 **(61)**

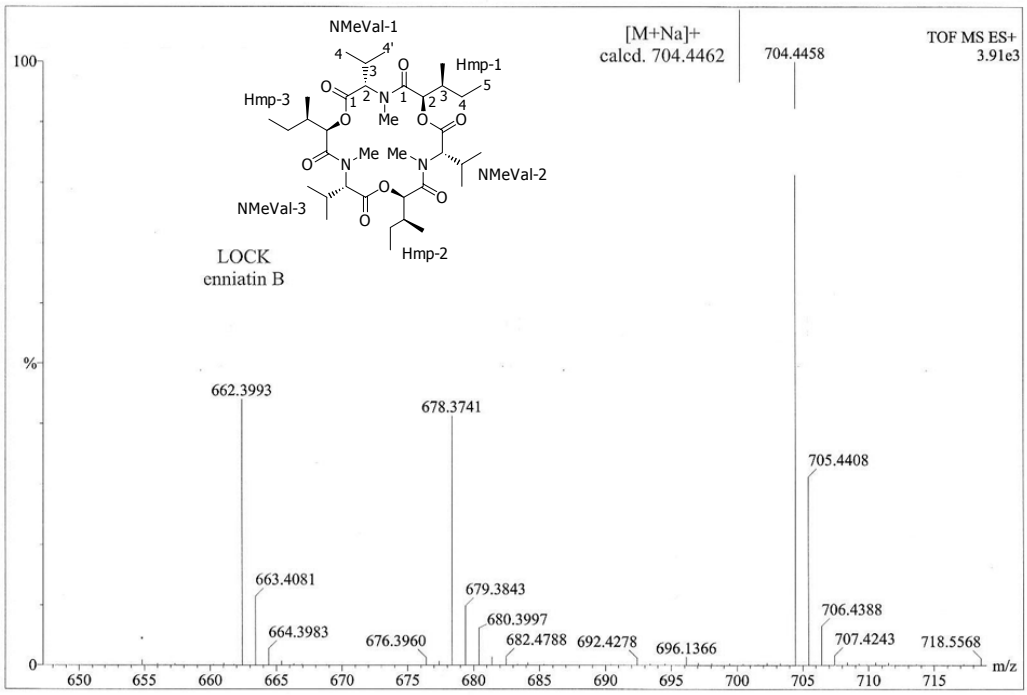

Figure 262. HRMS spectrum of MK 1688 **(61)**

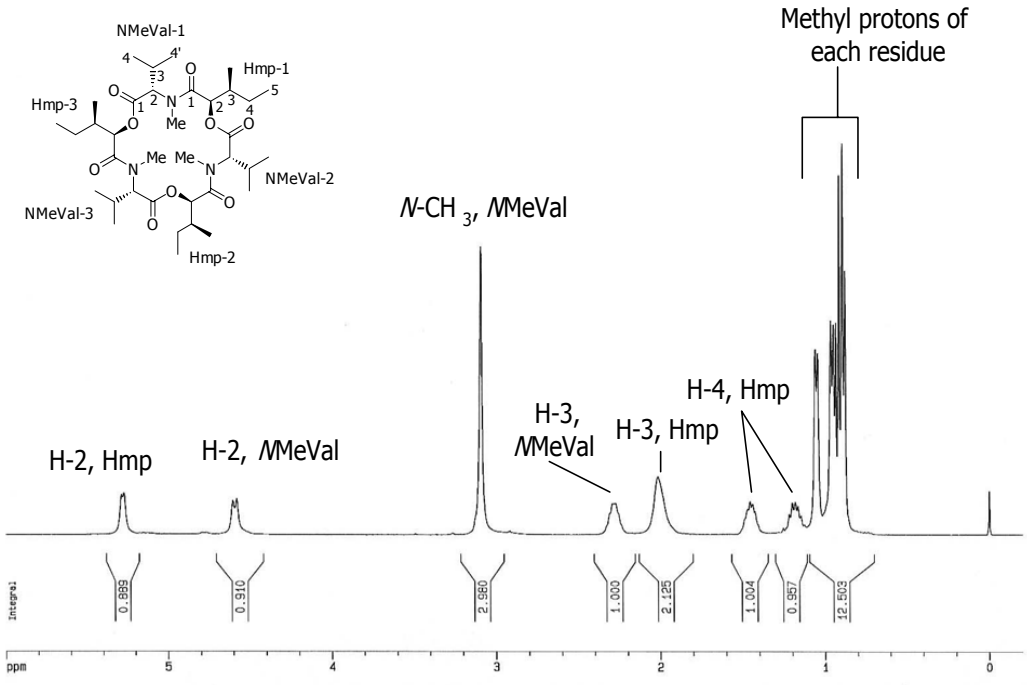

Figure 263. ^{1}H-NMR ($CDCl_3$) spectrum of MK 1688 **(61)**

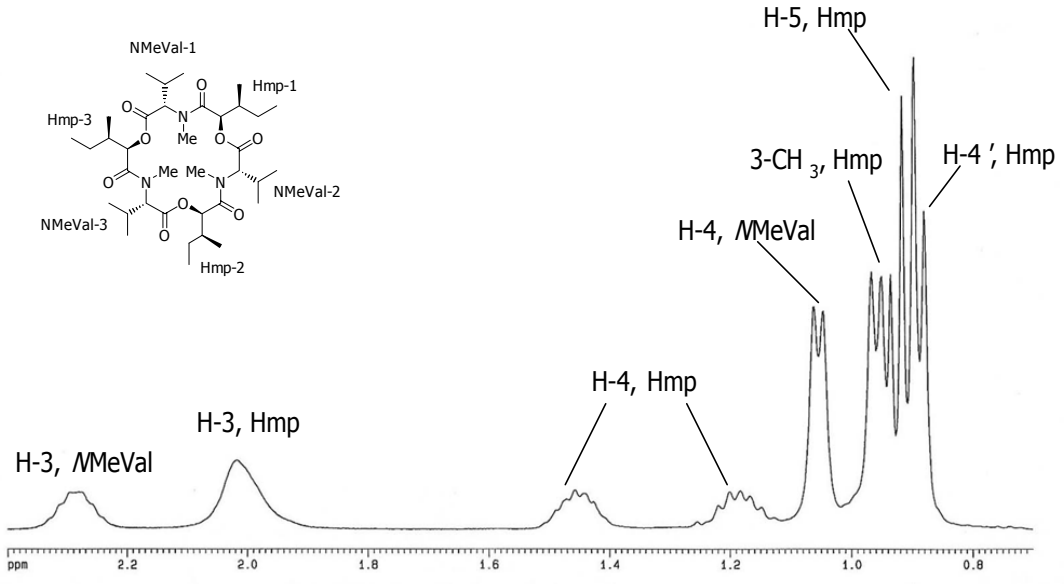

Figure 264. Expansion A of ^{1}H-NMR ($CDCl_3$) spectrum of MK 1688 **(61)**

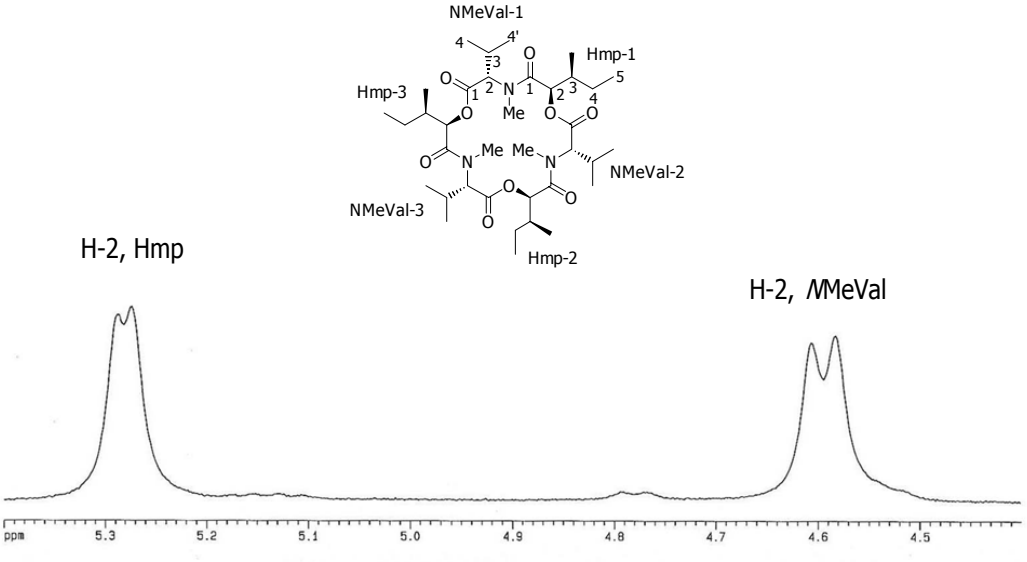

Figure 265. Expansion B of ^{1}H-NMR ($CDCl_3$) spectrum of MK 1688 **(61)**

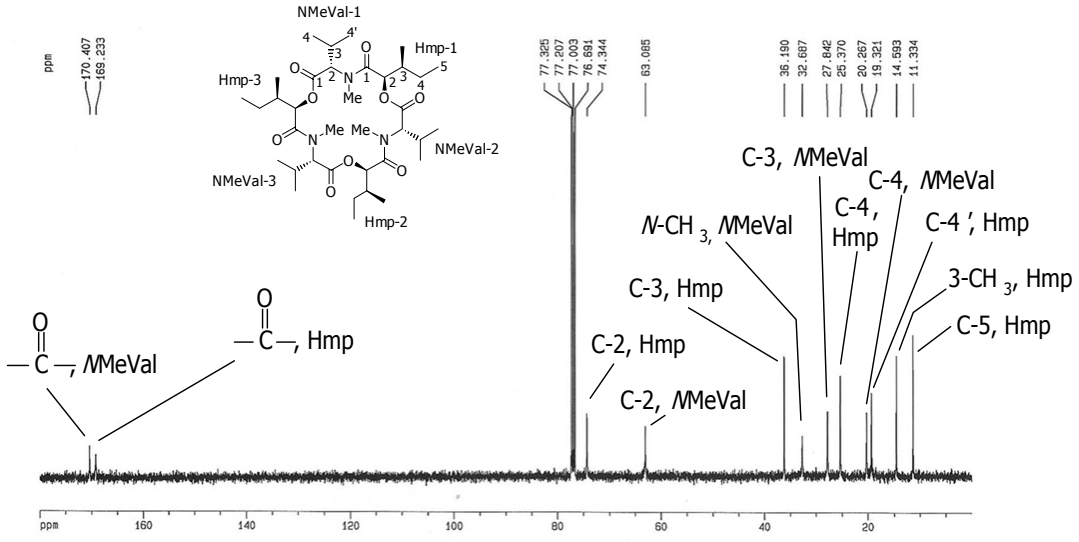

Figure 266. ^{13}C-NMR spectrum of MK 1688 **(61)**

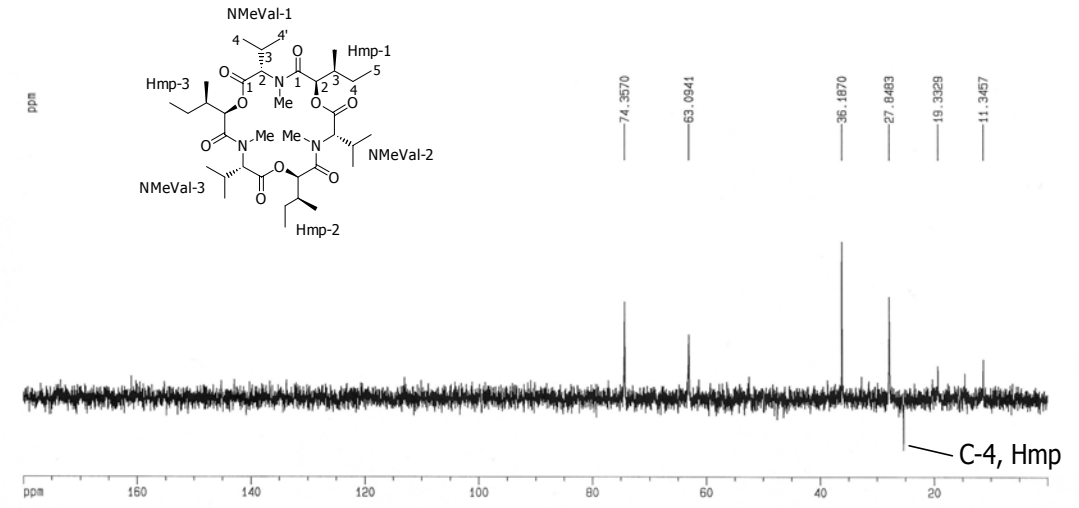

Figure 267. DEPT 135 spectrum of MK 1688 **(61)**

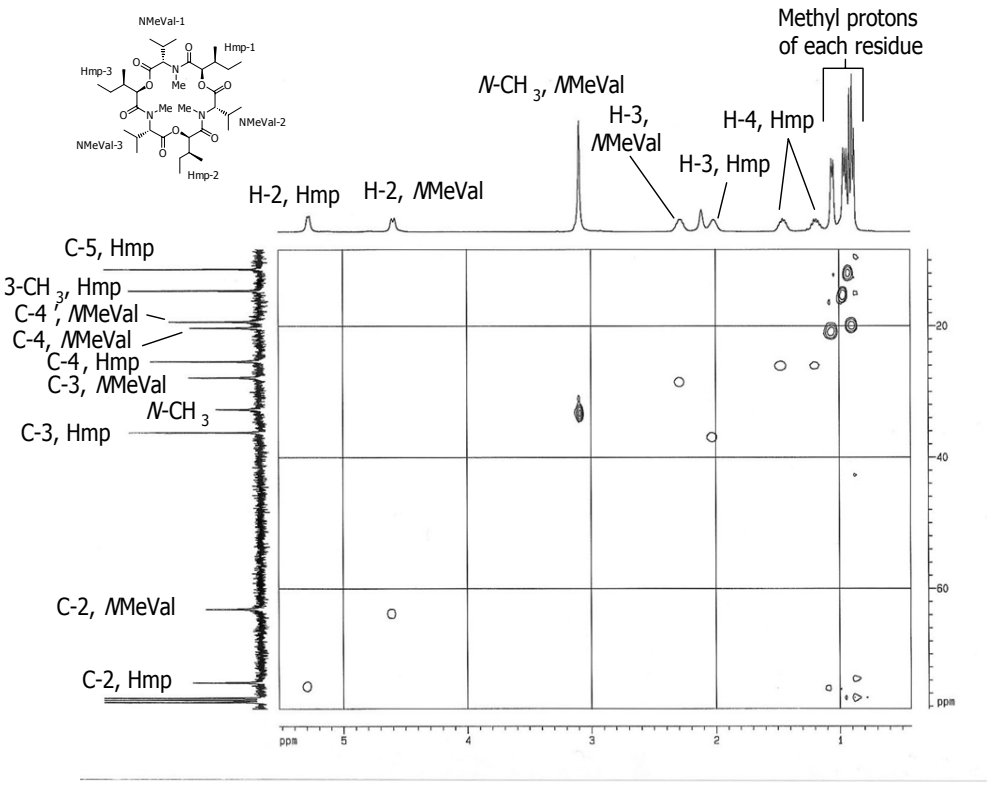

Figure 268. HMQC spectrum of MK 1688 **(61)**

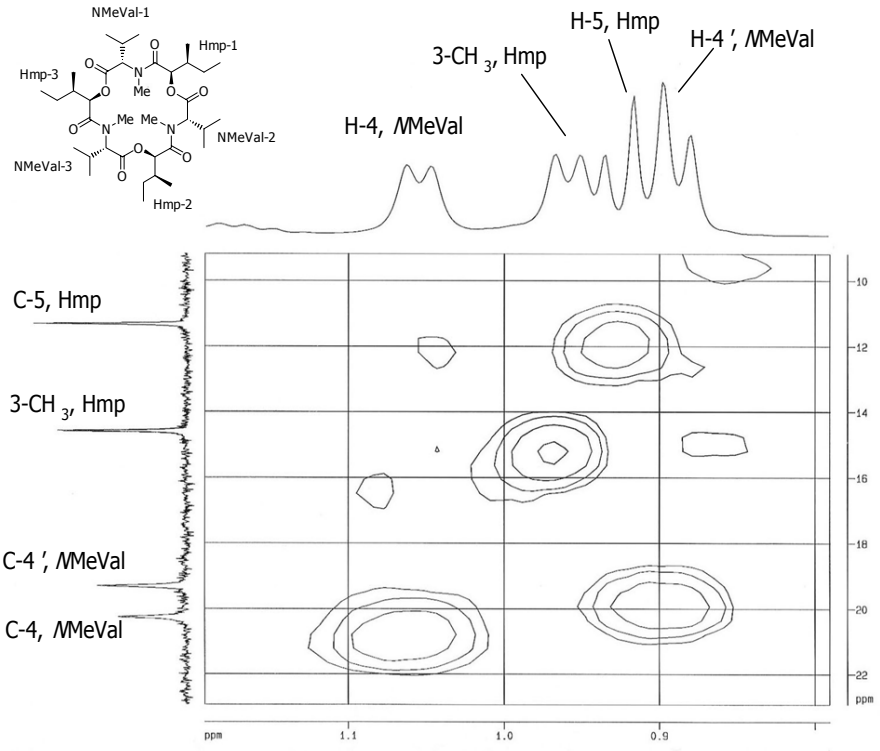

Figure 269. Expansion of HMQC spectrum of MK 1688 **(61)**

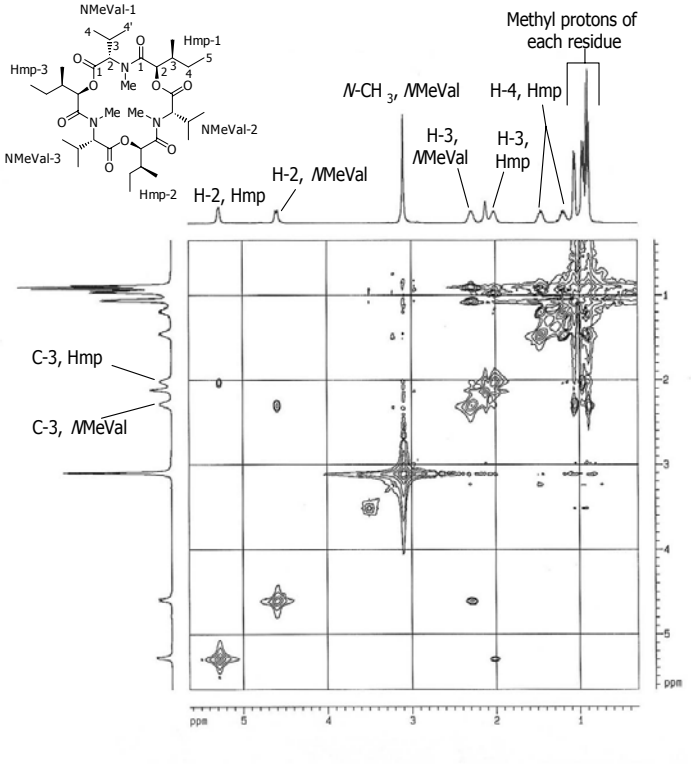

Figure 270. COSY spectrum of MK 1688 **(61)**

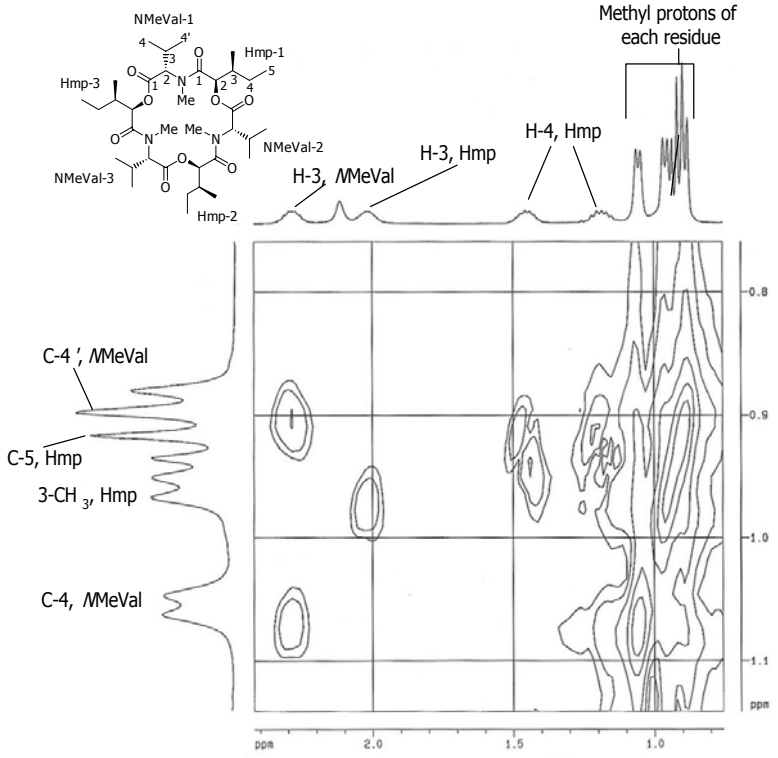

Figure 271. Expansion A of COSY spectrum of MK 1688 **(61)**

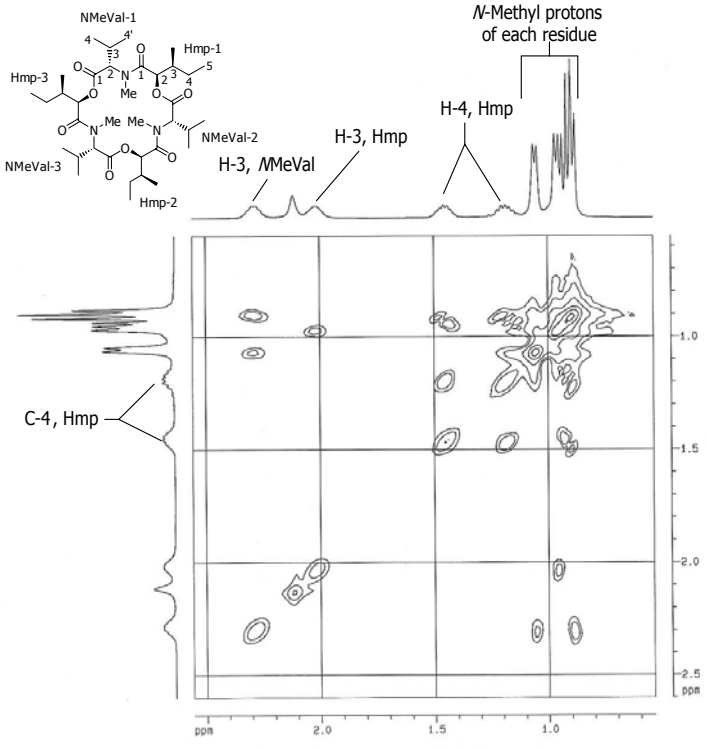

Figure 272. Expansion B of COSY spectrum of MK 1688 **(61)**

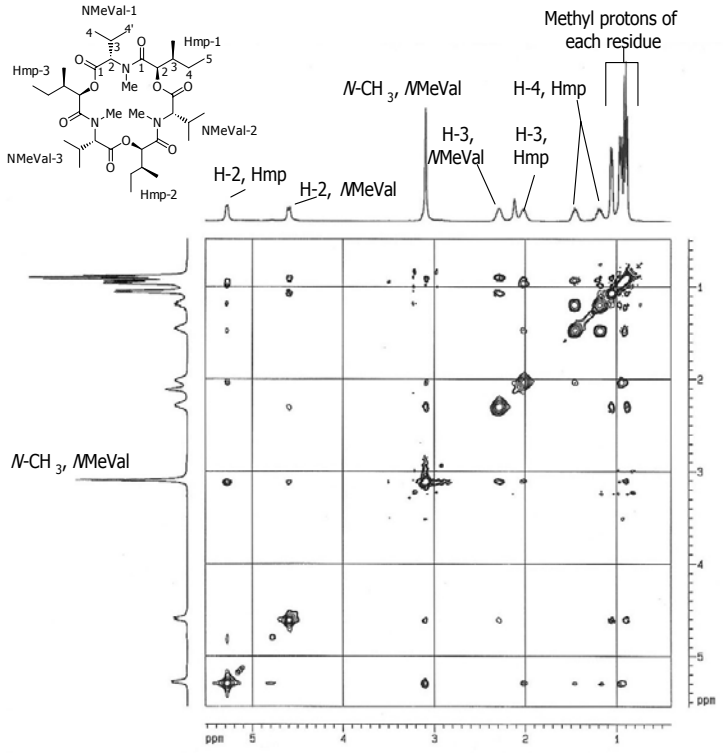

Figure 273. NOESY spectrum of MK 1688 **(61)**

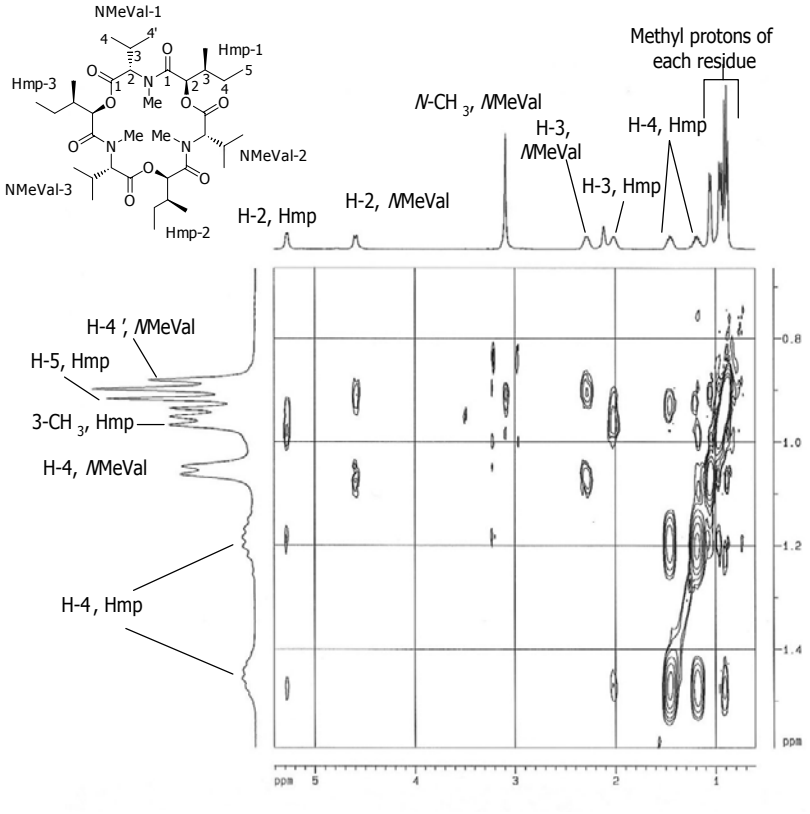

Figure 274. Expansion of NOESY spectrum of MK 1688 **(61)**

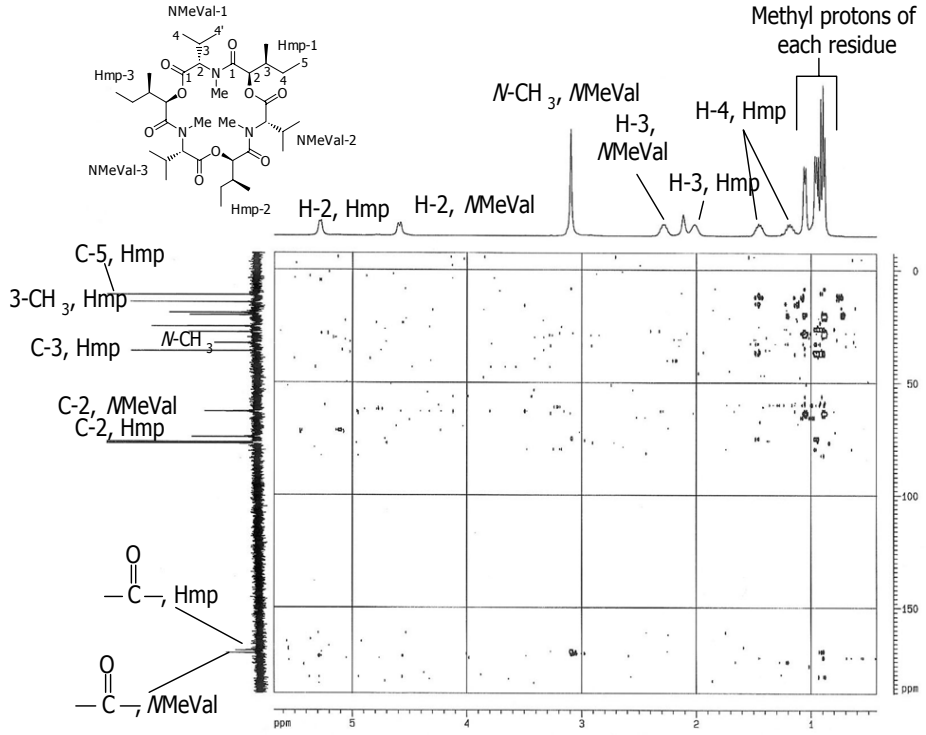

Figure 275. HMBC spectrum of MK 1688 **(61)**

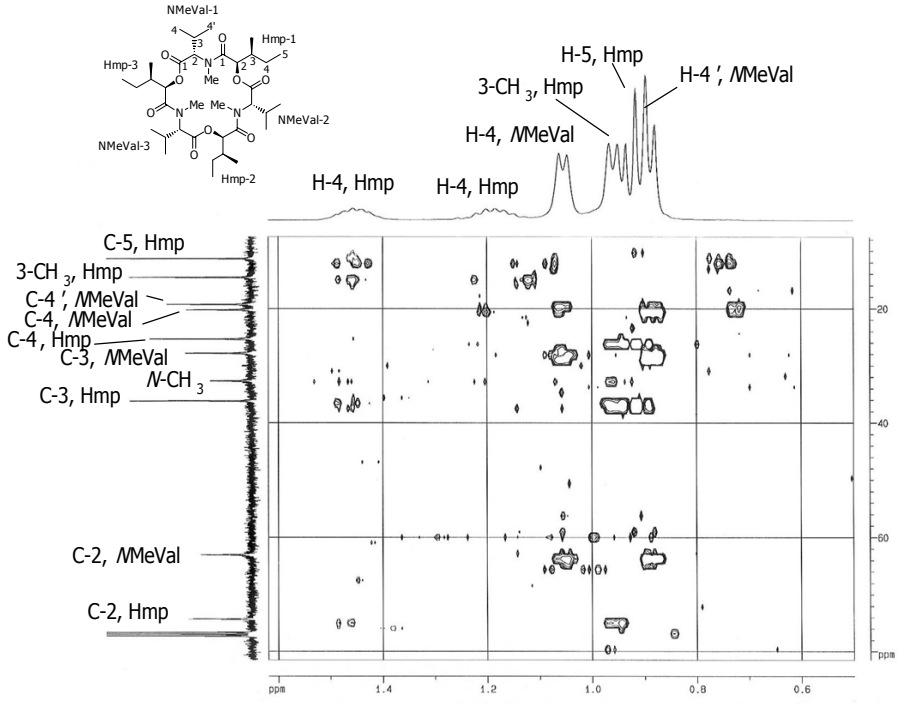

Figure 276. Expansion A of HMBC spectrum of MK 1688 **(61)**

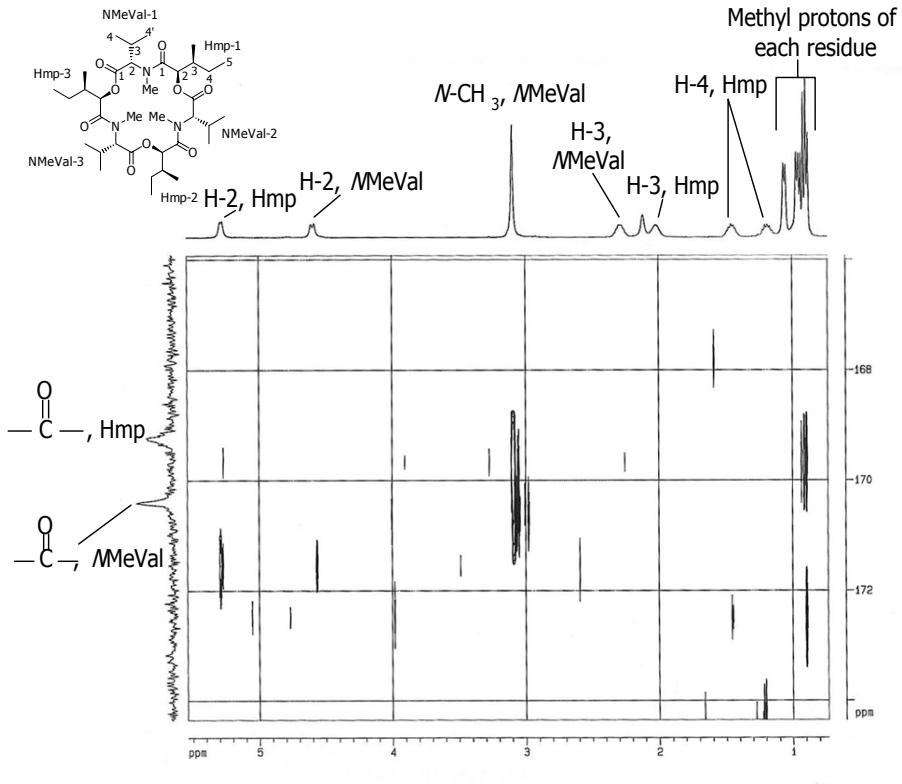

Figure 277. Expansion B of HMBC spectrum of MK 1688 **(61)**

PUBLICATIONS

1. Nilanonta, C., Isaka, M., Kittakoop, P., Saenboonrueng, J., Rukachaisirikul, V., Kongsaeree, P. and Thebtaranonth, Y. 2003. "New Diketopiperazines from the Entomopathogenic Fungus *Verticillium hemipterigenum* BCC 1449" *J. Antibiot.* 56, 647-651.

2. Nilanonta, C., Isaka, M., Chanphen, R., Thong-orn, N., Tanticharoen, M. and Thebtaranonth, Y. 2003. "Unusual enniatins produced by the insect pathogenic fungus *Verticillium hemipterigenum*: isolation and studies on precursor-directed biosynthesis" *Tetrahedron*. 59, 1015-1020.

THE JOURNAL OF ANTIBIOTICS Vol. 56, No. 7 pp. 647–651 July 2003

New Diketopiperazines from the Entomopathogenic Fungus *Verticillium hemipterigenum* BCC 1449

CHONGDEE NILANONTA,[a] MASAHIKO ISAKA,[b,*] PRASAT KITTAKOOP,[b] JUNYA SAENBOONRUENG,[b] VATCHARIN RUKACHAISIRIKUL,[a] PALANGPON KONGSAEREE[c] and YODHATHAI THEBTARANONTH[b,c]

[a] Department of Chemistry, Faculty of Science, Prince of Songkla University, Songkhla 90112, Thailand
[b] National Center for Genetic Engineering and Biotechnology (BIOTEC), 113 Phaholyothin Road, Klong 1, Klong Luang, Pathumthani 12120, Thailand
[c] Department of Chemistry, Faculty of Science, Mahidol University, Rama 6 Road, Bangkok 10400, Thailand

JAPAN ANTIBIOTICS RESEARCH ASSOCIATION

New Diketopiperazines from the Entomopathogenic Fungus *Verticillium hemipterigenum* BCC 1449

CHONGDEE NILANONTA,[a] MASAHIKO ISAKA,[b,*] PRASAT KITTAKOOP,[b] JUNYA SAENBOONRUENG,[b] VATCHARIN RUKACHAISIRIKUL,[a] PALANGPON KONGSAEREE[c] and YODHATHAI THEBTARANONTH[b,c]

[a] Department of Chemistry, Faculty of Science, Prince of Songkla University, Songkhla 90112, Thailand
[b] National Center for Genetic Engineering and Biotechnology (BIOTEC), 113 Phaholyothin Road, Klong 1, Klong Luang, Pathumthani 12120, Thailand
[c] Department of Chemistry, Faculty of Science, Mahidol University, Rama 6 Road, Bangkok 10400, Thailand

(Received for publication February 12, 2003)

Two new diketopiperazines, bisdethiodi(methylthio)-1-demethylhyalodendrin and 1-demethylhyalodendrin tetrasulfide, together with two known cyclodepsipeptides, enniatins B and B_4, and two known pyrones, pyrenocines A and B, were isolated from a culture broth of the entomopathogenic fungus *Verticillium hemipterigenum* BCC 1449. These structures were elucidated using spectroscopic methods and X-ray crystallography. Antimalarial and cytotoxic activities of these compounds were evaluated.

The fungal genus *Verticillium* has been known to be a rich source of bioactive secondary metabolites of diverse structures, for examples, balanol (a protein kinase C inhibitor) from *V. balanoides*,[1] ES-242-1 (a bioxanthracene, NMDA receptor antagonist) from *Verticillium* sp. SPC-15898,[2] 11α,11'α-dihydroxychaetocin (antibiotic) from *V. tenerum*,[3] verticillins A~C (diketopiperazine dimers, antibiotics) from *Verticillium* sp. TM-759,[4] and (−)-vertinolide (a β-tetronic acid derivative, mycotoxin) and bisvertinols (dimeric vertinoids) from *V. intertextum*.[5,6] Recently we reported the isolation of two new enniatins H and I, together with known enniatins B and B_4, from a mycelial extract of *V. hemipterigenum* BCC 1449 as antimalarial constituents.[7] Further investigation on EtOAc extract of the culture filtrate from this strain led to the identification of two new diketopiperazines **1** and **2**, together with four known compounds, enniatins B (**3**) and B_4 (**4**), and pyrenocines A (**5**) and B (**6**). We report herein the isolation, structural elucidation, and biological activities of these compounds.

Fermentation and Isolation

V. hemipterigenum was collected from Khlong Nakha Wildlife Sanctuary, Phetchaboon province, northern Thailand, on Homoptera–adult leafhopper, and identified by Dr. NIGEL L. Hywel-Jones of Mycology Research Unit, BIOTEC. The fungus is deposited at the Thailand BIOTEC Culture Collection as BCC 1449.

A culture of BCC 1449 maintained on potato dextrose agar was inoculated into potato dextrose broth (4× 250 ml). After 7 days, the primary inoculum (total 1 liter) was transferred into 40×1 liter Erlenmeyer flasks, each containing 250 ml of potato dextrose broth medium, and incubated at 30°C for 14 days. The culture filtrate (10 liters) was extracted twice with equal volume of EtOAc, and the combined organic layer was concentrated under reduced pressure to obtain a brown gum (481 mg). Trituration in MeOH (2 ml) gave light yellow crystals (123 mg). The filtrate was concentrated to obtain a brown gum (320 mg). Recrystallization of the crystals from EtOH-H_2O gave pure enniatin B (**3**; colorless crystals, 80 mg). The dried filtrate was purified by Sephadex LH-20 column (MeOH eluent)

* Corresponding author: isaka@biotec.or.th

Structures of **1**~**6**.

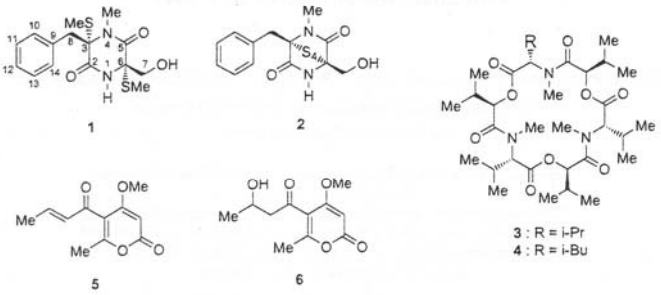

followed by column chromatography on silica gel (0~20% MeOH in CH_2Cl_2, gradient elution) to obtain, in the order of elution, five fractions: Fr-1 (62 mg), Fr-2 (17 mg), Fr-3 (21 mg), Fr-4 (24 mg) and Fr-5 (33 mg). Each fraction was subjected to preparative HPLC using a reversed-phase column (Prep Nova-Pak® HRC_{18}, 6 μm, 40×100 mm) with MeCN/H_2O as eluent, followed by column chromatography on silica gel (5~40% EtOAc in hexane, gradient elution). Compound **5** (43 mg) was obtained from Fr-1. Compounds **2** (3.6 mg) and **6** (5.9 mg) were obtained from Fr-2. From Fr-3 was isolated compound **1** (8.1 mg). Compounds **3** (5.2 mg) and **4** (3.3 mg) were isolated from Fr-4. Fr-5 mainly provided enniatin B (**3**).

Fig. 1. Selected HMBC correlations for **1** and **2**.

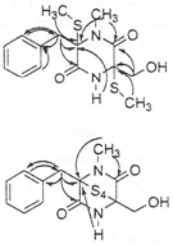

Structure Elucidation

The ^{13}C NMR spectrum ($CDCl_3$) of compound **1** showed twelve carbon signals where two carbonyl carbon signals were superimposed at δ_C 164.9 ppm; this was evident by the detection of two separate signals at δ_C 167.3 and δ_C 167.4 ppm in the spectrum acquired in MeOH-d_4 (total 13 signals). Combined analyses of ^1H, ^{13}C, DEPTs, COSY and HMQC spectra revealed that this compound possesses a benzyl group, a hydroxymethyl group, two methylthio groups (δ_C 13.5, δ_H 2.23 ppm; and δ_C 14.4, δ_H 2.20 ppm), a methyl group attached to an amide nitrogen (δ_C 30.3, δ_H 3.28 ppm), a secondary amide proton (δ_H 6.39 ppm, exchangeable with D_2O), two quaternary carbons at δ_C 64.8 and 75.7 ppm, and two carbonyls. The molecular formula of **1**, $C_{15}H_{20}S_2N_2O_3$, was determined by HRMS (ESI-TOF) analysis. The presence of amide groups was evident by strong IR absorptions at ν_{max} 1693 and 1634 cm^{-1}. HMBC correlations (in MeOH-d_4) demonstrated that the benzyl group, one of the methylthio groups (δ_H 2.27 ppm), one carbonyl (δ_C 167.3 ppm), and the methylated amide nitrogen were attached to the quaternary carbon at δ_C 76.5 ppm. Considering also other HMBC correlations (Fig. 1), the structure of **1** was elucidated as depicted.

The structure of **1** was confirmed by X-ray crystallographic analysis and it revealed that the two methylthio groups of **1** are attached to the same side of the six-membered ring (Fig. 2). The absolute configuration of **1** was elucidated unambiguously to be (3*S*,6*S*) by the standard anomalous scattering method.

The NMR, IR and UV spectra of compound **2** were close to those of **1** except for the lack of the two NMR signals of

sulfur-connected methyl groups both in ^1H and ^{13}C spectra. The molecular formula of $C_{13}H_{14}S_4N_2O_3$, established by HRMS, requested a structure bearing $-S_4-$ bridge depicted as **2**. Since compound **2** was isolated from the same extract as that of **1**, it is more likely to possess (3*S*,6*S*)-configuration rather than its optical antipode.

Compounds **1** and **2** are new 1-demethyl analogs of the known bisdethiodi(methylthio)hyalodendrin[8~10] and hyalodendrin tetrasulfide,[9~11] respectively. (3*S*,6*S*)-bisdethiodi(methylthio)hyalodendrin and (3*S*,6*S*)-hyalodendrin tetrasulfide have previously been isolated from *Hyalodendron* spp.,[8,11] while the (3*R*,6*R*)-isomers of these compounds were isolated from *Penicillium turbatum*.[9] In the extract of *V. hemipterigenum* BCC 1449, these known compounds were not detected.

Fig. 2. X-Ray crystal structure of **1**.

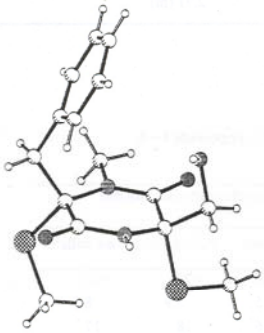

The spectral data (^1H and ^{13}C-NMR, IR, MS, and UV) of enniatins B (**3**: colorless crystals; mp 173~175°C; $[\alpha]_D^{29}$ −96, *c* 1.04, $CHCl_3$) and B_4 (**4**: amorphous solid; $[\alpha]_D^{27}$ −57, *c* 0.09, $CHCl_3$) were identical to those previously isolated from the mycelial extract by our group,[7] and also identical to literature data.[12~15] Structures of compounds **5** (colorless oil) and **6** (colorless oil) were elucidated by NMR, MS and IR analyses as known α-pyrones, pyrenocines A and B, respectively. Spectral data (^1H and ^{13}C NMR, IR, MS, UV) were consistent with those reported in literatures.[16~18]

Biological Activities

Compounds **1**~**6** were tested for *in vitro* antimalarial activity and cytotoxicity against two cancer cell lines (KB and BC-1) and Vero cells (Table 2). Assay for activity against *P. falciparum* (K1, multi-drug resistant strain) was performed using the standard protocol[19] which follows the microculture radioisotope technique.[20] Cytotoxic activities against human epidermoid carcinoma (KB) and human breast cancer (BC-1) cell lines and African green monkey kidney fibroblast (Vero cells) were evaluated using the colorimetric method.[21] IC_{50} values of a standard compound ellipticine are 0.46 μg/ml for KB, and 0.60 μg/ml for BC-1.

A number of diketopiperazines from fungal strains have been reported to show variety of biological activities such as antibacterial,[9,22] antiviral,[9] and antifungal.[10] This class of compounds also exhibit inhibitory activities against plasminogen activator inhibitor-1,[23] calpain[24] and farnesyltransferase.[25] In the present research, however, we found first that compound **2** shows antimalarial activity.

Table 1. Physico-chemical properties of **1** and **2**.

	1	2
Appearance	Colorless crystals	Colorless crystals
MP	154~157 °C	152~156 °C
Molecular formula	$C_{15}H_{20}N_2O_3S_2$	$C_{13}H_{14}N_2O_3S_4$
HRMS (ESI-TOF, negative)		
Found (*m/z*)	339.0841 $[M-H]^-$	372.9820 $[M-H]^-$
Calcd.	339.0837	372.9808
$[\alpha]_D$	−70° (*c* 0.21, $CHCl_3$, 26 °C)	−123° (*c* 0.16, $CHCl_3$, 26 °C)
UV λ_{max} nm (log ε) in EtOH	205 (4.35), 258 (2.94)	204 (4.35), 299 (3.59)
IR ν_{max} (KBr) cm^{-1}	3399, 3205, 3108, 1693, 1634, 1435, 1389, 1042, 701	3290, 3102, 1694, 1634, 1436, 1436, 1388, 1054, 752, 711

Table 2. ^{1}H and ^{13}C NMR data of compounds **1** and **2**.

position	1			2	
	^{1}H ($CDCl_3$)	^{13}C ($CDCl_3$)	^{13}C (MeOH-d_4)	^{1}H ($CDCl_3$)	^{13}C ($CDCl_3$)
2		164.9[a](s)	167.3[c](s)		168.0[b](s)
3		75.7 (s)	76.5 (s)		78.1 (s)
5		164.9[a](s)	167.4[c](s)		168.0[b](s)
6		64.8 (s)	66.6 (s)		71.0 (s)
7	2.74 (brd, 11.6) 3.42 (d, 11.8)	65.2 (t)	66.3 (t)	3.79 (dd, 12.2, 8.7) 3.94 (dd, 12.2, 4.7)	65.4 (t)
8	3.15 (d, 13.8) 3.54 (d, 13.9)	42.3 (t)	43.1 (t)	3.30 (d, 14.6) 3.87 (d, 14.6)	39.4 (t)
9		133.7 (s)	135.6 (s)		133.4 (s)
10, 14	7.11-7.32 (m)	128.8 (d)	129.7 (d)	7.25-7.31 (m)	128.9 (d)
11, 13	7.11-7.32 (m)	130.0 (d)	131.1 (d)	7.16-7.19 (m)	129.4 (d)
12	7.11-7.32 (m)	128.0 (d)	128.7 (d)	7.25-7.31 (m)	127.9 (d)
N-CH_3	3.28 (s)	30.3 (q)	30.9 (q)	3.17 (s)	30.3 (q)
N-*H*	6.39 (brs)			6.60 (brs)	
3-SCH_3	2.20 (s)	14.4 (q)	14.1 (q)		
6-SCH_3	2.23 (s)	13.5 (q)	13.7 (q)		
7-O*H*	1.85 (brs)			2.71 (m)	

[a,b] Two ^{13}C signals are overlapping. [c] Assignment can be interchanged.

Table 3. Antimalarial and cytotoxic activities of compounds **1**~**6**.

compound	antimalarial activity *P. falciparum* K1 (IC_{50}, μg/ml)	cytotoxicity (IC_{50}, μg/ml)		
		KB cells[a]	BC-1 cells[b]	Vero cells[c]
compound **1**	>20	>20	>20	>20
compound **2**	2.5	15	3.9	8.9
enniatin B (**3**)	0.27	16	18	17
enniatin B_4 (**4**)	0.20	11	12	18
pyrenocine A (**5**)	7.1	3.2	1.2	2.3
pyrenocine B (**6**)	22	>20	4.3	7.2
chloroquine diphosphate[d]	0.16	>20	16	>20

[a] Human epidermoid carcinoma in the mouth (oral cavity). [b] Human breast cancer cells. [c] African green monkey kidney fibroblast. [d] Standard antimalarial compound.

Thus, compound **2** moderately inhibited the proliferation of *P. falciparum* K1 while the bisdimethylthio ether **1** was inactive (Table 3).

Enniatin B, the major secondary metabolite, was most active against the malaria parasite, thus, it is most likely that this compound was responsible for the antimalarial activity as detected in the extract of the fungus BCC 1449. It should be noted that compounds **2**~**6** exhibited both antimalarial activity and cytotoxicity, therefore, the *in vitro* antimalarial activity of these compounds may be due to their cytotoxicity.

Acknowledgments

Financial support from the Biodiversity Research and Training Program (BRT) is gratefully acknowledged. One of us (Y. T.) thanks BIOTEC for the Senior Research Fellowship Award.

References

1) KULANTHAIVEL, P.; Y. F. HALLOCK, C. BOROS, S. M. HAMILTON, W. P. JANZEN, L. M. BALLAS, C. R. LOOMIS & J. B. JIANG: Balanol: a novel and potent inhibitor of protein kinase C from the fungus *Verticillium balanoides*. J. Am. Chem. Soc. 115: 6452~6453, 1993
2) TOKI, S.; K. ANDO, M. YOSHIDA, I. KAWAMOTO, H. SANO & Y. MATSUDA: ES-242-1, a novel compound from *Verticillium* sp., binds to a site on *N*-methyl-D-aspartate receptor that is coupled to the channel domain. J. Antibiotics 45: 88~93, 1992
3) HAUSER, D.; H. R. LOOSLI & P. NIKLAUS: Isolierung von 11α,11'α-dihydroxychaetocin aus *Verticillium tenerum*. Helv. Chim. Acta 55: 2182~2186, 1972
4) MINATO, H.; M. MATSUMOTO & T. KATAYAMA: Studies on the metabolites of *Verticillium* sp. Structures of verticillins A, B, and C. J. Chem. Soc. Perkin Trans. I. 1819~1825, 1973
5) TRIFONOV, L. S.; A. S. DREIDING, L. HOESCH & D. M. RAST: Isolation of four hexaketides from *Verticillium intertextum*. Helv. Chim. Acta 64: 1843~1846, 1981
6) TRIFONOV, L. S.; H. HILPERT, P. FLOERSHEIM & A. S. DREIDING: Bisvertinols: a new group of dimeric vertinoids from *Verticillium intertextum*. Tetrahedron 42: 3157~3179, 1986
7) NILANONTA, C.; M. ISAKA, R. CHANPHEN, N. THONG-ORN, M. TANTICHAROEN & Y. THEBTARANONTH: Unusual enniatins produced by the insect pathogenic fungus *Verticillium hemipterigenum*: isolation and studies on precursor-directed biosynthesis. Tetrahedron 59: 1015~1020, 2003
8) STRUNZ, G. M.; C. J. HEISSNER, M. KAKUSHIMA & M. A. STILLWELL: Metabolites of *Hyalodendron* sp.: bisdethiodi(methylthio)hyalodendrin. Can. J. Chem. 52: 325~326, 1974
9) MICHEL, K. H.; M. O. CHANEY, N. D. JONES, M. M. HOEHN & R. NAGARAJAN: Epipolythiopiperazinedione antibiotics from *Penicillium turbatum*. J. Antibiotics 27: 57~64, 1974
10) DEVAULT, R. L. & W. ROSENBROOK, Jr.: A novel class of diketopiperazinesics J. Antibiotics 26: 532~534, 1973
11) STRUNZ, G. M.; M. KAKUSHIMA & M. A. STILLWELL: An epitetrathiodioxopiperazine with 3*S*,6*S* configuration from *Hyalodendron* sp. Can. J. Chem. 53: 295~297, 1975
12) PLATTNER, PL. A.; U. NAGER & A. BOLLER: Über die isolierung neuartiger antibiotika aus Fusarien. Helv. Chim. Acta 31: 594~602, 1948
13) TSANTRIZOS Y. S.; X.-J. XU, F. SAURIOL & R. C. HYNES: Novel quinazolinones and enniatins from *Fusarium lateritium* Nees. Can. J. Chem. 71: 1362~1367, 1993
14) TOMODA, H.; H. NISHIDA, X. HUANG, R. MASUMA, Y. K. KIM & S. ŌMURA: New cyclodepsipeptides, enniatins D, E and F produced by *Fusarium* sp. FO-1305. J. Antibiotics 45: 1207~1215, 1992
15) VISCONTI, A.; L. A. BLAIS, J. W. APSIMON, R. GREENHALGH & J. D. MILLER: Production of enniatins by *Fusarium acuminatum* and *Fusarium compactum* in liquid culture: isolation and characterization of three new enniatins, B_2, B_3, and B_4. J. Agric. Food Chem. 40: 1076~1082, 1992
16) NIWA, M.; S. OGISO, T. ENDO, H. FURUKAWA & S. YAMAMURA: Isolation and structure of citreopyrone, a metabolite of *Penicillium citreo-viride* Biourge. Tetrahedron Lett. 21: 4481~4482, 1980
17) SATO, H.; K. KONOMA & S. SAKAMURA: Phytotoxins produced by onion pink root fungus, *Pyrenochaeta terrestris*. Agric. Biol. Chem. 43: 2409~2411, 1979
18) SATO, H.; K. KONOMA, S. SAKAMURA, A. FURUSAKI, T. MATSUMOTO & T. MATSUZAKI: X-Ray crystal structure of pyrenocine A, a phytotoxin from *Pyrenochaeta terrestris*. Agric. Biol. Chem. 45: 795~797, 1981
19) JATURAPAT, A.; M. ISAKA, N. L. HYWEL-JONES, Y. LERTWERAWAT, S. KAMCHONWONGPAISAN, K. KIRTIKARA, M. TANTICHAROEN & Y. THEBTARANONTH: Bioxanthracenes from the insect pathogenic fungus *Cordyceps pseudomilitaris* BCC 1620. I. Taxonomy, fermentation, isolation and antimalarial activity. J. Antibiotics 54: 29~35, 2001
20) DESJARDINS, R. E.; C. J. CANFIELD & J. D. CHULAY: Quantitative assessment of antimalarial activity *in vitro* by semiautomated microdilution technique. Antimicrob. Agents Chemother. 16: 710~718, 1979
21) SKEHAN, P.; R. STORENG, D. SCUDIERO, A. MONKS, J. MCMAHON, D. VISTICA, J. T. WARREN, H. BOKESCH, S. KENNEY & M. R. BOYD: New colorimetric cytotoxicity assay for anticancer-drug screening. J. Natl. Cancer Inst. 82: 1107~1112, 1990
22) SUGIE, Y.; H. HIRAI, T. INAGAKI, M. ISHIGURO, Y.-J. KIM, Y. KOJIMA, T. SAKAKIBARA, S. SAKEMI, A. SUGIURA, Y. SUZUKI, L. BRENNAN, J. DUIGNAN, L. H. HUANG, J. SUTCLIFFE & N. KOJIMA: A new antibiotic CJ-17,665 from *Aspergillus ochraceus*. J. Antibiotics 54: 911~916, 2001
23) WANG, S.; J. GOLEC, W. MILLER, S. MILUTINOVIC, A. FOLKES, S. WILLIAMS, T. BROOKS, K. HARDMAN, P. CHARLTON, S. WREN & J. SPENCER: Novel inhibitors of plasminogen activator inhibitor-1: development of new templates from diketopiperazines. Bioorg. Med. Chem. Lett. 12: 2367~2370, 2002
24) DONKOR, I. O. & M. L. SANDERS: Synthesis of a reported calpain inhibitor isolated from *Streptomyces griseus*. Bioorg. Med. Chem. Lett. 11: 2647~2649, 2001
25) DINSMORE, C. J.; J. M. BERGMAN, D. D. WEI, C. B. ZARTMAN, J. P. DAVIDE, I. B. GREENBERG, D. LIU, T. J. O'NEILL, J. B. GIBBS, K. S. KOBLAN, N. E. KOHL, R. B. LOBERT, I.-W. CHEN, D. A. MCLOUGHLIN, T. V. OLAH, S. L. GRAHAM, G. D. HARTMAN & T. M. WILLIAMS: Oxopiperazine derivatives of *N*-arylpiperazinones as inhibitors of farnesyltransferase. Bioorg. Med. Chem. Lett. 11: 537~540, 2001

Pergamon

SCIENCE DIRECT®

TETRAHEDRON

Tetrahedron 59 (2003) 1015–1020

Unusual enniatins produced by the insect pathogenic fungus *Verticillium hemipterigenum*: isolation and studies on precursor-directed biosynthesis

Chongdee Nilanonta,[a] Masahiko Isaka,[b,*] Rachada Chanphen,[b] Nuntawan Thong-orn,[b] Morakot Tanticharoen[b] and Yodhathai Thebtaranonth[b]

[a]*Department of Chemistry, Prince of Songkla University, Songkhla 90112, Thailand*
[b]*National Center for Genetic Engineering and Biotechnology (BIOTEC), 113 Phaholyothin Road, Klong 1, Klong Luang, Pathumthani 12120, Thailand*

Received 10 October 2002; revised 26 November 2002; accepted 12 December 2002

Abstract—Two new enniatins H (**3**) and I (**4**), whose substituents on 2-hydroxycarboxylic acid moieties were different from those of known compounds, were isolated, together with known enniatins B (**1**) and B_4 (**2**), from the insect pathogenic fungus *Verticillium hemipterigenum* BCC 1449. Structures of these compounds were elucidated by spectroscopic means. Studies on precursor-directed biosynthesis with strain BCC 1449 led to the production and identification of three analogs, enniatins G (**5**), C (**6**) and MK1688 (**7**), as well as the stereochemical elucidation of **3** and **4**. Enniatins **1**–**7** were evaluated for their antiplasmodial and antimycobacterial activities.

1. Introduction

Enniatins are well-known cyclohexadepsipeptide antibiotics produced by various *Fusarium* species.[1] This class of compounds have been known to exhibit antibiotic,[1b,c,2] insecticidal,[1d,3] and phytotoxic[1e,4] activities, and also inhibit acyl-CoA: cholesterol acyltransferase (ACAT).[5] Enniatins consist of three each of D-2-hydroxyisovaleric acid (Hiv) and L-*N*-methylamino acid residues linked alternately to furnish an 18-membered cyclodepsipeptide structure. Several isomers of enniatins, e.g. enniatin B (**1**) (Fig. 1), have previously been isolated and their differences are the R^1, R^2 and R^3 substituents on the three L-*N*-methylamino acid residues: L-*N*-methylvaline (*N*MeVal), L-*N*-methylleucine (*N*MeLeu) or L-*N*-methylisoleucine (*N*MeIle).[1] However, all the naturally occurring enniatins reported in the literature have fixed substructure at the D-2-hydroxycarboxylic acid residues; R^4=R^5=R^6=*i*-Pr.

In our search for novel bioactive compounds from insect pathogenic fungi,[6] we came across an enniatin mixture as antimalarial constituents in the extract from *Verticillium hemipterigenum* BCC 1449. Together with known enniatins B (**1**) and B_4 (**2**; also reported as enniatin D),[1c,f] two new analogs, enniatins H (**3**) and I (**4**), which, respectively, bear one and two 2-hydroxy-3-methylpentanoic acid (Hmp) residues instead of Hiv, were subsequently isolated. We report herein the isolation and structural elucidation of these unusual enniatins, production of other analogs by precursor-directed biosynthesis employing the fungus BCC 1449, and the evaluation of their biological activities. During the late stage of our experimental works, Zocher's group reported a related study on the precursor-directed biosynthesis of unnatural enniatins using *Fusarium scirpi* (enniatin B producer) and *F. sambucinum* (enniatin A producer).[7]

2. Results and discussion

Enniatins **1**–**4** were isolated from the methanolic extract of mycelia of *V. hemipterigenum* BCC 1449. Structures of known enniatins B (**1**) and B_4 (**2**)[1f] were elucidated by spectroscopic analyses (NMR, MS, IR) with their physicochemical properties being identical to those reported in the literature in all respects. The IR spectrum of enniatin H (**3**), $C_{34}H_{59}N_3O_9$ as shown by HRMS, ^1H and ^{13}C NMR, was very similar to those of **1** and **2**, showing absorptions of esters (ν 1743 cm^{-1}) and amides (ν 1663 cm^{-1}). NMR analyses (^1H, ^{13}C, DEPTs, COSY, HMQC and HMBC; in $CDCl_3$) revealed that this compound consists of three *N*MeVal, two Hiv and one Hmp residues. Thus, in the ^1H NMR spectrum of enniatin H (**3**), protons of three *N*MeVal residues and two Hiv residues appeared as superimposed signals with the chemical shifts very close to those of

Keywords: *Verticillium hemipterigenum*; enniatin; insect pathogenic fungus.

* Corresponding author. Tel.: +66-2-5646700x3554; fax: +66-2-5646707; e-mail: isaka@biotec.or.th

0040–4020/03/$ - see front matter
PII: S0040-4020(02)01631-9

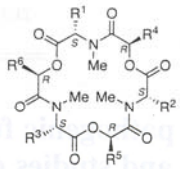

	R^1	R^2	R^3	R^4	R^5	R^6
enniatin B (**1**)	i-Pr	i-Pr	i-Pr	i-Pr	i-Pr	i-Pr
enniatin B_4 (**2**)	i-Bu	i-Pr	i-Pr	i-Pr	i-Pr	i-Pr
enniatin G (**5**)	i-Bu	i-Bu	i-Pr	i-Pr	i-Pr	i-Pr
enniatin C (**6**)	i-Bu	i-Bu	i-Bu	i-Pr	i-Pr	i-Pr
enniatin H (**3**)	i-Pr	i-Pr	i-Pr	*s*-Bu	i-Pr	i-Pr
enniatin I (**4**)	i-Pr	i-Pr	i-Pr	*s*-Bu	*s*-Bu	i-Pr
MK1688 (**7**)	i-Pr	i-Pr	i-Pr	*s*-Bu	*s*-Bu	*s*-Bu

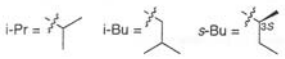

Figure 1. Structures of enniatins.

enniatin B (**1**). In addition to these, signals assignable to another 2-hydroxycarboxylic acid residue were present. Signal at δ_H 5.27 (1H, d, J=6.8 Hz) assigned to the proton situated at the α-position (H-2; attached to C-2, δ_C 74.3) showed vicinal coupling (COSY) to a multiplet signal at δ_H 2.00 (1H, H-3; attached to C-3, δ_C 36.1). This methine (C-3) which, in turn, was connected to a methyl group (δ_H 0.96, overlapping signal; δ_C 14.6) and a methylene (δ_H 1.46 and 1.19, 2H, H-4; δ_C 25.4, C-4). The C-4 methylene was attached to a terminal methyl (δ_H 0.92, overlapping signal, H-5; δ_C 11.3, C-5) as indicated by the COSY cross signal. Therefore, the 2-hydroxycarboxylic acid residue was assigned to Hmp, and this was consistent with HMBC correlations: H-2 to a carbonyl (δ_C 170.3), C-3 and 3-CH_3; and H-4 to C-2, C-5 and 3-CH_3. ^{1}H and ^{13}C NMR assignments of the three *N*MeVal residues for enniatin H could not be distinguished due to the very close signals overlap, however, this partial structure was confirmed by 2D NMR analyses (COSY and HMBC) as a set of signals. Important HMBC correlations for *N*MeVal residues are H-2 to C-3, C-4, C-4′, N–CH_3 and two carbonyl signals at δ_C 169.3 and 170.3, and from both H-4 and H-4′ to C-2. Two Hiv residues were also assigned as a set of signals (Table 1; full HMBC data are shown in Section 3). Analysis of NOESY spectral data revealed the connectivity of six residues, three *N*MeVal and three 2-hydroxycarboxylic acid. Thus, intense correlations were observed for the three *N*-methyl singlet signals at δ_H 3.11, 3.13 and 3.14, respectively, with the α-protons (H-2) of the 2-hydroxycarboxylic acid residues at δ_H 5.27 (Hmp), 5.13 (Hiv) and 5.15 (Hiv), which clearly indicated that three *N*MeVal residues are linked alternately with the three 2-hydroxycarboxylic acid residues. Finally, ^{13}C NMR assignment of the carbonyl carbons, which appeared as only two signals at δ_C 169.3 and 170.3, was achieved based on the HMBC correlations from the three *N*-methyl proton signals to the δ_C 169.3 peak, not to δ_C 170.3. Therefore, the δ_C 169.3 signal was assigned to that of amide carbonyls (C-1 for two Hiv and a Hmp), and δ_C 170.3 signal to ester carbonyls (C-1 for three *N*MeVal). Another possibility of enniatin H structure bearing one *N*MeIle instead of *N*MeVal in **1**, thus enniatin B_1 (R^1=*s*-Bu, R^2=R^3=*i*-Pr; R^4=R^5=R^6=*i*-Pr), was clearly ruled out by these spectroscopic analyses. Furthermore, NMR spectral data (^{1}H and ^{13}C) of enniatin H in $CDCl_3$ were apparently different from those reported for enniatin B_1.[1g,5]

Enniatin I (**4**), molecular formula $C_{35}H_{61}N_3O_9$ (HRMS), showed IR and UV spectra similar to those of **3** and other

Table 1. NMR data for enniatins H and I and compound **7** in $CDCl_3$

Position	Enniatin H (**3**)		Enniatin I (**4**)		**7**	
	^{13}C	^{1}H (mult, J in Hz)	^{13}C	^{1}H (mult, J in Hz)	^{13}C	^{1}H (mult, J in Hz)
*N*MeVal	3 units		3 units		3 units, symmetrical	
1 *C*=O	170.3×3	–	170.3×3	–	170.4	–
2	63.3, 63.2, 63.1	4.57–4.55 (3H, m)	63.1×3	4.56–4.55 (3H, m)	63.1	4.59 (3H, brd, 9.4)
3	28.0, 27.9, 27.8	2.29–2.28 (3H, m)[a]	27.9×2, 27.8	2.30–2.28 (3H, m)[a]	27.8	2.29 (3H, m)
4	20.4, 20.3×2	1.06 (9H, m)	20.3×3	1.06 (9H, m)	20.3	1.06 (9H, d, 6.1)
4′	19.5, 19.4, 19.3	0.90–0.89 (9H, m)	19.4, 19.3, 19.2	0.89 (9H, m)	19.3	0.89 (9H, d, 6.9)
N–*CH*$_3$	33.1, 32.9×2	3.14 (3H, s)	32.9×2, 32.7	3.12 (3H, s)	32.7	3.10 (9H, s)
		3.13 (3H, s)		3.11 (3H, s)		
		3.11 (3H, s)		3.09 (3H, s)		
Hiv	2 units		1 unit			
1 *C*=O	169.3×2	–	169.2	–		
2	75.9, 75.6	5.15–5.13 (2H, m)	75.7	5.15 (1H, d, 8.2)		
3	29.9×2	2.28 (2H, m)[a]	29.9	2.29 (1H, m)[a]		
4	18.7[b], 18.6[b]	0.98 (6H, m)[a]	18.6[b]	0.98 (3H, m)[a]		
4′	18.5×2[b]	0.96 (6H, m)[b]	18.5[b]	0.95 (3H, m)[a]		
Hmp	1 unit		2 units		3 units, symmetrical	
1 *C*=O	169.3	–	169.2×2	–	169.2	–
2	74.3	5.27 (1H, d, 6.8)	74.4, 74.2	5.28–5.27 (2H, m)	74.3	5.28 (3H, brd, 5.6)
3	36.1	2.00 (1H, m)	36.1×2	2.02 (2H, m)	36.2	2.02 (3H, m)
4	25.4	1.46 (1H, m)	25.3×2	1.46 (2H, m)	25.4	1.45 (3H, m)
		1.19 (1H, m)		1.19–1.18 (2H, m)		1.19 (3H, m)
5	11.3	0.92 (3H, m)	11.3×2	0.92 (6H, t, 7.5)	11.3	0.92 (9H, t, 7.4)
3-*CH*$_3$	14.6	0.96 (3H, m)[a]	14.6×2	0.96 (6H, m)[a]	14.6	0.96 (9H, d, 6.4)

[a] ^{1}H signals are overlapping.
[b] Assignments can be interchanged.

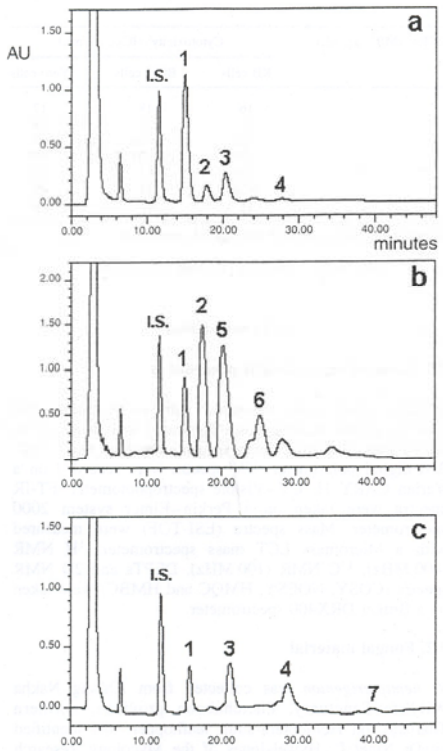

Figure 2. HPLC chromatogram of the EtOAc extracts from supernatant (detection at 210 nm): (**a**) control (non-additive); (**b**) L-leucine fed (20 mM); (**c**) L-isoleucine fed (20 mM). Internal standard (I.S.): ethyl 4-phenylbenzoate (0.50 mg).

enniatins. ^{1}H and ^{13}C NMR spectra of enniatin I were also similar to those of **3** where chemical shifts of the protons and carbons in each residue were superimposed but with different composition: three *N*MeVal, one Hiv, and two Hmp. Analyses of 2D NMR spectra (COSY, NOESY, HMQC and HMBC) further confirmed the connectivity and assignment of each residue (Table 1; HMBC correlations are shown in Section 3).

Enniatin synthetase, a multifunctional enzyme catalyzing enniatin biosynthesis, has previously been isolated from *F. oxysporum*,[8] and the cell-free synthesis of enniatins has also been reported.[8,9] It is known that the biosynthetic precursor for L-*N*MeVal residues of the major metabolite enniatin B (**1**) is L-valine as shown by the uptake of radioactive substrate. The D-Hiv residues are also derived from L-valine via 2-ketoisovalerate as reported in the literature.[10] Production of the unusual analogs **3** and **4** by *V. hemipterigenum* BCC 1449 suggested that the nature of enniatin synthetase of this strain might be different from those of previously investigated enniatins-producing *Fusarium* species, especially at the region associated with Hiv substrate recognition. With the characteristic enniatins-producing strain (BCC 1449) in hand, we decided to examine the precursor-directed biosynthesis,[11] since it was anticipated that feeding the substrate analog, L-leucine and L-isoleucine, might result in the incorporation of these mimics as either L-*N*-methylamino acid or D-2-hydroxy-carboxylic acid residues in the enniatin molecules.

A feeding experiment with 20 mM of L-leucine (fermentation: 4×1 L Erlenmeyer flasks, each containing 250 mL of potato dextrose broth) led to the enhanced production of enniatins as compared to controlled fermentation (no additive) (Fig. 2). HPLC/UV analysis (ODS column: MeCN/H_2O=70:30; detection at 210 nm) of the extract from supernatant showed that enniatin B_4 (**2**) and a new analog (**5**), corresponding to the peak at t_R 20 min, were produced in higher amounts relative to enniatin B (**1**). In addition, HPLC peaks due to several other minor isomers were observed. It should also be noted that the total amount of enniatins in the L-leucine-fed culture, 16 mg of total enniatins per 1 L culture broth (calculated using an internal standard), was higher than that of the control (5 mg per 1 L culture broth). Similar results were observed for the analysis of the extract from mycelia. Thus, extracts from supernatant and mycelia were combined and subjected to chromatographic separation. Compounds **1**, **2**, **5** and a minor product corresponding to the HPLC peak at t_R 25 min (**6**) were isolated (see Section 3). Although the HPLC retention time (in MeCN/H_2O) of compound **5** was very close to **3**, the prep. HPLC fraction corresponding to this peak contained mainly compound **5** and a trace amount of **3** which was removed by subsequent re-chromatography employing MeOH/H_2O as the solvent system. Spectral data for enniatins B (**1**) and B_4 (**2**) obtained from this feeding experiment were identical to those obtained from non-additive fermentation. NMR analyses of another major product, **5**, having a molecular formula of $C_{35}H_{61}N_3O_9$ (HRMS, ^{13}C NMR), revealed that this molecule consists of one *N*MeVal, two *N*MeLeu and three Hiv residues, hence, the structure, assigned as depicted (Fig. 1), was identical to enniatin G which was very recently isolated from the mangrove fungus *Halosarpheia* sp. (strain 732).[12] The minor product, **6**, exhibited a C_3-symmetric structure as indicated by its molecular formula ($C_{36}H_{63}N_3O_9$, HRMS) and ^{1}H and ^{13}C NMR spectra. Analyses of the 2D NMR spectral data revealed that this compound consists of *N*MeLeu and Hiv residues, therefore, it is identical to enniatin C which is a synthetically known compound but not a naturally occurring enniatin analog.[13]

A feeding experiment with L-isoleucine (20 mM) gave dramatically different results in which enhanced production of enniatins H (**3**) and I (**4**), and the appearance of another derivative, **7**, at t_R 40 min, were observed by HPLC/UV analysis (Fig. 2). Due to the small amounts of enniatin products, a 10 L fermentation (250 mL×40 flasks) was conducted from which four compounds, **1**, **3**, **4**, and **7**, were isolated. Spectral data of **1**, **3** and **4**, obtained from the L-isoleucine-fed culture were identical in all respects to those from non-additive fermentation. The newly produced analog, **7**, molecular formula $C_{36}H_{63}N_3O_9$ (HRMS), possessed a C_3-symmetric structure as indicated by its

Table 2. Antiplasmodial, antimycobacterial and cytotoxic activities of enniatins 1–7

Compound	*P. falciparum* K1[a] (IC_{50}, μg/mL)	*M. tuberculosis* H37Ra[b] (MIC, μg/mL)	Cytotoxicity[c] (IC_{50}, μg/mL)		
			KB cells	BC-1 cells	Vero cells
Enniatin B (**1**)	0.27	3.12	16	18	17
Enniatin B_4 (**2**)	0.20	3.12	11	12	18
Enniatin G (**5**)	0.46	6.25	>20	>20	45
Enniatin C (**6**)	1.1	6.25	>20	>20	>50
Enniatin H (**3**)	1.9	6.25	>20	5.5	38
Enniatin I (**4**)	0.24	6.25	>20	18	38
Compound **7**	0.22	1.56	11	8.1	1.4

[a] IC_{50} values of the standard antimalarial compouds, chloroquine diphosphate and artemisinin, were 0.16 and 0.0011 μg/mL, respectively.
[b] MIC value of the standard drug, isoniazide, was 0.050 μg/mL.
[c] IC_{50} values of the standard compound, ellipticine, were 0.46 μg/mL for KB cells, 0.60 μg/mL for BC-1 cells, and 1.0 μg/mL for Vero cells.

NMR spectra. NMR analyses also revealed that this compound bears three *N*MeVal and three Hmp residues. Results from L-isoleucine-feeding experiments also confirmed the (3*S*)-configuration at the β-position of Hmp residues in the naturally occurring enniatins H (**3**) and I (**4**), and the missing analog, **7**. A related compound MK1688, obtained from *F. oxysporum* D338, was claimed as an antifungal substance in a Japanese patent,[14] although its stereochemistries at the Hmp residues have not been presented. By comparison of ^{1}H NMR (taken in methanol-d_6) and IR spectrum, and optical rotation data of **7**, with those of MK1688 in the patent, we have concluded that they are the same compound. Therefore, MK1688 possesses (2*R*,3*S*)-configuration at the Hmp residues.

The present results are of particular interest concerning specificity of the substrate recognition domain of the enzyme enniatin synthetase in strain *V. hemipterigenum* BCC 1449. It is evident that the enzyme favors L-leucine over L-isoleucine as a substrate of the L-*N*-methylamino acid residue in enniatin biosynthesis. In contrast, the domain which recognizes 2-hydroxycarboxylic acid substrates readily accepts Hmp, derived from L-isoleucine, as indicated by the enhancement of production of enniatins H (**3**), I (**4**) and MK1688 (**7**) in the feeding experiment as well as by the production of **3** and **4** even in the standard fermentation. It should be noted that this observation is of marked contrast to the study of substrate specificity in the precursor-directed biosynthesis of *Fusarium* spp, recently reported by Zocher's group.[7]

Enniatins **1**–**7** were tested for their activities against *Plasmodium falciparum* (K1 strain) and *Mycobacterium tuberculosis* (H37Ra strain), and also for their cytotoxic activity towards two cancer cell-lines (KB, BC-1) and Vero cells. Enniatins **1**–**7** strongly inhibited the proliferation of the human malaria parasite (*P. falciparum* K1), they also exhibited inhibitory activity against the growth of mycobacteria (*M. tuberculosis* H37Ra) (Table 2). To the best of our knowledge, this is the first report on the in vitro activities of enniatins against *P. falciparum* and *M. tuberculosis*, although enniatin B was previously reported to be active against *M. paratuberculosis* and *M. phlei*.[1h] It should also be commented that these enniatins also exhibited cytotoxic activities, but these were rather weak when compared to their antimalarial activities.

3. Experimental

3.1. General experimental procedures

Melting points were measured with an Electrothermal IA9100 digital melting point apparatus and were uncorrected. Optical rotations were measured with a JASCO DIP-370 digital polarimeter. UV spectra were recorded on a Varian CARY 1E UV–Visible spectrophotometer. FT-IR spectra were taken on a Perkin–Elmer system 2000 spectrometer. Mass spectra (ESI-TOF) were measured with a Micromass LCT mass spectrometer. ^{1}H NMR (400 MHz), ^{13}C NMR (100 MHz), DEPTs and 2D NMR spectra (COSY, NOESY, HMQC and HMBC) were taken on a Bruker DRX400 spectrometer.

3.2. Fungal material

V. hemipterigenum was collected from Khlong Nakha Wildlife Sanctuary, Phetchaboon province, northern Thailand, on Homoptera-adult leafhopper, and identified by Dr Nigel L. Hywel-Jones of the Mycology Research Unit, BIOTEC. The fungus was deposited at the Thailand BIOTEC Culture Collection as BCC 1449.

3.3. Extraction and isolation

The flask cultures (40×1 L Erlenmeyer flask), each containing 250 mL of potato dextrose broth, were incubated at 22°C for 21 days, and filtered to separate into mycelia and supernatant. The mycelial cakes were extracted with methanol (2 L, rt, 2 days) and the solvent concentrated to 500 mL. H_2O (50 mL) was added, washed with hexane (300 mL), and the aqueous methanol layer was concentrated under reduced pressure. The residual oil was dissolved in EtOAc (500 mL), washed with H_2O (150 mL), and concentrated to obtain a brown semi-solid (0.85 g). This mycelial extract was subjected to Sephadex LH20 column chromatography (CH_2Cl_2/MeOH) followed by CC on silica gel (MeOH/CH_2Cl_2) to obtain a mixture of enniatins. Continuous separation by preparative HPLC using a reversed-phase column (MeCN/H_2O, then MeOH/H_2O) gave enniatin isomers in the following order of elution: enniatins B (**1**, 52 mg), B_4 (**2**, 14 mg), H (**3**, 8.3 mg) and I (**4**, 2.8 mg).

3.3.1. Enniatin H (3). Colorless solid; mp 105–106°C;

$[\alpha]_D^{29}=-102$ (*c* 0.22, $CHCl_3$); UV (EtOH) λ_{max} (log ε) 206 (4.23) nm; IR (KBr) ν_{max} 2967, 1743, 1663, 1470, 1203, 1012 cm^{-1}; HRMS (ESI-TOF) *m/z* 676.4121 $[M+Na]^+$ (calcd for $C_{34}H_{59}N_3O_9Na$ 676.4149; Δ=2.8 mmu); ^1H and ^{13}C NMR data, Table 1. HMBC correlations ($CDCl_3$, 400 MHz, 50 and 100 ms): *N*MeVal (3 units), H-2 to C-1 (δ_C 170.3), C-3, C-4, C-4′, δ_C 169.3 (amide) and N–CH_3; H-4 to C-2, C-3 and C-4′; H-4′ to C-2, C-3 and C-4; N–CH_3 to C-1 and δ_C 169.3 (amide): Hiv (2 units), H-2 to C-3, C-4 and C-4′; H-3 to C-2, C-4 and C-4′; H-4 to C-2, C-3 and C-4′; H-4′ to C-2, C-3 and C-4: Hmp (1 unit), H-2 to C-3, 3-CH_3 and δ_C 170.3 (ester); H-4a (δ_H 1.46) to C-2, C-5 and 3-CH_3; H-5 to C-3: 3-CH_3 to C-3 and C-4.

3.3.2. Enniatin I (4). Colorless gum; $[\alpha]_D^{29}=-87$ (*c* 0.12, $CHCl_3$); UV (EtOH) λ_{max} (log ε) 207 (4.23) nm; IR (KBr) ν_{max} 2965, 1745, 1665, 1468, 1281, 1192, 1012 cm^{-1}; HRMS (ESI-TOF) *m/z* 690.4277 $[M+Na]^+$ (calcd for $C_{35}H_{61}N_3O_9Na$ 690.4306; Δ=2.9 mmu); ^1H and ^{13}C NMR data, Table 1. HMBC correlations ($CDCl_3$, 400 MHz, 100 ms): *N*MeVal (3 units), H-2 to C-1 (δ_C 170.3), C-3, C-4, C-4′, δ_C 169.2 (amide) and N–CH_3; H-3 to C-2, C-4 and C-4′; H-4 to C-2, C-3 and C-4′; H-4′ to C-2, C-3 and C-4; N–CH_3 to C-1 and δ_C 169.2 (amide): Hiv (1 unit), H-3 to C-4 and C-4′; H-4 to C-2, C-3 and C-4′; H-4′ to C-2, C-3 and C-4: Hmp (2 units), H-4a (δ_H 1.46, 2H) to C-3, C-5 and 3-CH_3; H-5 to C-3 and C-4; 3-CH_3 to C-2, C-3 and C-4.

3.4. Precursor-directed biosynthesis

V. hemipterigenum BCC 1449 was incubated in 4×1 L Erlenmeyer flasks, each containing 250 mL of potato dextrose broth with 20 mM of L-leucine. The flask cultures were filtered to separate into mycelia and supernatant (ca. 1 L). Extraction from mycelia was performed as described above. Supernatant was extracted with EtOAc (1 L), dried over $MgSO_4$, and concentrated in vacuo to obtain a crude extract. To each extract from mycelia and supernatant was added ethyl 4-phenylbenzoate (0.50 mg) as an internal standard. Each sample was subjected to HPLC/UV analysis using a reversed-phase column (NovaPak 8NV4μ; 8×100 mm), elution with MeCN/H_2O=70:30 with a flow rate of 1 mL/min (detection at 210 nm). Calibration was made for pure enniatin B, and for the calculation of the amounts of enniatin analogs. The L-isoleucine-feeding and control (no additive) experiments were carried out in the same manner. After HPLC analyses, the extracts from mycelia and supernatant of the L-leucine-fed culture were combined, and subjected to chromatographic separation/purification to obtain pure enniatins B (**1**, 2.5 mg), B_4 (**2**, 5.7 mg), G (**5**, 6.8 mg) and C (**6**, 2.2 mg). The L-isoleucine-feeding experiment was repeated on a larger scale (40 flasks; total 10 L) from which enniatins B (**1**, 8.1 mg), H (**3**, 22 mg) and I (**4**, 25 mg), and MK1688 (**7**, 10 mg) were isolated.

3.4.1. Enniatin G (5). Colorless solid; mp 143–145°C; $[\alpha]_D^{26}=-75$ (*c* 0.21, $CHCl_3$); UV (MeOH) λ_{max} (log ε) 206 (4.28) nm; HRMS (ESI-TOF) *m/z* 690.4301 $[M+Na]^+$ (calcd for $C_{35}H_{61}N_3O_9Na$ 690.4306; Δ=0.5 mmu); IR and NMR spectral data were identical to those listed in the literature.[12]

3.4.2. Enniatin C (6). Colorless solid; mp 159–160°C; $[\alpha]_D^{27}=-47$ (*c* 0.11, $CHCl_3$); UV (MeOH) λ_{max} (log ε) 205 (4.23) nm; IR (KBr) ν_{max} 2964, 1748, 1659, 1471, 1268, 1204, 1014 cm^{-1}; HRMS (ESI-TOF) *m/z* 704.4443 $[M+Na]^+$ (calcd for $C_{36}H_{63}N_3O_9Na$ 704.4462; Δ=1.9 mmu); ^1H NMR (400 MHz, $CDCl_3$) δ *N*MeLeu (3 units, symmetrical) 5.33 (3H, brd, *J*=7.1 Hz, H-2), 3.10 (9H, s, NCH_3), 1.73 (3H, m, H-3a), 1.66 (3H, m, H-3b), 1.45 (3H, m, H-4), 0.95 (9H, d, *J*=6.5 Hz, H-5), 0.91 (3H, d, *J*=6.5 Hz, H-5′): Hiv (3 units, symmetrical) 4.91 (3H, d, *J*=8.2 Hz, H-2), 2.20 (3H, m, H-3), 1.01 (9H, d, *J*=6.4 Hz, H-4), 0.94 (9H, d, *J*=6.7 Hz, H-4′); ^{13}C NMR (100 MHz, $CDCl_3$) δ, *N*MeLeu (3 units, symmetrical) 171.1 (s, C-1), 54.2 (d, C-2), 37.8 (t, C-3), 31.4 (q, NCH_3), 25.3 (d, C-4), 23.4 (q, C-5), 20.9 (q, C-5′): Hiv (3 units, symmetrical) 170.3 (s, C-1), 75.7 (d, C-2), 30.0 (d, C-3), 18.6 (q, C-4), 18.0 (q, C-4′).

3.4.3. Compound 7 (MK1688). Colorless gum; $[\alpha]_D^{26}=-89$ (*c* 0.25, $CHCl_3$); UV (MeOH) λ_{max} (log ε) 207 (4.17) nm; IR ($CHCl_3$) ν_{max} 2970, 1737, 1662, 1465, 1191, 1007 cm^{-1}; HRMS (ESI-TOF) *m/z* 704.4458 $[M+Na]^+$ (calcd for $C_{36}H_{63}N_3O_9Na$ 704.4462; Δ=0.4 mmu); ^1H NMR (400 MHz, methanol-d_6) (symmetrical) δ 5.43 (3H, d, *J*=6.6 Hz), 4.80 (3H, d, *J*=9.8 Hz), 3.21 (9H, s), 2.33 (3H, m), 2.00 (3H, m), 1.51 (3H, m), 1.29 (3H, m), 1.12 (9H, d, *J*=6.6 Hz), 1.04 (9H, d, *J*=6.7 Hz), 1.00 (9H, t, *J*=7.4 Hz), 0.97 (9H, d, *J*=6.7 Hz); ^1H and ^{13}C NMR data in $CDCl_3$, Table 1.

3.5. Biological assays

The assay for activity against *P. falciparum* K1 was performed using a standard protocol,[15] which follows the microculture radioisotope technique as described by Desjardins.[16] IC_{50} represents the concentration that causes 50% reduction of parasite growth as indicated by the *in vitro* uptake of [^{3}H]-hypoxanthine by *P. falciparum*. Growth inhibitory activity against *M. tuberculosis* H37Ra was performed using the Microplate Alamar Blue Assay (MABA).[17] Cytotoxic activities of the purified compounds against human epidermoid carcinoma (KB cells), human breast cancer (BC-1 cells) and African green monkey kidney fibroblast (Vero cells) were evaluated using colorimetric method.[18]

Acknowledgements

Financial support from the Thailand Research Fund (TRF) is gratefully acknowledged. One of us (Y. T.) thanks BIOTEC for the Senior Research Fellowship Award.

References

1. (a) Gaumann, E.; Roth, S.; Ettlinger, L.; Plattner, P. A.; Nager, U. *Experientia* **1947**, *3*, 202. (b) Tsantrizos, S. Y.; Xu, X.-J.; Sauriol, F.; Hynes, R. C. *Can. J. Chem.* **1993**, *71*, 1362–1367. (c) Tomoda, H.; Nishida, H.; Huang, X.; Masuma, R.; Kim, Y. K.; Omura, S. *J. Antibiot.* **1992**, *45*, 1207–1215. (d) Strongman, D. B.; Strunz, G. M.; Giguere, P.; Yu, C.-M.;

Calhoun, L. *J. Chem. Ecol.* **1988**, *14*, 753–764. (e) Burmeister, H. R.; Plattner, R. D. *Phytopathology* **1987**, *77*, 1483–1487. (f) Visconti, A.; Blais, L. A.; ApSimon, J. W.; Greenhalgh, R.; Miller, J. D. *J. Agric. Food Chem.* **1992**, *40*, 1076–1082. (g) Blais, L. A.; ApSimon, J. W.; Blackwell, B. A.; Greenhalgh, R.; Miller, J. D. *Can. J. Chem.* **1992**, *70*, 1281–1287. (h) Plattner, P. A.; Nager, U.; Boller, A. *Helv. Chim. Acta* **1948**, *31*, 594–602. (i) Deol, B. S.; Ridley, D. D.; Singh, P. *Aust. J. Chem.* **1978**, *31*, 1397–1399. (j) Bishop, G. C.; Isley, A. H. *Aust. J. Biol. Sci.* **1978**, *31*, 93–96. (k) Madry, N.; Zocher, R.; Kleinkauf, H. *Eur. J. Appl. Microbiol. Biotechnol.* **1983**, *17*, 75–79. (l) Minasyan, A. E.; Chermenskii, D. N.; Ellanskaya, I. A. *Mikrobiologiya* **1978**, *47*, 67–71.

2. Tirunarayanan, M. O.; Sirsi, M. *J. Ind. Inst. Sci.* **1957**, *39*, 185–194.
3. Grove, J. F.; Pople, M. *Mycopathologia* **1980**, *70*, 103.
4. Gauman, E.; Naef-Roth, St.; Kern, H. *Phytopathol. Z.* **1960**, *40*, 45–51.
5. Tomoda, H.; Huang, X.-H.; Cao, J.; Nishida, H.; Nagao, R.; Okuda, S.; Tanaka, H.; Omura, S.; Arai, H.; Inoue, K. *J. Antibiot.* **1992**, *45*, 1626–1632.
6. (a) Isaka, M.; Tanticharoen, M.; Kongsaeree, P.; Thebtaranonth, Y. *J. Org. Chem.* **2001**, *66*, 4303–4308. (b) Isaka, M.; Kongsaeree, P.; Thebtaranonth, Y. *J. Antibiot.* **2001**, *54*, 36–43. (c) Seephonkai, P.; Isaka, M.; Kittakoop, P.; Trakulnaleamsai, S.; Rattanajak, R.; Tanticharoen, M.; Thebtaranonth, Y. *J. Antibiot.* **2001**, *54*, 751–752. (d) Isaka, M.; Tanticharoen, M.; Thebtaranonth, Y. *Tetrahedron Lett.* **2000**, *41*, 1657–1660. (e) Nilanonta, C.; Isaka, M.; Kittakoop, P.; Palittapongarnpim, P.; Kamchonwongpaisan, S.; Pittayakhajonwut, D.; Tanticharoen, M.; Thebtaranonth, Y. *Planta Med.* **2000**, *66*, 756–758.
7. Krause, M.; Lindemann, A.; Glinski, M.; Hornbogen, T.; Bonse, G.; Jeschke, P.; Thielking, G.; Gau, W.; Kleinkauf, H.; Zocher, R. *J. Antibiot.* **2001**, *54*, 797–804.
8. Zocher, R.; Keller, U.; Kleinkauf, H. *Biochemistry* **1982**, *21*, 43–48.
9. (a) Zocher, R.; Salnikow, J.; Kleinkauf, H. *FEBS Lett.* **1976**, *71*, 13–17. (b) Zocher, R.; Kleinkauf, H. *Biochem. Biophys. Res. Commun.* **1978**, *81*, 1162–1167. (c) Pieper, R.; Kleinkauf, H.; Zocher, R. *J. Antibiot.* **1992**, *45*, 1273–1277.
10. Lee, C.; Gorisch, H.; Kleinkauf, H.; Zocher, R. *J. Biol. Chem.* **1992**, *267*, 11741–11744.
11. (a) Recent reports in the production of unnatural analogs of secondary metabolites by precursor-directed biosynthesis: Nilanonta, C.; Isaka, M.; Kittakoop, P.; Trakulnaleamsai, S.; Tanticharoen, M.; Thebtaranonth, Y. *Tetrahedron* **2002**, *58*, 3355–3360. (b) Gerard, J.; Lloyd, R.; Barsby, T.; Haden, P.; Kelly, M. T.; Andersen, R. J. *J. Nat. Prod.* **1997**, *60*, 223–229. (c) Perellino, N. C.; Malyszko, J.; Ballabio, M.; Gioia, B. *J. Nat. Prod.* **1992**, *55*, 424–427. (d) Kozikowski, A. P.; Okita, M.; Kobayashi, M.; Floss, H. G. *J. Org. Chem.* **1988**, *53*, 863–869. (e) Jacobsen, J. R.; Huchinson, C. R.; Cane, D. E.; Khosla, C. *Science* **1997**, *277*, 367–369. (f) Hunziker, D.; Wu, N.; Kenoshita, K.; Cane, D. E.; Khosla, C. *Tetrahedron Lett.* **1999**, *40*, 635–638.
12. Lin, Y.; Wang, J.; Wu, X.; Zhou, S.; Vrijmoed, L. L. P.; Jones, E. B. G. *Aust. J. Chem.* **2002**, *55*, 225–227.
13. Ovchinnikov, Yu. A.; Ivanov, V. T.; Mikhaleva, I. I.; Shemyakin, M. M. *Izv. Akad. Nauk. SSSR, Ser. Khim.* **1964**, 1823.
14. Mikawa, T.; Chiba, N.; Ogishi, H.; Gomi, S.; Miyaji, S.; Sezaki, M. Japanese Patent JP 02229177-A2; *Chem. Abstr.* **1991**, *114*, 227487k.
15. Jaturapat, A.; Isaka, M.; Hywel-Jones, N. L.; Lertwerawat, Y.; Kamchonwongpaisan, S.; Kirtikara, K.; Tanticharoen, M.; Thebtaranonth, Y. *J. Antibiot.* **2001**, *54*, 29–35.
16. Desjardins, R. E.; Canfield, C. J.; Chulay, J. D. *Antimicrob. Agents Chemother.* **1979**, *16*, 710–718.
17. Collins, L.; Franzblau, S. G. *Antimicrob. Agents Chemother.* **1997**, *41*, 1004–1009.
18. Skehan, P.; Storeng, R.; Scudiero, D.; Monks, A.; McMahon, J.; Vistica, D.; Warren, J. T.; Bokesch, H.; Kenney, S.; Boyd, M. R. *J. Natl Cancer Inst.* **1990**, *82*, 1107–1112.